# Geologic Controls on Porosity and Permeability in the Bethany Falls Limestone, Collier Flats Oil Field

## Comanche County, Kansas

By

Jay Allen LeBeau

August, 1997

# Geologic Controls on Porosity and Permeability in the Bethany Falls Limestone, Collier Flats Oil Field

## Comanche County, Kansas

By

Jay Allen LeBeau
B.S., Fort Lewis College, 1987

Submitted to the Department of Geology and the Faculty of the Graduate School of the University of Kansas in partial fulfillment of the requirements for the degree of Master of Science.

Thesis Chairman - Robert H. Goldstein

Thesis Cochairman - W. Lynn Watney

Committee Member - Ernest E. Angino

Committee Member - G. Paul Willhite

3-5-97

Date thesis accepted

Geologic Controls On Porosity and Permeability

in the Bethany Falls Limestone, Collier Flats Oil Field

Comanche County, Kansas

**Abstract**

The Bethany Falls limestone reservoir of the Collier Flats Oil Field is composed of fossiliferous wackestones, peloidal and fossiliferous packstones, mixed oolitic-bioclastic grainstones and oolitic grainstones capped by a paleosol. These sediments were deposited on a paleotopographic high of the northern Anadarko shelf of Kansas. The paleotopographic high focused wave and current energy to form regressive oolitic and bioclastic sand shoals with a north-south marine sand belt morphology. The location of this paleotopographic high is likely related to rejuvenation of Pre-Pennsylvanian-age structures that form a hinge-line or flexural zone in the vicinity of the Collier Flats Oil Field.

Effective porosity in the Bethany Falls limestone resulted from four dissolution and five cementation events. The first two dissolution and the first three cementation events are attributed to meteoric diagenesis, subaerial exposure and paleosol formation after Bethany Falls limestone deposition and during Galesburg shale deposition. The final two dissolution and the last two cementation events are related to burial diagenesis and occurred after Canville limestone deposition, burial and fracturing. A majority of the effective porosity is secondary porosity reduced by ferroan saddle dolomite, the final cementation event. Late post-burial fluid flow was focused preferentially in the center of the thickest portions of the carbonate sand shoals by preserved primary and secondary porosity connected by fractures caused by differential subsidence along the underlying flexural zone.

Two porosity-permeability distributions are interpreted based on whole core analysis, depositional and diagenetic models. Oil wells were classified as high or low permeability to select a porosity-permeability correlation equation to estimate average permeability of an oil

well in the Collier Flats Oilfield. The cementation factor, used in the Archie water saturation equation, was also modified to compensate for the higher percentage of secondary pores compared to primary interparticle pores, m= 2.5 and m=3.0 for oomoldic porosity.

Bethany Falls limestone reservoir characterization of the Collier Flats Oil Field identified four reservoir heterogeneity types based on the Weber (1986) classification: (1) Type 6, Microscopic textural; (2) Type 2, Genetic Unit; (3) Type 3, Permeability Zonation within a genetic unit; and (4) Fracture. Identification and mapping of these reservoir heterogeneities will assist enhancement of oil recovery.

Geologic Controls On Porosity and Permeability

in the Bethany Falls Limestone, Collier Flats Oil Field

Comanche County, Kansas

**Acknowledgments**

I wish to express my gratitude to Robert H. Goldstein, Thesis Chairman. Your patience and generous support led to the completion of this thesis. I would also like to express my gratitude to W. Lynn Watney, Thesis Cochairman, for sharing your wealth of geologic expertise on Kansas petroleum geology. A special word of thanks to G. Paul Willhite and the staff of the Tertiary Oil Recovery Project, you provided the much needed financial and technical support during the early phases of my Master of Science studies. It was during this time, I was able to define this thesis topic which has subsequently led me into a rewarding career in the petroleum industry.

# Table of Contents

# List Of Figures

## Chapter 1



## Chapter 2



## Chapter 3

## Chapter 4

## Chapter 5

# List of Tables

## Chapter 1



## Chapter 4



## Chapter 5

Geologic Controls On Porosity and Permeability

in the Bethany Falls Limestone, Collier Flats Oil Field

Comanche County, Kansas


## Abstract

The Bethany Falls limestone reservoir of the Collier Flats Oil Field is composed of fossiliferous wackestones, peloidal and fossiliferous packstones, mixed oolitic-bioclastic grainstones and oolitic grainstones capped by a paleosol. These sediments were deposited on a paleotopographic high of the northern Anadarko shelf of Kansas. The paleotopographic high focused wave and current energy to form regressive oolitic and bioclastic sand shoals with a north-south marine sand belt morphology. The location of this paleotopographic high is likely related to rejuvenation of Pre-Pennsylvanian-age structures that from a hinge-line or flexural zone in the vicinity of the Collier Flats Oil Field.

Effective porosity in the Bethany Falls limestone resulted from four dissolution and five cementation events. The first two dissolution and the first three cementation events are attributed to meteoric diagenesis, subaerial exposure and paleosol formation after Bethany Falls limestone deposition and during Galesburg shale deposition. The final two dissolution and the last two cementation events are related to burial diagenesis and occurred after Canville limestone deposition, burial and fracturing. A majority of the effective porosity is secondary porosity reduced by ferroan saddle dolomite, the final cementation event. Late post-burial fluid flow was focused preferentially in the center of the thickest portions of the carbonate sand shoals by preserved primary and secondary porosity connected by fractures caused by differential subsidence along the underlying flexural zone.

Two porosity-permeability distributions are interpreted based on whole core analysis, depositional and diagenetic models. Oil wells were classified as high or low permeability to select the appropriate porosity-permeability correlation equation to estimate average

permeability of an oil well in the Collier Flats Oilfield. The cementation factor, used in the Archie water saturation equation, was also modified to compensate for the higher percentage of secondary pores compared to primary interparticle pores, m= 2.5 and m=3.0 for oomoldic porosity.

Bethany Falls limestone reservoir characterization of the Collier Flats Oil Field identified four reservoir heterogeneity types based on the Weber (1986) classification: (1) Type 6, Microscopic textural; (2) Type 2, Genetic Unit; (3) Type 3, Permeability Zonation within a genetic unit; and (4) Fracture. Identification and mapping of these reservoir heterogeneities will assist enhancement of oil recovery.

Geologic Controls On Porosity and Permeability

in the Bethany Falls Limestone, Collier Flats Oil Field

Comanche County, Kansas

**Acknowledgments**

I wish to express my gratitude to Robert H. Goldstein, Thesis Chairman. Your patience and generous support led to the completion of this thesis. I would also like to express my gratitude to W. Lynn Watney, Thesis Cochairman, for sharing your wealth of geologic expertise on Kansas petroleum geology. A special word of thanks to G. Paul Willhite and the staff of the Tertiary Oil Recovery Project, you provided the much needed financial and technical support during the early phases of my Master of Science studies. It was during this time, I was able to define this thesis topic which has subsequently led me into a rewarding career in the petroleum industry.

# Chapter 1

## Introduction

### Purpose of Investigation

Kansas petroleum production is a significant part of the Kansas economy and as such has been studied intensely by industry, state agencies and academia in the search for understanding and to enhance petroleum production. More than 350,000 wells have been drilled within the state producing approximately 5 billion barrels of oil with an estimated 11 billion barrels yet to be produced (Baars et al., 1989). Pennsylvanian carbonates of the Lansing-Kansas City group have produced over two billion barrels of oil in central and western Kansas, and southern Nebraska. The productive Lansing-Kansas City strata are generally located on and adjacent to the Central Kansas Uplift (CKU). Many recent Lansing-Kansas City discoveries are located west of the CKU extending from the Collier Flats field in Comanche County in south central Kansas to the Northrup field in Cheyenne County in the extreme northwestern corner of the state (Figure 1.1).

One focus of petroleum production, occurrence, and engineering research at the University of Kansas is enhanced oil recovery. This focus has brought together the geology and petroleum engineering departments in a cooperative effort to perform reservoir characterization to better understand the mechanisms and processes that govern petroleum production. Determining the geologic controls that affect porosity and permeability development and their distribution is a significant component in simulating primary production and assessing enhanced oil recovery (EOR) potential. This investigation is an attempt to identify the geologic processes that impact porosity and permeability development, reservoir continuity and heterogeneity in the Bethany Falls limestone of the Collier Flats oil field, Comanche County, Kansas (Figure 1.1).

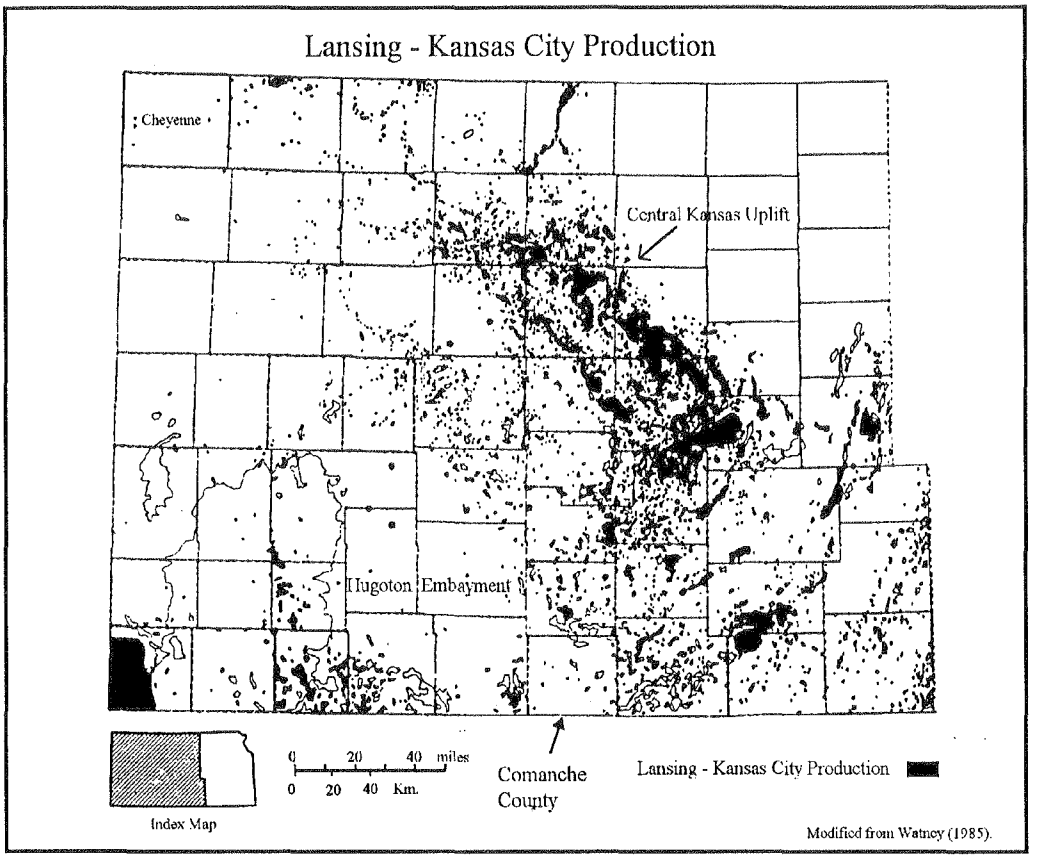


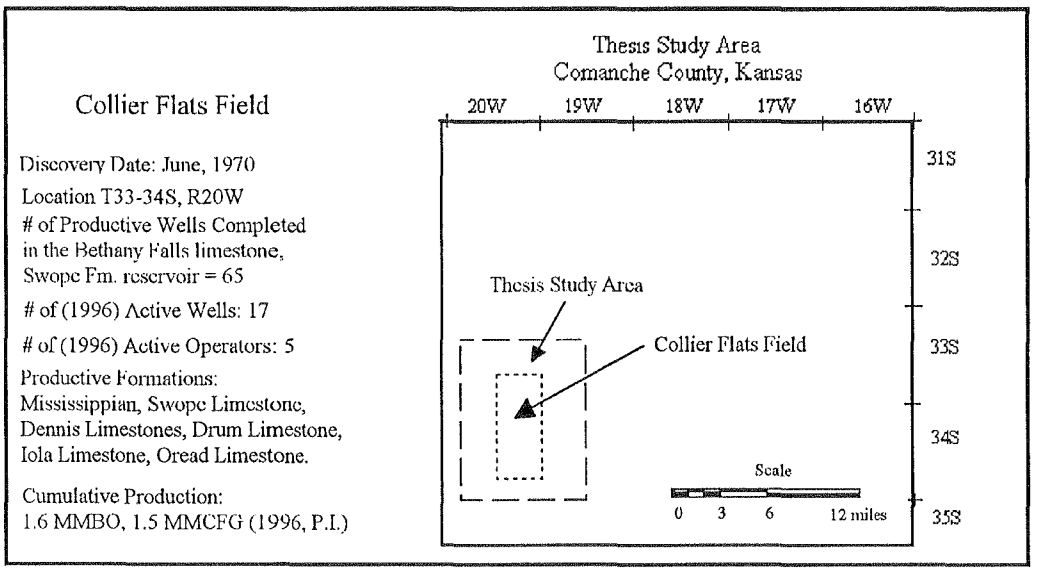


Figure 1.1 Lansing-Kansas City Group production and location of Collier Flats oil field study area.

The Collier Flats field is a good candidate for this type of investigation because: (1) sufficient amounts of geologic data are available, (modern well logs with core); (2) the relative youth of the fields, (discovered in the 1970's); and (3) the wealth of geologic knowledge regarding Kansas cyclothems. This oil field has produced approximately 1.6 million barrels of oil and 4.5 billion cubic feet of gas in township 20 west, ranges 33 and 34 south, Comanche County, Kansas (Figure 1.1). The majority of oil production occurs from the Missourian age Bethany Falls limestone member, Swope Limestone Formation, Kansas City Group, Missourian Stage, Upper Pennsylvanian Series (Figure 1.2).

Objectives of this investigation are:

- to describe the lithofacies and paragenetic features observed in the producing interval
- to develop geologic models of the reservoir that can be used to calibrate well logs and predict permeability
- to construct a grid of reservoir engineering data that delineates reservoir continuity and heterogeneity.

The data and conclusions from this study will begin a process where primary and secondary performance can be assessed by the staff of the Tertiary Oil Recovery Project (TORP). Additionally, it is hoped that this study will provide a framework that will allow assessment of enhanced oil recovery potential.

This investigation has been conducted under the auspices of the Tertiary Oil Recovery Project (TORP), Kansas Geological Survey (KGS) and the Department of Geology. TORP provided financial support and engineering expertise. The KGS provided geologic data, computer software and geologic expertise for this effort. The Department of Geology provided financial assistance, support facilities and direct oversight.

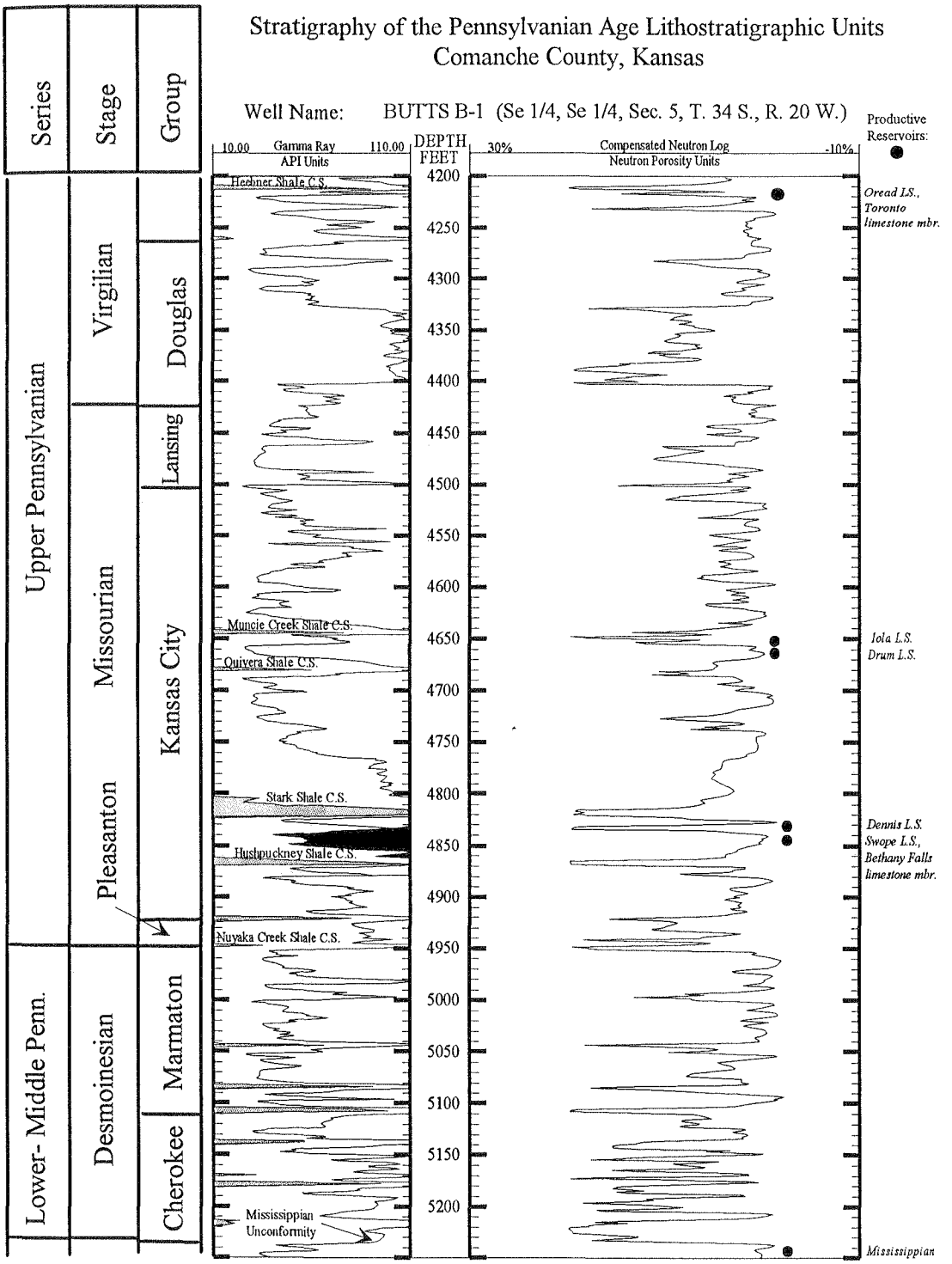


Figure 1.2 Pennsylvanian series stratigraphy in the study area. Stratigraphy based on picks from type logs of western Kansas from the Kansas Geological Survey. Well location is presented on the regional database maps. Productive intervals are noted by productive oil wells symbols and by formation name. Iola and Dennis Formation production are from the transgressive limestone members Paola and Canville limestones respectively.

## Field History (Collier Flats)

The Nomenclature Committee of the Kansas Geological Society has designated the Lemon Ranch field as part of the Collier Flats field. In order to simplify oil field references and comply with the KGS, all further references to the Collier Flats field will include the Lemon Ranch field unless otherwise noted. The Collier Flats field was discovered in June of 1970 by Halliburton Oil Production Company with the completion of the #1 Schweitzer well, NE 1/4, NE 1/4, T20W, R33S. Field development occurred in three distinct stages:

- 12 wells were drilled by five operators in 1970, sections 23, 24, 25, 26, T20W, R33S (Figure 1.3)
- 14 wells were drilled by one operator in 1978-79, sections 13, 14, 23, 24, 33, T20W, R34S (Figure 1.3)
- 72 wells were drilled by twelve operators in 1980-85 (Figure 1.3).

Sixty-five of these wells were completed in the Bethany Falls limestone member including 15 wells listed as dual producers (Figure 1.4). As of December 1996, five operators were producing 16 oil and gas wells on nine leases (P.I., 1996).

The main productive zone is the Bethany Falls limestone member, Swope Limestone Formation, Kansas City Group, Missourian Stage, Upper Pennsylvanian Series (Figure 1.5). Bethany Falls production occurs from discontinuous porosity along the one to one-and-a-half mile wide crest and southeastern flank of a southwest plunging anticline. The trapping mechanism is primarily stratigraphic with dry and non-productive wells reflecting a decrease in porosity and/or permeability. There are five additional pay zones in the Collier Flats field and in stratigraphic order they are:

- **Mississippian Limestone** - The Mississippian Limestone produces primarily gas along the Collier Flats Anticline.

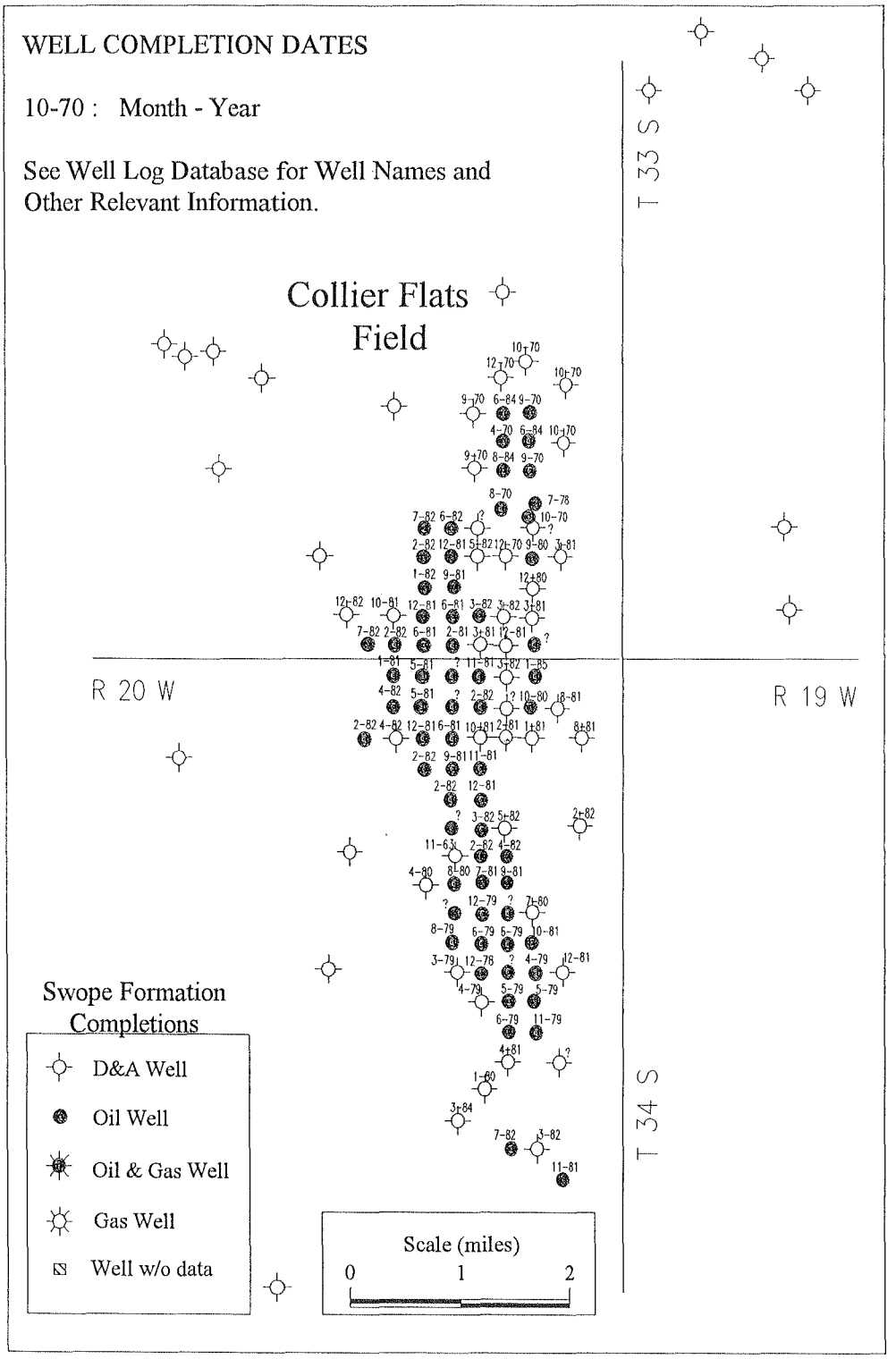


Figure 1.3 Collier Flats field oil well completion dates.

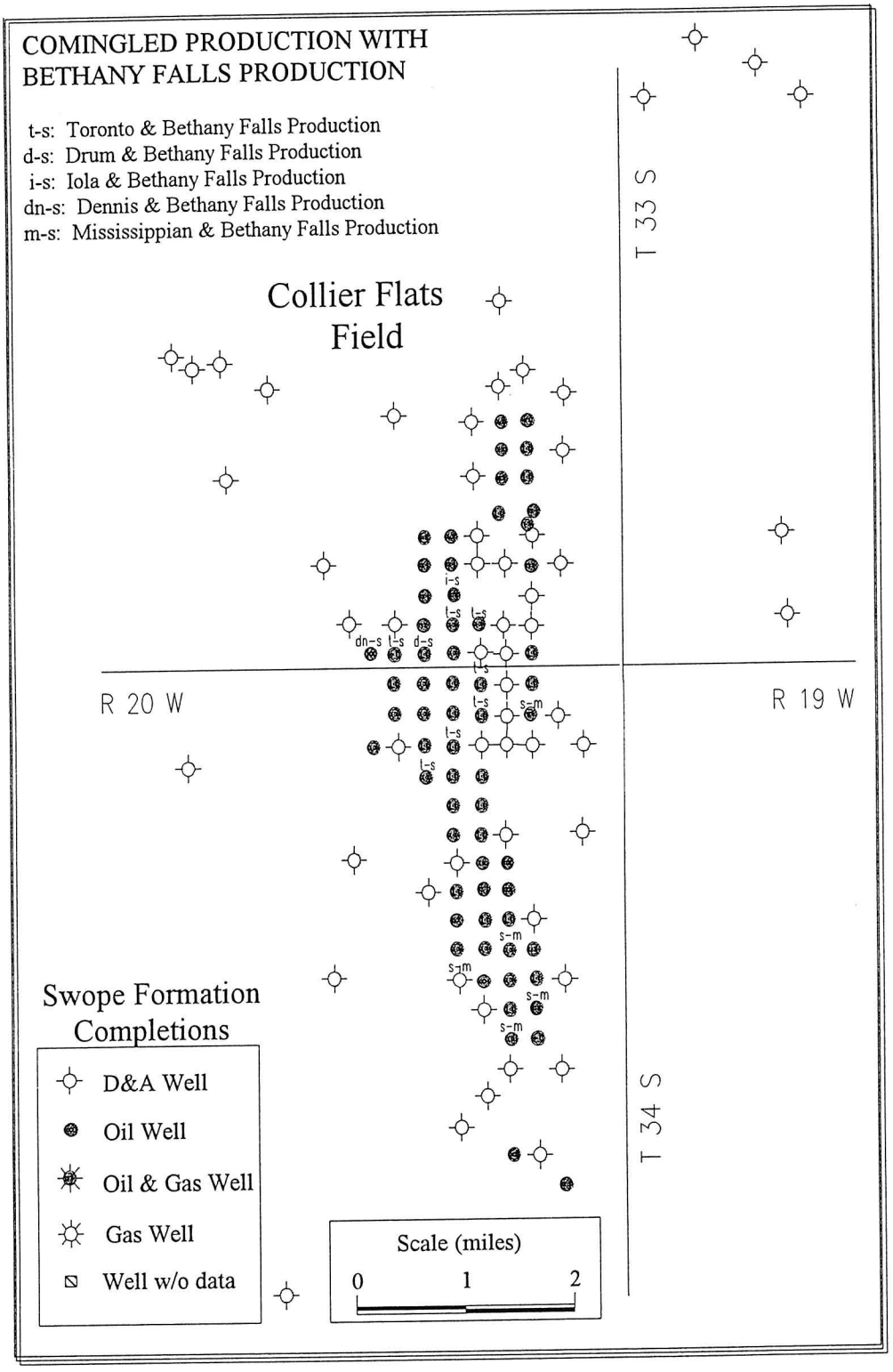


Figure 1.4 Collier Flats field, comingled oil production.

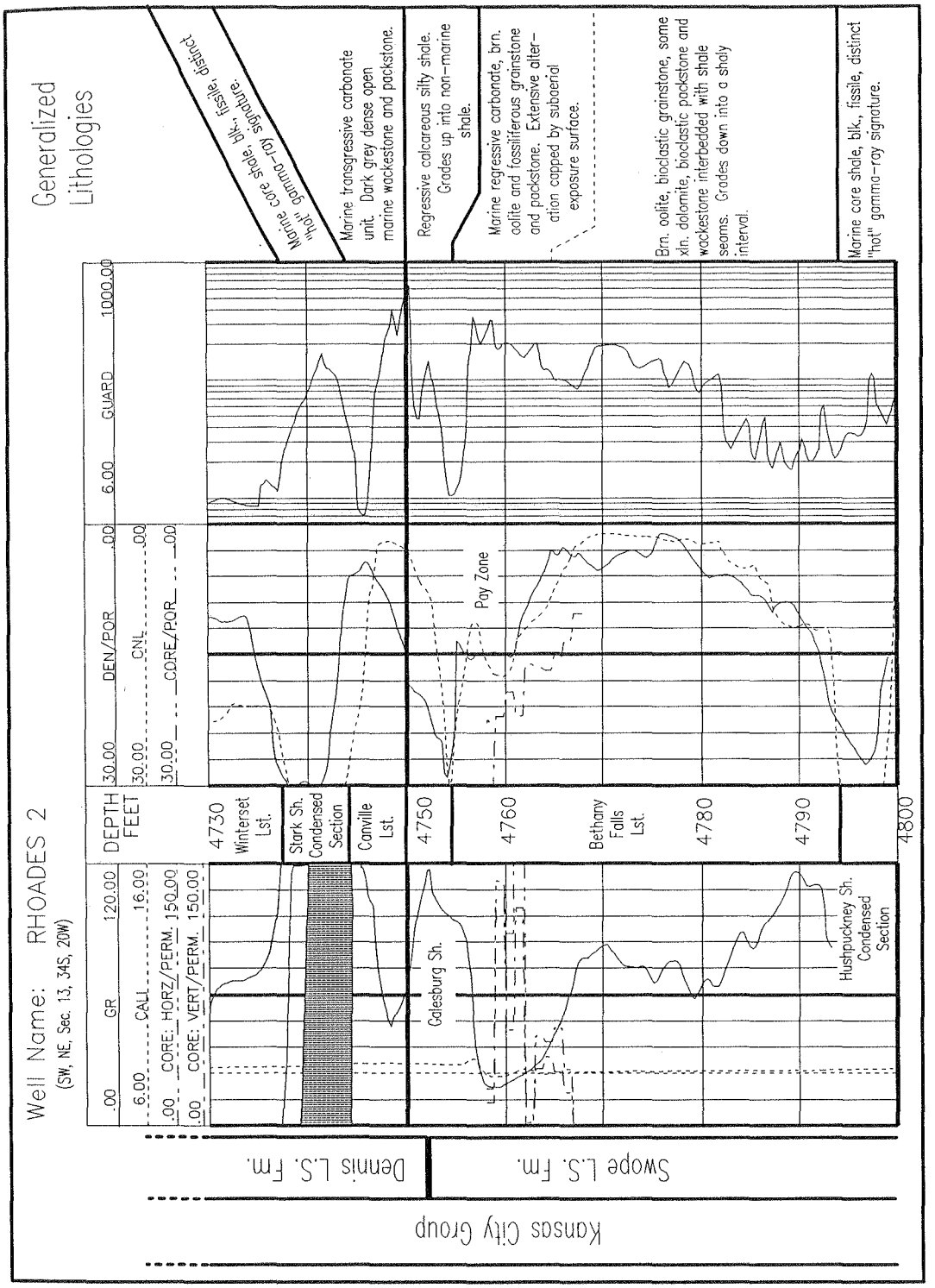


Figure 1.5 Typical well log signature of the Bethany Falls Limestone reservoir and other lithostratigraphic units. Whole core analysis data are also presented with log data.

Mississippian gas and condensate production is commingled with five Bethany Falls wells (Figures 1.2, 1.4). This productive zone is found approximately 350 feet below Bethany Falls production.

- **Missourian Dennis Limestone Formation** - Only one scout card reported Dennis Limestone perforations (Figures 1.2, 1.4).
- **Missourian Drum Limestone Formation** - The Drum Limestone is productive in only three wells. Drum production commingles with one Bethany Falls well (Figures 1.2, 1.4). This productive zone is found approximately 155 feet above the Stark Shale.
- **Missourian Iola Limestone Formation** - Only one scout card reported Iola Limestone perforations (Figures 1.2, 1.4).
- **Virgilian Toronto Limestone Member**- The Toronto limestone member produces from about a dozen wells in the study area with production from seven wells commingled with Bethany Falls production (Figures 1.2, 1.4). Perforations are generally 25-30 feet below the Heebner Shale.

Drilling and completion of the pay zone typically consisted of drilling through the Bethany Falls limestone pay-zone, running well logs, setting casing and perforating with acid stimulation. Acid treatments commonly consisted of 2000 to 3000 gallons of 15% to 28% HCL acid. Well logs were run on all wells with drill stem test data reported on scout tickets and 36 KRM well files. The most common log suites consist of:

- Gamma-Ray / Neutron / Guard,
- Gamma-Ray / Compensated Neutron/Density / Dual Induction Laterolog,
- Gamma-Ray / Compensated Neutron/Density / Guard logs (see Appendix A, for a list of well-log suites for each well).

Primary production occurred from liquid expansion and solution gas drive supplemented by reinjection of produced gas to maintain reservoir pressures (Henderson &

Co., 1981). KRM, the primary operator of the Lemon Ranch leases in 1979, began water-flooding their leases in 1983 with good results (Anchor Bay, per. comm., 1990). At the time this investigation began, Anchor Bay Company of Denver Colorado purchased a majority of Petro leases with plans to implement a waterflood in the areas north of the Lemon Ranch leases.

## Geologic Setting and Previous Studies

Heckel (1977, 1980, 1984), Merriam (1963), Moore (1979), Rascoe and Adler (1983) and Watney (1980, 1984, 1985) and many other authors have developed a widely accepted paleogeographic model for the Upper Pennsylvanian age strata in western Kansas. This model is used to place the Collier Flats field in a geologic and paleogeographic context for subsequent analysis.

During Missourian and Virgilian time, the super-continent Pangea was in the final stages of development producing the Marathon-Ouachita mountains to the south, Appalachian mountains to the east and ancestral Rocky mountains to the west (Heckel, 1980; Watney, 1980). Associated with the continental collisions are many uplifts and basins formed in the Mid-Continent including the Central Kansas Uplift and Anadarko Basin.

The Hugoton embayment, during the Missourian, was a stable carbonate shelf extending into a subsiding Anadarko Basin. Subsidence on the western Kansas shelf appears to have been significant because Permo-Pennsylvanian strata represent nearly 45 - 75% of the Paleozoic sedimentary column, even though Permo-Pennsylvanian time only represents 23% of Paleozoic time (Watney, 1989). Sedimentation rates also appear to have been high. The cyclic strata of the western Kansas shelf thicken and merge southward to the northern edge of the Anadarko basin to form a constructive shelf margin (Watney, 1984). Farther south, western shelf carbonates merge into deep water basinal lithologies. Collier Flats reservoir facies developed on the western flank of the Pratt Anticline, Central Kansas Uplift, and the

eastern edge of the Hugoton Embayment on what was a stable carbonate shelf during the Upper Pennsylvanian, Missourian (Figure 1.6).

The Missourian age Lansing and Kansas City groups in the Mid-Continent have been described as a repetitive sequence of interbedded carbonates and clastics. These rocks were classified as cyclothems by the early works of Moore (1929, 1936, 1949) and Merriam, (1963). Cyclicity of these sediments is attributed to glacio-eustatic changes in sea-level based on the insightful work of Wanless and Shepard (1936), Heckel (1977) and Watney (1985). However, the effects of tectonism on paleogeography during the Pennsylvanian must not be dismissed especially in areas near uplifts and buried structures.

The ideal four component "Kansas Type" cyclothem as described by Heckel (1977; 1980; 1983) consists of an outside shale, middle limestone, core shale and upper limestone sequence (Figure 1.7). Each cyclothem is attributed to one rise and fall of sea-level depositing a transgressive middle limestone, core shale, regressive upper limestone and non-marine outside shale. Watney (1984) provided an excellent regional summary of cyclothem lithofacies in western Kansas (Table 1.1).

| Lithofacies | Northern Shelf | Central Kansas Uplift | West Central | Southwest |
|---|---|---|---|---|
| **Regressive Shale (Outside Shale: Heckel, 1977)** **(Upper Shale Watney, 1985)** | Red-brown (oxidized) siltstone with soil characteristics: greatest thickness northwestern shelf | Unfossiliferous silty shale; gray, green reduced on south end of uplift; oxidized to occasionally reduced on north end (Cambridge Arch); thinner locally, missing over uplift north and south. | Reduced, occasionally oxidized on northern reaches; unfossil-iferous to locally restricted shallow-water fauna to south commonly very thin to missing in southern reaches. | Reduced, sparsely fossiliferous to unfoss-iliferous, absent in many areas or extremely thin, i.e. difficult to map using wireline logs; most cycles contain sparse indications of soil formation. |

Table 1.1 General Lithofacies Components of Kansas City Group Cyclothems in Western Kansas.

| | | | | |
|---|---|---|---|---|
| **Regressive Carbonate**<br>**(Upper Limestone: Heckel, 1977)**<br><br>**(Upper Limestone: Watney, 1985)** | **Northern Shelf**<br>Regional thinning to north; lower interval commonly shalier and more silty to north; siltier in upper interval; top locally eroded and more heavily weathered northward, secondary porosity more important; limited coated grains and thin interval of grainstones; shaly intervals in lower portion are light color tones. | **Central Kansas Uplift**<br>Thin over uplift, sometimes extreme thinning; evidence of weathering apparent across uplift; secondary porosity important reservoir parameter; cleaner carbonate overall in southern area; light-colored carbonates are the rule; locally very thin or missing subtital quiet water carbonate with diverse fossils. | **West Central**<br>Gradual thickening to south; local thickening due to bioherm or grainstone accumulation or combination; well-developed subtital, open marine with light colored micrite shalier to north; oolitic shoal-water grainstones more significant to south; thicker and more extensive grainstones, but still isolated patches; east west trend of shoal carbonates, north-south trend w/ east-west secondary trend in oolite tract; more effects of weathering to south. | **Southwest**<br>Relatively dark-colored lower interval of open marine carbonates with more abundant organic matter macerals preserved in this relatively thick subtital portion; more chert replacement; extensive thick oolite developed as large sheet-like lobes that cover area; north-south lobes with east-west elongated fingers; major trends commonly run northwest to south-east. |
| **Marine Shale**<br><br>(Core Shale: Heckel, 1977)<br><br>(Lower Shale: Watney, 1985) | **Northern Shelf**<br>Silty, calcareous, gray and green shale commonly oxidized to maroon color; brachiopods and crinoids common; occasionally restricted facies, pelecypods and ostracods associated with limestone nodules including layers of silty grainstones; interval is thick and continues to thicken northward in excess of 20 feet. | **Central Kansas Uplift**<br>Gray-green to black color; black shale is hard with conchoidal and platy fractures; sparse fossils including conodonts, fish scales orbiculoid brachiopods; gray-green shale contains predominately brachiopods; thickness varies from zero to several feet. | **West Central**<br>As in area of CKU except is thicker; consistent thickness of several feet. | **Southwest**<br>Dark gray to black shales are the rule outside the extreme southwestern area of study where unit becomes abruptly thicker, silty and contains more diverse fossils. |

Table 1.1 cont. General Lithofacies Components of Kansas City Group Cyclothems in Western Kansas.

| Transgressive Limestone<br><br>(Middle Limestone: Heckel, 1977)<br><br>(Lower Limestone: Watney, 1985) | Northern Shelf<br><br>Thin, laterally extensive (good marker bed to denote lower boundary of cycle); coated (osagia) grainstone - packstone with diverse fossil assemblage; locally carbonate buildup as mud mound (phylloid algae) or oolitic shoal; moderate to very silty at the base with occasionally local sandstone development and conglomerate (localized reservoir play); base is erosional. | Central Kansas Uplift<br>Thin, extensive silty to sandy grainstone to packstone commonly with Osagia at base; occasionally conglomeratic at base; persists even when marine shale is missing; base is erosional. | West Central<br><br>As in North. | Southwest<br><br>Generally thicker than to north; darker gray-brown with diverse fossils in silty wackestone to occasionally packstone; preserved flecks of organic matter; clean intervals w/ phylloid algae; base less distinctly erosional although hiatus is noted. |
|---|---|---|---|---|

Table 1.1 cont. General Lithofacies Components of Kansas City Group Cyclothems in Western Kansas. Modified from Watney (1985).

Watney's research clearly points out the relationship between location on the carbonate shelf and cyclothem lithofacies development. One of the more significant cyclothem features delineated by Watney's investigations is paleosol development on top of the regressive upper limestone members. Diagenetic processes associated with subaerial exposure typically alter primary porosity, impact reservoir porosity and permeability development and ultimately contribute to reservoir heterogeneity (Heckel 1983, Prather 1984, Watney 1983;1985).

The earliest reported Swope Limestone Formation investigations were performed by Payton (1966) and Mossler (1971; 1973) on outcrops in Missouri, Iowa and southeastern Kansas. In recent years, additional work on these outcrops have been performed by the Kansas University geology faculty, students and the staff of the Kansas Geological Survey (KGS) (Watney et al., 1983; 1985; 1989; 1991). Watney (1984; 1985 and 1989) has focused on regional studies of Missourian age cyclothems, including the Swope Formation, in western Kansas.

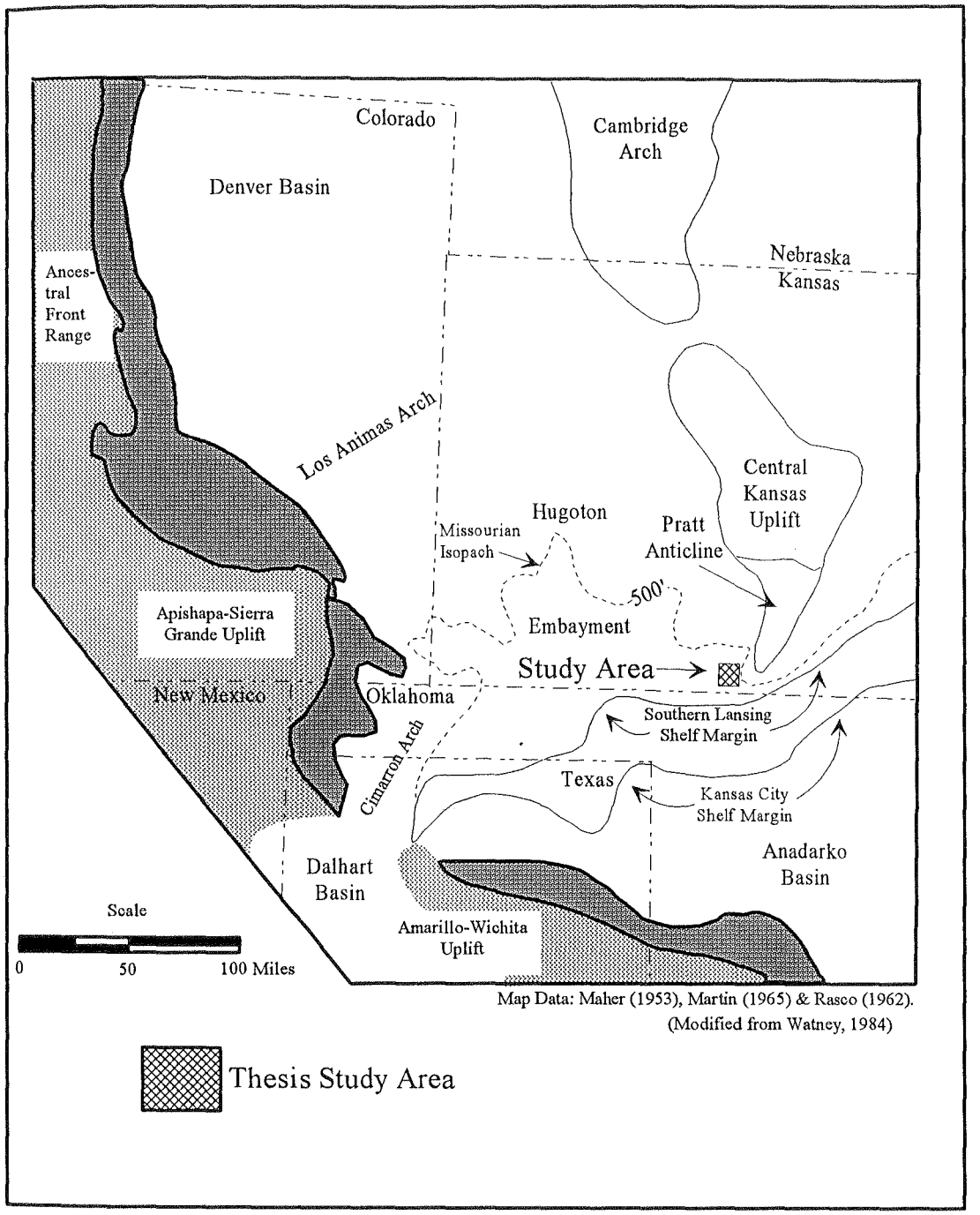


Figure 1.6 Late Pennsylvanian Mid-Continent Paleogeography (Missourian Stage) with location of study area.

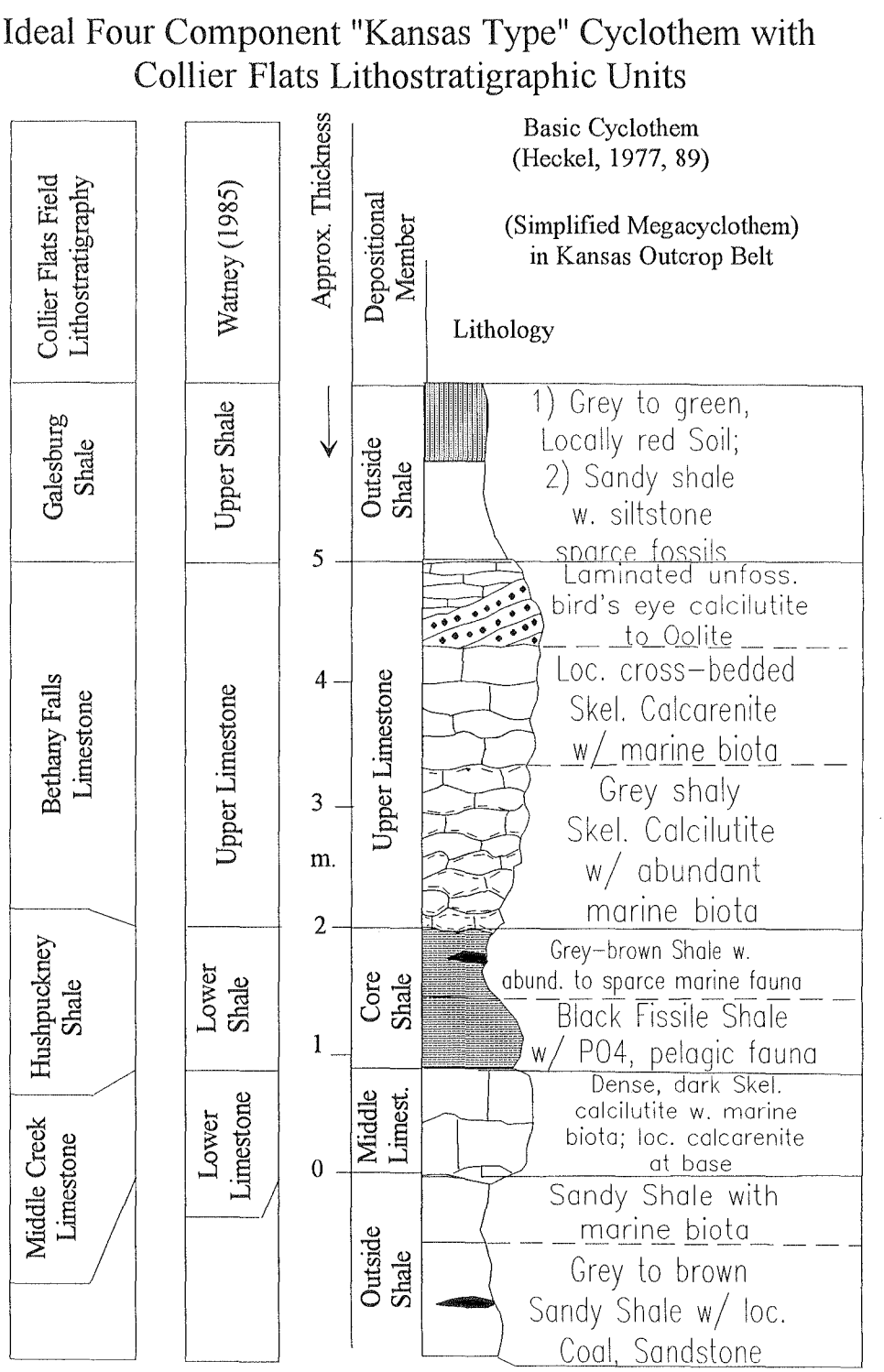


Figure 1.7 Initial correlation between Heckel's and Watney's cyclothem nomenclatures and Collier Flats field lithostratigraphy. (Modified after Watney et al., 1989) and Heckel (1977, 1989).

There are many lithologic similarities between the Swope Limestone Formation in eastern and western Kansas. However, there are differences in paleogeography between eastern and western Kansas during the Missourian which may impact many geologic aspects of Swope Formation deposition and diagenesis.

## Study Area and Reservoir Analysis Methodology

This investigation is focused on identifying the geologic controls on porosity and permeability in the Bethany Falls limestone in the Collier Flats oil field. Geologic mapping and analysis is limited to this area and the Bethany Falls limestone member. Several rough regional maps were constructed to aid in establishing a paleogeographic model for the study area.

Depositional environment is interpreted from analysis of 13 slabbed cores in the Lemon Ranch leases of the Collier Flats field and 153 well logs in the study area. Structure and isopach maps of relevant strata were generated using TerraSciences well log analysis software provided by the Kansas Geological Survey (KGS).

Paragenesis and reservoir analysis is interpreted from thin-section petrography. Petrography was performed using plane-light microscopy, cathodoluminescence, ultra-violet epifluoresence and alizarin red-S and potassium ferricyanide stained thin-sections to identify mineralogy, pore-types and diagenetic features from over 100 blue-epoxy impregnated thin-sections from core.

Reservoir characterization is based on 10 whole-core analysis data sets, thin section petrography, computer analysis of 100 digitized well logs using TerraSciences well log analysis software, 18 detailed drill stem tests, production data and Collier Flats depositional and diagenetic models. All geologic and reservoir engineering data are tabulated and digitally stored in computer files.

# Chapter 2

## Study Area Paleogeography

### Introduction

As stated earlier, Heckel (1977, 1980, 1984), Merriam (1963), Moore (1979), Rascoe and Adler (1983) and Watney (1980, 1984, 1985) and many other authors have developed a widely accepted regional paleogeographic model for Upper Pennsylvanian age strata in western Kansas. In order to establish a geological model for Collier Flats production, a study area paleogeographic model must be established to frame depositional and diagenetic models.

An additional twenty-five well-logs, outside the study area, were digitized into Terra-sciences well log analysis software to create a series of computer generated regional maps and cross-sections (Figure 2.1). Formation boundary picks are based on "type well-logs" from the Kansas Geological Survey (Figure 1.2).

### Mississippian Unconformity and Overlying Strata

Tectonism associated with the Ouachita orogeny resulted in widespread uplift and erosion of Mississippian strata in the Midcontinent including much of the Hugoton embayment and the Central Kansas Uplift. Morrowan and Atokan age fluvial-deltaic siliciclastics were deposited in the deeper portions of the Hugoton embayment and Anadarko basin onlapping onto the Mississippian unconformity south and west of the study area (Brown et al., 1993). In the study area, thin Upper Morrowan estuarine and shallow marine sandstones are reported in the southwestern portion of Comanche county indicating thin Atokan age sediments may also be preserved (Mannhard and Busch, 1974).

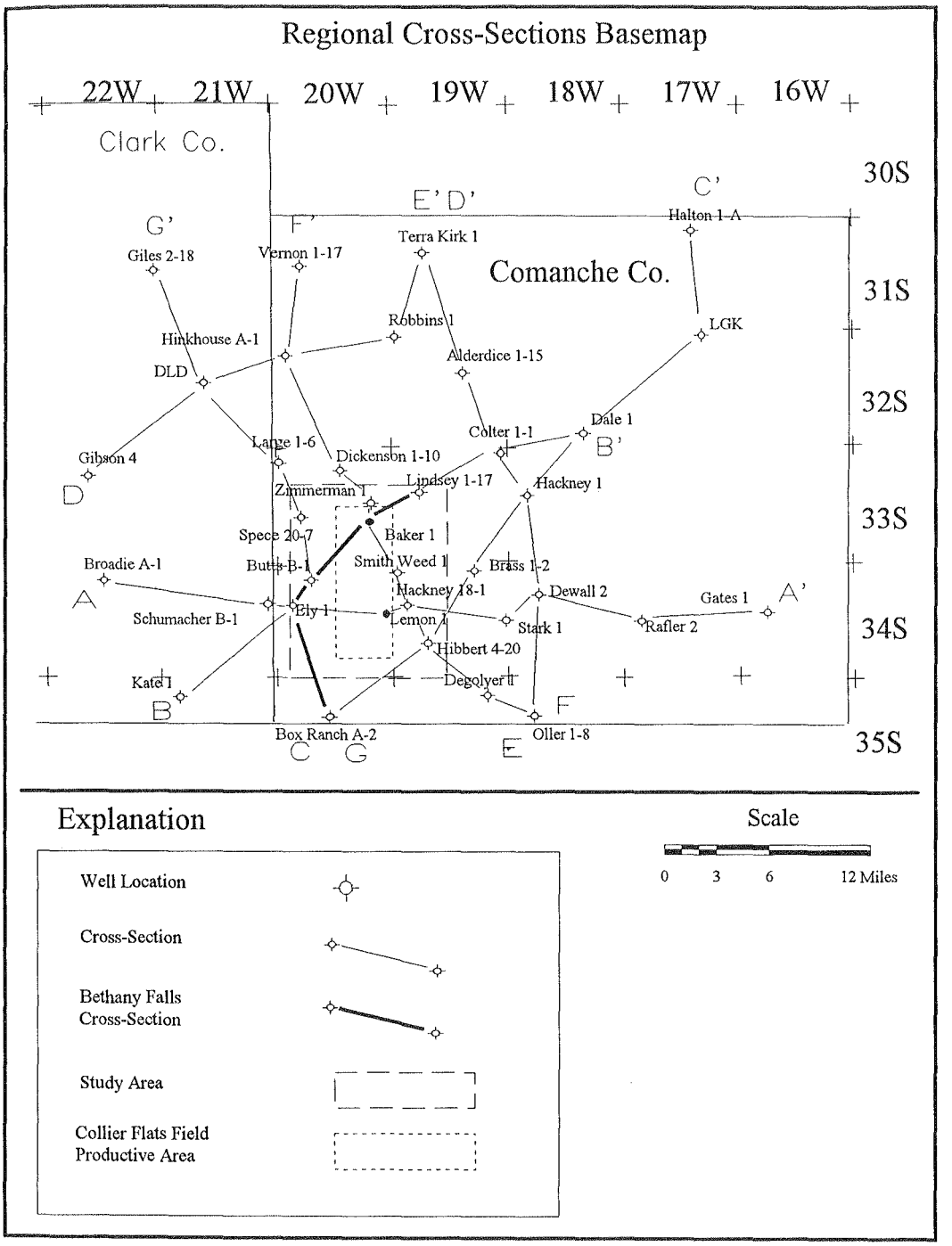


Figure 2.1 Regional cross sections base map in the thesis study area. The Bethany Falls cross section is shown in detail in Figure 2.12 with paleogeography and depositional environment interpretations.

Early Desmoinesian transgressive marine sandstones and scattered regressive fluvial-deltaic strata of the Cherokee Group prograded to the south and southwest over the Mississippian unconformity and Morrowan and Atokan age sediments (Figure 2.2). Sediment source is interpreted primarily as the exposed strata on the Central Kansas Uplift. Figure 2.3 is a structure contour map on top of the Mississippian unconformity that delineates pre-Pennsylvanian topography. Figure 2.4 is a Cherokee Group isopach map that shows thinning over structurally high areas to the north and east and thickening into the Anadarko basin to the southwest. Collier Flats production overlies this structural high on the Mississippian unconformity.

Up on the shelf of the Anadarko basin, Upper Desmoinesian Marmaton Group strata conformably overlie Cherokee Group strata and consist almost entirely of cyclic carbonates. The Anadarko basin to the south continued to receive clastic sediments from the Amarillo-Wichita and Ouachita fold belts (Moore, 1979; Rascoe and Adler, 1983; Houseknecht, 1986). In the study area, Marmaton Group strata are relatively uniform in thickness over the Collier Flats productive area, thicken to the south and southwest, and thin to the north and to the south-east (Figure 2.4).

Lower to Middle Pennsylvanian strata, (Morrowan, Atokan and Desmoinesian), record a gradual transition from marine clastic sedimentation to cyclic marine carbonate sedimentation in the study area, as the early Pennsylvanian seas transgressed onto the Anadarko shelf.

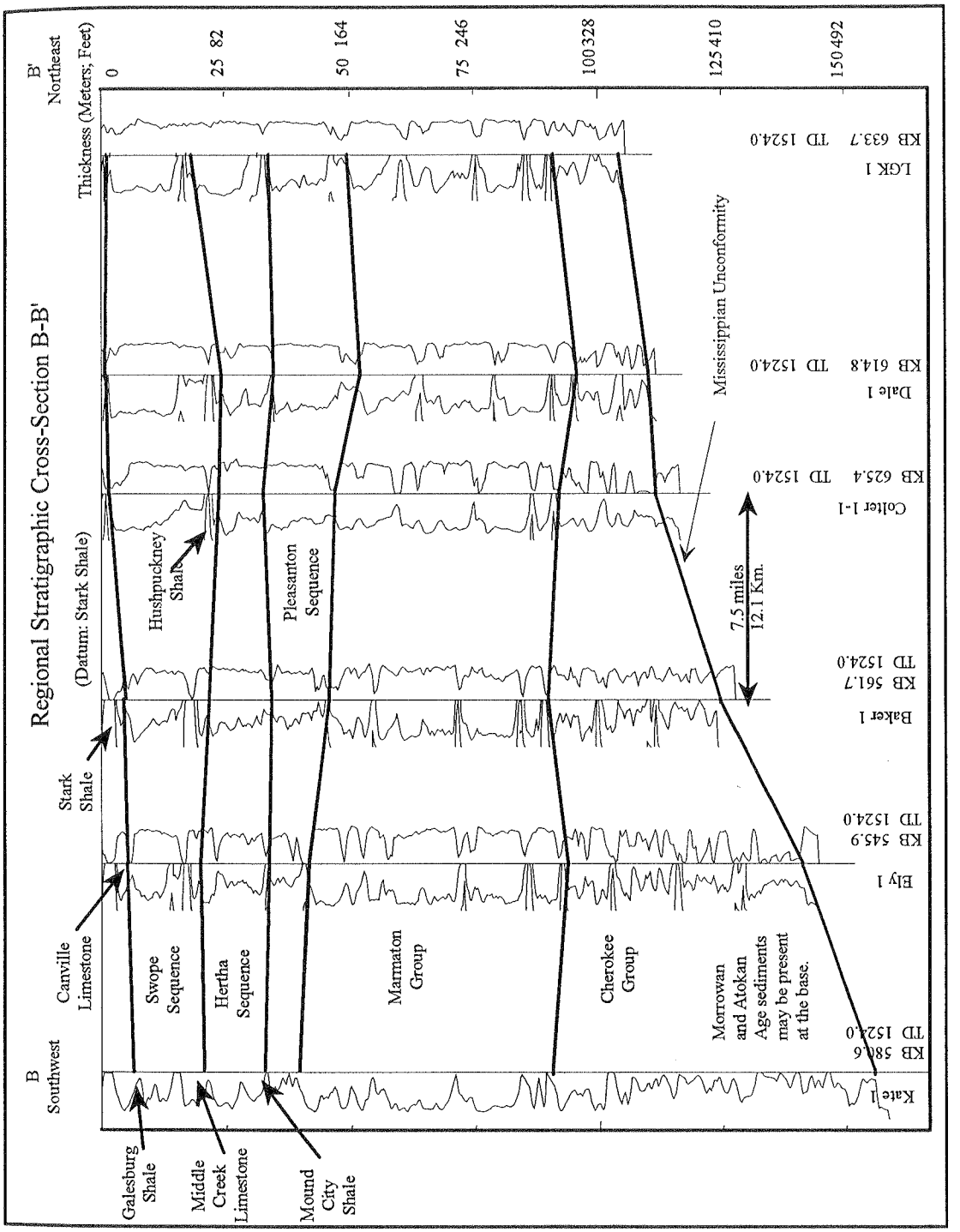


Figure 2.2 Regional cross section of the Pennsylvanian age strata, up to the Swope sequence, in the thesis study area. Well log picks are based on KGS type logs.

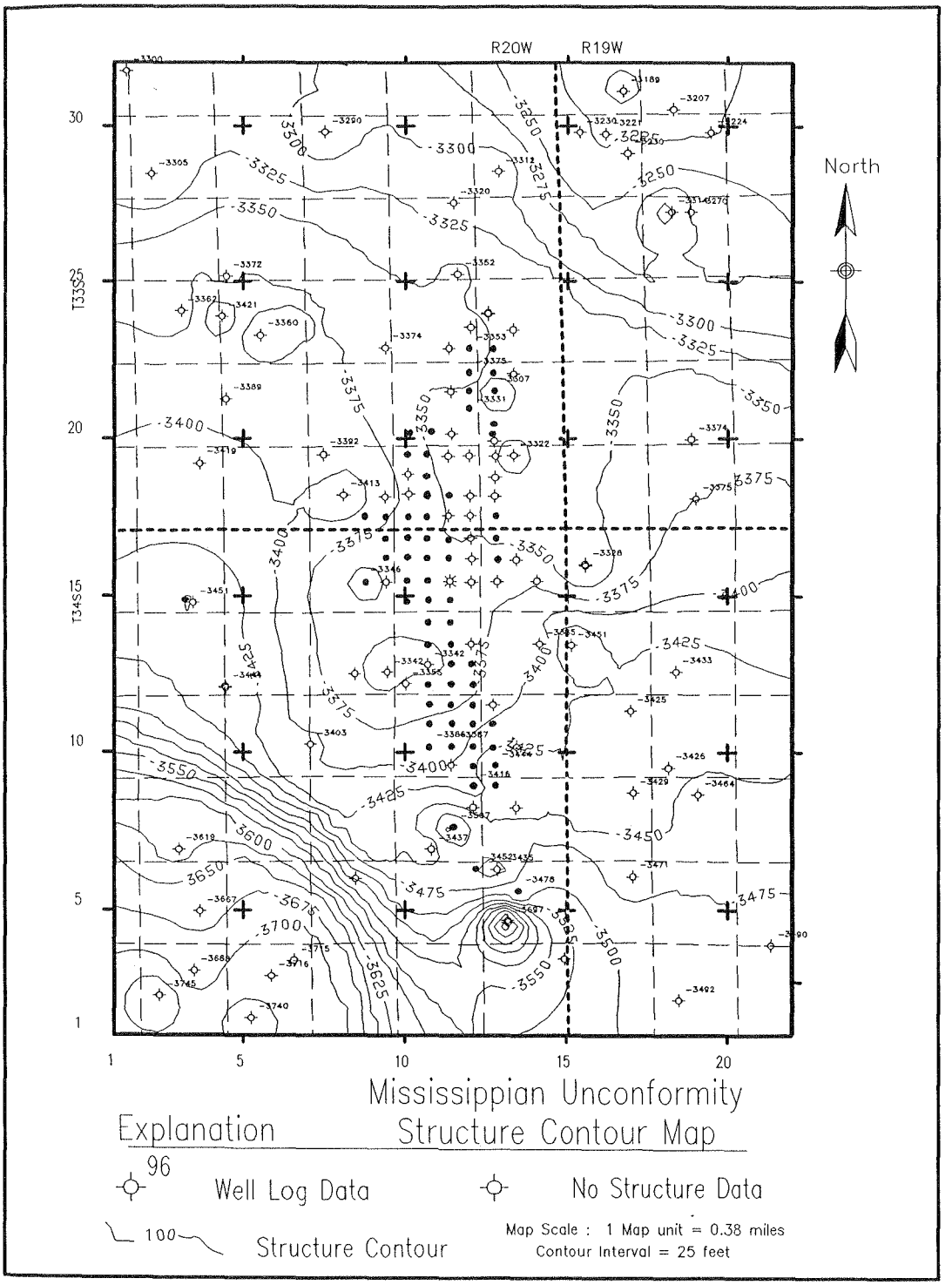


Figure 2.3 Structure contour map on top of the Mississippian unconformity.

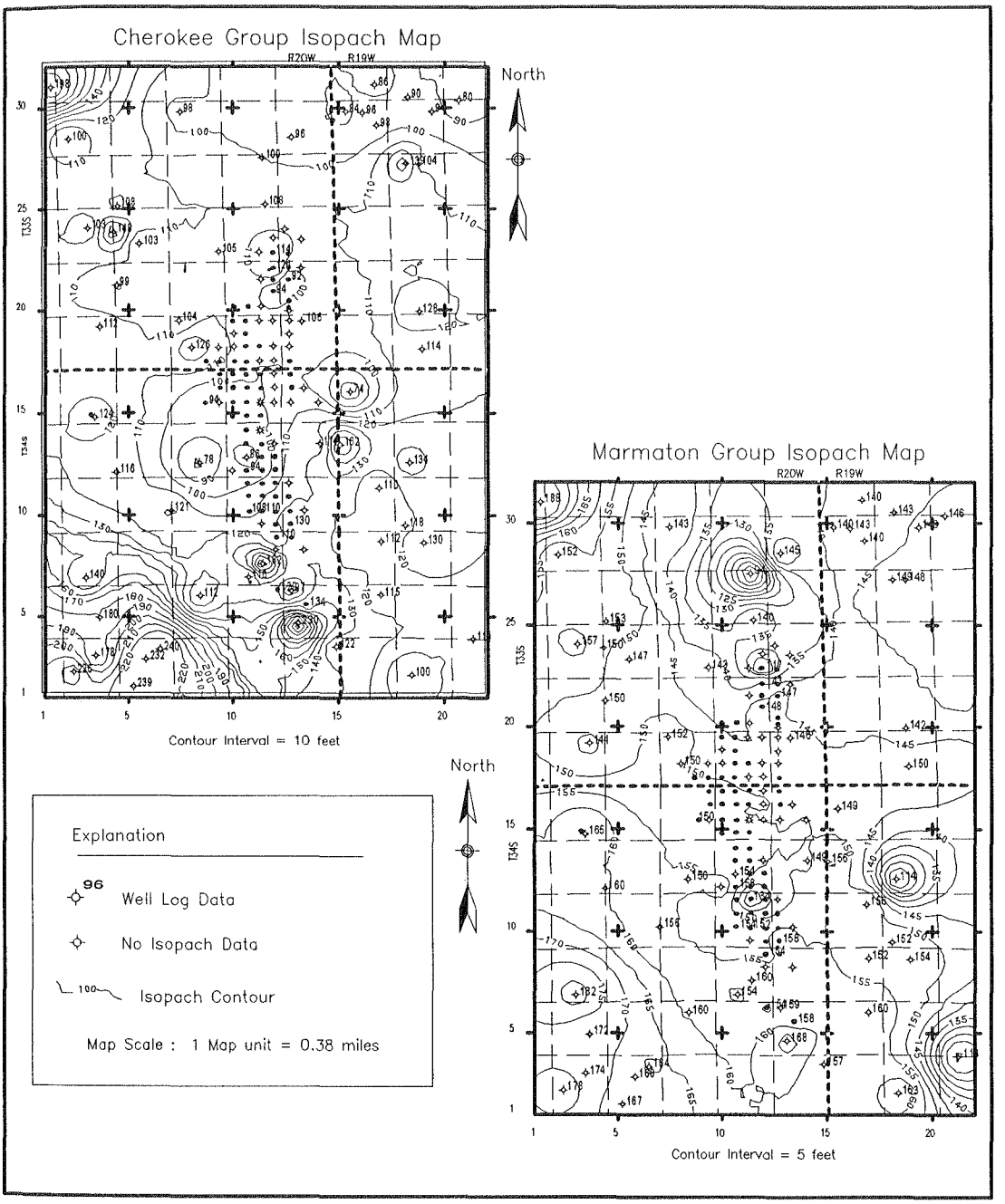


Figure 2.4 Cherokee and Marmaton Group isopach maps. Cherokee Group strata thin over the Mississippian unconformity underlying Collier Flats production and thicken into the Anadarko Basin to the southwest. Marmaton Group strata are fairly uniform underlying Collier Flats production.

Differential subsidence between the Anadarko basin and Anadarko shelf is recorded by thickening Lower Pennsylvanian strata toward the Anadarko basin and thinning over paleo-topographical high areas in the study area and to the northeast on the Central Kansas uplift.

## Upper Pennsylvanian, Missourian Age Strata

The KGS has developed shelf to slope sequence stratigraphic correlations of Missourian age strata including the Pleasanton, Hertha and Swope sequences in eastern Kansas (Watney et al., 1989). In order to facilitate isopach mapping and geologic interpretations, Missourian age strata in the thesis area are subdivided using sequence stratigraphic boundaries identified by subaerial exposure surfaces mapped in eastern Kansas by the KGS (Figure 2.5). Missourian-age strata began with deposition of the Pleasanton Sequence. In eastern Kansas, the upper portion of the Pleasanton Group deltaic strata conformably merges into the Critzer limestone member of the Hertha Formation and is included in the Pleasanton sequence (Watney et al 1989), (Figure 2.5). In the study area, black fissile shales are easily identified in well-logs and generally identified as the core shale of Heckel's (1977) cyclothem model (Figure 1.7). These relationships allowed isopach mapping of the Pleasanton sequence between the Nuyaka Creek Shale and Mound City Shale in the study area (Figure 2.5). Analysis of well log signatures of regional cross sections (Figure 2.6) indicate the Pleasanton sequence is primarily a shaly carbonate unit in the study area. Farther northeast toward the Central Kansas Uplift, the Pleasanton sequence grades into clean carbonate units reflecting shallow water shoaling conditions. In the study area, thickening of the Pleasanton sequence carbonates trends approximately north to south underlying Collier Flats production (Figure 2.7). Pleasanton thickening underlying Collier flats production indicates that carbonates fill in paleotopographic lows or may have accumulated at a higher rate to create a carbonate build-up.

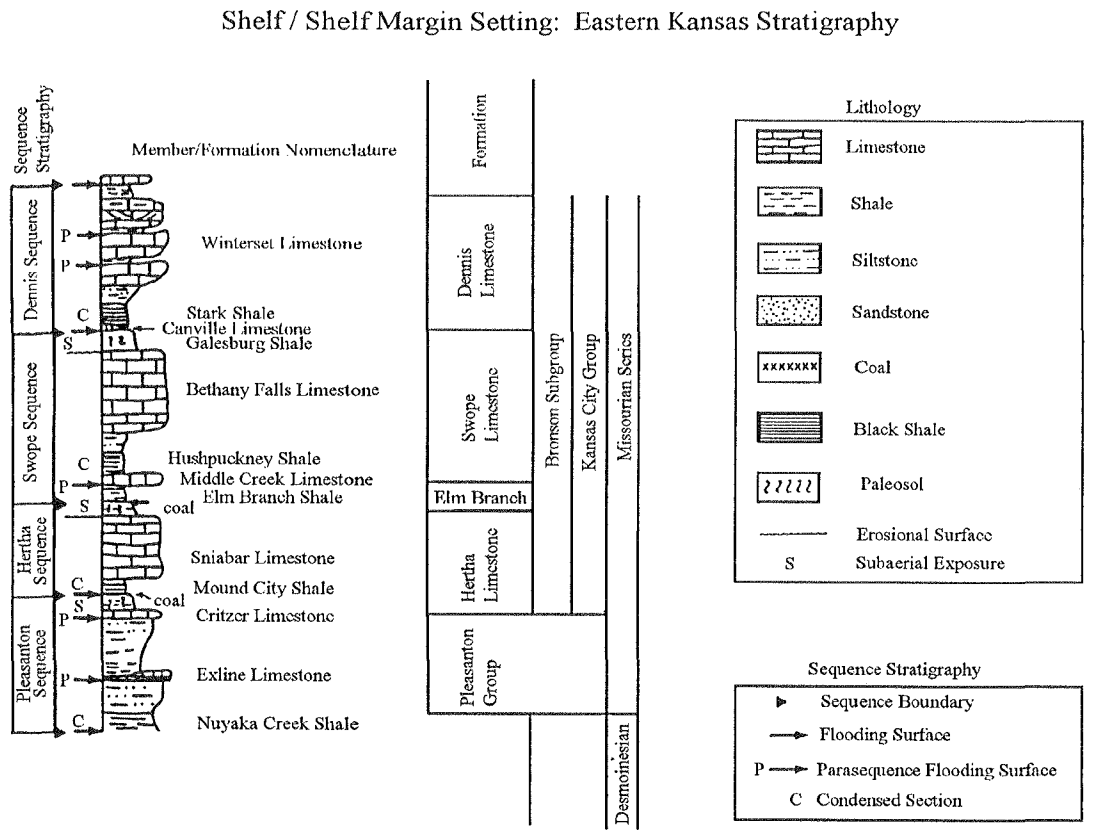


Figure 2.5 Sequence stratigraphy of the Lower Kansas City Group in easten Kansas by Watney et al., 1989.

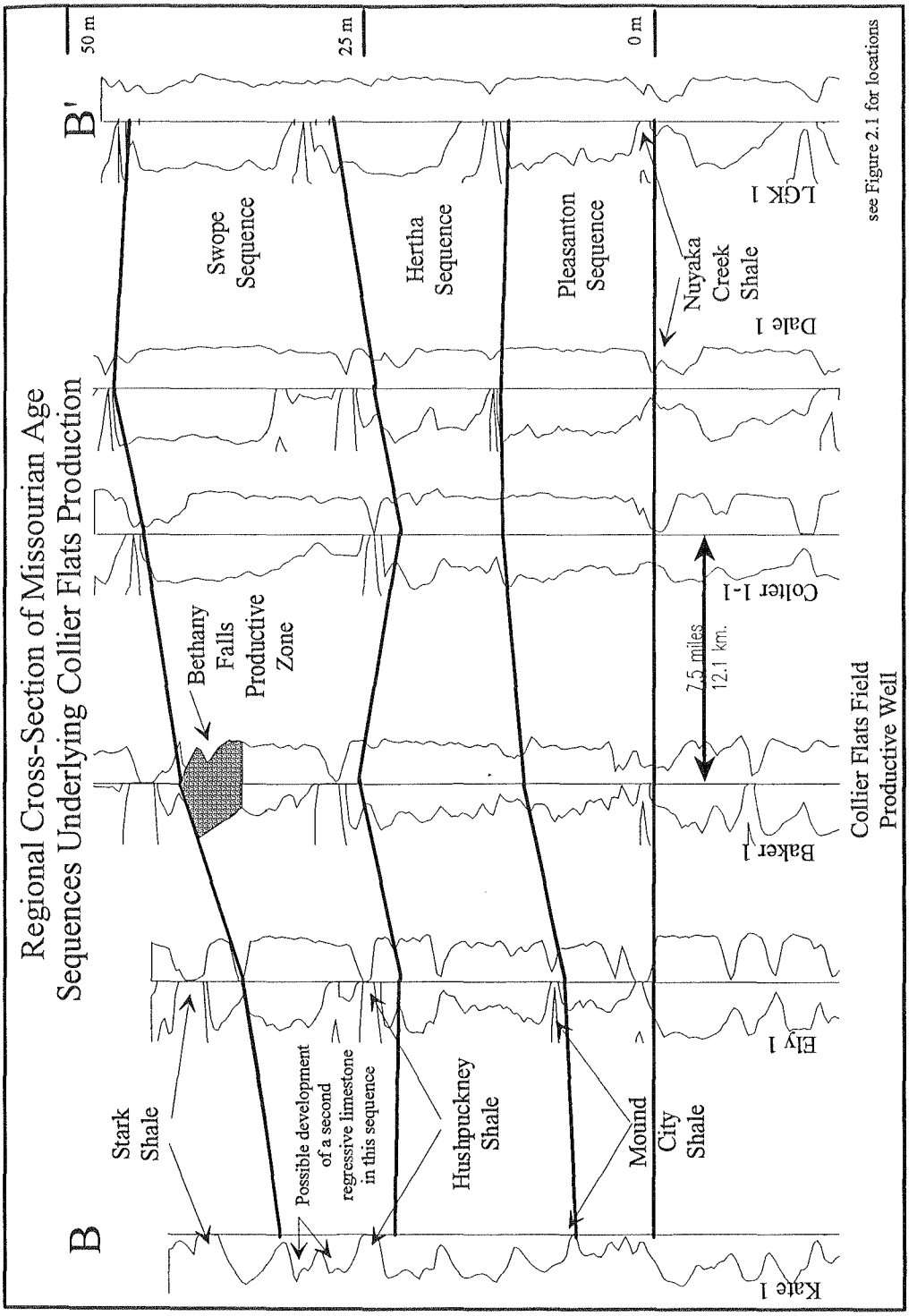


Figure 2.6 Regional cross section of the lower Missourian age sequences underlying Collier Flats production.

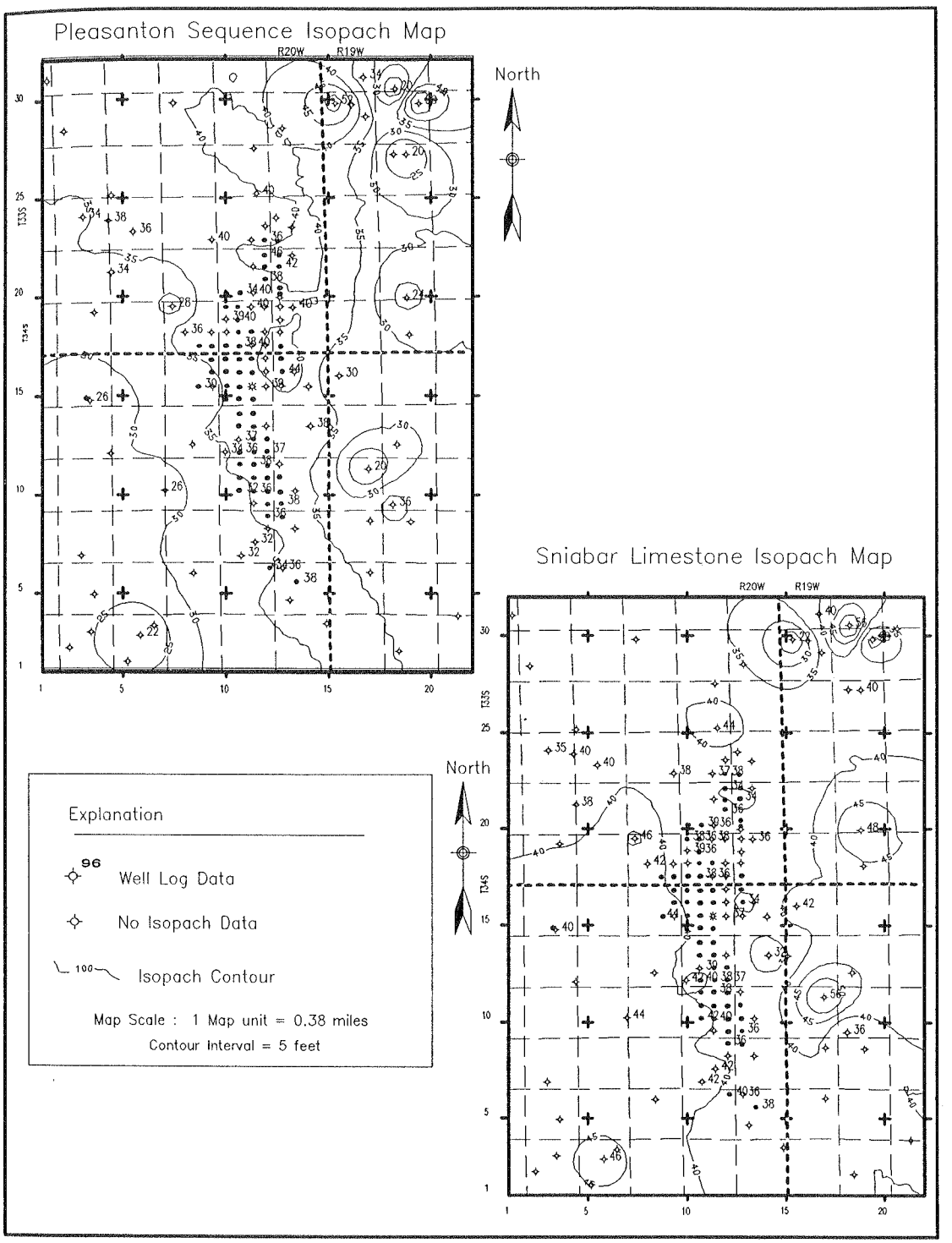


Figure 2.7 Pleasanton sequence and Sniabar limestone isopach maps. Under Collier Flats production, the Pleasanton sequence thickens where the Sniabar limestone thins.

Analysis of regional well-log cross-sections reveal lower gamma ray and neutron well-log responses indicating Pleasanton sequence thickening correlates with a decrease in shale content, suggesting higher carbonate sedimentation rates and possibly a carbonate buildup (Figure 2.6).

The Hertha sequence consists of the Mound City shale, Sniabar limestone and Elm Creek shale members (Figure 2.5). Under Collier flats production, isopach maps of the Sniabar and Elm Creek members indicate thinning over a thick area of the Pleasanton sequence arguing for Hertha sequence thinning over a paleo-topographic high (Figure 2.7 and 2.8). Additionally, Mound City shale's characteristic high gamma ray well-log response does not develop in this area possibly due to localized diminished water-column stratification causing an increase in oxygen and reduction of organics in the shale over this paleotopographic high area (Figure 2.9).

The Swope sequence in eastern Kansas consists of the Middle Creek limestone, Hushpuckney shale, Bethany Falls limestone and Galesburg shale members (Figure 2.5). Bethany Falls limestone isopach mapping displays a north-south area of uniform thickness, between 32 to 38 feet, that correlates with petroleum production. This unit thickens to the northeast and eastern portions of the study area (Figure 2.10). Also, Bethany Falls limestone thins toward the west and southwest. Isopach mapping of low gamma ray response in the Bethany Falls correlates with porosity development and may delineate a north-south oriented marine sand belt morphology (Ball, 1967) (Figure 2.10). The Galesburg shale and Canville limestone display a unique isopach pattern in the study area. Both members pinch-out northeast and east of Collier Flats production (Figures 2.10 and 2.11).

Thinning of the Bethany Falls limestone to the southwest and west and high gamma-ray well-log signatures indicate thinning is due to reduced carbonate sedimentation in deeper water farther down the Swope sequence shelf (Figure 2.6).

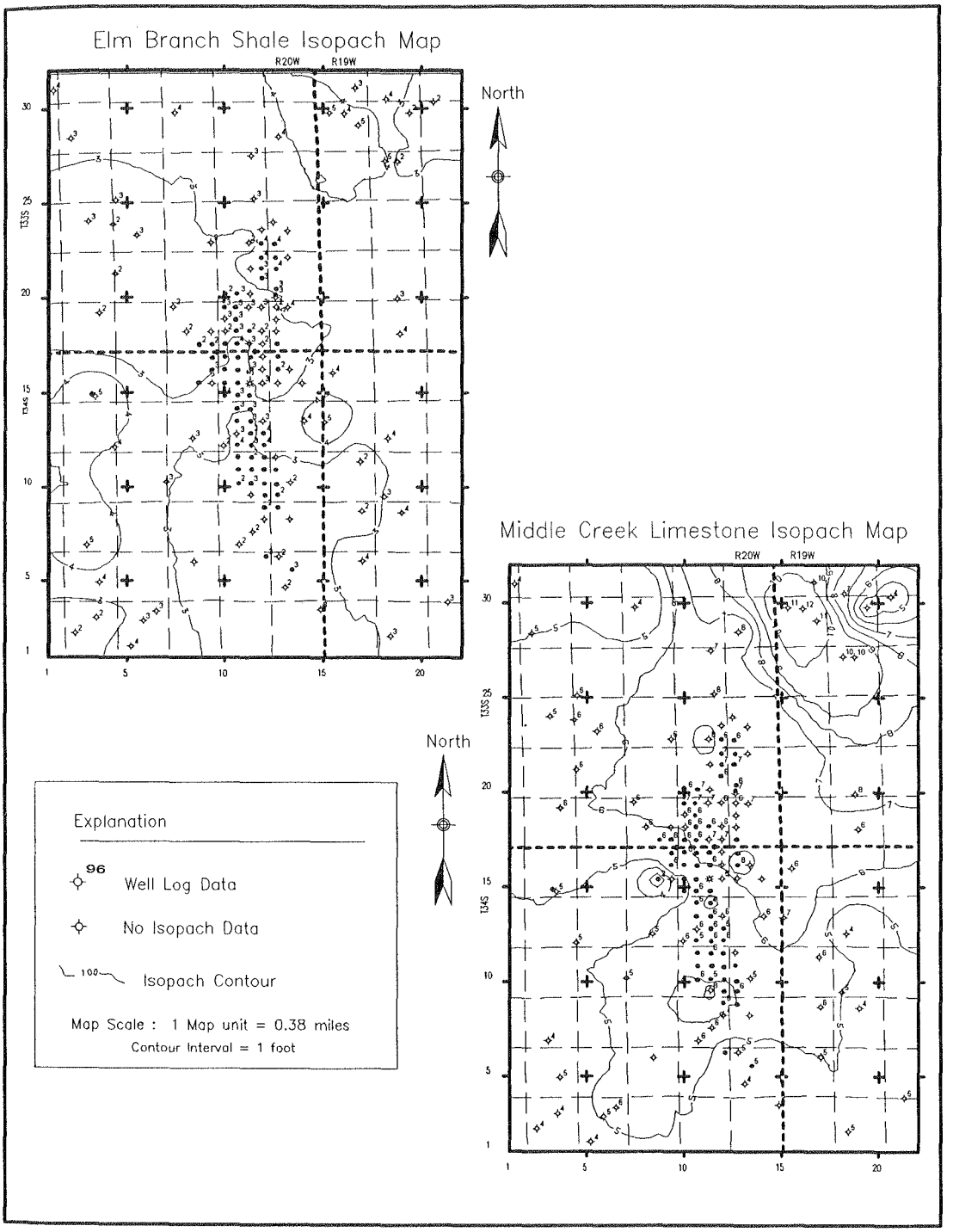


Figure 2.8 Elm Branch shale and Middle Creek limestone isopach maps. The regressive Elm Branch shale thins over the Sniabar limestone and thickens to the east and southwest. The transgressive Middle Creek limestone thins to the southeast, south and southwest.

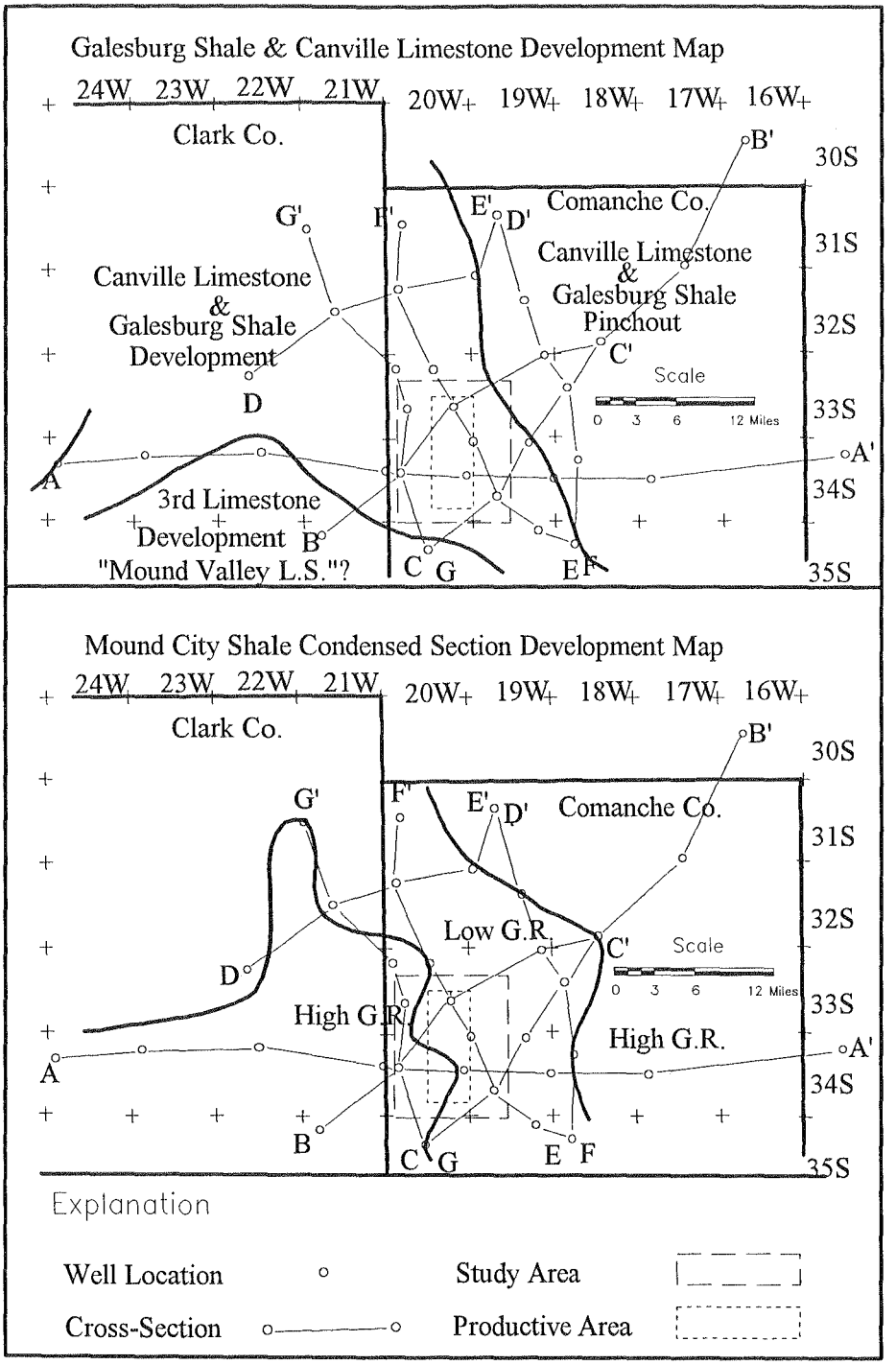


Figure 2.9 Regional maps of the Canville limestone, Galesburg shale and Mound City shale. The Canville limestone and Galesburg shale pinchout to the east higher up on the Swope sequence shelf while a third limestone member of the Swope sequence is present farther down the shelf. The Mound City shale characteristic high gamma-ray signature dissappears under Collier Flats production.

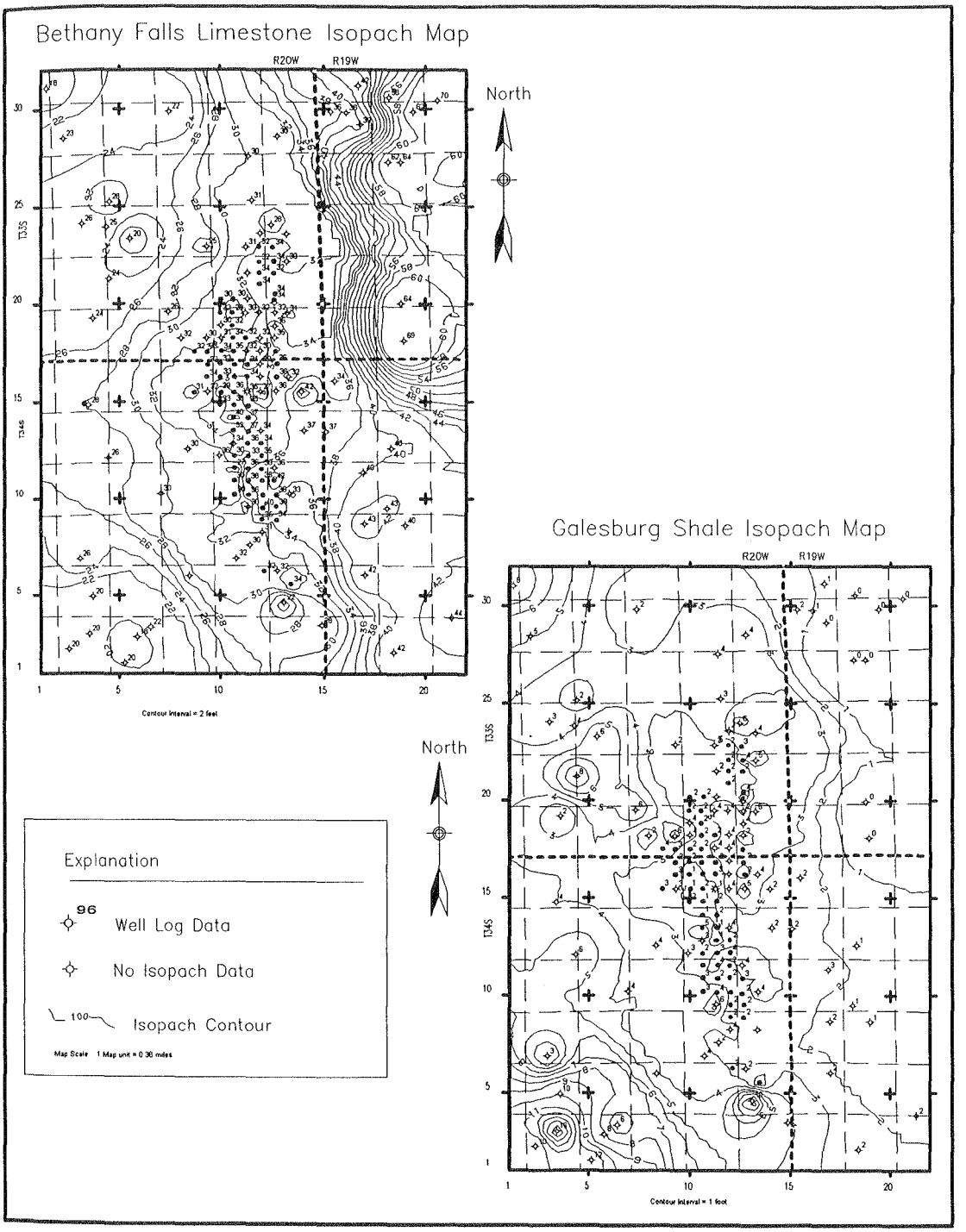


Figure 2.10 Bethany Falls limestone and Galesburg shale isopach maps. The 32 foot contour line is the boundary between productive wells and non-productive wells farther down the Swope sequence shelf. There is significant Bethany Falls thickening to the northeast. The Galesburg shale pinches-out over thick Bethany Falls areas and thickens to the southwest down the Swope sequence shelf.

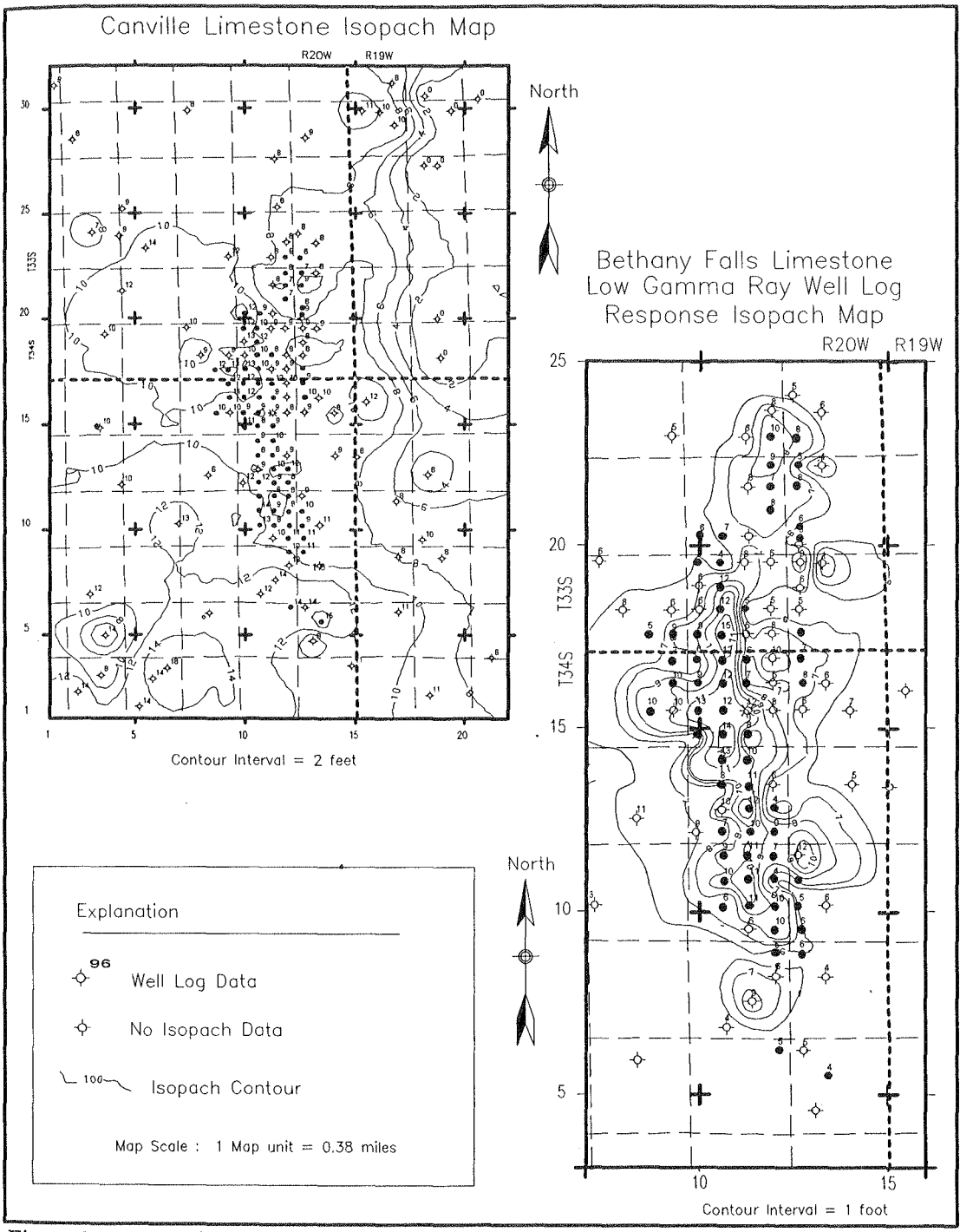


Figure 2.11 Canville limestone and net thickness of low gamma ray facies isopach maps. The Canville limestone mirrors the isopach pattern of the Galesburg shale. The low gamma ray facies isopach map indicates shoal water carbonates and possibly grainstone lithofacies.

Regional cross-section analysis indicates development of a third limestone member of the Swope sequence (Mound Valley limestone) to the southwest farther down the paleoshelf (Figure 2.12). The Mound City limestone in eastern Kansas is interpreted as a parasequence within the Swope sequence that developed in a more basinal setting overlying the Bethany Falls limestone (Figure 2.13).

Thickening of the Bethany Falls limestone occurs to the northeast and east of Collier Flats petroleum production(Figure 2.10). Well log signatures and thickening to the northeast and east indicate this area was in a deeper water setting possibly an embayment on the Swope shelf (Figure 2.12). Carbonate sedimentation rates remained high suggested by a progressive decrease in gamma-ray and neutron porosity well log response culminating in shoal water Bethany Falls limestone deposition (Figure 2.12).

### Paleogeography Conclusions

Swope Sequence isopach maps along with observations from core and well-log signature analysis indicate Collier Flats reservoir facies developed in the regressive Bethany Falls upper limestone which localized on a paleo-topographic high area on the Swope sequence shelf (Figure 2.12). The location of this paleotopographic high area may be related to Pre-Pennsylvanian age structures. Both the Cherokee and Marmaton Groups thicken to the west and southwest along a hinge-line or flexure zone that trends northwest to southeast one section southwest of Collier Flats production. Isopach patterns indicate clastic sedimentation rates of these groups and subsidence in the Anadarko basin to the south and to the west outpaced sedimentation and subsidence along this hinge-line underlying Collier Flats field production. Well log signatures of the Pleasanton, Hertha and Swope carbonate sequences indicate a lithologic transition from shoal water carbonates to shaly carbonates to the west and southwest of this hinge line. Additionally, the study area was subaerially exposed with significant erosion and/or non-deposition of regressive nonmarine shale and the subsequent transgressive Canville limestone member of the Dennis sequence just a few miles to the northeast.

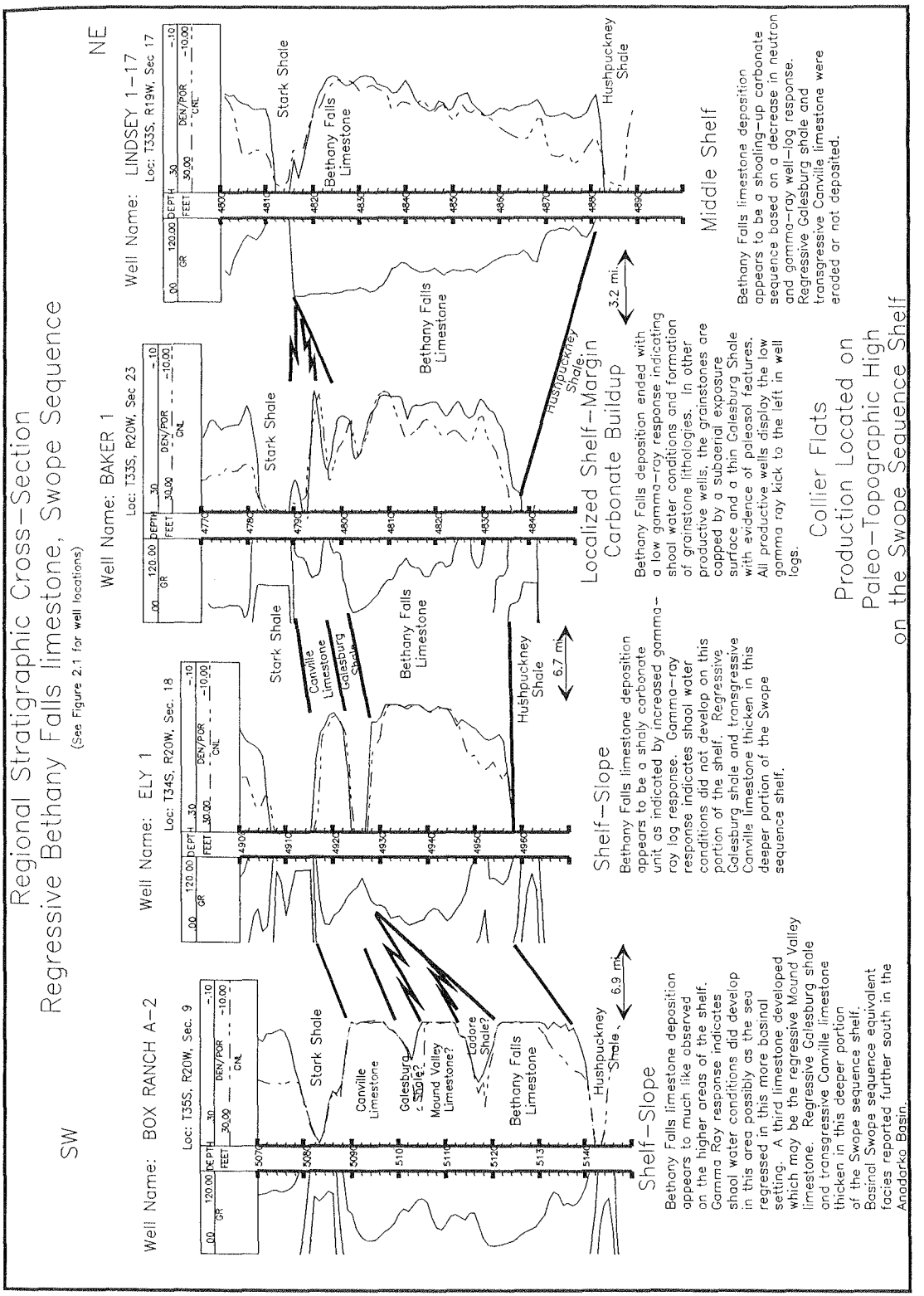


Figure 2.12 Regional cross section of the Bethany Falls limestone indicating inferred location of productive Bethany Falls wells relative to paleoshelf location. Box Ranch A-2 illustrates the potential location of the Mound Valley limestone.

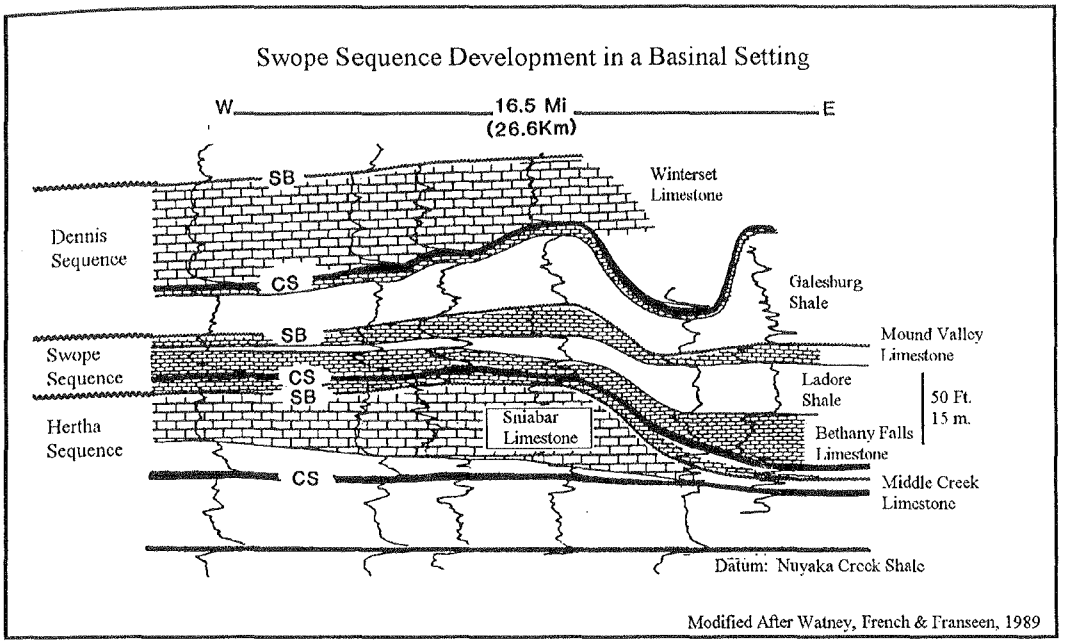


Figure 2.13 Cross section and interpreted sequence boundaries based on outcrop and core descriptions, Neosho County Kansas by Watney et al., 1989. The Mound Valley limestone is a separate unit in the more basinal setting to the east and merges with the Bethany Falls limestone higher up on the shelf to the west.

# Chapter 3

## Bethany Falls Depositional Environments

### Introduction

Interpretations of Bethany Falls limestone depositional environments are based on 13 slabbed cores in the Lemon Ranch leases and 153 wire-line well logs in the study area. Additionally, approximately 110 thin-sections were prepared from the cores which aided in identifying lithologies and biotic constituents. Stratigraphic picks are based on KGS type-logs and verified by comparing cores with well log signatures. Isopach maps were computer generated using TerraSciences well log analysis software and imported into Micrografx Designer software for presentation.

Lithologic descriptions of cores are based on Dunham's (1962) textural classification.

### Cored Intervals

Collier Flats field cores are only present in the Lemon Ranch and Rhoades leases. Core data consist of the upper intervals of the Bethany Falls limestone reservoir zone, the Galesburg shale, and the lower Canville limestone intervals. Detailed core descriptions are presented in Appendix B.

### Bethany Falls Lithofacies

The Bethany Falls limestone is interpreted as the shoaling upward, regressive member of the Swope sequence and consists of the following lithofacies:

- interbedded fossiliferous wackestone and black fissile shale
- fossiliferous wackestone
- peloidal and fossiliferous packstone
- mixed oolitic and bioclastic grainstone
- and oolitic grainstone altered by paleosol formation (Figure 3.2).

Figure 3.3 is a core location map that identifies the cored intervals and core analysis database. The following descriptions of the Bethany Falls limestone are based on this database. Thin-sections and well log data also provide data for depositional environment interpretations. Figures 3.4 and 3.5 present macroscopic observations and significant features observed in the Bethany Falls limestone. The lithologies are described from the base to the top of the unit.

Fossiliferous wackestone interbedded with calcareous fissile black shale is present in most cores approximately 3 to 6 feet below grainstone intervals (Figures 3.2 & 3.6). These wackestones are generally dark gray to brown, mottled, burrowed, crinoidal and brachiopod wackestones. Minor biota observed include mollusks, bryozoans, fusulinids and other foraminifera that decreases in abundance down section. Mottling is generally centimeter to decimeter scale, dark gray to gray, and decrease in abundance upward in the wackestones (Figure 3.7). Contacts between mottled and non-mottled areas are gradational. Mottling is caused by micrite (dark gray) versus microspar (gray) textures. Interbedded brachiopod and crinoidal fissile calcareous shales are generally 1 to 3 centimeters thick and uncommonly grade into stylolites. Spacing between interbedded black shales decreases down section.

There is considerable variability in the fossiliferous wackestone that immediately overlying the interbedded black shale and fossiliferous wackestone. In most cores above the black shale and wackestone interval, the fossiliferous wackestone interval is 1 to 4 feet thick and consists of dark gray to brown, mottled and bioturbated fossiliferous wackestone (Figure 3.8). Mottling is generally centimeter to decimeter scale, dark gray to tan, and decreases in abundance upward in the wackestones. Contacts between mottled and non-mottled areas are gradational.

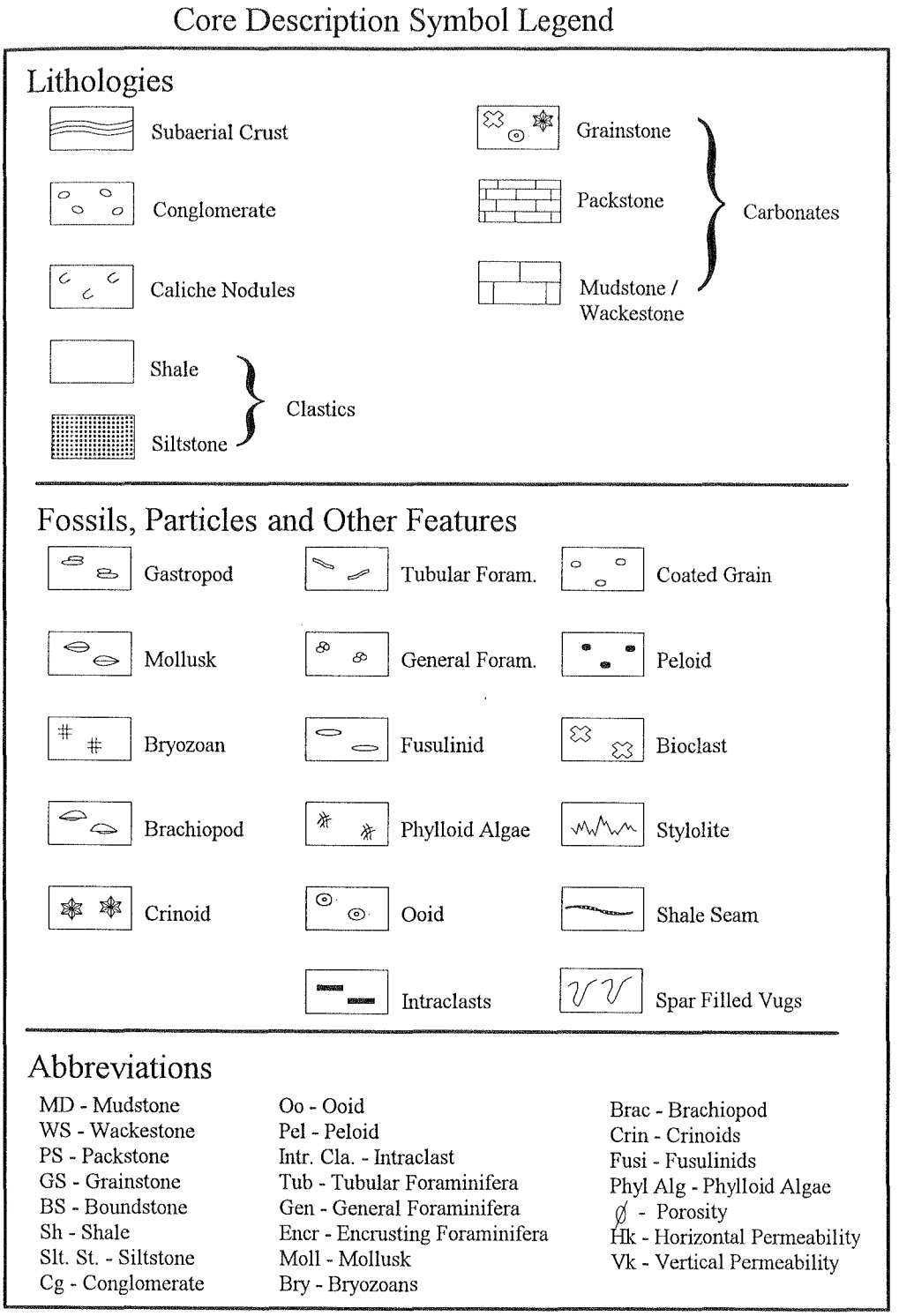


Figure 3.1 Core description symbol and abbreviations legend.

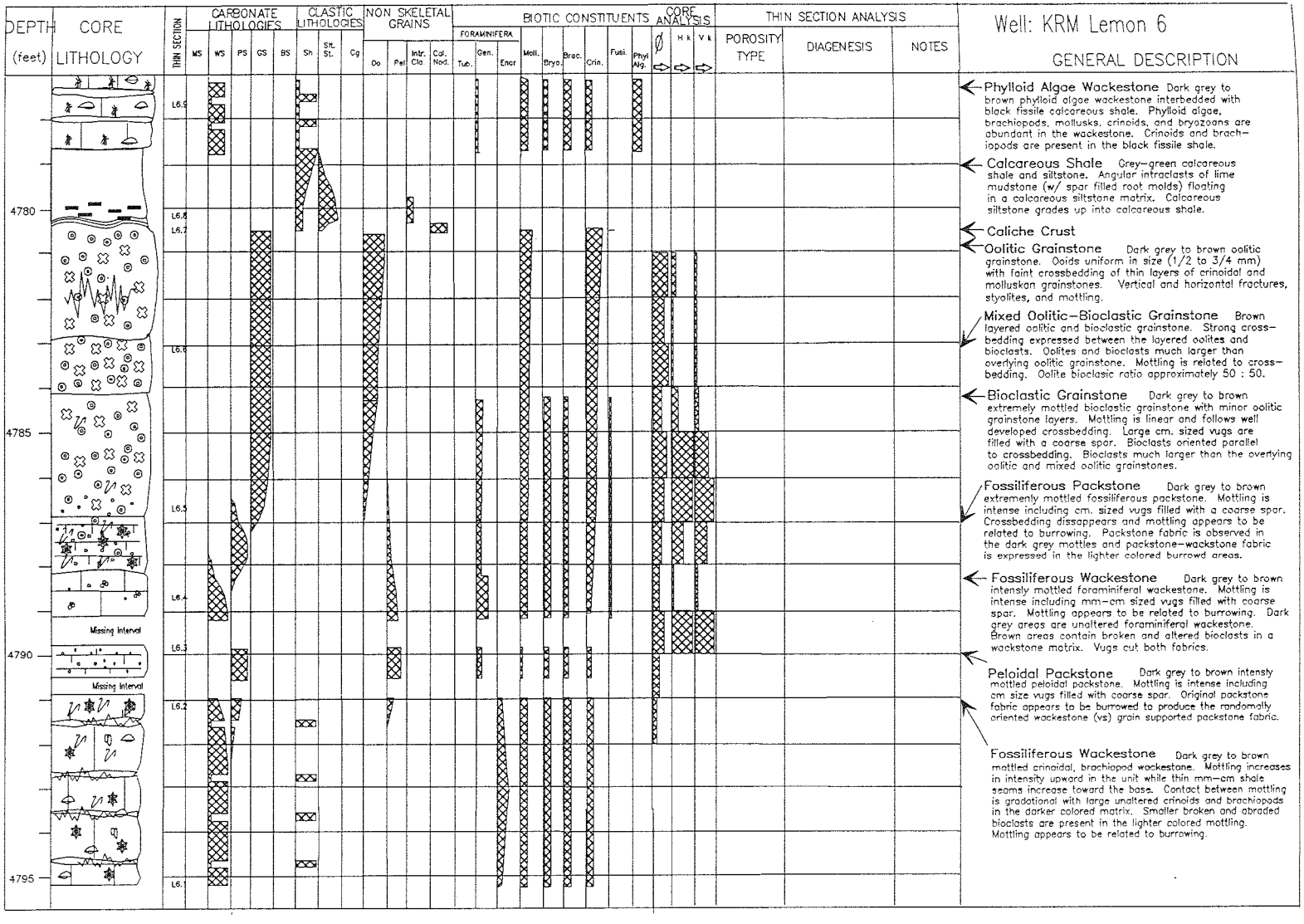


Figure 3.2 Lemon 6 core lithological description. Key to symbols is illustrated in Figure 3.1.

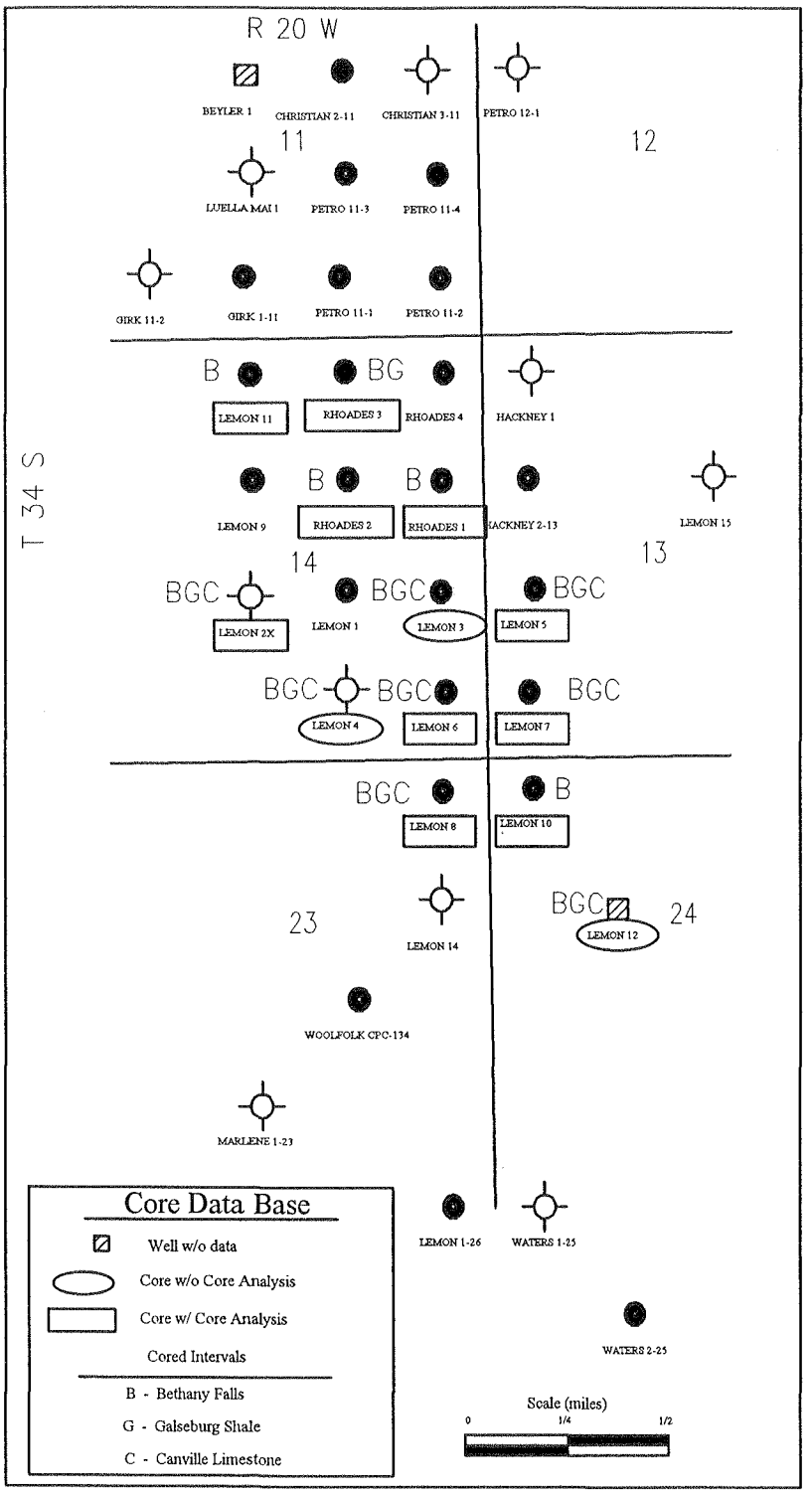


Figure 3.3 Core database and locations (Lemon Ranch leases).

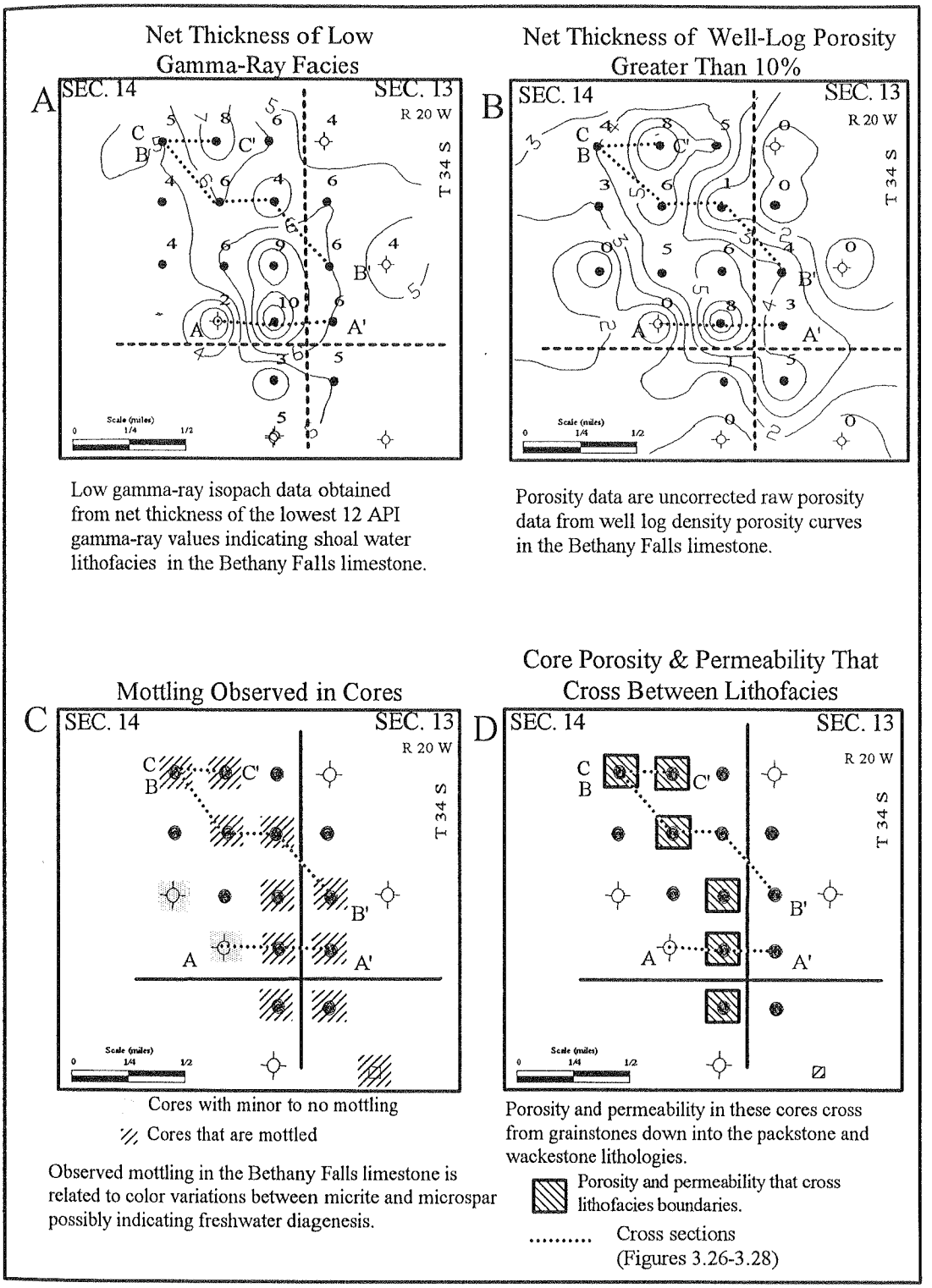


Figure 3.4 Core and wireline well log observations, Bethany Falls limestone
A) Net thickness of Low Gamma Ray facies (thickness of the lowest 12 API units) which indicate grainstone lithofacies. B) Net thickness of well log porosity greater than 10%. C) Cores that are mottled. D) Location of cores with porosity and permeability that cross from the grainstones down into the mud supported lithologies.

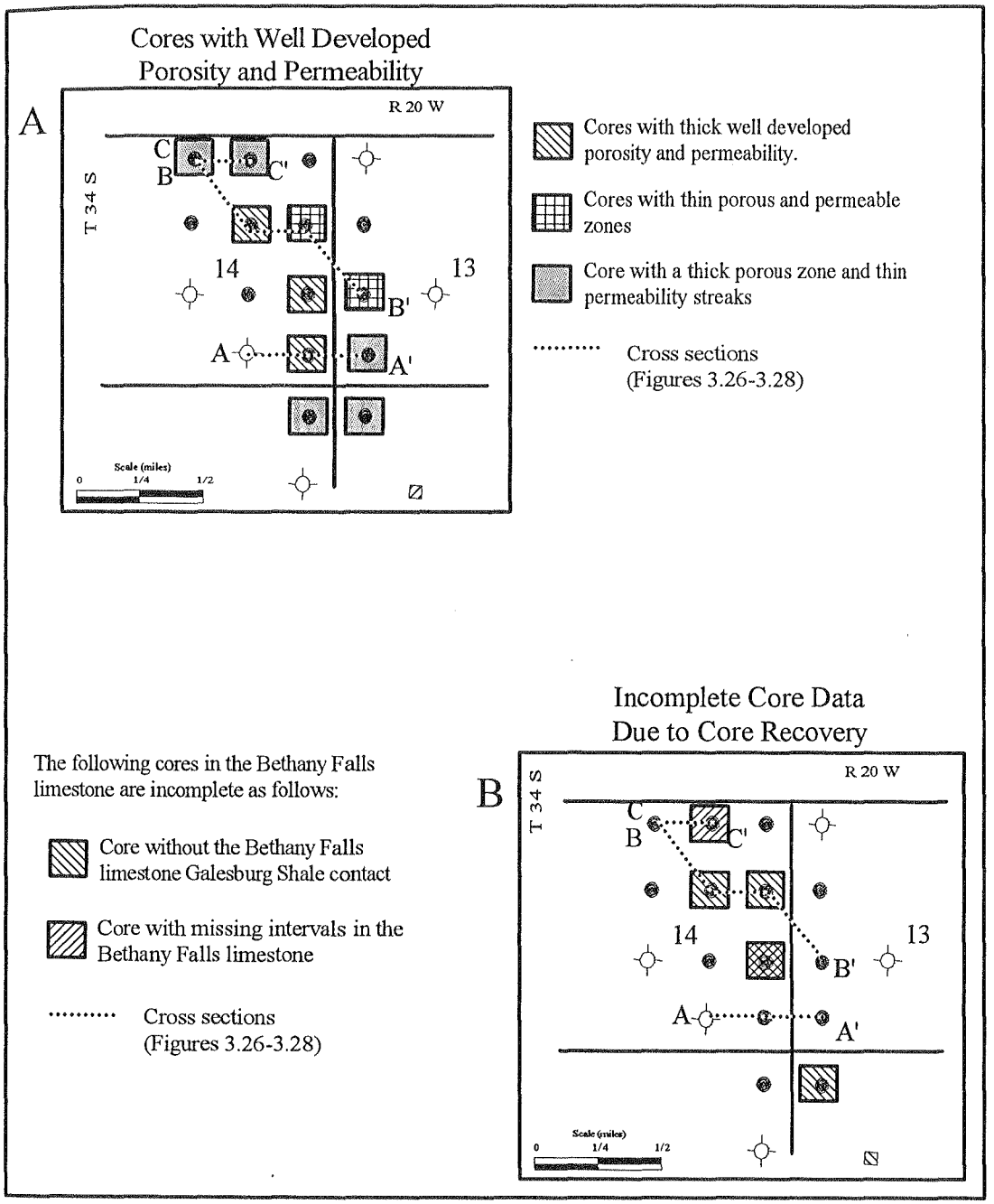


Figure 3.5 Core and wireline well log observations, Bethany Falls limestone.
A) Core with well developed porosity and permeability. B) Incomplete core data.

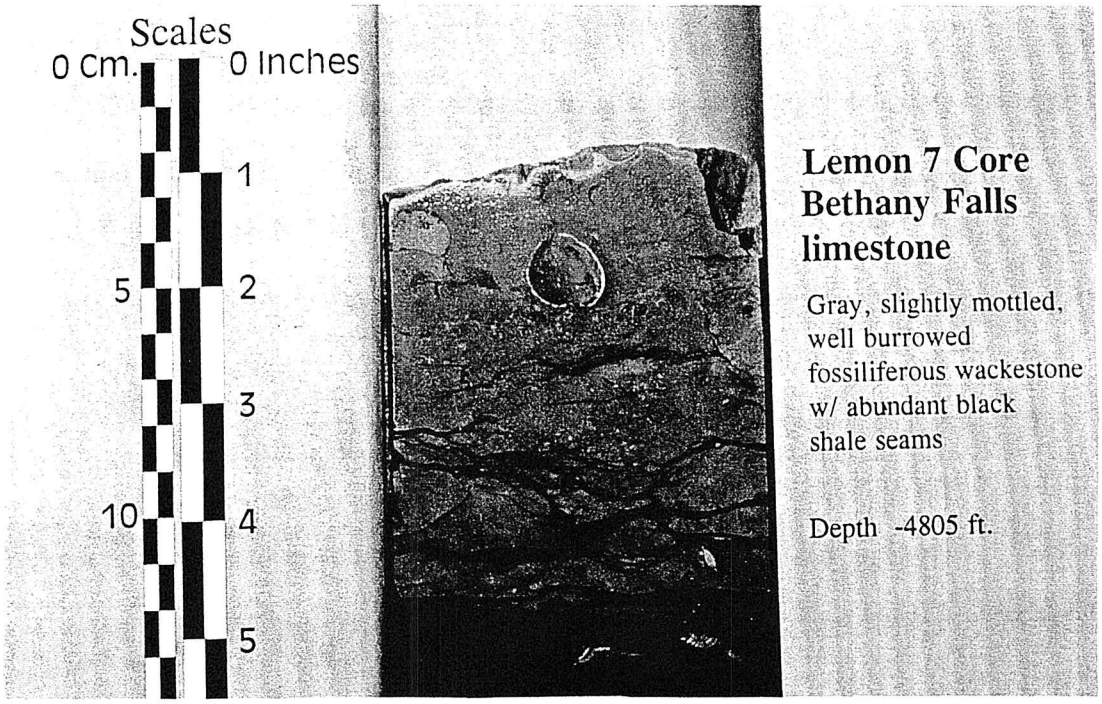


Figure 3.6 Lemon 7 core, fossiliferous wackestone, Bethany Falls limestone.

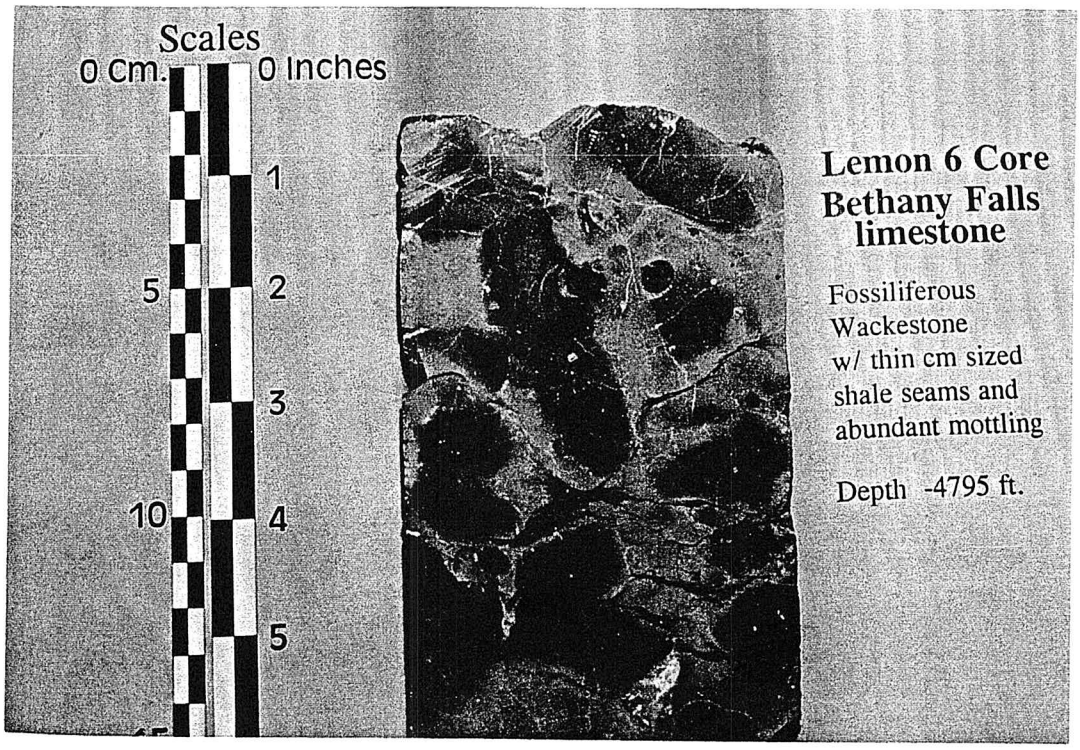


Figure 3.7 Lemon 6 core, fossiliferous wackestone, Bethany Falls limestone.

Color mottling is caused by micrite (dark gray) versus microspar (gray) textures. In the Lemon 2X, Lemon 4, Lemon 7 and Rhoades 1 cores, this interval is 3 to 4 feet thick, brown to tan, bioturbated, non-mottled fossiliferous wackestone (Figures 3.6 & 3.9). Biota in this interval include brachiopods, crinoids, mollusks, bryozoa, ostracods and foraminifera. Wispy millimeter-thick clay seams are present and grade into stylolites in places. Porosity if present is vuggy, moldic and microvugular and correlates with light brown to tan mottling.

Wackestone lithologies grade up into packstones in most cores. This interval is 1 to 3 feet thick, gray to brown, mottled, peloidal and fossiliferous packstone and forms the lowest portion of the Bethany Falls reservoir zone. Mottling is generally more intense and smaller in scale than in the lower fossiliferous wackestone interval. Mottling is not well developed in the Lemon 2X and Lemon 4 cores but is very intense in the cores located in the center of the field (Figures 3.4, 3.10 & 3.11). Biota in this lithology include foraminifera, ostracods, bryozoans and mollusks. Porosity, if present, is vuggy, moldic and microvugular and correlates with light brown to tan mottling. Porosity and permeability is enhanced by vertical fractures.

Mixed oolitic and bioclastic grainstone lithologies are 1 to 6 feet thick and form the lower portion of the reservoir zone. Biota include crinoids, mollusks, brachiopods, brachiopod spines, encrusting bryozoans and foraminifera. Bioclasts become smaller and ooid percentages increase toward the top of this interval. Other features include oolite lithoclasts, extensive micritization of allochems and lithoclasts, cross stratification and extensive mottling. Mottling is dark gray to brown and merges with mottling in the packstone and wackestone lithologies (Figures 3.4, 3.12 and 3.13). Porosity if present is vuggy, moldic and microvugular. Highly porous and permeable cores are fractured.

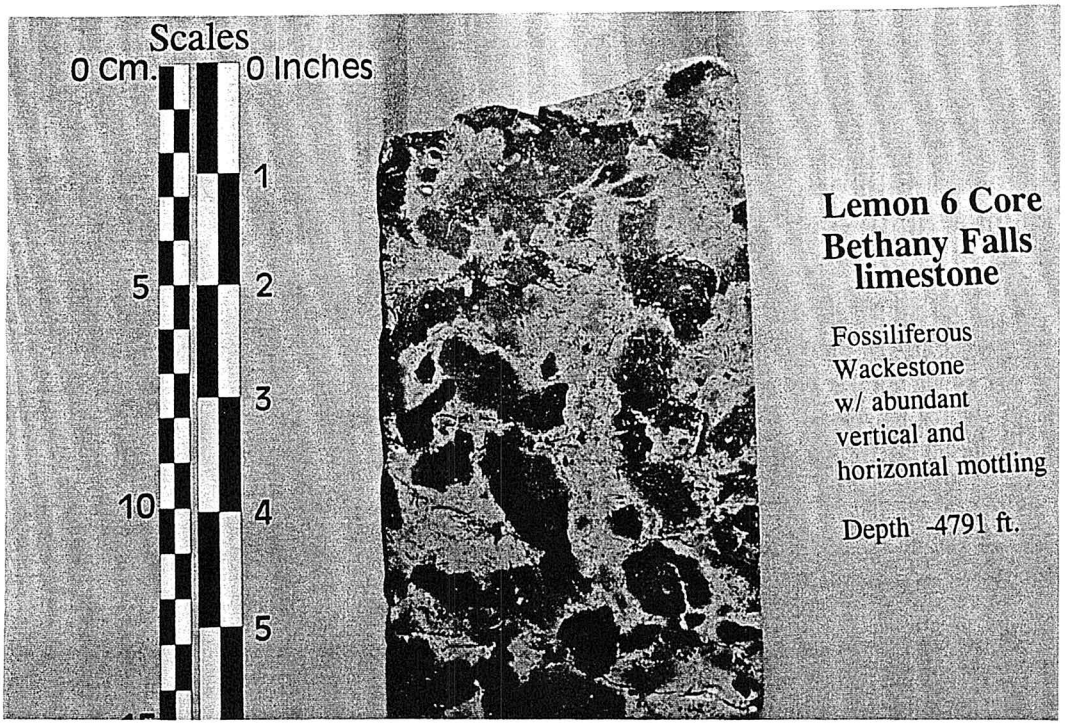


Figure 3.8 Lemon 6 core, fossiliferous wackestone, Bethany Falls limestone.

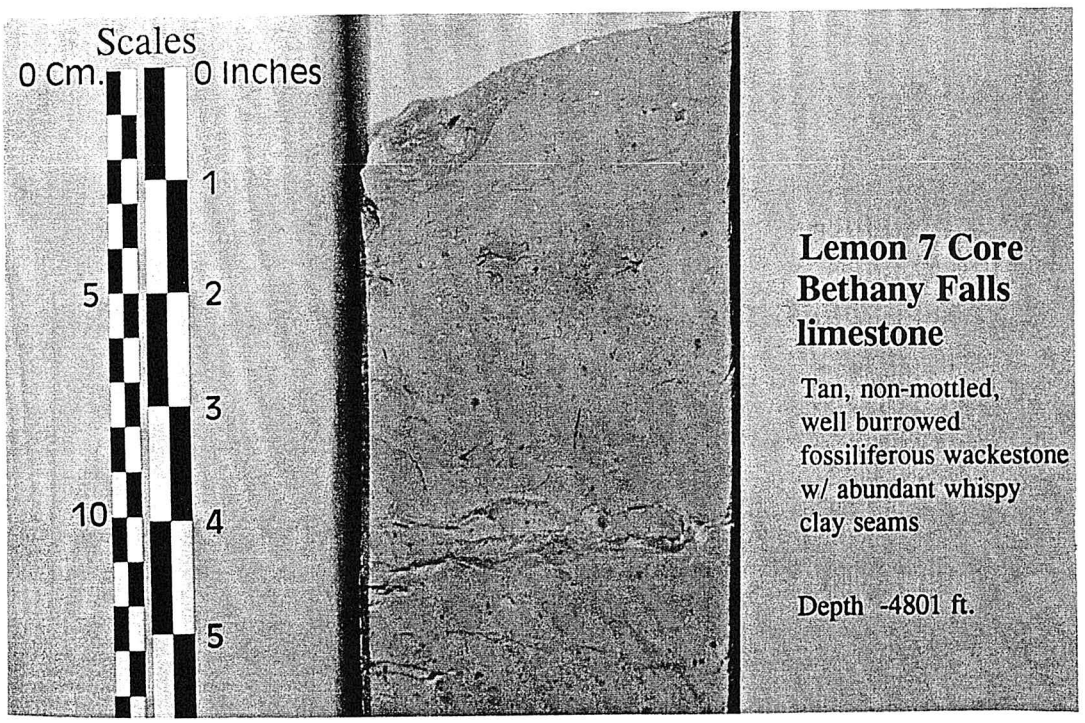


Figure 3.9 Lemon 7 core, fossiliferous wackestone, Bethany Falls limestone.

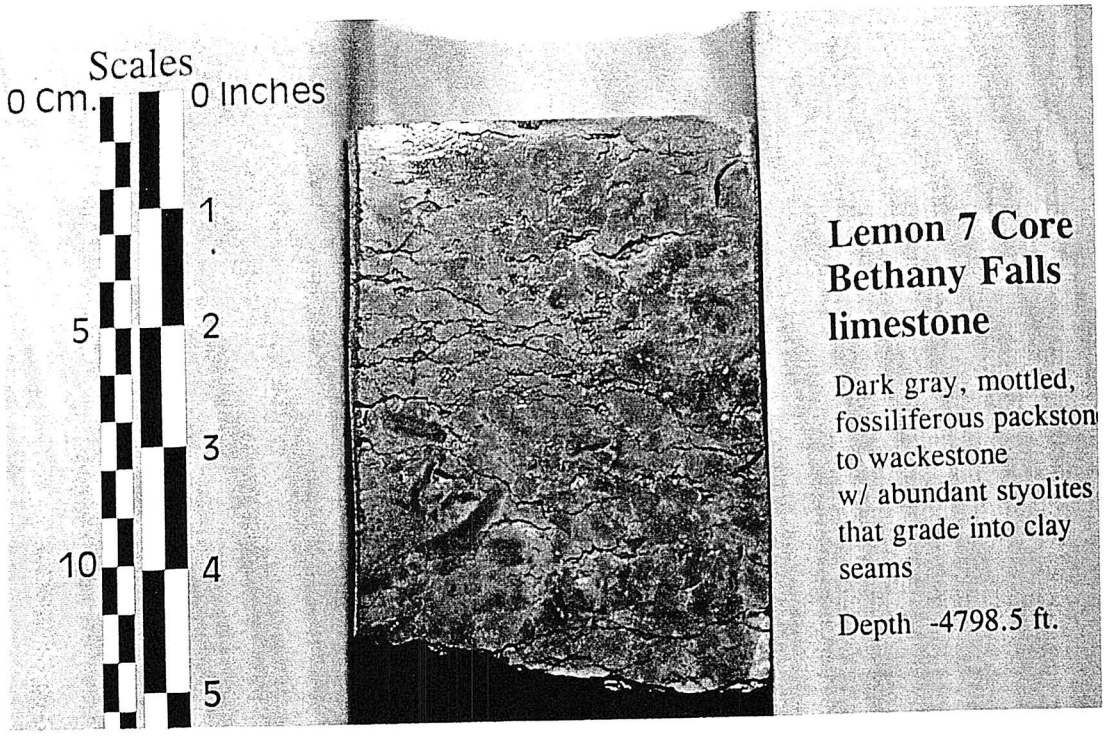


Figure 3.10 Lemon 7 core, fossiliferous packstone, Bethany Falls limestone.

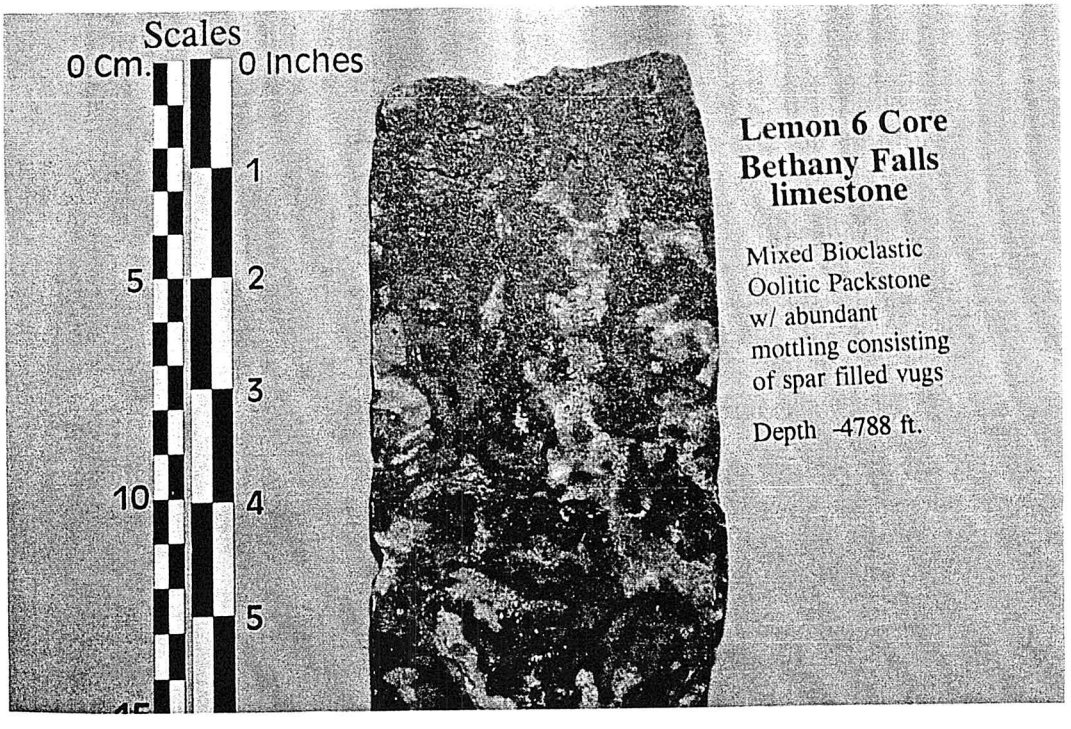


Figure 3.11 Lemon 6 core, mixed bioclastic-oolitic packstone, Bethany Falls limestone.

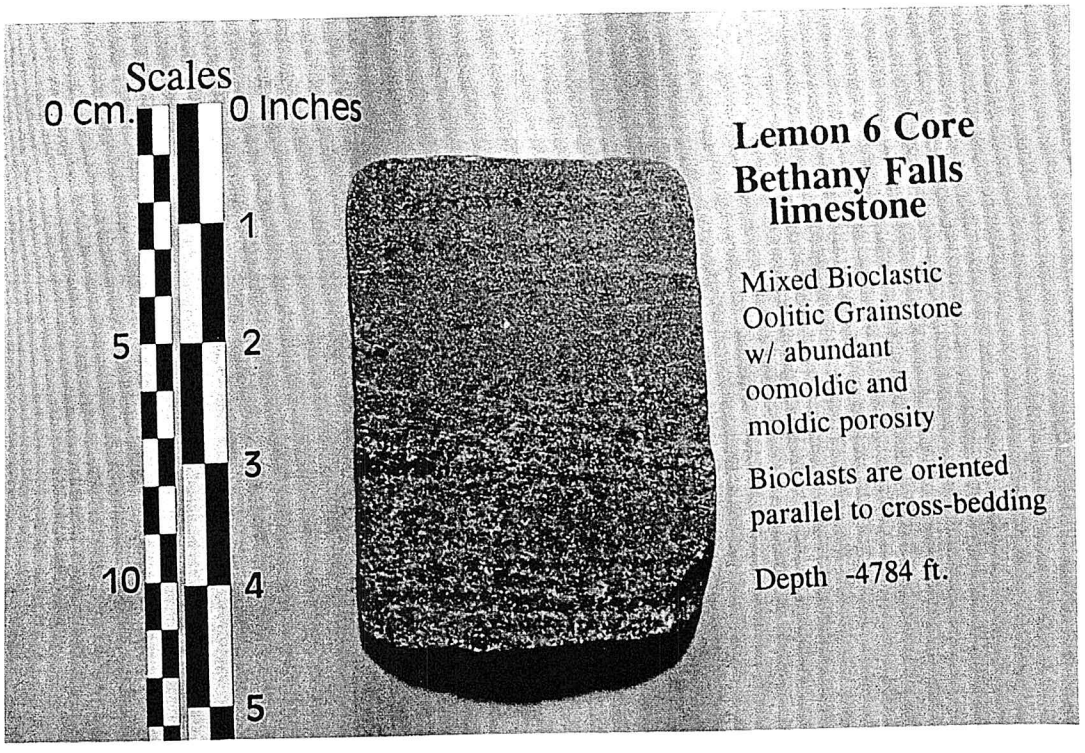


Figure 3.12 Lemon 6 core, mixed bioclastic-oolitic grainstone, Bethany Falls limestone.

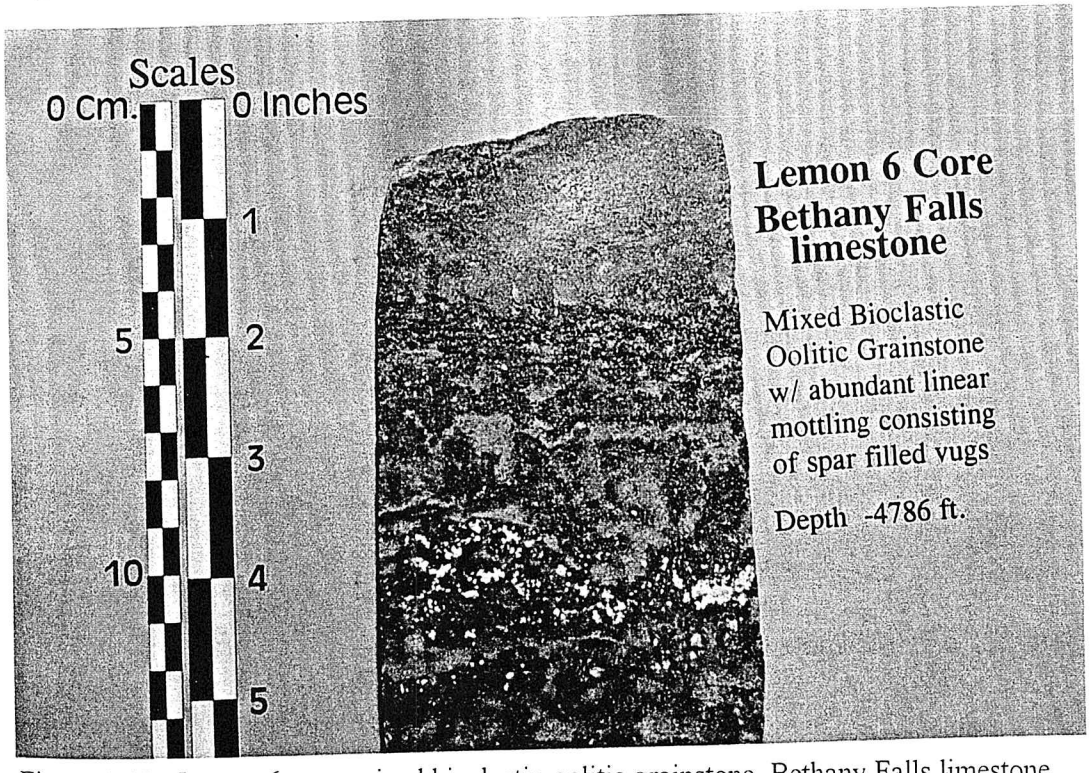


Figure 3.13 Lemon 6 core, mixed bioclastic-oolitic grainstone, Bethany Falls limestone.

Mixed oolitic and bioclastic grainstone grades up into well cemented mottled to non-mottled oolitic grainstone that are 1 to 3 feet thick (Figures 3.14, 3.15). Biota include crinoids, mollusks, foraminifera and brachiopods. The upper few inches to one foot of this interval typically contains rhizoliths and an over-compacted fabric possibly related to soil formation processes. Ooids and bioclasts generally are smaller in diameter than in the underlying grainstone lithologies. Porosity is predominantly oomoldic and moldic. Permeability generally is poorly developed due to calcite cementation, oomoldic porosity, lack of vuggy porosity and only minor fracturing.

The upper interval of the Bethany Falls limestone is a 1 to 3 cm thick paleosol. Several paleosol features are observed in thin section and include rhizoliths, circumgranular cracking and a caliche crust. These features are observed in the Lemon 6 and Lemon 7 cores (Figures 3.14, 3.16).

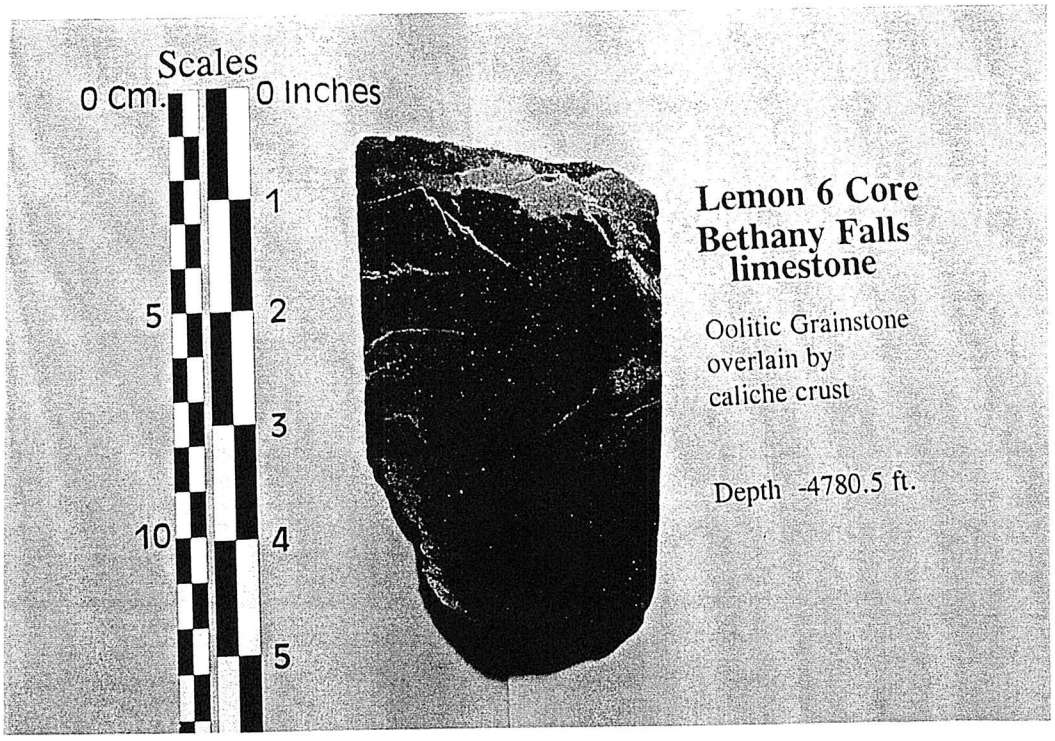


Figure 3.14 Lemon 6 core, oolitic grainstone, Bethany Falls limestone.

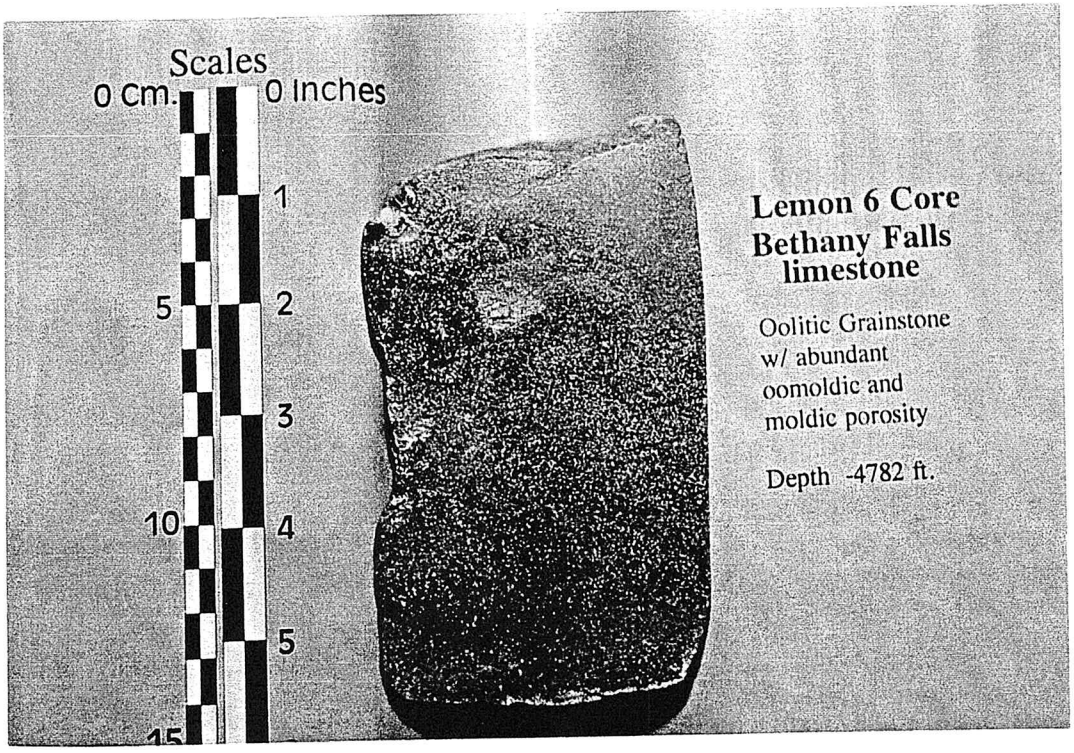


Figure 3.15 Lemon 6 core, oolitic grainstone, Bethany Falls limestone.

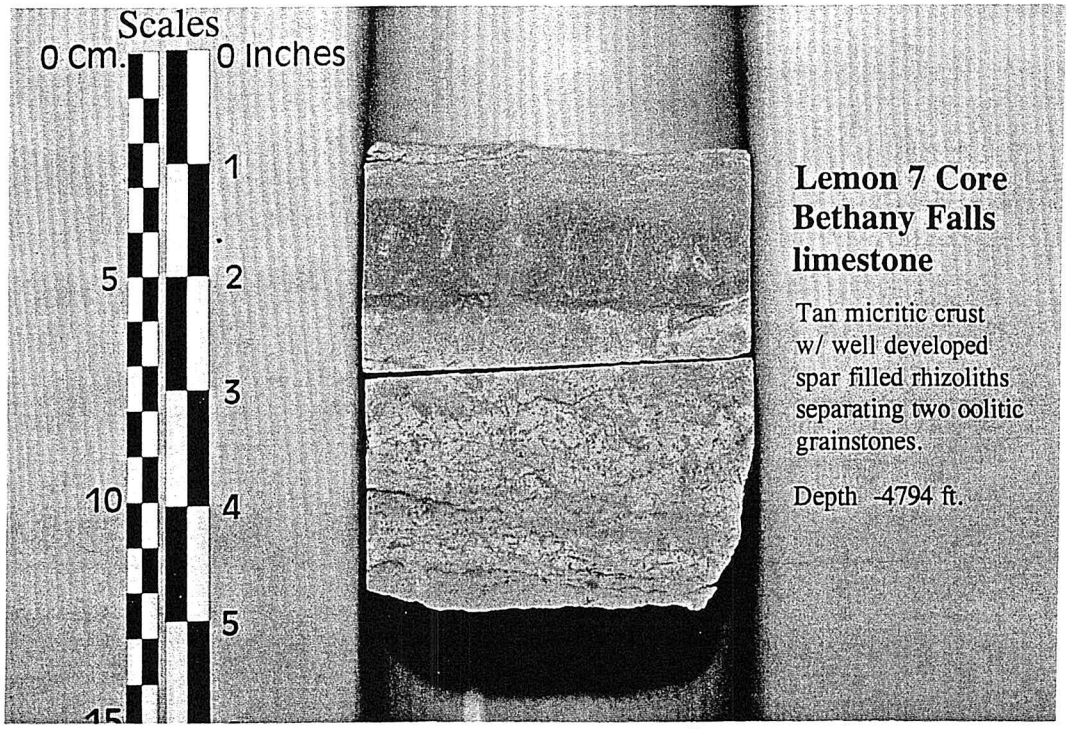


Figure 3.16 Lemon 7 core, calcrete crust, Bethany Falls limestone.

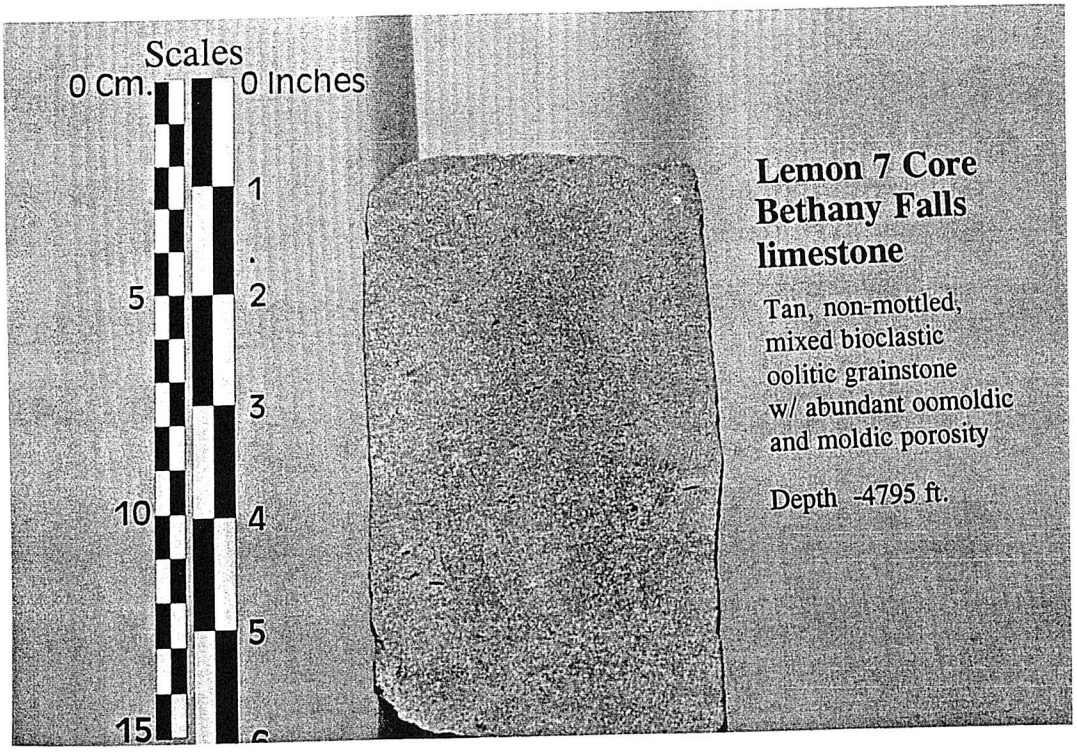


Figure 3.17 Lemon 7 core, oolitic grainstone, Bethany Falls limestone.

## Galesburg Shale Interval Lithofacies

The Galesburg shale is interpreted as a lithologic component of the regressive Swope sequence and consists of the following lithofacies from the base to the top:

- fissile, green/gray mottled, calcareous shale w/ evidence of paleosol development
- gray blocky shale
- fissile gray shale w/ carbonized plant material.

The Galesburg shale is generally 1 to 2 feet thick in most cores except for the Lemon 4 core where it is 5.5 feet thick and displays all the lithofacies described above. In all other cores, the Galesburg shale consists of only fissile green/gray calcareous shale and gray blocky shale (Appendix B).

The lower green/gray calcareous shale is present in all the cores that recovered the Galesburg shale (Figure 3.3) and is 1 to 2 feet thick. This interval contains no fossils except for those in the reworked oolite lithoclasts from the Bethany Falls limestone. The most significant feature of this interval is evidence of paleosol development. Gray micritic lithoclasts are observed 3 feet above the Bethany Falls limestone / Galesburg shale contact. These lithoclasts appear to be the result of autobrecciation in a green laminated shale. Rhizoliths are also observed in the lithoclasts (Figures 3.18, 3.19, 3.20 and 3.21).

Overlying the calcareous shale is a nondescript gray blocky shale 1 to 2 feet thick. This lithofacies is present in all cores that recovered the complete Galesburg shale interval.

The uppermost Galesburg shale lithofacies observed in core is a one foot thick fissile gray shale with plant debris. This unit is only observed in the Lemon 4 core and grades up section into black calcareous brachiopod shale of the Canville limestone (Figure 3.20).

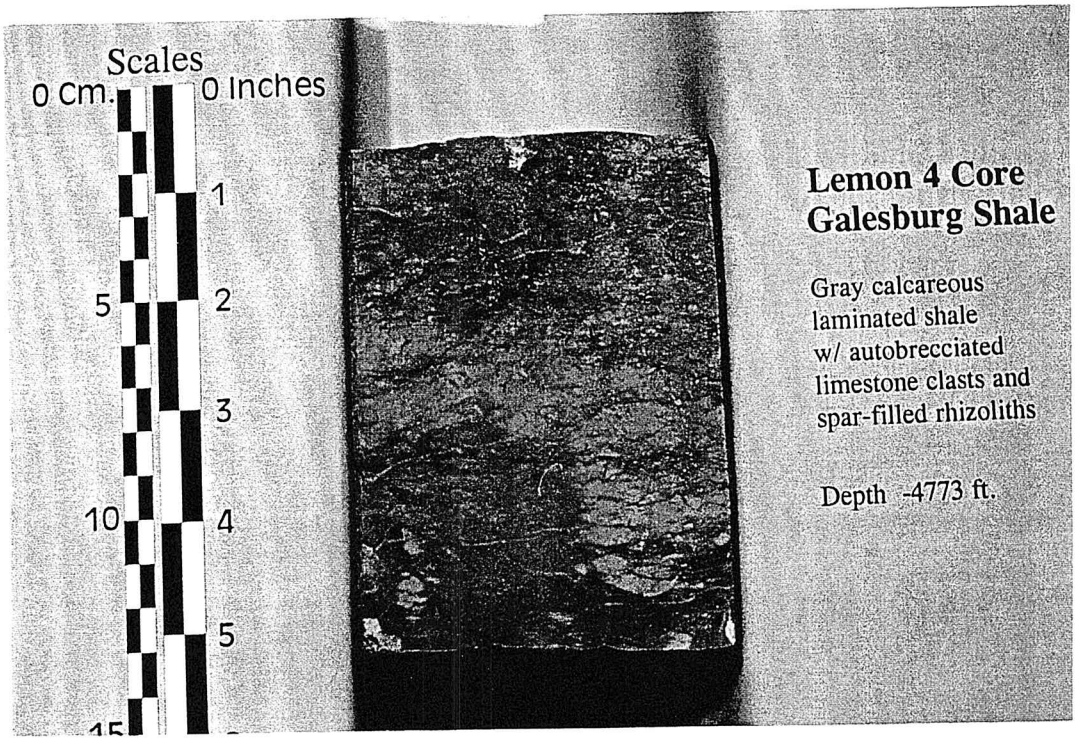


Figure 3.18 Lemon 4 core, Galesburg shale.

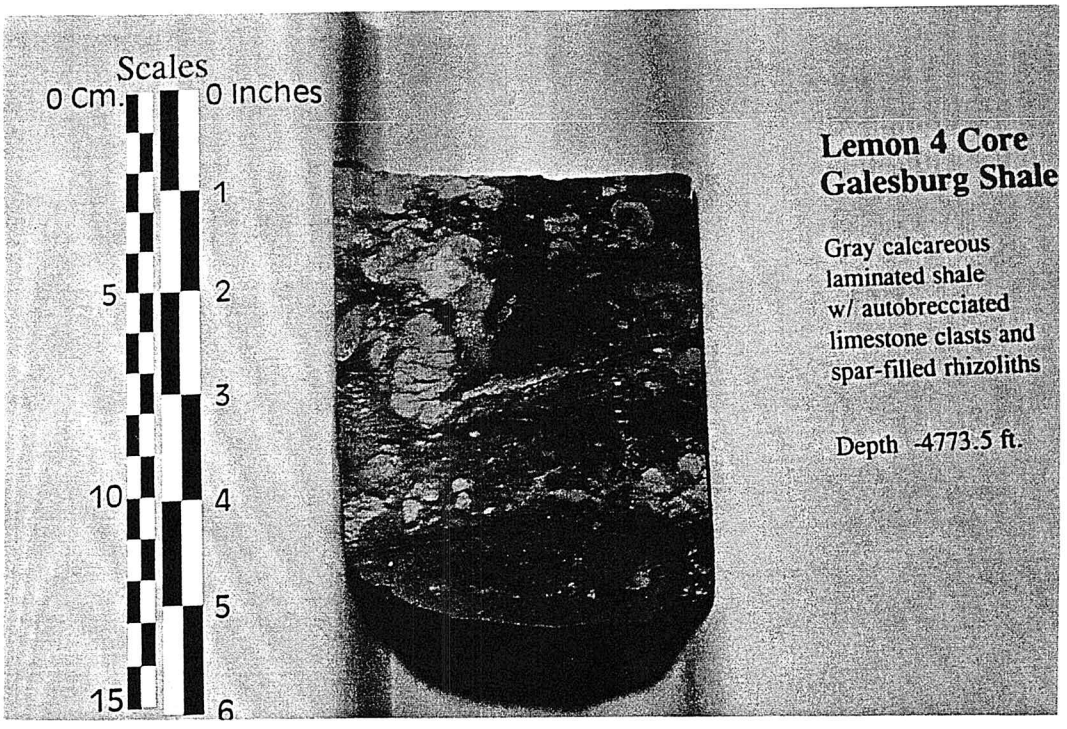


Figure 3.19 Lemon 4 core, Galesburg shale.

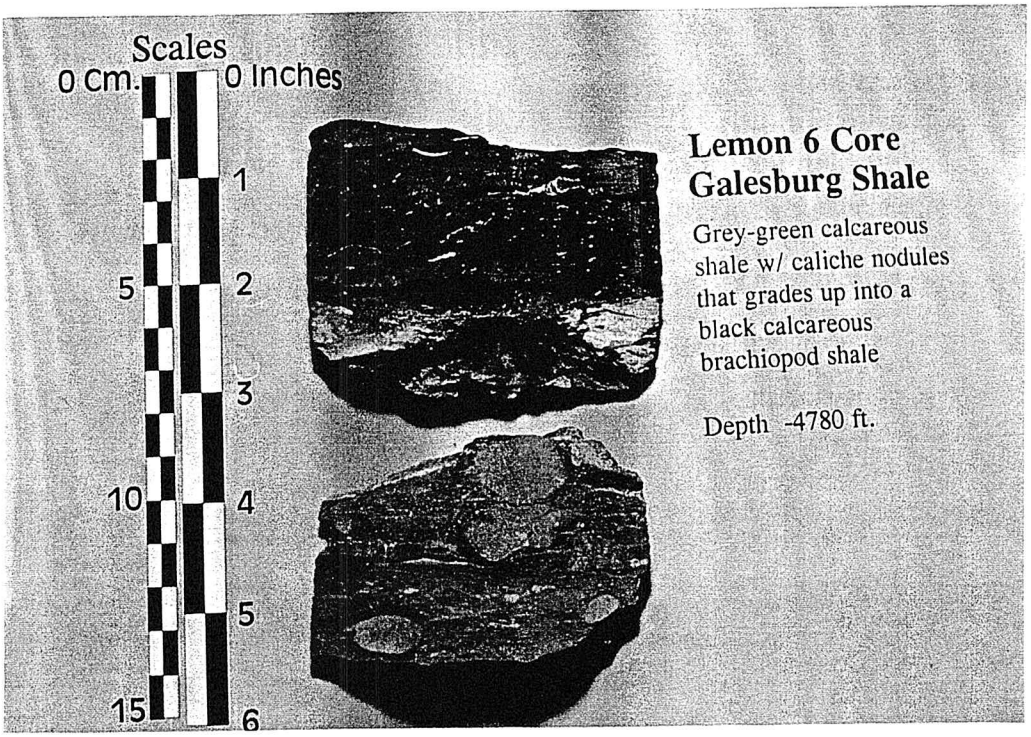


Figure 3.20 Lemon 6 core, Galesburg shale.

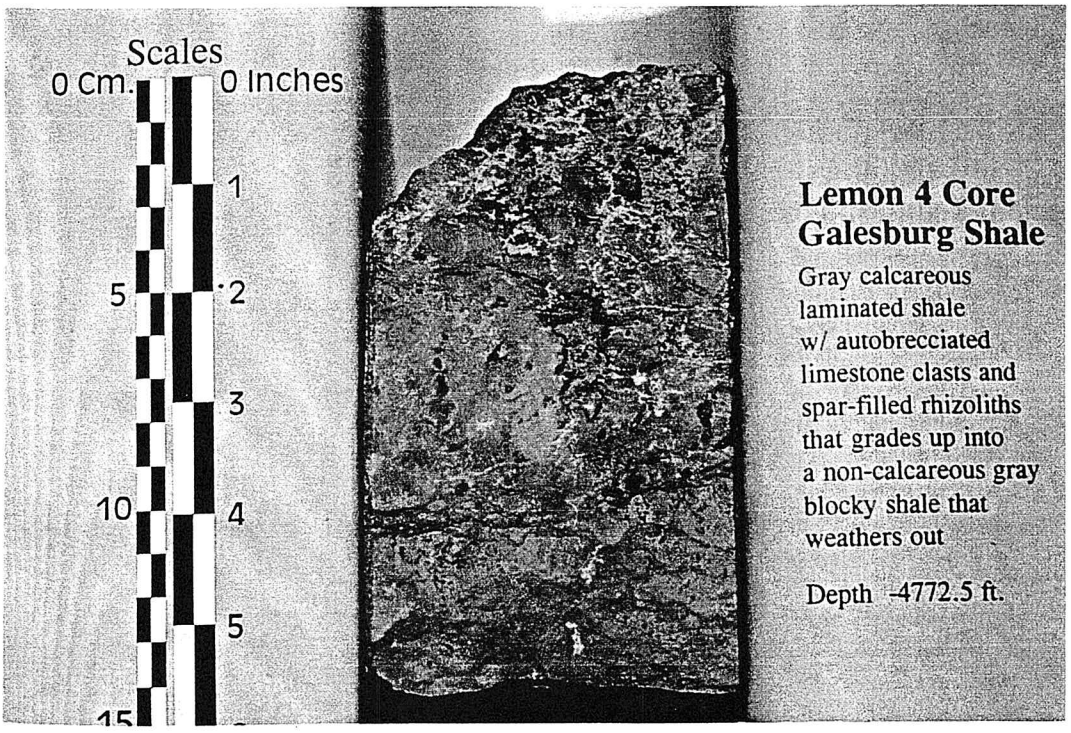


Figure 3.21 Lemon 4 core, Galesburg shale.

## Canville Limestone

The Canville limestone is interpreted as a transgressive component of the Dennis Sequence and consists of interbedded calcareous black fissile shale and dark gray phylloid algal wackestone. Unfortunately, none of the cores recovered the entire Canville limestone because the operators only cored the productive interval.

The wackestone facies of the Canville limestone can be characterized as a dark gray, argillaceous, dense, phylloid algal, brachiopod wackestone. Minor biota include bryozoans, mollusks, crinoids, ostracods and foraminifera. Porosity is generally absent except for minor open fractures.

Black calcareous fissile shale occurs in one foot intervals and increases in frequency up-section. This lithology contains only brachiopods and crinoids oriented parallel to laminations.

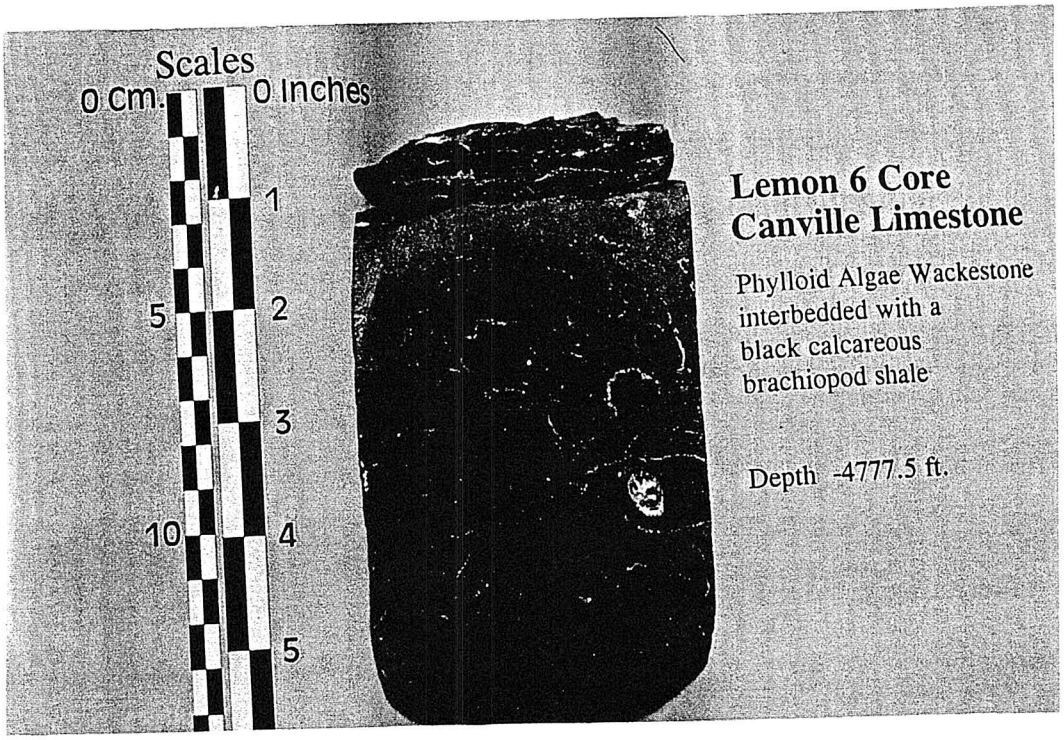


Figure 3.22 Lemon 6 core, Canville limestone.

## Bethany Falls Depositional Environment Interpretation

### "Kansas Type" Cyclothem Member

It has been demonstrated that the Bethany Falls limestone member of the Swope sequence was deposited on a topographic high area on a broad carbonate shelf (Figure 2.12). Further, regional mapping demonstrates that the underlying Mound City core shale's high gamma ray response did not develop under the Collier Flats field (Figure 2.9). This suggests that this area of the Swope sequence shelf may have been topographically higher than the adjacent areas to the west and east. Additionally, the Collier Flats field may have developed on a flexure zone between the Anadarko Basin and the Swope sequence shelf causing differential subsidence.

To classify the Bethany Falls limestone as a regressive upper limestone member of a cyclothem, one would expect to see:

- lithofacies that indicate a general marine shallowing-upward succession,
- evidence of subaerial exposure at the top of the unit,
- and an underlying shale possibly of deep marine origin and an overlying non-marine shale.

As the Swope sequence sea started to regress, open marine interbedded wackestone and black shale was deposited on the shelf. Interbedded wackestone and fossiliferous black shale indicate open marine deposition in which carbonate mud and organic rich shale accumulated below storm wave-base. This environment also allowed typical Pennsylvanian deep-water marine invertebrates to survive (crinoids, bryozoans, brachiopods and mollusks). Interbedded black shales are organic, calcareous, and contain brachiopods and crinoids that were deposited during periods when the carbonate mud production was likely constrained by variations in water depth, increases in detrital sedimentation rates and/or decreases in oxygen content due to different water circulation patterns on the shelf.

Carbonate sedimentation rates were likely low because carbonate mud and fossiliferous black shale assemblage indicate carbonate sedimentation conditions were intermittent.

As sea-level continued to fall, carbonate sedimentation conditions prevailed and 4 to 6 feet of fossiliferous wackestone and packstone were deposited. These lithologies indicate open marine carbonate sedimentation continued uninterrupted at/or below storm wave-base. Fossil abundance and burrowing increased, suggesting relative sea-level fall created the conditions where marine invertebrates could thrive.

Sea-level continued to fall and mixed bioclastic-oolite grainstone lithologies were deposited, overlain by shoal-water oolitic grainstones. Ooid lithoclasts in the lower portions of the grainstone intervals indicate early marine cementation may have stabilized the grainstone shoals. Bioclast size decreases up-section with a gradual increase in ooid abundance culminating in oolite deposition. Bethany Falls limestone deposition ended with a subaerial exposure event that created a paleosol on top of the Bethany Falls limestone.

Overall the Bethany Falls lithofacies assemblage is characteristic of a shallowing-upward marine carbonate succession. Additionally, core data clearly show a non-marine shale lithology overlying it and well logs indicate a core shale underlies the Bethany Falls strata.

## Reservoir Lithofacies

Identification of Bethany Falls limestone productive reservoir lithofacies is based on core descriptions and core analysis performed by Core Laboratories, 1981. Nonporous and nonpermeable wells, Lemon 2x and 4, have cores that lack Bethany Falls grainstone lithofacies. High porosity and permeability (>15% porosity and > 20 md) is generally restricted to grainstone lithologies of the Bethany Falls limestone on the eastern and western margins of the Collier Flats field, (Lemon 5, 7, 11, and 10 cores) (Figure 3.4d). High porosity and permeability zones in the center and thickest intervals of the grainstone lithofacies of the Lemon Ranch and Rhoades leases can pass down into the underlying packstone/wackestone lithofacies (Lemon 6, Rhoades 2 and Rhoades 3 cores) (Figure 3.4d). Based on these observations, Bethany Falls limestone highly porous and permeable lithofacies consist of: (1) grainstone lithofacies along the margins of the field, and (2) grainstone, packstone and wackestone lithofacies in the center portion of the field where the grainstone lithofacies are the thickest. Non-permeable Bethany Falls limestone lithofacies are packstone and wackestone lithologies along the western and eastern margins of the Collier Flats field.

Delineation of Bethany Falls reservoir geometry is based on several lines of evidence: Bethany Falls limestone isopach maps, core data, net thickness of low gamma ray isopach map, net porosity greater than 10% isopach map, paleogeographic and depositional environment interpretations. The foundation for these maps is the correlation of core lithofacies with well-log responses (Figure 3.23). These correlations show two characteristics used to delineate reservoir geometry: (1) low gamma ray values correlate with Bethany Falls "clean carbonates" which are grainstone and packstone lithologies; and (2) interbedded fossiliferous wackestone and black fissile shale correlate with higher gamma ray responses (Figure 3.23). These two correlations are consistent for all cores.

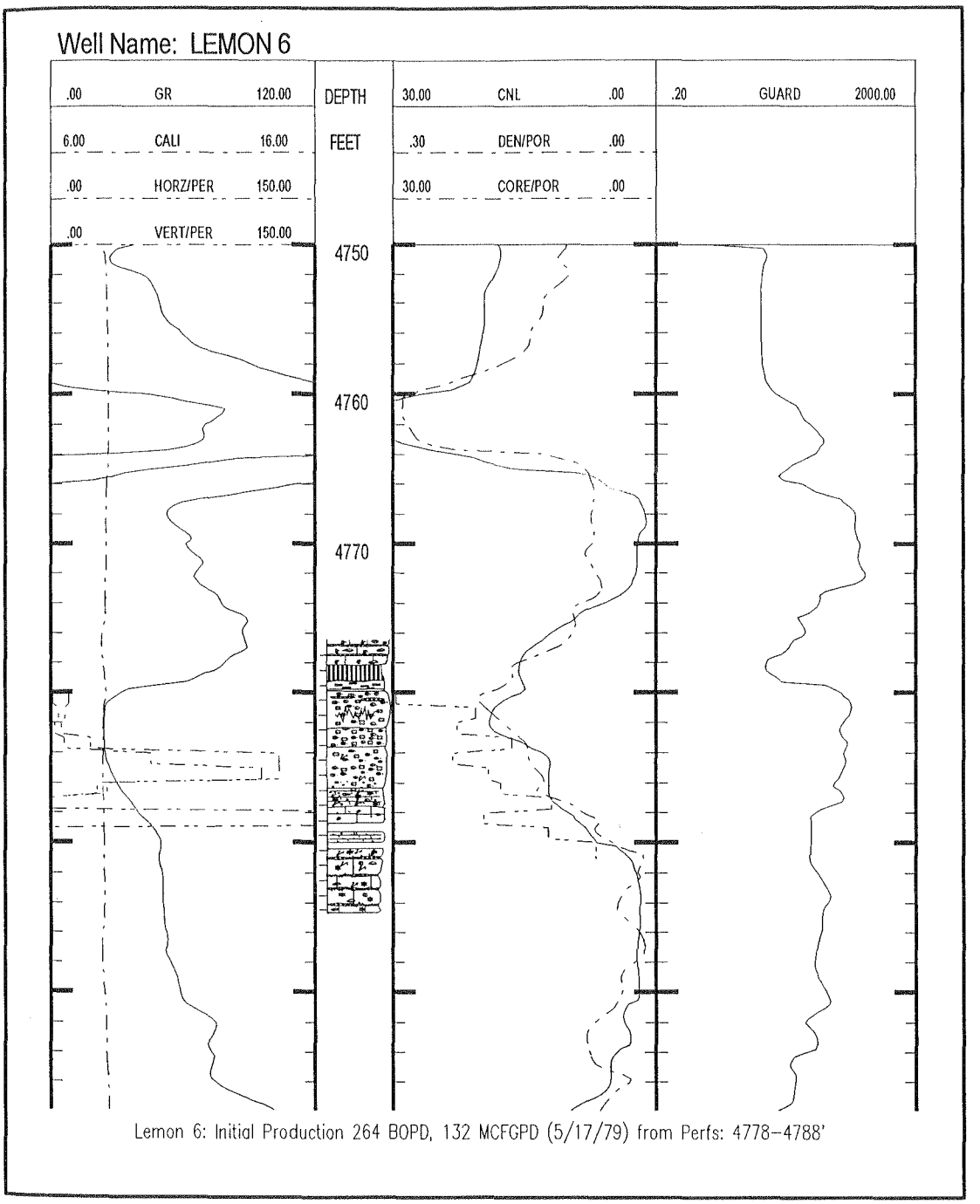


Figure 3.23 Core lithologies and well log response correlation. The most significant feature that is revealed in these correlations is the low gamma ray values correlating with Bethany Falls "clean carbonates". The lowest gamma ray response is in the grainstone lithologies. The fossiliferous wackestones correlate with higher gamma ray well log responses. The Galesburg shale has a yet higher gamma ray well log response.

Bethany Falls limestone isopach map data are based on well log signatures presented in Figure 1.5. The Bethany Falls limestone isopach map shows the north-south thickness trend, (between 32 and 38 feet), which coincides with Collier Flats field production (Figure 3.24). The elongate nature of Bethany Falls production is further expressed by the net feet of well log low gamma ray responses and density porosity isopach maps (Figure 3.25). These observations suggest reservoir lithofacies developed as a marine sand body parallel to depositional slope much like the ooid shoals of the western Bahama platform (Ball, 1967). Other lines of evidence for this interpretation are as follows:

- Reservoir lithofacies are absent in Lemon 2x and 4 cores as a result of non-deposition. Additionally, there are non-productive wells to the west of the Collier Flats field where well log signatures, based on core correlations, indicate reservoir lithofacies did not develop. These observations indicate a change in depositional environment possibly due to a change in paleotopography and deposition of lower energy carbonate lithofacies.
- The low gamma ray well log response isopach map indicates a north-south localized carbonate grainstone build up in the center of the Collier Flats field and thinning to the east and west. Lobate features are present in sections 1,3,12,13 and 14, T20W, R34S, which may be spillover lobes that formed as a result of tidal or storm currents flowing across the sand body.
- A band of oolite shoals, running northwest to southeast, extends from west-central to south-central Kansas (Watney, 1984). These oolite shoals lie parallel and immediately west of what was a positive shelf area, the Pratt Anticline (Watney, 1984).

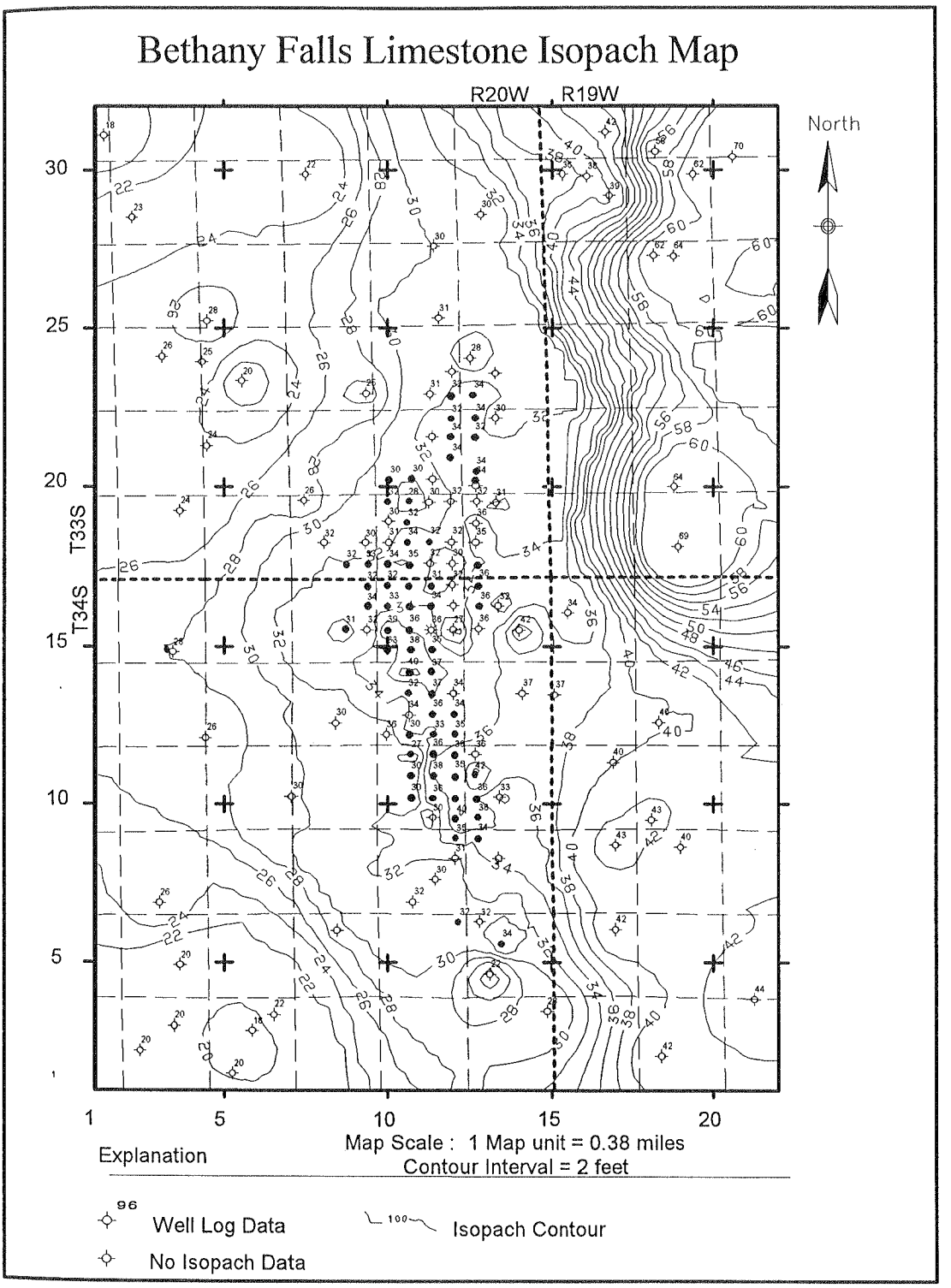


Figure 3.24 Isopach map of the Bethany Falls limestone.

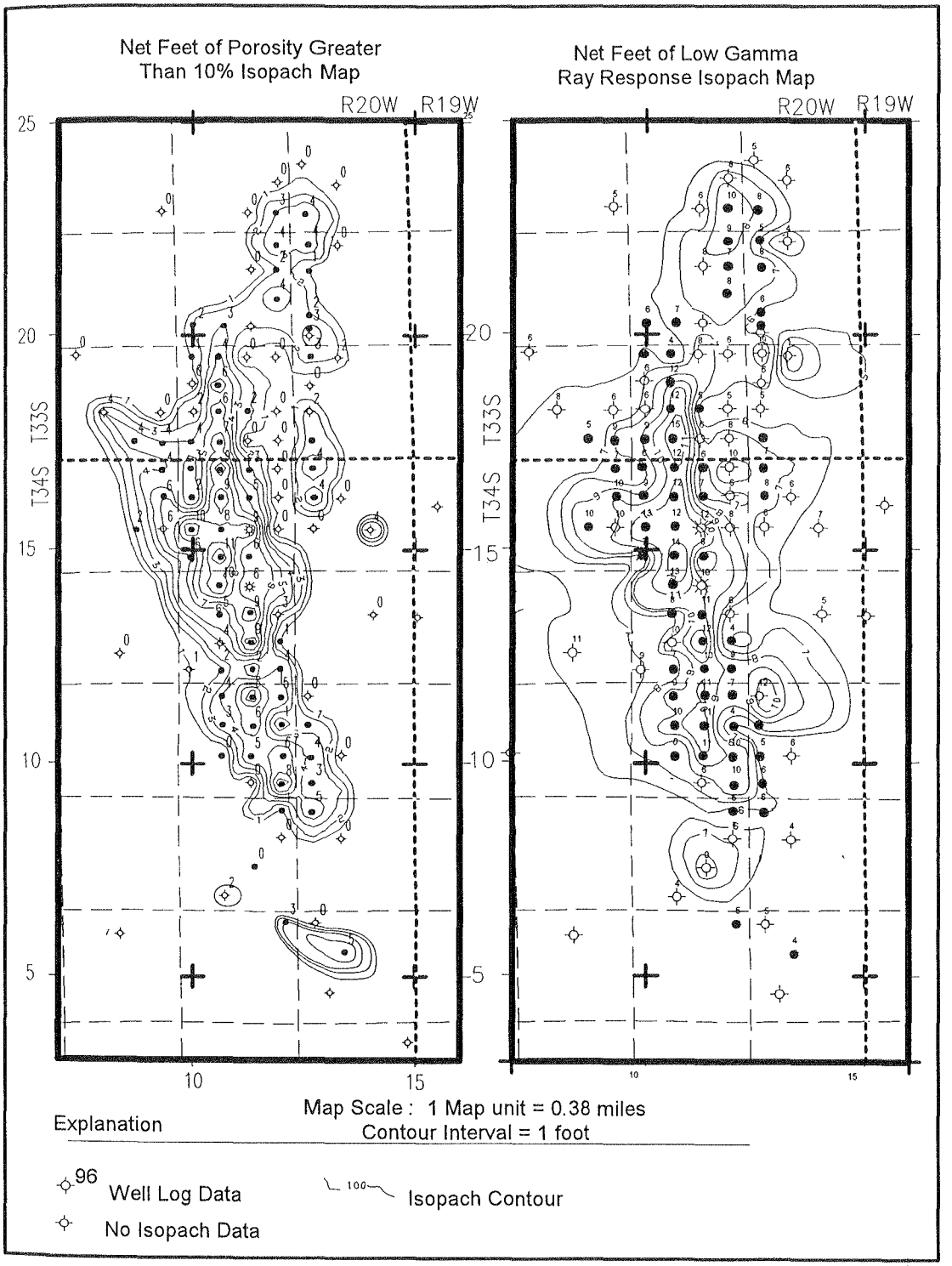


Figure 3.25 Net thickness of porosity > 10% and net thickness of low gramma ray facies isopach maps. Porosity data are from well log density curves and converted to porosity using standard well-log corrections. Low gamma ray data are based on a strong kick to lower GR API values relative to the shaly carbonate response (see Figure 3.24).

Wells with high porosity and permeability, intense mottling, and porosity/permeability that cross from the grainstone lithofacies down into the underlying packstone/wackestone lithofacies mirror the thickest portion of the low gamma ray response isopach map (Figures 3.4 and 3.5).

Vertical distribution of reservoir lithofacies and engineering data trends presented in Figures 3.4 ands 3.5 are summarized in a series of lithostratigraphic cross sections (Figures 3.26, 3.27 and 3.28). These figures clearly illustrate the heterogeneous distribution of porosity and permeability in the Bethany Falls limestone reservoir.

The complex nature of porosity and permeability development cannot be attributed solely to primary depositional features and geologic processes such as formation of primary porosity in the grainstones (Figures 3.26 to 3.28). Preliminary correlations between core porosity and well log porosity data do not show a 1 to 1 correlation. Additionally, core porosity and permeability relationships do not display any obvious correlation. Thus, depositional processes are only part of the answer to porosity and permeability development in the Collier Flats field.

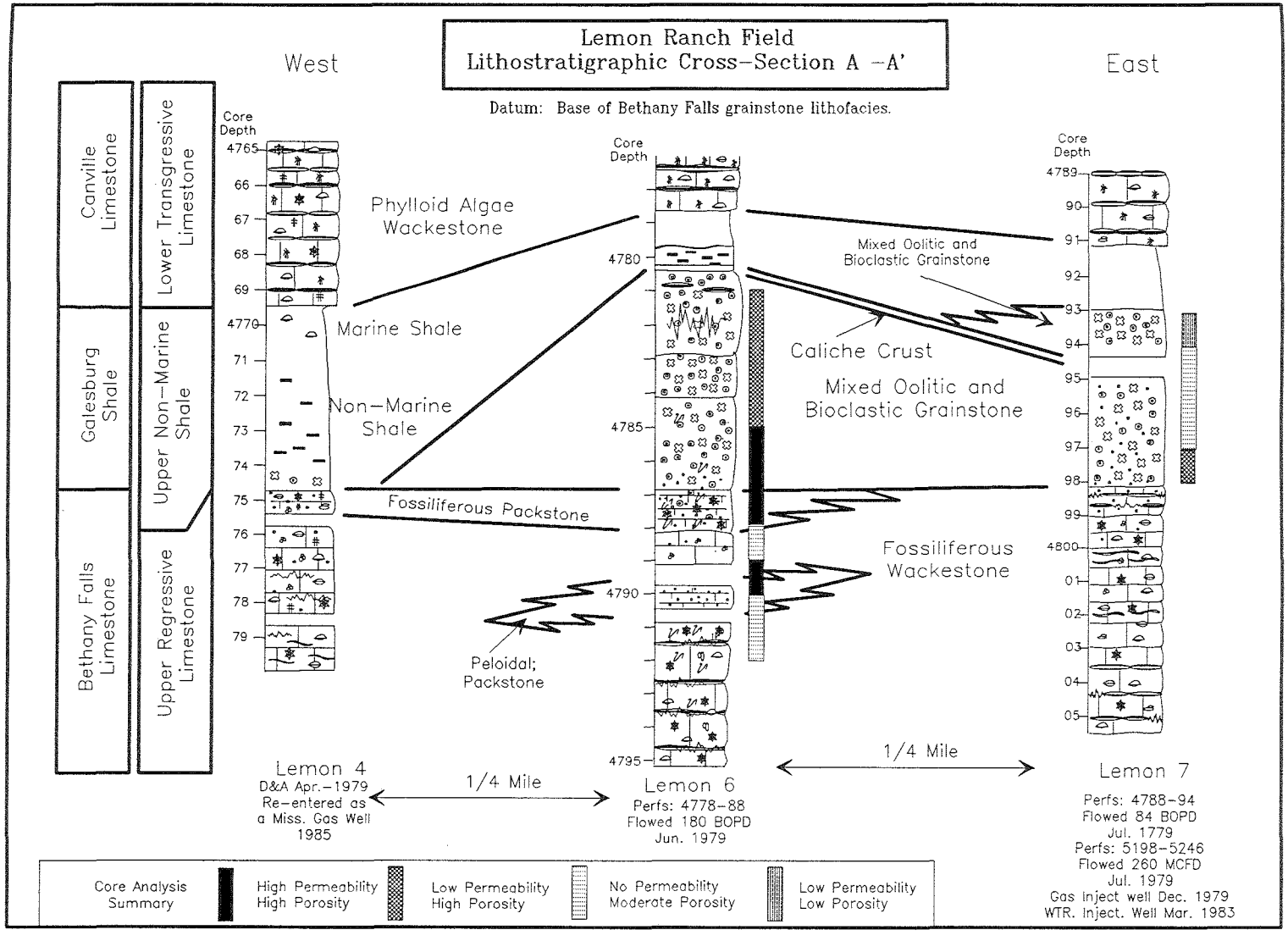


Figure 3.26 Lithostratigraphic cross section A-A'. See Figures 3.1 and 3.4 for location and symbol explanation. Datum base of Bethany Falls grainstone lithofacies.

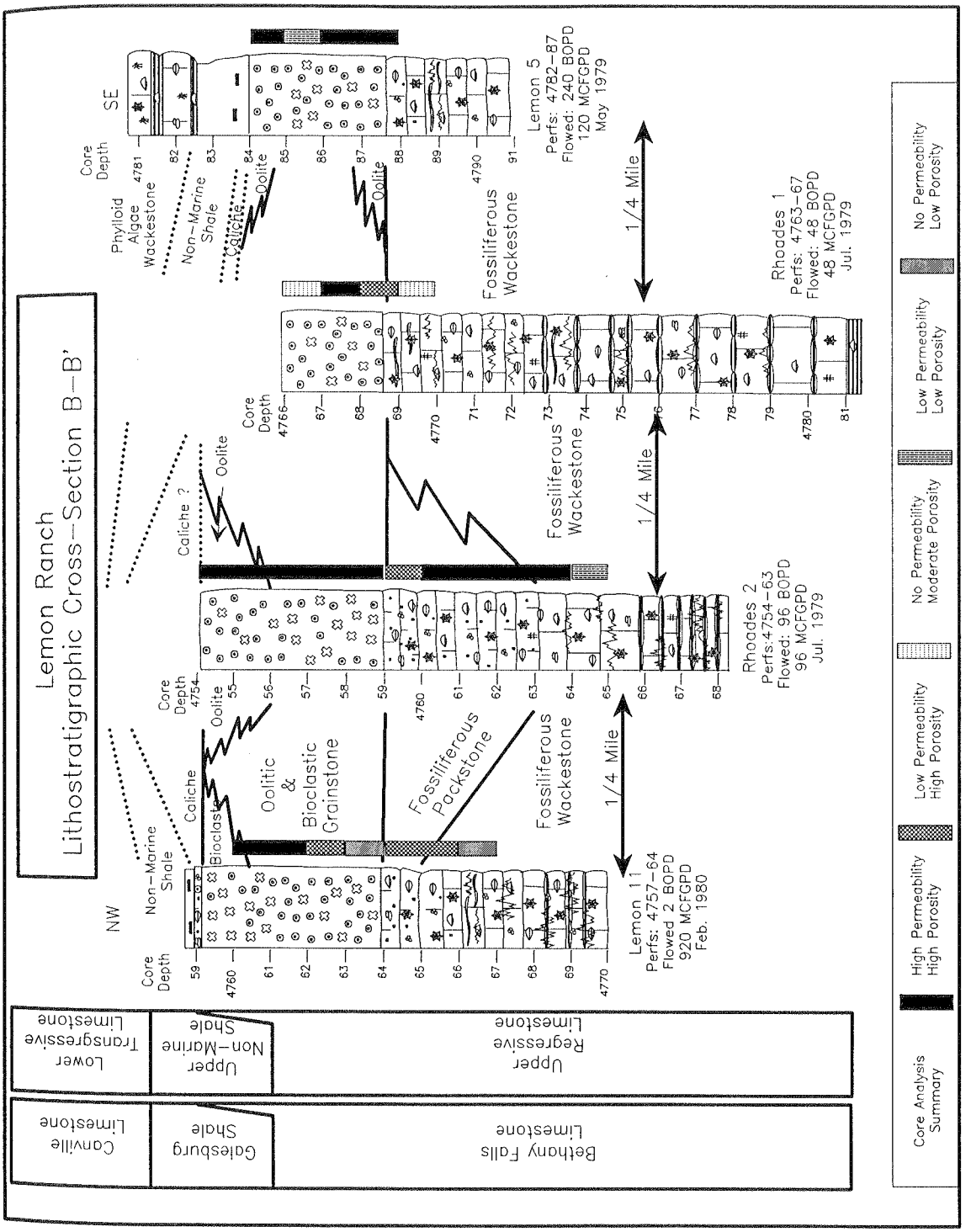


Figure 3.27 Lithostratigraphic cross section B-B'. See Figures 3.1 and 3.4 for location and symbol explanation. Datum base of Bethany Falls grainstone lithofacies.

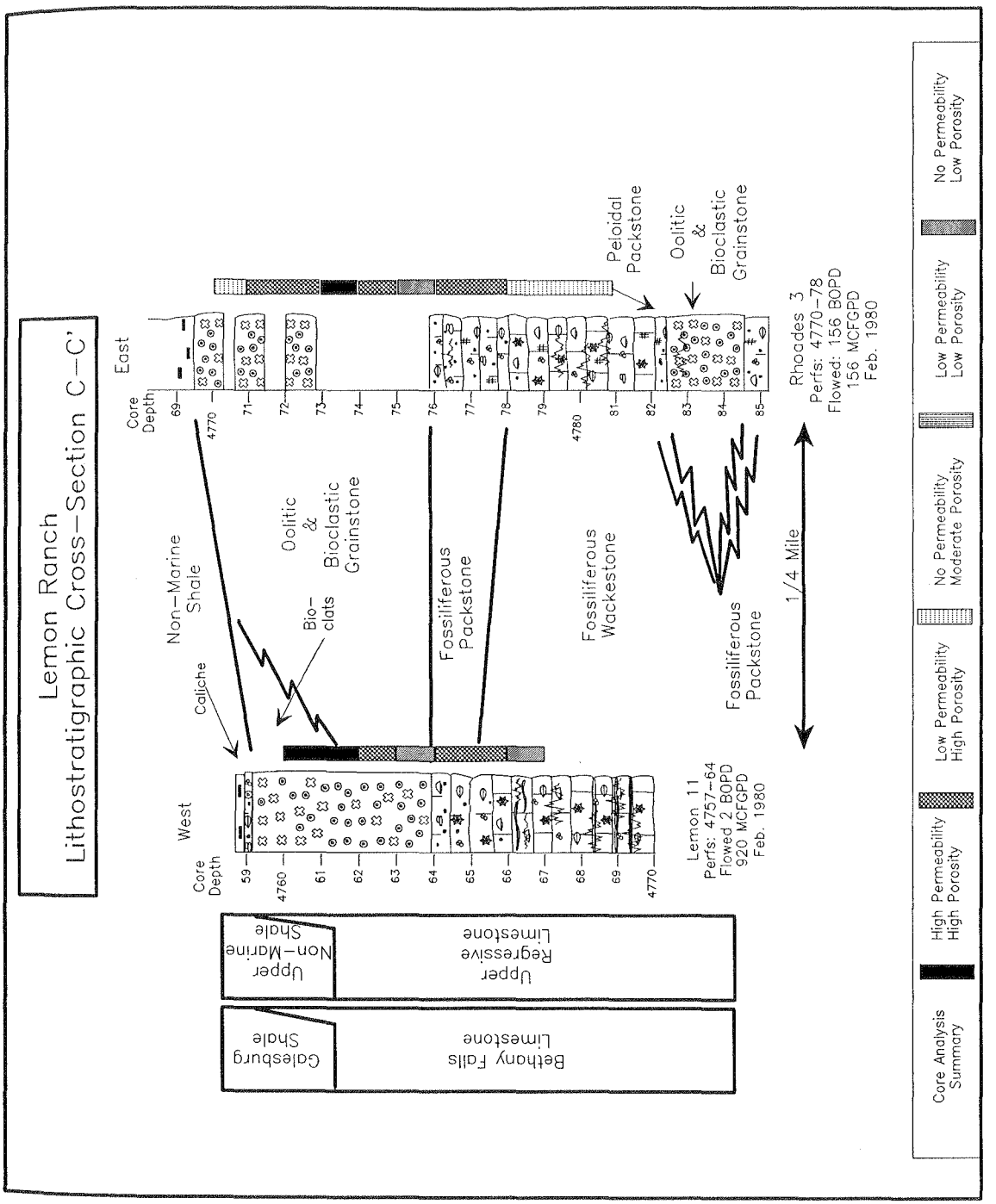


Figure 3.28 Lithostratigraphic cross section C-C'. See Figures 3.1 and 3.4 for location and symbol explanation. Datum base of Bethany Falls grainstone lithofacies.

## Galesburg Shale Depositional Environment Interpretations

The Galesburg shale overlies the Bethany Falls limestone and is easily identified in well logs. Galesburg shale lithofacies consists of: 1) fissile, green/gray mottled, calcareous shale w/ evidence of paleosol development; 2) gray blocky shale and 3) fissile gray shale w/ carbonized plant material that grade up into marine black shale with crinoids and brachiopods. This lithofacies assemblage indicates a transition from non-marine to marine sedimentation. A paleosol in the Galesburg shale is observed 3 feet above the Bethany Falls limestone in the Lemon 4 core (Figures 3.18 and 3.19).

The paleosol in the Galesburg shale cannot be differentiated from the paleosol on top of the Bethany Falls limestone. This indicates that the two paleosols likely formed during the same subaerial exposure event at the end of Bethany Falls limestone deposition.

## Canville Limestone Depositional Environment Interpretations

The Canville limestone has been identified as a transgressive member of the Dennis sequence by stratigraphic position and well log correlations. Unfortunately, the Canville limestone was not completely cored since it is not the main reservoir zone. However, the cored zones clearly show the transition from Galesburg shale non-marine deposition to Canville limestone marine carbonate deposition. The Canville limestone consists of interbedded black fissile shale and dark gray phylloid algal wackestone. The black fissile shales contain brachiopods and crinoids whereas the wackestones contain an open marine biotic assemblage including: phylloid algae, brachiopods, crinoids, mollusks, foraminifera, ostracods and bryozoans. This type of lithology is characteristic of quiet subtidal carbonate deposition below effective wave base. Fossil abundance is high in the lowest portion of the Canville limestone and decreases up-section (Lemon 12 core).

The Canville limestone cements and pore types are very useful in the process of determining Bethany Falls limestone paragenesis. These features provide a reference to compare Bethany Falls limestone cementation events and porosity formation events in the underlying units.

# CHAPTER 4

## Collier Flats Field Diagenetic History

### Introduction

It has been established that Collier Flats field porosity and permeability development and distribution cannot be attributed totally to depositional environment. Effective porosity is secondary indicating diagenetic processes are a significant component to porosity and permeability development. In order to characterize the Collier Flats field reservoir, a diagenetic model must be constructed to help establish porosity and permeability relationships. This model can then be used to predict porosity and permeability throughout the entire field without core.

Paragenesis and diagenetic history are interpreted from thin-section petrography. Petrography was performed using plane-light microscopy, cathodoluminescence, ultra-violet epifluoresence and stained thin-section (alizarin red-S and potassium ferricyanide staining) techniques to identify mineralogy, pore-types and diagenetic features from over 100 blue-epoxy impregnated thin-sections from core.

### Paragenesis Interpretation Methodology

Several geological events and features have already been identified which may constrain cementation and porosity formation events and assist with interpreting Bethany Falls limestone reservoir paragenesis. Deposition of the Bethany Falls limestone, subaerial exposure after deposition of the Bethany Falls limestone, Galesburg shale deposition and Canville limestone deposition can be used to constrain diagenetic features and infer timing.

Cathodoluminescence proved to be a significant tool for distinguishing between individual calcite and dolomite cements. Stained thin-sections were useful in identifying

ferroan calcite and dolomite cements whereas blue-epoxy impregnated thin-sections identify effective porosity.

The following cement and spar descriptions are presented in interpreted paragenetic order. Cement descriptions generally include:

- fabric criteria for cement identification (Bathurst, 1975),
- mineralogy,
- cement type and character (Folk nomenclature, 1965),
- cathodoluminescent signature,
- stratigraphic location,
- what type of pore the cement fills or reduces,
- and cross-cutting relationships.

Folk's (1965) classification of authigenic calcite is used to describe cements observed in thin-section. It should be recognized that a fundamental interpretation on mode of formation of authigenic calcite spar has been made to construct a list of cements used to interpret diagenetic history. The remaining components of this classification are purely descriptive (Table 4.1).

| **Mode of Formation Code** | **Description** | **Other Features** |
|---|---|---|
| P | Passive Precipitation | Normal Pore Filling |
| Ps | Passive Precipitation | Solution Fill |
| D | Displacive Precipitation | |
| N | Neomorphic | Unknown Processes |
| Ni | Inversion | Original Aragonite |
| Nr | Recrystallization | Original Calcite |
| Nd | Degrading | |
| Ns | Strained | |
| Nc | Coalescive | |
| R | Replacement | |

Table 4.1 Folk's Classification of Authigenic Calcite (Folk, 1965).

| Shape Code | Description | Other Features |
|---|---|---|
| E | Equant | Axial Ratio <1.5:1 |
| B | Bladed | Axial Ratio 1.5:1 to 6:1 |
| F | Fibrous | Axial Ratio >6:1 |
| **Crystal Size Code** | **Description** | **Size, mm** |
| 1 | Aphanocrystalline | 0.001 |
| 2 | Very Finely Crystalline | 0.004 |
| 3 | Finely Crystalline | 0.016 |
| 4 | Medium Crystalline | 0.062 |
| 5 | Coarsely Crystalline | 0.25 |
| 6 | Very Coarsely Crystalline | 1.0 |
| 7 | Extremely Coarsely Crystalline | 4.0 |
| **Foundation Code** | **Description** | **Other Features** |
| O | Overgrowth | In Optical Continuity |
| Om | Overgrowth | Monocrystal |
| Ow | Overgrowth | Widens Outward From Nucleus |
| C | Crust | Oriented By a Nucleant Surface |
| Cw | Crust | Widens Outward From Nucleus |
| S | Spherulitic | No Obvious Orientation |

Table 4.1 Folk Classification of Authigenic Calcite (Folk, 1965) continued.

Dolomite descriptions are based on Sibley and Gregg's (1987) classification of dolomite textures (Figure 4.1). This classification is largely descriptive in nature. Other features such as cathodoluminescent signature, staining characteristics and distribution are noted.

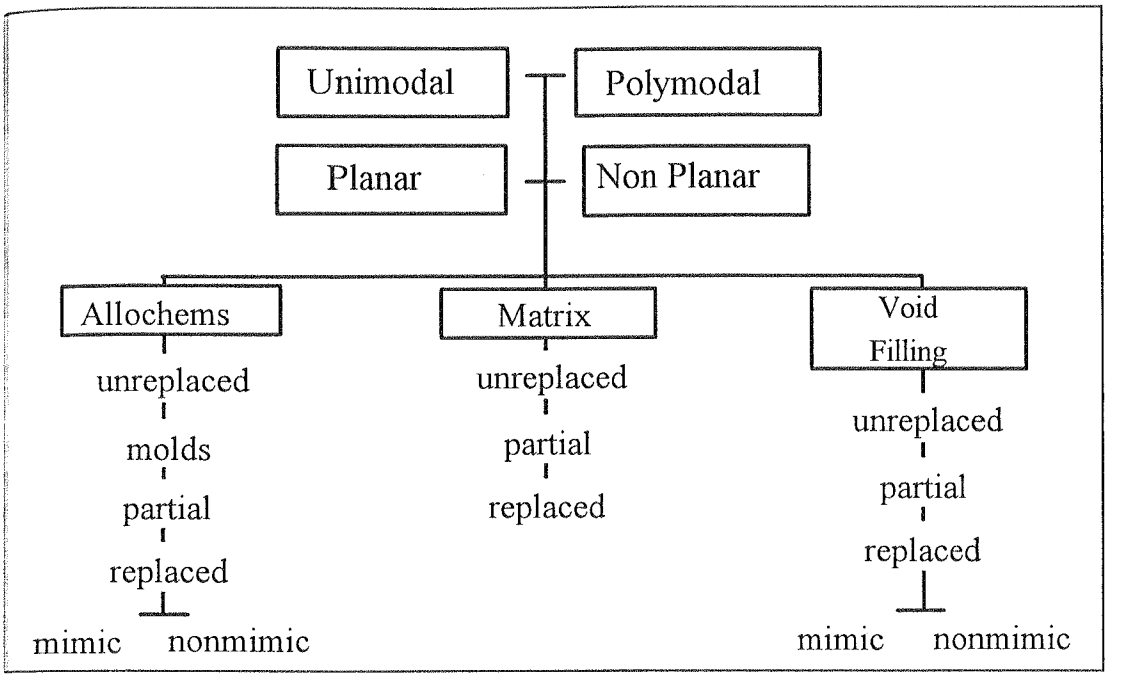


Figure 4.1 Classification of dolomite textures (Sibley and Gregg, 1977).

Porosity descriptions used in this study are based on Choquette and Pray, 1970, nomenclature and classification of porosity in sedimentary carbonates (Figure 4.2). This classification is generally descriptive except when time of secondary porosity formation is implied (eogenetic, mesogenetic and telegenetic).

## Bethany Falls Paragenesis

### Cementation Event A - Nonferroan calcite cementation in Bethany Falls limestone primary porosity.

Nonferroan, calcite cements #C1, #C2 and #C3 fill or reduce primary interparticle porosity in the Bethany Falls limestone grainstone lithofacies. These cements (1) pre-date compactional features, (2) are truncated by a later dissolution event, (3) are not found in overlying strata of the Galesburg shale and Canville limestone and (4) are not found in the paleosol zone on top of the Bethany Falls limestone and the paleosol in the Galesburg shale. These observations suggest that these three cements precipitated prior to any dissolution events that created secondary porosity in the Bethany Falls limestone.

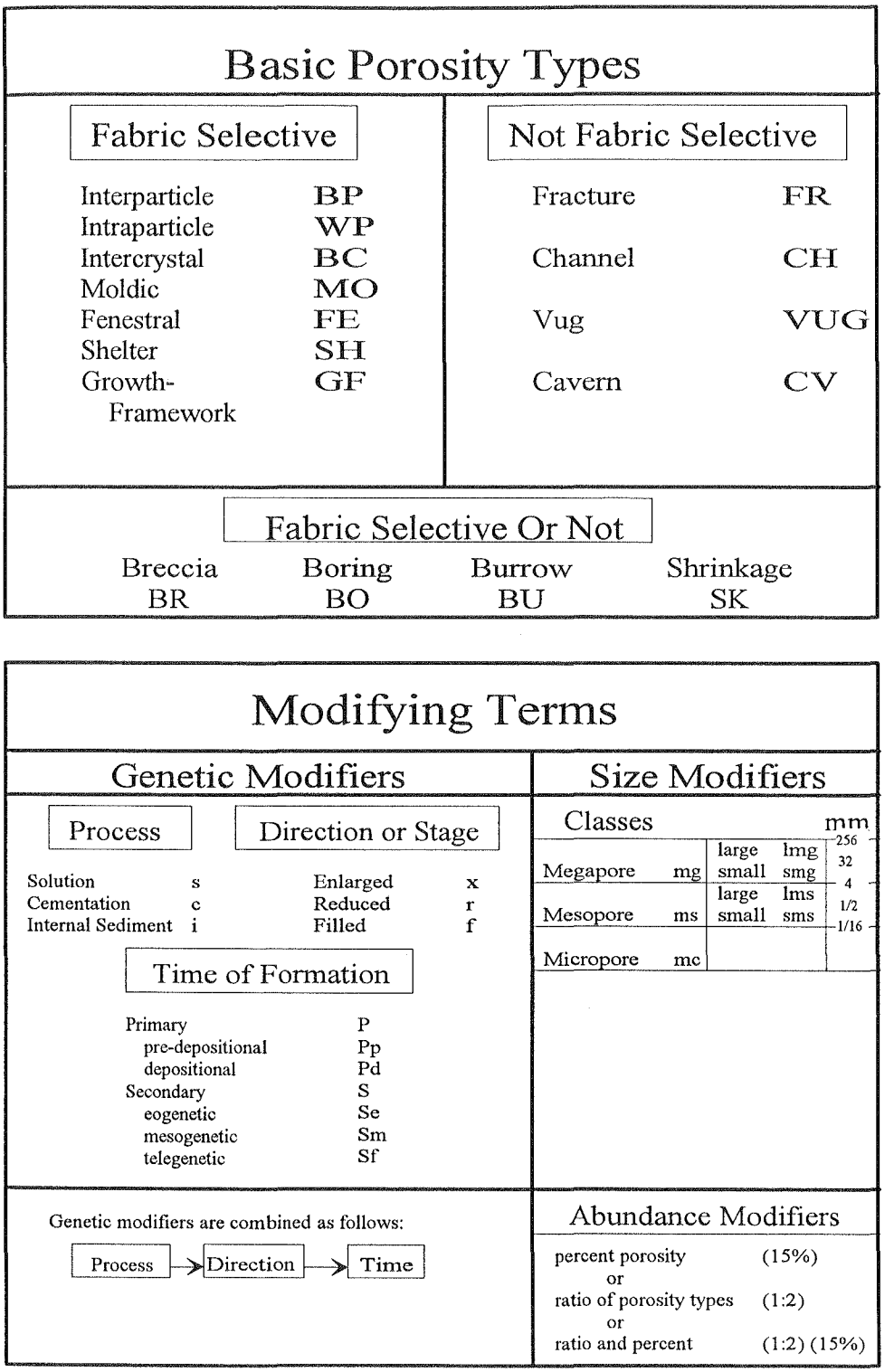


Figure 4.2 Geologic classification of pores and pore systems in carbonate rocks (Choquette and Pray, 1970).

Later cements are observed in Bethany Falls limestone primary interparticle porosity indicating that this pore type remained open at the end of this cementation event.

**Cement #C1: $PB_2C$, Nonferroan, zoned cathodoluminescent calcite.**

Cement #C1 is a bladed to equant, isopachous, nonferroan calcite cement that displays a zoned cathodoluminescent signature. This cement reduces and lines primary interparticle porosity in the Bethany Falls oolitic and bioclastic grainstones and is truncated by fractures. Because this cement is only observed in Bethany Falls grainstone primary interparticle porosity, a reasonable interpretation is that this cement precipitated prior to any dissolution event that created secondary porosity in the Bethany Falls limestone. Figure 4.3 illustrates cement #C1 reducing and lining primary interparticle porosity. Figure 4.4 illustrates the cathodoluminescent signature of this cement.

**Cement #C2: $PE_{3-5}O$, Poikilotopic, nonferroan, nonluminescent syntaxial calcite.**

Cement #C2 is a nonferroan, nonluminescent, syntaxial calcite cement overgrowth on crinoid grains in the Bethany Falls limestone grainstone lithofacies. This cement generally fills primary interparticle porosity in the Bethany Falls oolitic and bioclastic grainstones. As ooid abundance decreases in the lower portion of the grainstone lithofacies, the abundance of this cement increases because more non-coated crinoid bioclasts are available as nucleation sites. Because cement #C2 is observed reducing and filling Bethany Falls grainstone primary interparticle porosity, a reasonable interpretation is that this cement and cement #C1 precipitated prior to dissolution events that created secondary porosity in the Bethany Falls limestone. Figure 4.3 illustrates cement #C2 filling primary interparticle porosity. Figure 4.4 illustrates the cathodoluminescent signature of this cement.

Figure 4.3 Stained thin section photomicrograph of Cements #C1, #C2 and #C5. Sample L6.5 in the Lemon 6 Core, Bethany Falls limestone.

Cement #C1 grades into syntaxial cement #C2 which reduces primary interparticle porosity surrounding a crinoid grain in a bioclastic grainstone. Cement #C5 fills secondary vug porosity.

Arrow Explanation
(1) Nonferroan bladed calcite cement #C1 reduces primary interparticle porosity and nucleated on a crinoid grain.
(2) Nonferroan syntaxial calcite cement #C2 reduces and fills primary interparticle porosity also nucleated on a crinoid grain.
(3) Ferroan calcite cement #C5 fills vug porosity overlying cements #C1.

Figure 4.4 Thin section cathodoluminescent photomicrograph of cements #C1, #C2 and #C5. Sample L6.5 in the Lemon 6 Core, Bethany Falls limestone.

Cement #C1 grades into syntaxial cement #C2 which reduce primary interparticle porosity surrounding a crinoid grain in a bioclastic grainstone. Cement #C5 fills secondary vug porosity.

Arrow Explanation
(1) Non ferroan bladed calcite cement #C1 reduces primary interparticle porosity and nucleated on a crinoid grain.
(2) Non ferroan syntaxial calcite cement #C2 reduces and fills primary interparticle porosity also nucleated on a crinoid grain.
(3) Ferroan calcite cement #C5 fills vug porosity overlying cements #C1
(4) Ferroan calcite cement #C5 fills vug porosity that truncates neomorphic spar.

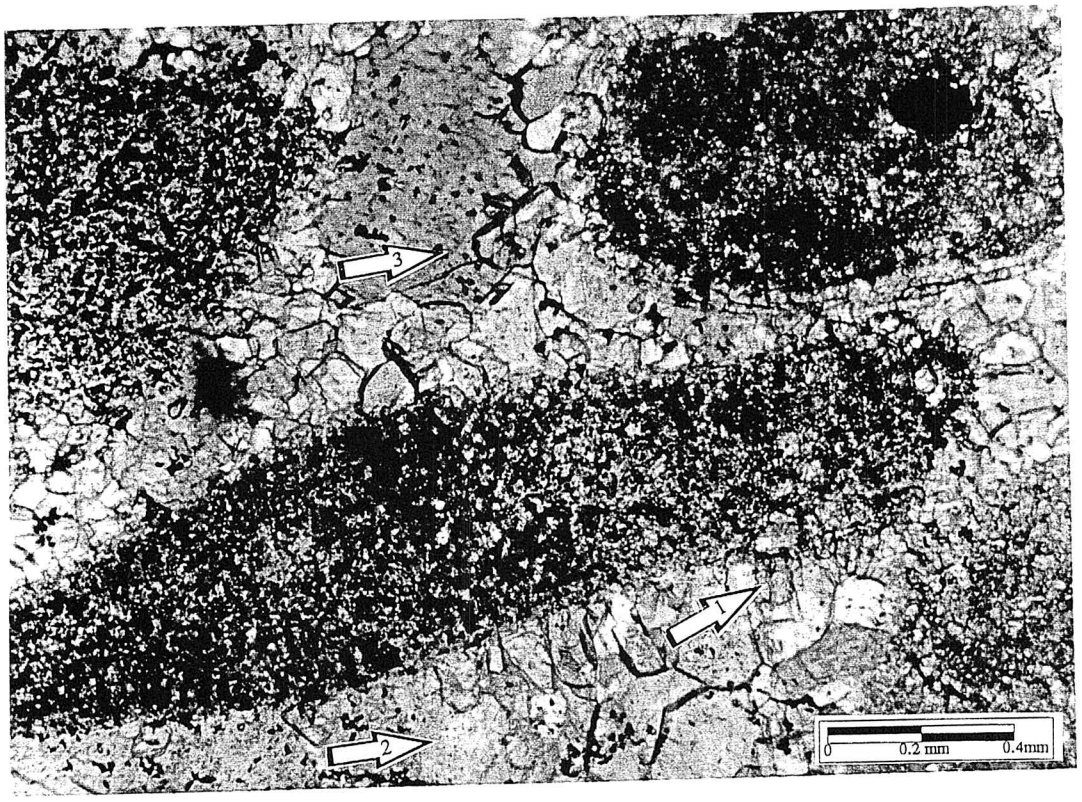
3
1
2
0
0.2 mm
0.4mm

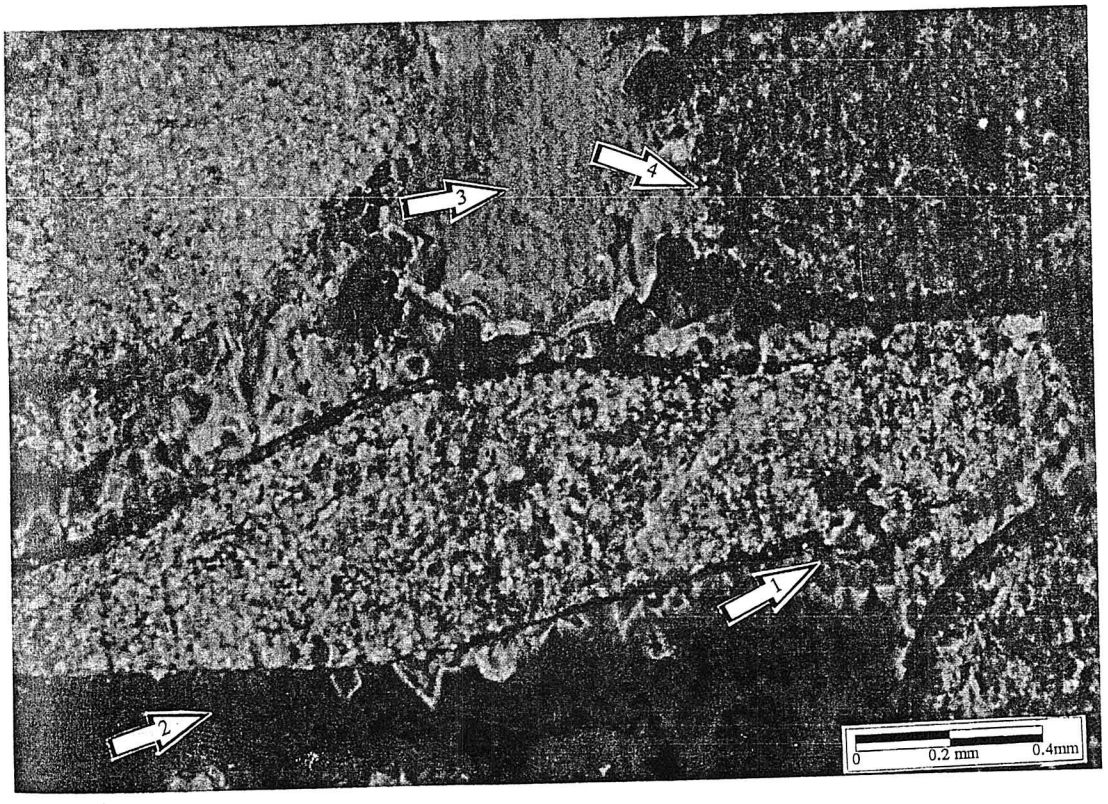
4
3
1
2
0
0.2 mm
0.4mm

### #C2 Fluid Inclusions

During a 1990 fluid inclusion seminar, primary and secondary fluid inclusions were identified in syntaxial cement #C2 overgrowths on crinoids in the grainstone lithofacies of the Bethany Falls limestone, Lemon 11 core. A preliminary fluid inclusion study of the syntaxial calcite overgrowths was initiated. Single phase (all liquid) fluid inclusions are located adjacent to echinoderm grains along growth zones and within inferred crystal boundaries. Two phase (liquid-vapor) fluid inclusions are also distributed along with the one-phase inclusions. These two populations of fluid inclusions were interpreted as primary.

Two phase (liquid-vapor) fluid inclusions in this cement displayed a wide distribution of homogenization and freezing temperatures. Based on wide distribution of homogenization and freezing temperatures, it is likely that the two phase fluid inclusions record the effects of reequilibration of the primary single phase fluid inclusions. The presence of single phase all liquid fluid inclusions indicates precipitation of this cement occurred at temperatures below about 50 degrees centigrade.

### Cement #C3: $PE_2C$, Nonferroan, zoned cathodoluminescent calcite.

Cement #C3 is an equant, isopachous, nonferroan, zoned cathodoluminescent calcite cement. This cement also lines Bethany Falls grainstone primary interparticle porosity. The abundance of this cement increases in areas where syntaxial cement #C2 is minor. It is likely that an increase in coated crinoid grains provide fewer places for the syntaxial cement #C2 to nucleate. As with cements #C1 and #C2, this cement is observed reducing and filling primary interparticle porosity in the Bethany Falls limestone. Thus, a reasonable interpretation is that this cement also precipitated prior to dissolution events that created secondary porosity in the Bethany Falls limestone. Figures 4.5 and 4.6 illustrates cement #C3 reducing primary interparticle porosity.

Figure 4.5 Stained thin section photomicrograph of Cements #C3 and #C5. Sample L6.6 in the Lemon 6 Core, Bethany Falls limestone.

Arrow Explanation
(1) Nonferroan calcite cement #C3 reducing primary interparticle porosity between ooids.
(2) Open porosity in high porous and permeable areas in the mixed oolitic and bioclastic grainstone lithologies. Other types of effective porosity are primary interparticle and secondary moldic and vug porosity.
(3) Ferroan calcite cement #C5 fills secondary moldic porosity.
(4) Ferroan calcite cement #C5 fills secondary moldic porosity and appears to have been truncated by a later dissolution event.

Figure 4.6 Thin section cathodoluminescent photomicrograph of Cements #C2, #C3 and #C5. Sample L6.6 in the Lemon 6 Core, Bethany Falls limestone.

Arrow Explanation
(1) Non ferroan calcite cement #C3 reducing primary interparticle porosity between ooids.
(2) Open porosity in high porous and permeable areas in the mixed oolitic and bioclastic grainstone lithologies. Other types of effective porosity are primary interparticle and secondary moldic and vug porosity.
(3) Ferroan calcite cement #C5 fills secondary moldic porosity.
(4) Ferroan calcite cement #C5 fills secondary moldic porosity and appears to have been truncated by a later dissolution event.

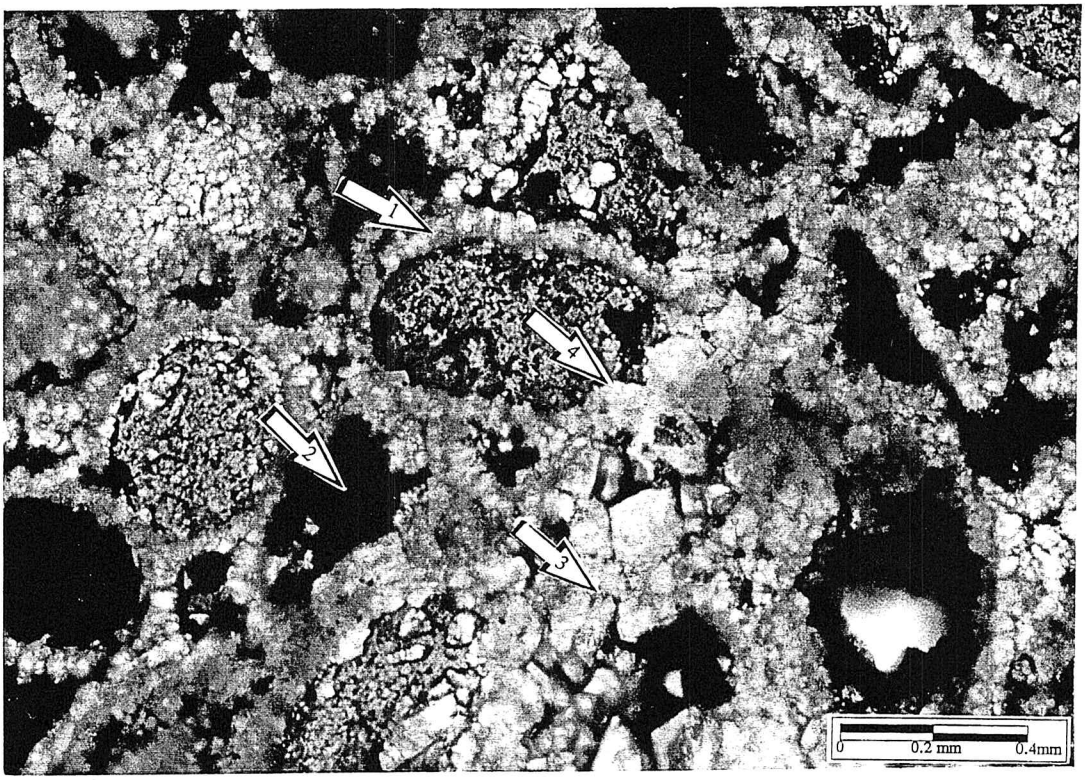
1
2
3
4
0
0.2 mm
0.4mm

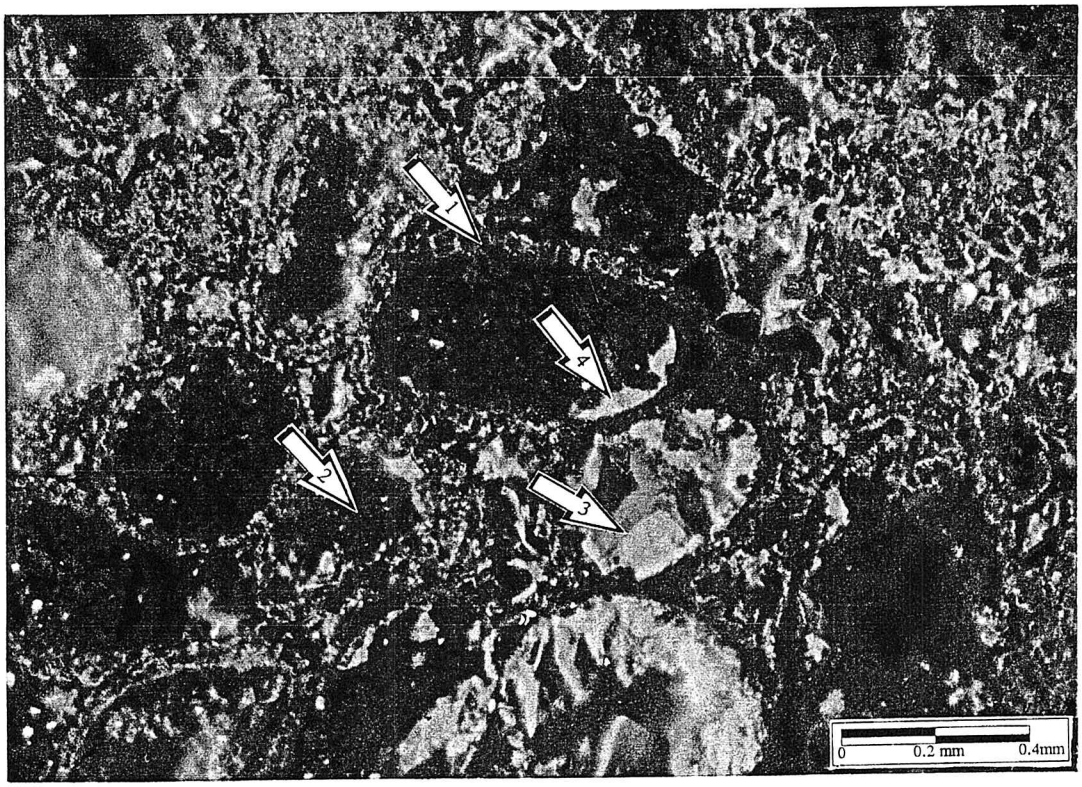
1
2
3
4
0
0.2 mm
0.4mm

### Cementation Event B - Nonferroan calcite cementation and Bethany Falls limestone primary and secondary porosity reduction.

Nonferroan, calcite #C4 cement lines and reduces primary interparticle and secondary moldic porosity in the Bethany Falls limestone grainstone lithofacies. This cement (1) is restricted to the Bethany Falls limestone grainstone lithofacies, (2) is present in the paleosol on top of the Bethany Falls limestone and (3) is not present in the overlying Galesburg shale. Cement #C4 is the first cement to line secondary porosity, therefore, it must post date Bethany Falls limestone deposition and the first dissolution event that created Bethany Falls limestone secondary porosity. The first dissolution event is likely associated with subaerial exposure, paleosol formation and meteoric diagenesis at the end of Bethany Falls limestone deposition. Later cements are observed in Bethany Falls limestone primary and secondary porosity indicating these pores remained open at the end of this cementation event.

#### Cement #C4: $PE_2C$, Nonferroan, nonluminescent calcite.

Cement #C4 is a nonferroan, nonluminescent calcite cement that generally ends with a bright luminescent band. This cement reduces and lines primary interparticle and secondary moldic porosity in the Bethany Falls limestone. Cement #C4 is observed in the upper one foot Bethany Falls limestone paleosol influenced zone. Cement #C4 lines interparticle pores after soil formation processes likely created grain-to-grain contacts between grains that are now molds in the paleosol influenced zone (Figure 4.8). The significance of this cement is that cement #C4 is the first cement to reduce Bethany Falls limestone secondary porosity. Thus, this cement must have precipitated after a dissolution event and paleosol formation at the end of Bethany Falls deposition. Figures 4.7 and 4.8 illustrate cement #C4 reducing and lining primary interparticle and secondary porosity.

Figure 4.7: Stained thin section photomicrograph of cements #C4 and #C5. Sample L6.8 in the Lemon 6 Core, Bethany Falls limestone.

Arrow Explanation
(1) Nonferroan calcite cement #C4 reduces and lines primary interparticle porosity overlying micritized ooids and bioclasts.
(2) Ferroan calcite cement #C5 fills secondary moldic porosity overlying cement #C4 in ooid molds.
(3) Ferroan calcite cement #C5 fills primary interparticle porosity overlying cements #C4.

Figure 4.8: Thin section cathodoluminescent photomicrograph of cements #C4 and #C5. Sample L6.8 in the Lemon 6 Core, Bethany Falls limestone.

Arrow Explanation
(1) Non ferroan calcite cement #C4 reduces and lines primary interparticle porosity overlying micritized ooids and bioclasts.
(2) Ferroan calcite cement #C5 fills secondary moldic porosity overlying cement #C4 in ooid molds.
(3) Ferroan calcite cement #C5 fills primary interparticle porosity overlying cements #C4.

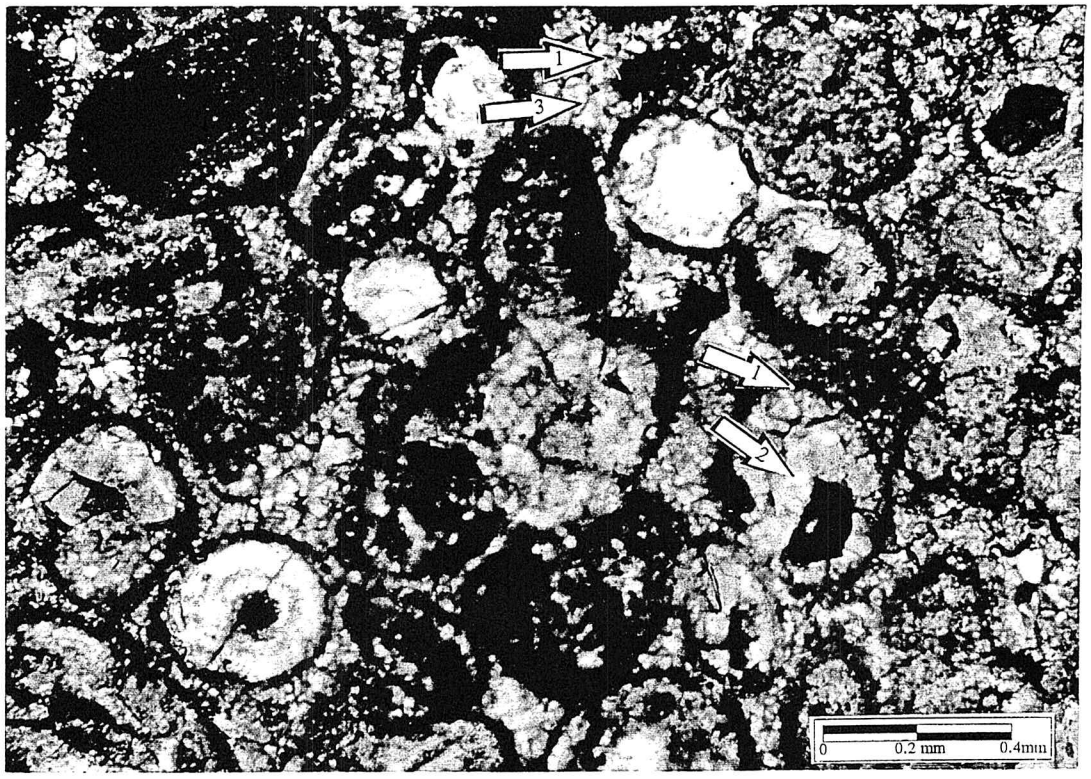
1
3
1
2
0
0.2 mm
0.4mm

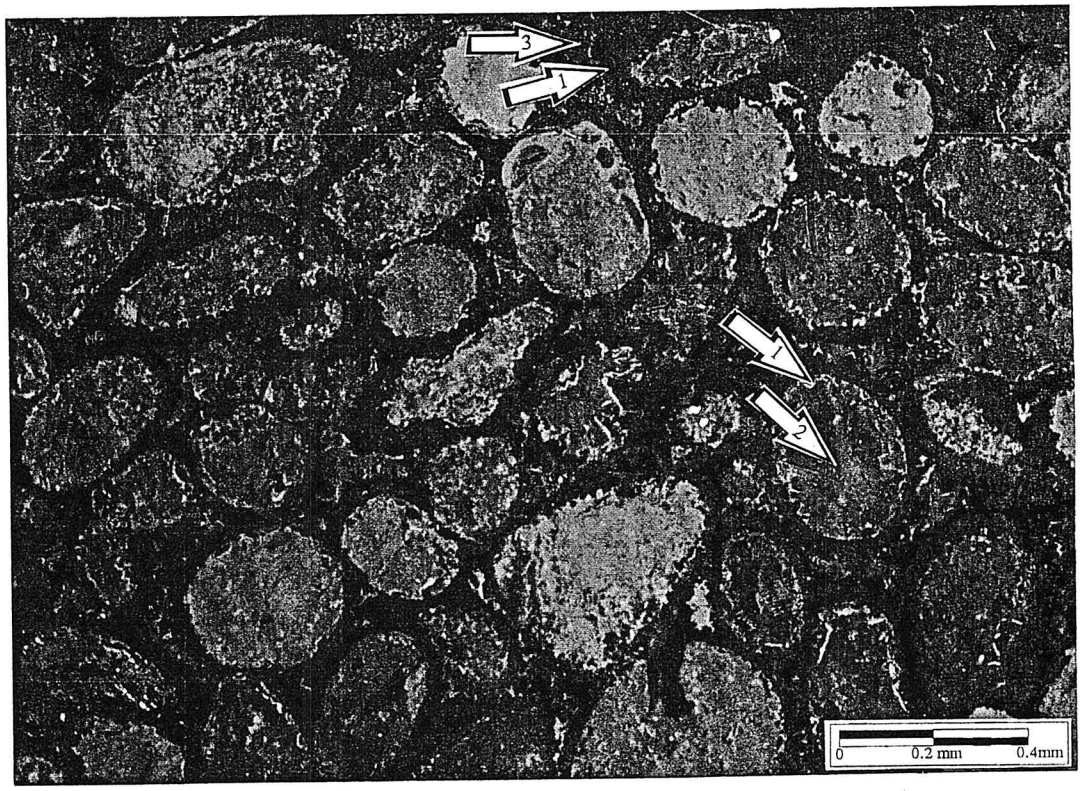
3
1
1
2
0
0.2 mm
0.4mm

### Cementation Event C - Ferroan calcite cementation and Bethany Falls limestone primary and secondary porosity reduction.

Ferroan calcite cement #C5 fills primary interparticle and secondary moldic and vug porosity in the Bethany Falls grainstone, packstone and wackestone lithofacies. This cement also fills rhizoliths in the Galesburg shale paleosol (Figure 4.11). Cement #C5 is also the first cement observed in secondary porosity in the Bethany Falls packstone and wackestone lithofacies. Additionally, this cement is not observed in the overlying Dennis sequence strata and is truncated by a later dissolution event. These observations suggest this cement formed: (1) after Bethany Falls limestone deposition, (2) after paleosol formation on top of the Bethany Falls limestone, (3) after the first dissolution event associated with the Bethany Falls paleosol, (4) after formation of a paleosol in the Galesburg shale and (5) prior to deposition of the Canville limestone. The presence of this cement in Galesburg shale rhizoliths indicates that this cement precipitated after a subaerial exposure event in the Galesburg shale. It is likely that a second dissolution event associated with formation of the Galesburg shale paleosol may be responsible for formation of the moldic and vug porosity, filled by cement #C5, in the mud-supported lithologies of the Bethany Falls limestone. Later cements are also observed in Bethany Falls limestone primary porosity indicating that this cementation event did not completely fill all Bethany Falls limestone primary and secondary porosity.

### Cement #C5: $PE_{2-3}$ Poikilotopic, ferroan, calcite.

Ferroan calcite #C5 cement fills primary interparticle and is the first cement that fills moldic and vug porosity throughout the Bethany Falls limestone grainstone, packstone and wackestone lithofacies. Additionally this cement is observed in the Galesburg shale paleosol rhizoliths. The cathodoluminescent signature of this cement is highly variable. In the upper Bethany Falls oolitic grainstone intervals, moldic and interparticle porosity is filled by a non-luminescent ferroan calcite (Figure 4.7 and 4.8). In the lower Bethany Falls bioclastic grainstone intervals, this cement fills primary interparticle and solution enlarged fracture porosity (Figure 4.9) Figure 4.10 from sample L6.7 shows zoned dull luminescent to bright luminescent ferroan calcite #C5 cement filling moldic porosity. Because these cathodoluminescent signatures are from a ferroan equant calcite filling moldic, vug and primary interparticle porosity and there are no other cross-cutting relationships differentiating the cathodoluminescent signatures, they are grouped together as one cement.

## Cementation Event D - Ferroan calcite cementation in the upper foot of the Bethany Falls limestone.

Cementation event D consists of precipitation of ferroan calcite cement #C7 in secondary porosity in the Canville limestone, Galesburg shale and upper one foot of the Bethany Falls limestone. This cementation event is minor since it only filled a very small percentage of secondary moldic porosity in the upper one foot of the Bethany Falls limestone. This cementation event is significant in the Canville limestone and Galesburg shale since it fills approximately 50%-70% of moldic porosity. There was no vug porosity observed in the Canville limestone.

Figure 4.9 Thin section photomicrograph of slightly ferroan cement #C5 filling a fracture in the grainstone lithofacies. Sample L6.5 in the Lemon 6 core, Bethany Falls limestone.

Arrow Explanation
(1) Slightly ferroan cement #C5 filling a fracture that truncates oolitic packstone lithoclasts and isopachous cement #C1.

Figure 4.10 Thin section cathodoluminescent photomicrograph of Cement #5 illustrating the variability in luminescent character. Sample L6.7 in the Lemon 6 Core, Bethany Falls limestone.

Arrow Explanation
(1) Ferroan calcite cement #C5 illustrating zoned cathodoluminescent character in moldic porosity.
(2) Ferroan calcite cement #C5 illustrating zoned cathodoluminescent character in primary interparticle porosity.
(3) Ferroan calcite cement #C5 illustrating dull cathodoluminescent character in primary interparticle porosity.
(4) Ferroan calcite cement #C5 illustrating dull cathodoluminescent character in moldic porosity.

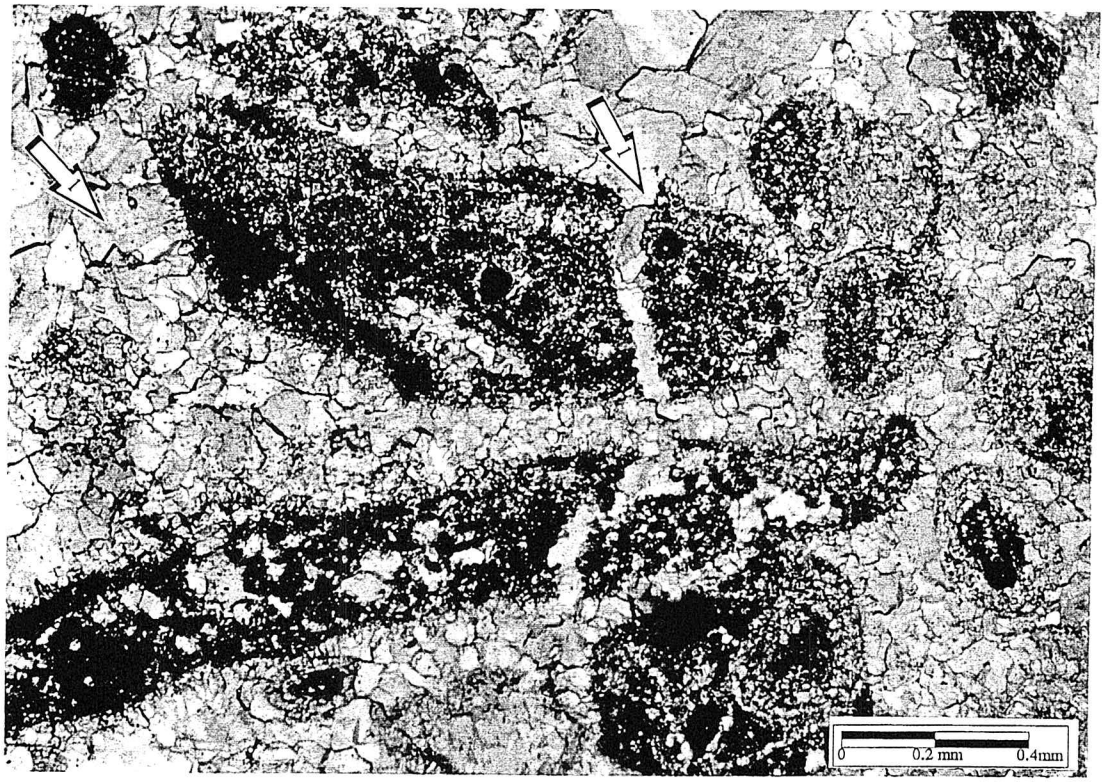
1
1
0
0.2 mm
0.4mm

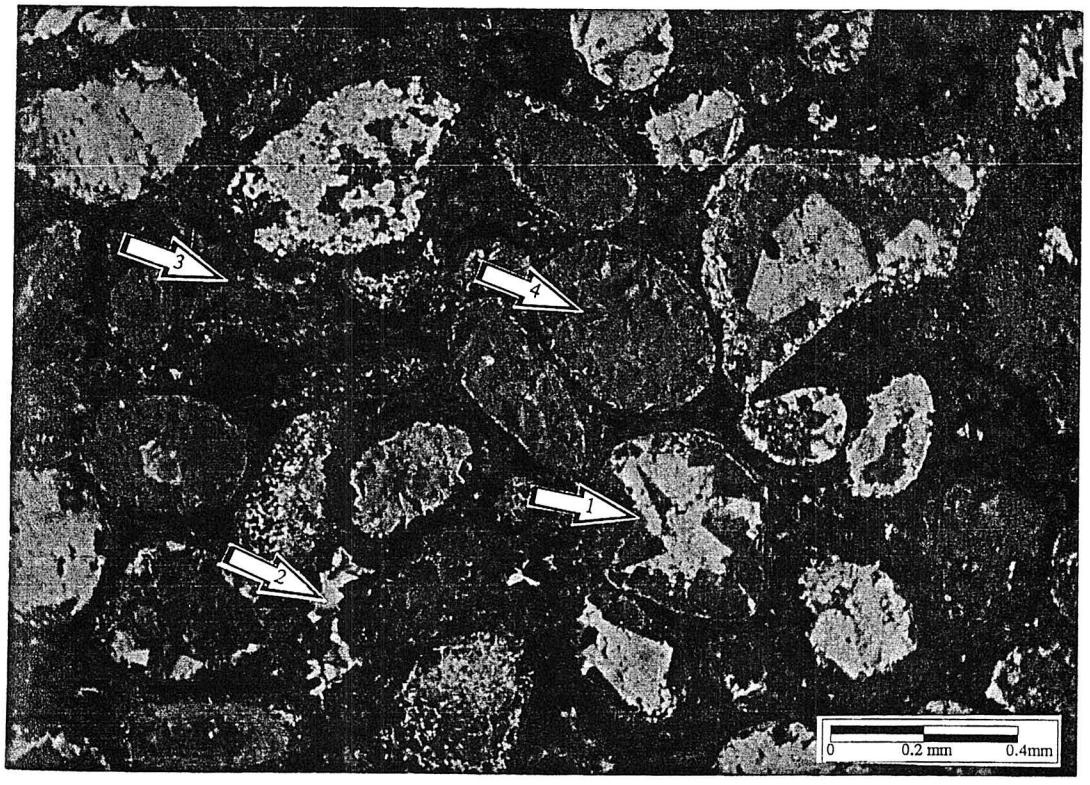
3
4
1
2
0
0.2 mm
0.4mm

Cementation Event D must have followed deposition of the Canville limestone and is likely after the same dissolution event that created more moldic porosity reduced by nonferroan calcite cement #C6 in the Canville limestone. There is no evidence of a dissolution event between precipitation of nonferroan calcite cement #C6 and ferroan calcite cement #C7 in the Canville limestone moldic pores. Ferroan calcite cement #C7 is also observed filling fracture porosity in the Canville limestone suggesting that this cementation event post dates burial compaction of the Canville limestone. Ferroan calcite cement #C7 is present in the Galesburg shale and the upper one foot of the Bethany Falls limestone indicating an open pore system extended from the Canville limestone, Galesburg shale and through at least the top one foot of the Bethany Falls limestone prior to Cementation Event D.

**Cement #C6: PE-$B_2$, Nonferroan, zoned cathodoluminescent calcite.**

Nonferroan, equant to bladed calcite cement #C6 lines and fills phylloid algal and mollusk moldic pores in the Canville limestone. It resembles cement #C4 because it also lines moldic porosity. However, cement #C4 in the Bethany Falls limestone does not show the complex cathodoluminescent signatures observed in cement #C6. Figures 4.11 and 4.12 illustrates cement #C6 lining and reducing moldic porosity overlain by ferroan calcite cement #C7 in the Canville limestone. Because this cement is not observed in the Bethany Falls limestone, it has no impact on porosity reduction except to say, this cement followed a third dissolution event after deposition of the Canville limestone which may have enhanced porosity in the Bethany Falls limestone.

Figure 4.11 Thin section photomicrograph of unstained cement #C6 reducing a phylloid algae mold overlain by cement #C7 in a phylloid algae wackestone. Sample L6.9 in the Lemon 6 Core, Canville Limestone.

Arrow Explanation
(1) Non ferroan calcite cement #C6 lines a phylloid algae mold.
(2) Non ferroan calcite cement #C6 continuing to reduce the mold. In other sample, this cement completely fills phylloid and mollusk molds.
(3) Ferroan calcite cement #C7 fills remaining porosity in the phylloid mold. In other areas of this sample, this cement completely fills allochem molds and fractures.

Figure 4.12 Thin section cathodoluminescent photomicrograph of unstained cement #C6 reducing a phylloid algae mold overlain by cement #C7 in a phylloid algae wackestone. Sample L6.9 in the Lemon 6 Core, Canville Limestone.

Arrow Explanation
(1) Non ferroan calcite cement #C6 lines a phylloid algae mold.
(2) Non ferroan calcite cement #C6 continuing to reduce the mold. In other sample, this cement completely fills phylloid and mollusk molds.
(3) Ferroan calcite cement #C7 fills remaining porosity in the phylloid mold. In other areas of this sample, this cement completely fills allochem molds and fractures.

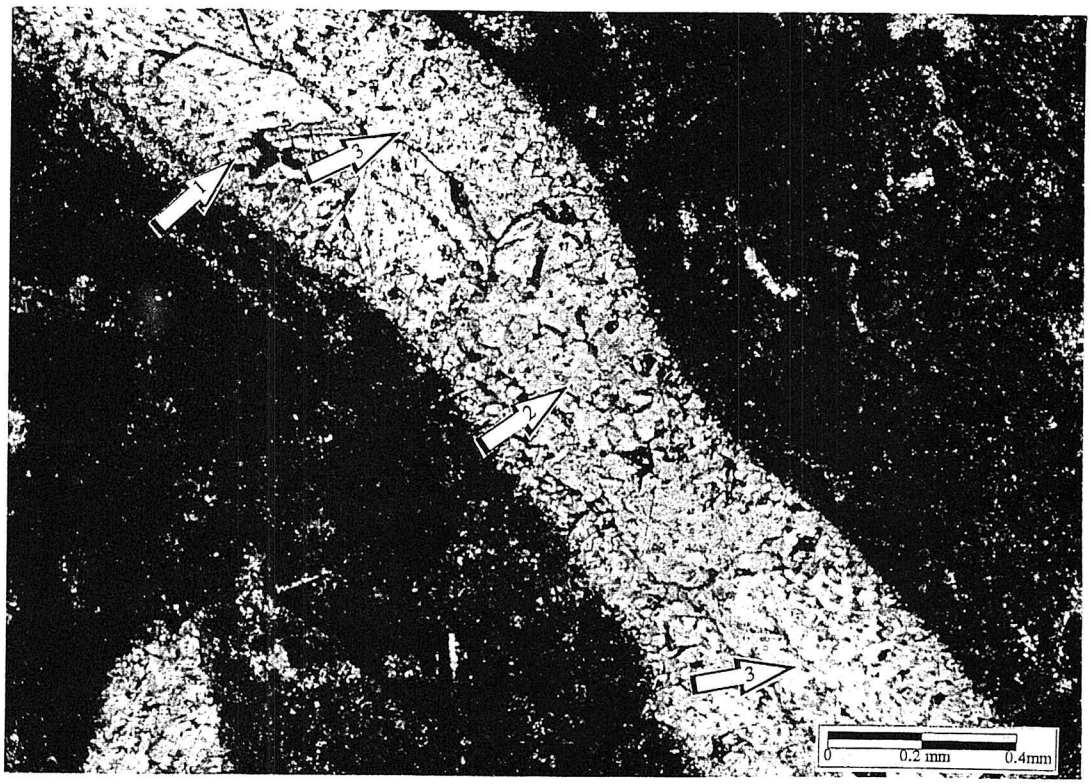
1
3
2
3
0
0.2 mm
0.4mm

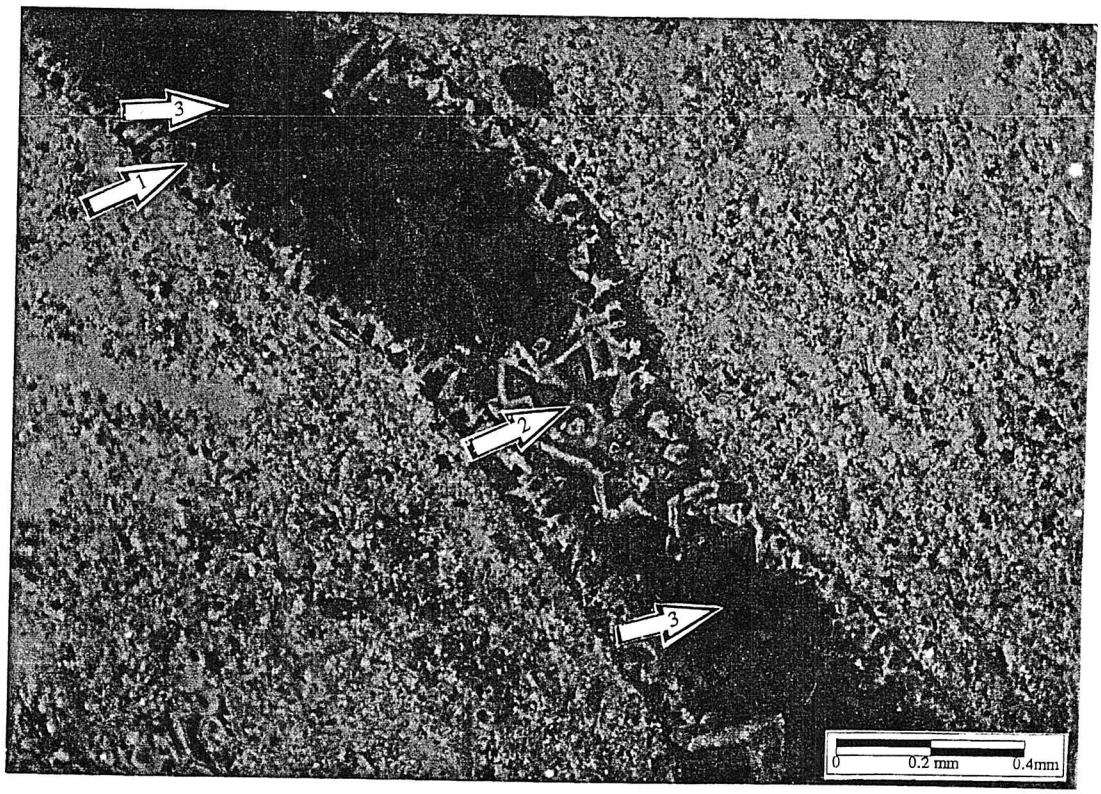
3
1
2
3
0
0.2 mm
0.4mm

### Cement #C7: $PE_{2-3}$, strongly ferroan, nonluminescent calcite.

Ferroan calcite cement #C7 fills phylloid algal and mollusk moldic porosity overlying cement #C6 in the Canville limestone. This cement is also observed filling rhizoliths in the Galesburg shale and moldic porosity in the upper one foot of the Bethany Falls limestone. (Figures 4.13-4.14). Additionally, cement #C7 fills fracture porosity which truncates allochem molds and all other fabrics observed in the Canville limestone. This cement resembles ferroan calcite #C5, however, cement #C7 shows a much stronger ferroan stain than cement #C5 (Figure 4.14).

## Cementation Event E - Ferroan saddle dolomite cementation in the Bethany Falls limestone primary and secondary porosity.

Ferroan saddle dolomite cement #D1 distribution is present throughout the entire Bethany Falls limestone whereas the earlier ferroan calcite cement #C7 is found only in the upper one foot of the the Bethany Falls limestone. Thus, it is likely that a fourth and final dissolution event opened up a new pore system prior to dolomite #D1 precipitation. Ferroan saddle dolomite #D1 is the last cement that reduces primary and secondary porosity in the Bethany Falls limestone reservoir.

### Cement #D1: Unimodal, nonplanar, void filling, nonluminescent, ferroan saddle dolomite cement.

Ferroan saddle dolomite #D1 reduces primary interparticle and secondary moldic, vug and fracture porosity in the Canville limestone, Galesburg shale and Bethany Falls limestone. This cement exhibits a patchy distribution throughout the Bethany Falls limestone extending from the grainstones down into the mud supported lithologies (Figures 4.15 and 4.16). This cement is cut by open fractures and fills fractures as well. This cement is the last cement that reduces but by no means fills all open effective primary and secondary porosity in the Bethany Falls limestone

Figure 4.13 Stained thin section photomicrograph of cements #C5 and #C7 filling rhizoliths in the Galesburg shale paleosol. Sample L12.8 in the Lemon 12 core, Galesburg Shale.

Arrow Explanation
(1) Ferroan calcite cement #C7 overlies ferroan calcite #C5 in a rhizolith mold.

Figure 4.14 Stained thin section photomicrograph of cement #C7 filling secondary porosity in the Bethany Falls oolitic grainstone. Sample L12.5 in the Lemon 12 core, Bethany Falls limestone.

Arrow Explanation
(1) Ferroan calcite cement #C7 fills moldic porosity.

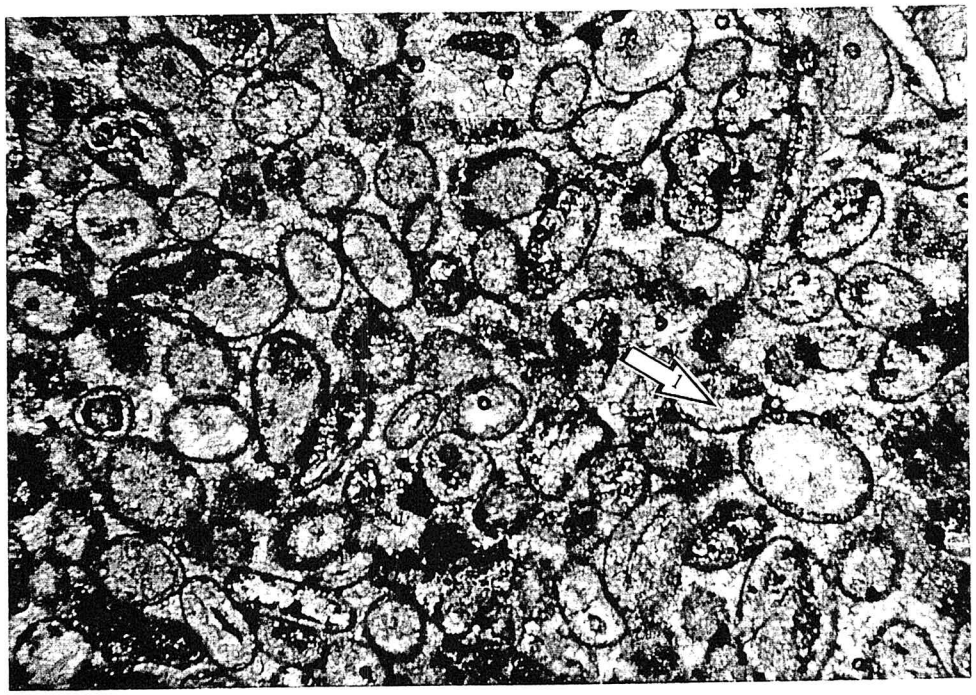

This cement overlies ferroan calcite cement #C5 in vug and moldic pores in the Bethany Falls limestone indicating that this cement is a late event. Dolomite cement D#1 is also truncated by open fractures that connect effective porosity and enhance permeability. Figures 4.15 and 4.16 illustrate the patchy distribution of this dolomite cement.

## Other Diagenetic Phases

### Spar #D2: Polymodal, nonplanar, partially replacing allochems, mimic, ferroan dolomite spar.

This dolomite spar partially replaces ooid laminae and nuclei in the Bethany Falls limestone paleosol zones. Dolomite spar #D2 is polymodal with dolomite microspar preserving crinoid or micritized ooid nuclei while subhedral to anhedral spar replaces ooid laminae and truncates ooid cortices (Figure 4.17). Since this spar is replacing ooids, the superposition criteria used to infer cement precipitation timing cannot be to used to infer when this spar began to replace its host. This spar is only found in the upper 1 foot of the Bethany Falls limestone and does not impact Bethany Falls limestone porosity distribution.

### #S1: Chert replacement.

Chert replacement is non-fabric selective in the Bethany Falls limestone. It replaces allochems, calcite cements and dolomite rhombs in the grainstone lithologies. Figure 4.18 illustrates the replacive nature of this phase. This diagenetic phase is minor in the Bethany Falls limestone and does not impact Bethany Falls limestone porosity distribution.

Figure 4.15 Thin section photomicrograph of saddle dolomite cement #D1 filling primary interparticle and secondary moldic porosity. Sample R2.12 in the Rhoades 2 core, Bethany Falls limestone.

Arrow Explanation
(1) Non ferroan calcite cement #C3 lining primary interparticle porosity.
(2) Ferroan saddle dolomite cement #D1 filling primary interparticle and secondary moldic porosity.
(3) Open fracture truncating cement #D1.

Figure 4.16 Thin section photomicrograph of saddle dolomite cement #D1 filling secondary vuggy porosity in a fossiliferous packstone. Sample L6.3 in the Lemon 6 core, Bethany Falls limestone.

Arrow Explanation
(1) Ferroan saddle dolomite cement #D1 filling secondary vuggy porosity in a fossiliferous packstone.
(2) Effective microvug porosity delineated by blue epoxy.

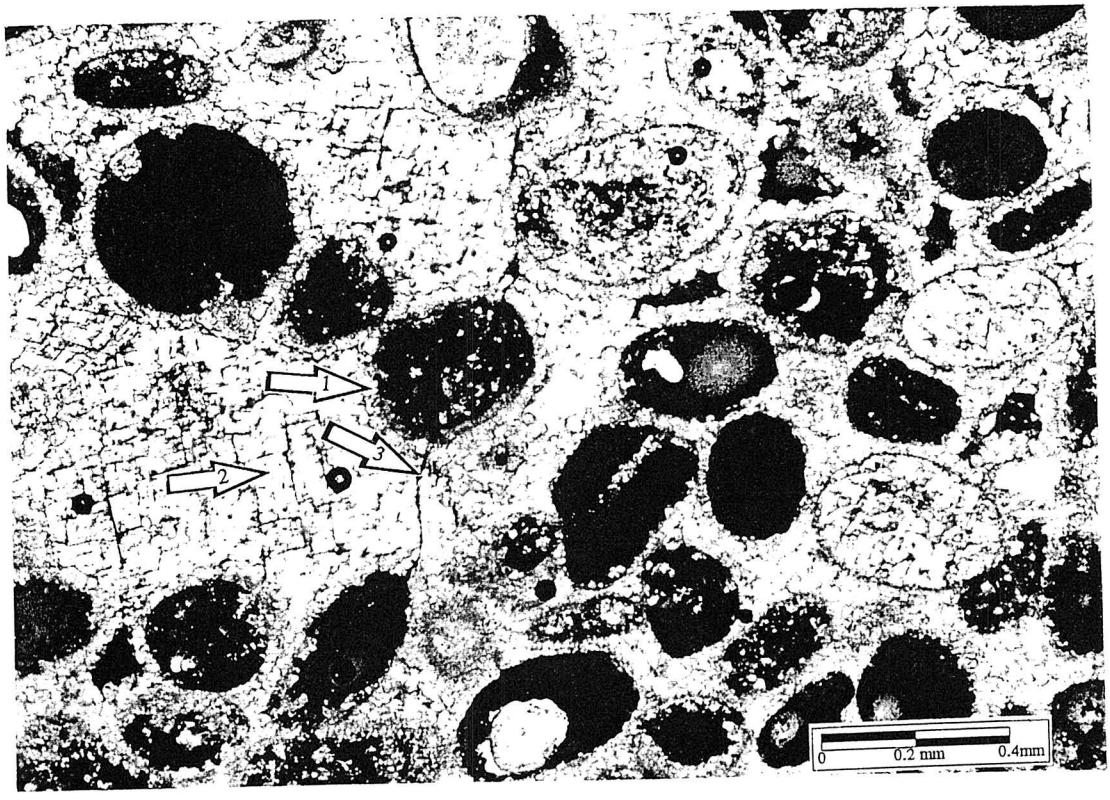
1
2
3
0
0.2 mm
0.4mm

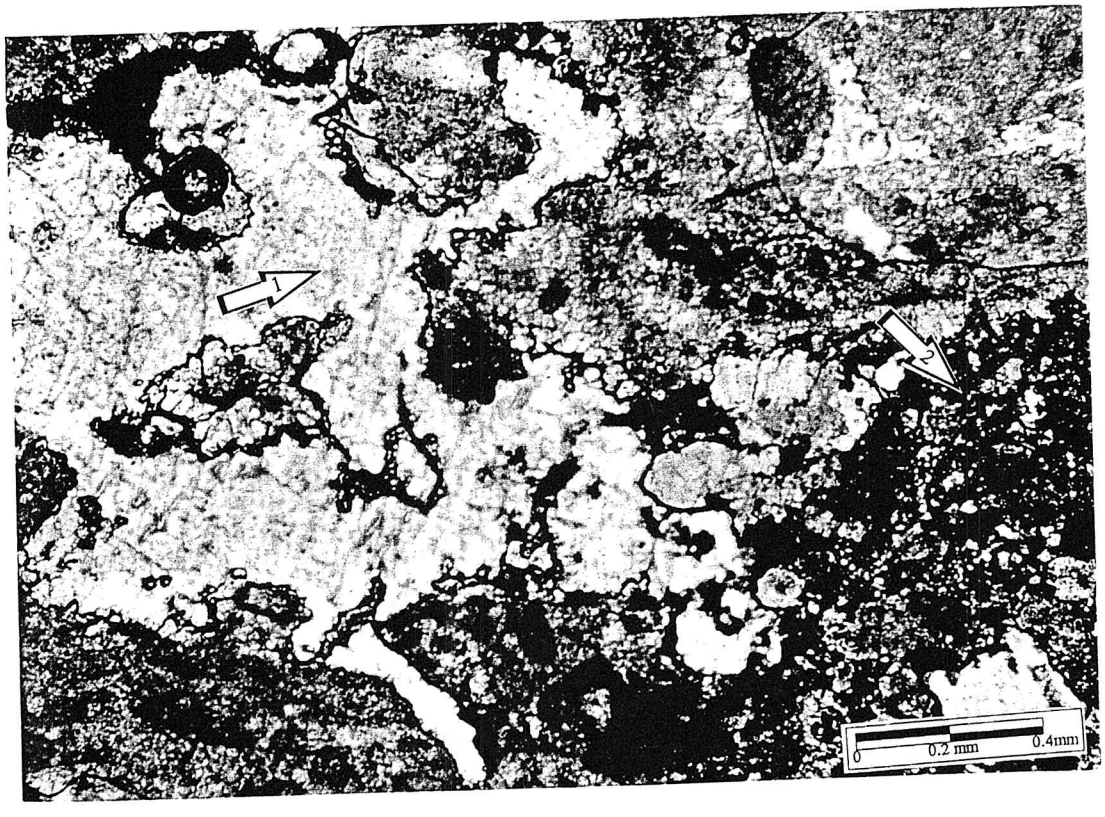
1
2
0
0.2 mm
0.4mm

Figure 4.17: Thin section photomicrograph of dolomite spar #D2 partially replacing an oolite in the Bethany Falls oolitic grainstone paleosol. Sample L6.8 in the Lemon 6 core, Bethany Falls limestone.

Arrow Explanation
(1) Slightly ferroan microcrystalline dolomite spar #D2 partially replacing a crinoid nucleus.
(2) Slightly ferroan dolomite spar #D2 partially replacing ooid laminae.
(3) Alveolar texture

Figure 4.18 Thin section photomicrograph of chert #S1 partially replacing an echinoid grain and cement #C5 in a fossiliferous packstone. Sample L6.4 in the Lemon 6 core, Bethany Falls limestone.

Arrow Explanation
(1) Chert #S1 partially replacing an echinoid grain and dolomite. Rhombic geometry of dolomite is preserved.
(2) Chert #S1 partially replacing cement #C5.

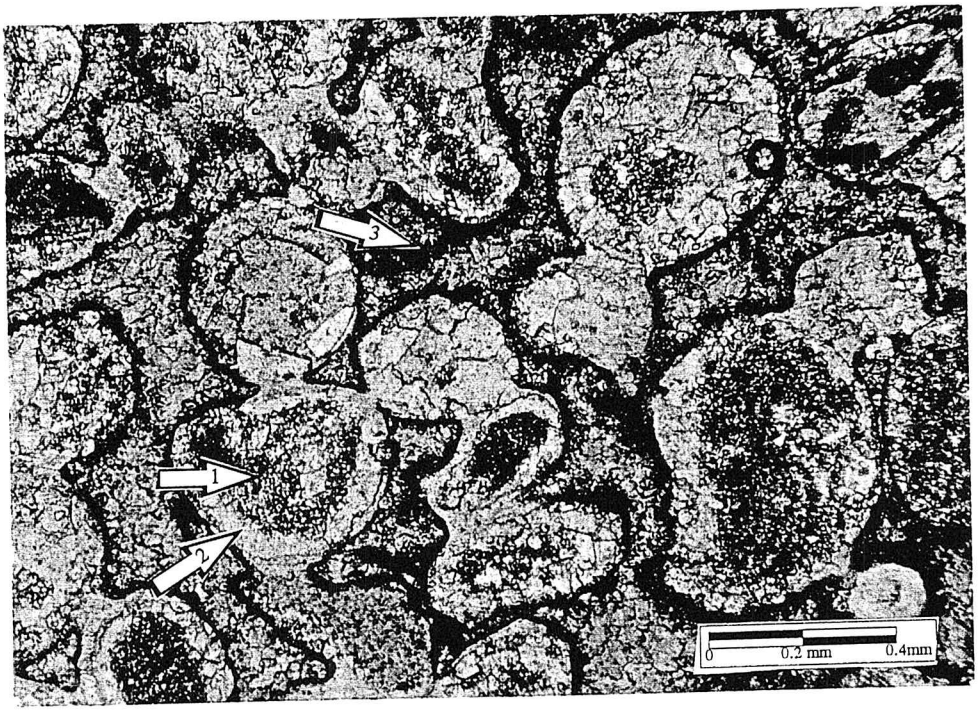
3
1
2
0
0.2 mm
0.4mm

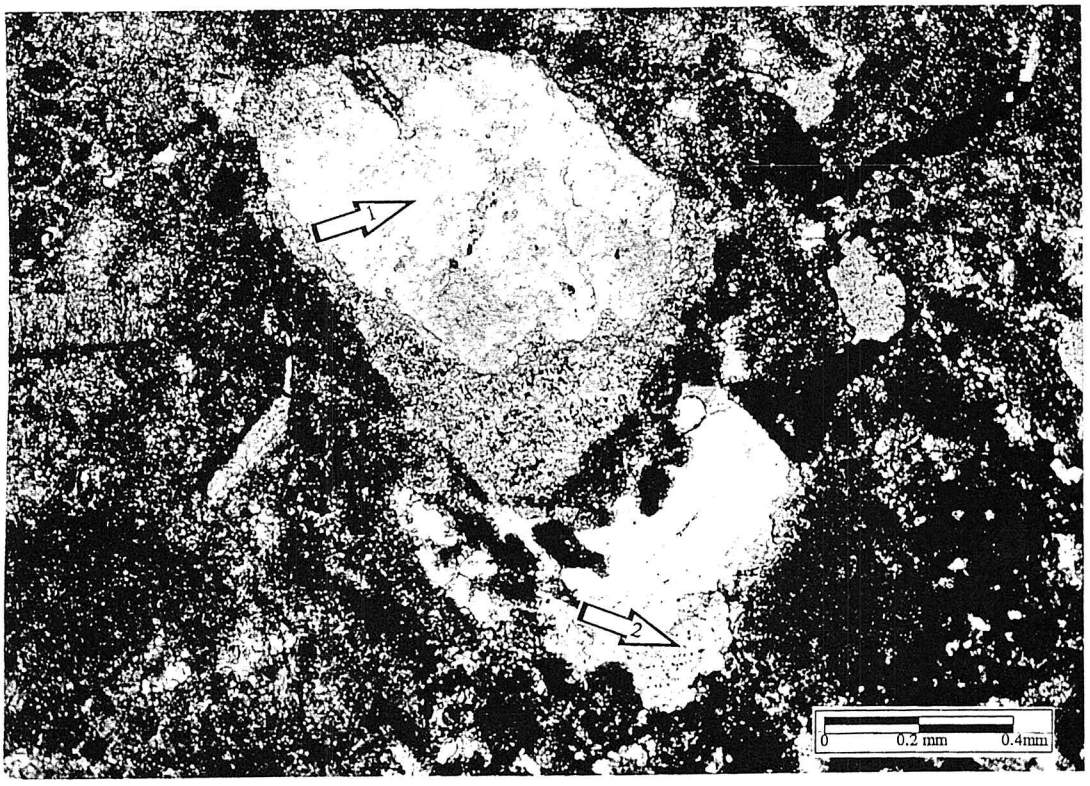
1
2
0
0.2 mm
0.4mm

**Spar #N1: $NE_{1-2}$, non ferroan, nonluminescent calcite spar.**

Neomorphosed ooids are located in the lower portions of the mixed oolitic and bioclastic grainstone lithofacies as oolite packstone intraclasts. Evidence used to identify this spar as neomorphic include: (1) original ooid laminae are visible in the spar and (2) boundaries between spar, ooid nuclei and surrounding micritic matrix is gradational unlike cemented fabrics. This spar also is observed in the mud supported lithologies of the Bethany Falls limestone as microspar which adds to the mottled appearance observed in core. This spar is not significant in the Bethany Falls limestone and does not impact Bethany Falls limestone porosity distribution.

## Porosity and Permeability Enhancement

### Fracturing

Spar filled and open fractures are observed in the Bethany Falls and Canville limestone. In terms of the Bethany Falls limestone reservoir, vertical fracturing appears to enhance permeability by linking effective porosity (Figures 4.19 and 4.20). Fracturing appears to be extensive. Selzer 7-2 (T34S, R20W, Sec. 2) was cored through the Stark shale and vertical fractures were common (Kansas Cores, 1981). Two wells are reported to be productive in the Canville limestone: (1) Baker 1-34 (T33S, R20W, Sec. 34) was perforated in the Canville and Bethany Falls limestone and (2) Selzer 8-2 (T34S, R20W, Sec. 2) was a gas well that was perforated in the Canville limestone. This fracturing system and interpreted late stage dissolution events following Canville limestone deposition and prior to ferroan saddle dolomite cementation may be responsible for porosity and permeability development in the Canville limestone.

Figure 4.19 Thin section photomicrograph of a fracture that connects oomoldic and moldic porosity. Sample R2.12 in the Rhoades 2 core, Bethany Falls limestone.

Arrow Explanation
(1) fracture that connects oomoldic and moldic porosity in the grainstone lithofacies.

Figure 4.20 Thin section photomicrograph of a fracture that connects vuggy porosity in a packstone lithofacies. Sample L6.3 in the Lemon 6 core, Bethany Falls limestone.

Arrow Explanation
(1) Fracture that connects vuggy porosity.

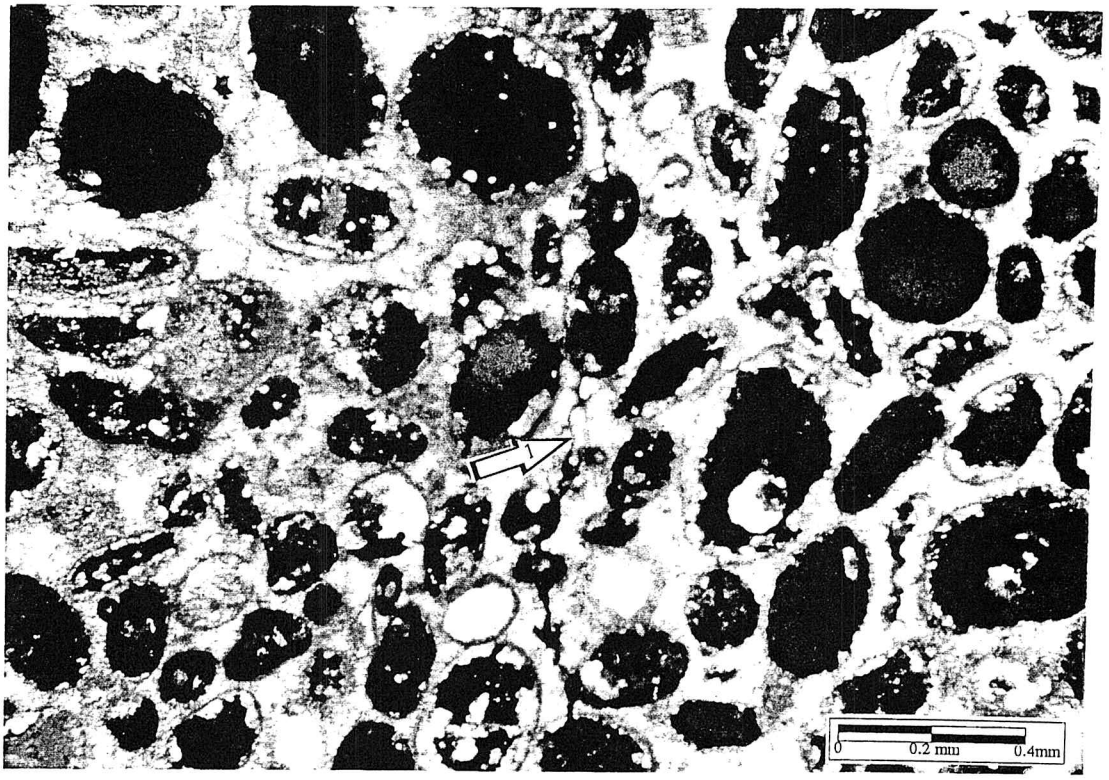
0
0.2 mm
0.4mm

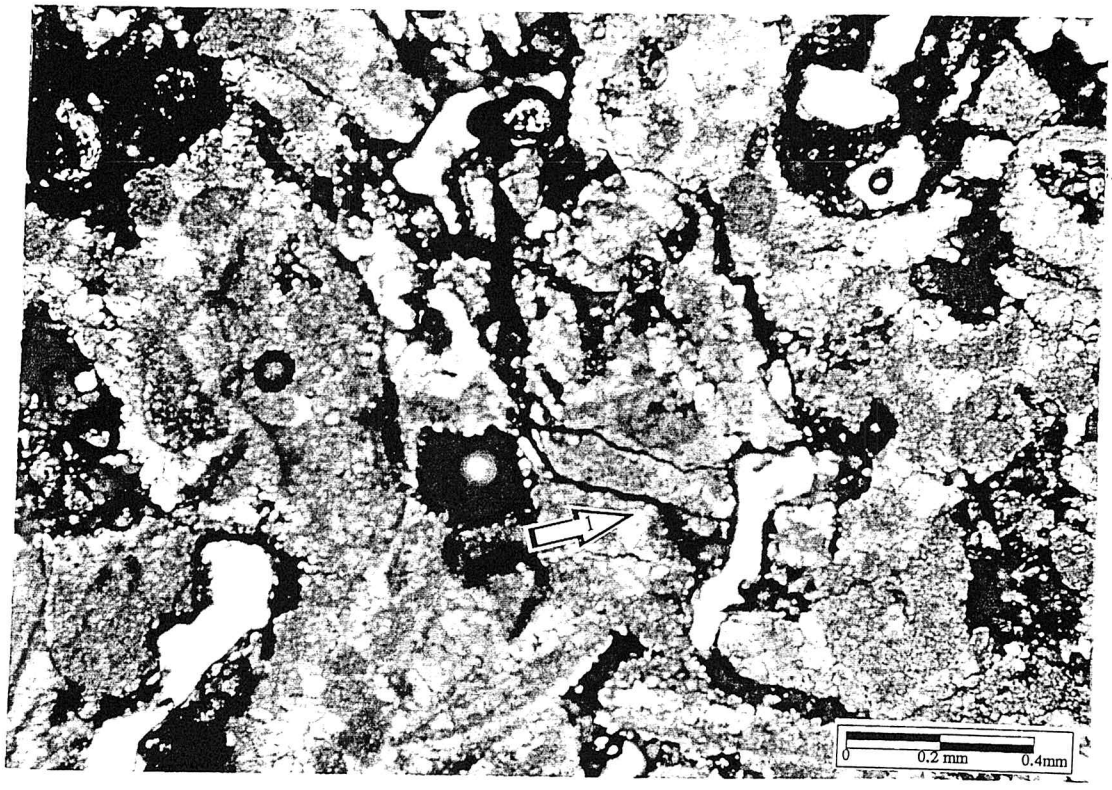
0
0.2 mm
0.4mm

## Bethany Falls Limestone Paragenesis Summary

Combining cement descriptions, thin section macroscopic and microscopic observations and Bethany Falls limestone, Galesburg shale and Canville limestone depositional models led to identification of 14 Bethany Falls limestone reservoir paragenetic events. Bethany Falls limestone paragenesis define diagenetic history, porosity and permeability development of the Collier Flats field (Table 4.2).

| Paragenetic Event | Significant Features or Cements | Cross-cutting Observations | Interpreted Diagenetic Environment | Additional Comments |
|---|---|---|---|---|
| **1) Deposition Of Bethany Falls Limestone**<br><br>***Creation of primary [BP] porosity in the Bethany Falls limestone*** | Oolitic and Bioclastic grainstones are deposited as carbonate sand shoals<br><br>Oolitic packstone lithoclasts are observed in the lower intervals of the grainstones.<br><br>Allochems and lithoclasts are extensively micritized. | Ooid laminae are truncated by abrasion in the lithoclasts.<br><br>The lithoclasts and primary [BP] porosity is reduced by nonferroan calcite cements. | Marine Phreatic<br><br>Formation of coated grains and micritization generally occurs in a marine phreatic diagenetic environment. | |

Table 4.2 Bethany Falls limestone paragenesis.

| Paragenetic Event | Significant Features or Cements | Cross-cutting Observations | Interpreted Diagenetic Environment | Additional Comments |
|---|---|---|---|---|
| **2) Cementation Event A:**<br><br>**Nonferroan calcite #C1, #C2 and #C3 cementation.**<br><br>***Reduction of primary [BP] porosity in the Bethany Falls limestone.*** | Minor isopachous bladed nonferroan calcite cement #C1, reduces primary [BP] porosity.<br><br>Isopachous non-ferroan calcite cement #C2 and #C3 reduce primary [BP] porosity. | All cements are precompactional and are not observed in secondary porosity.<br><br>These cements are restricted to the Bethany Falls limestone.<br><br>These cements are not present in the Bethany Falls or Galesburg shale paleosols. | Marine Phreatic<br><br>Isopachous bladed calcite cement #C1 is overlain by cement #C2. Fluid inclusion data suggest precip-itation below 50 degrees centigrade. | This cementation event must predate the end of Bethany Falls limestone deposition and paleosol formation.<br><br>Bethany Falls limestone primary [BP} porosity remain open after this cementation event. |
| **3) Subaerial Exposure And Dissolution Event #1:**<br><br>**Paleosol formation at the end of Bethany Falls limestone deposition.**<br><br>***Enhancement of primary [BP] porosity and creation of secondary [MO] porosity in the Bethany Falls limestone.*** | Calcrete crust, circumgranular cracking, rhizoliths, and alveolar textures are observed in the top 0.5 foot of the Bethany Falls limestone grainstones.<br><br>Soil formation processes create grain-to-grain contacts in the soil zone on top of the Bethany Falls limestone.<br><br>Enhancement of [BP] porosity and development of [MO] porosity in the Bethany Falls limestone. | Cements #C1-#C3 are not observed in secondary porosity.<br><br>Cement #C4 is observed in Bethany Falls limestone secondary porosity<br><br>These cements are not observed in the overlying lithologies. | Subaerial exposure and paleosol development indicate meteoric diagenesis.<br><br>Meteoric vadose diagenesis in the upper portion of the Bethany Falls grainstones and meteoric phreatic diagenesis in the middle to lower Bethany Falls limestone including the mud-supported lithologies. | |

Table 4.2 Bethany Falls limestone paragenesis (continued).

| Paragenetic Event | Significant Features or Cements | Cross-cutting Observations | Interpreted Diagenetic Environment | Additional Comments |
|---|---|---|---|---|
| **4) Cementation Event B:**<br><br>**Nonferroan calcite #C4 cementation.**<br><br>***Reduction of primary and secondary porosity in the Bethany Falls limestone.*** | Equant non-ferroan, nonlum-inescent calcite cement #C4 lines primary [BP] and secondary [Mo] porosity in the Bethany Falls limestone and paleosol.<br><br>This cement is generally nonluminescent but ends with a bright luminescent band. | This cement lines primary [BP] and secondary [MO] porosity in the Bethany Falls limestone<br><br>This cement is the first cement observed reducing secondary porosity in the Bethany Falls limestone.<br><br>This cement is not observed in the overlying lithologies | Meteoric Phreatic<br><br>Since this cement is limited to the Bethany Falls limestone, it must have been precip-itated prior to deposition of the Galesburg shale and Canville limestone and re-establishment of a marine depo-sitional environ-ment. | Bethany Falls limestone primary [BP} porosity remain open after this cementation event.<br><br>This cement must have precipitated after a dissolution event and paleosol formation at the end of Bethany Falls deposition. |
| **5) Deposition Of The Galesburg Shale.** | Intraclasts from the Bethany Falls limestone are observed at the base of the Galesburg shale. | The Galesburg shale paleosol is observed several feet above the Galesburg shale base. | | |

Table 4.2 Bethany Falls limestone paragenesis continued.

| Paragenetic Event | Significant Features or Cements | Cross-cutting Observations | Interpreted Diagenetic Environment | Additional Comments |
|---|---|---|---|---|
| **6) Subaerial Exposure And Dissolution Event #2:**<br><br>**Paleosol formation in the Galesburg shale.**<br><br>***Enhancement of primary porosity and creation of secondary porosity in the Bethany Falls limestone.*** | Circumgranular cracking and rhizoliths are observed 2-3 feet above the Bethany Falls limestone within the Galesburg shale.<br><br>Enhancement of [BP] porosity and development of [MO] porosity in the Bethany Falls limestone. | Ferroan calcite #C5 is observed in Galesburg shale rhizoliths and Bethany Falls limestone [BP], [MO] and [VUG] porosity.<br><br>Cement #C5 is not observed above the Galesburg shale paleosol.<br><br>Ferroan calcite cement #C7 and ferroan dolomite cement #D1 are observed in the Canville limestone, Galesburg shale and Bethany Falls limestone. | Subaerial exposure and paleosol development indicate meteoric diagenesis.<br><br>Meteoric vadose diagenesis in the upper portion of the Bethany Falls grainstones and meteoric phreatic diagenesis in the middle to lower Bethany Falls limestone including the mud-supported lithologies. | |

Table 4.2 Bethany Falls limestone paragenesis continued.

| Paragenetic Event | Significant Features or Cements | Cross-cutting Observations | Interpreted Diagenetic Environment | Additional Comments |
|---|---|---|---|---|
| **7) Cementation Event C:**<br><br>**Equant ferroan #C5 calcite cementation in the Bethany Falls limestone and Galesburg shale primary and secondary porosity.**<br><br>***Reduction of primary and secondary porosity in the Bethany Falls limestone.*** | Equant nonferroan, zoned luminescent calcite cement #C5 reduces and fills Bethany Falls limestone primary [BP] and secondary [MO] and [VUG] porosity.<br><br>This cement is also observed in the Galesburg shale paleosol. | Ferroan calcite #C7 and saddle dolomite #D1 are observed in the Canville limestone, Galesburg shale and Bethany Falls limestone.<br><br>Cement #C5 is restricted to the Bethany Falls limestone and Galesburg shale.<br><br>Cement #C5 is overlain by dolomite #D1 in Bethany Falls limestone vugs. | Meteoric Phreatic<br><br>Because this cement is limited to the Bethany Falls limestone, Galesburg shale, and Galesburg paleosol, this cement must have precipitated prior to deposition of the remaining Galesburg shale and Canville limestone. | Bethany Falls limestone primary [BP} porosity remain open after this cementation event. |
| **8) Deposition Of The Remaining Galesburg Shale.** | | There are several feet of Galesburg shale above the Galesburg paleosol. | Transition between meteoric and marine diagenetic environments. | |
| **9) Deposition Of Transgressive Canville Limestone** | Creation of phylloid algal wackestone.<br><br>Calcite cements #C6 and #C7 reduce and fill moldic porosity in the Canville limestone. | Calcite cement #C7 and dolomite #D1 are observed reducing moldic porosity in the Canville limestone, Galesburg shale and Bethany Falls limestone. | Marine Phreatic Diagenesis<br><br>Deposition of a open marine Phylloid Algae wackestone indicates marine phreatic diagenesis | Due the sealing nature of the Galesburg Shale, it is not known if re-establishment of the marine phreatic diagenetic environment affected the underlying lithologies. |

Table 4.2 Bethany Falls limestone paragenesis continued.

| Paragenetic Event | Significant Features or Cements | Cross-cutting Observations | Interpreted Diagenetic Environment | Additional Comments |
|---|---|---|---|---|
| **10) Dissolution Event #3:**<br><br>**Creation of secondary [MO] porosity in the Canville limestone, Galesburg shale and Bethany Falls limestone**<br><br>***Possible enhancement of primary and secondary porosity in the Bethany Falls limestone.*** | Creation of phylloid algal and mollusk molds in the Canville limestone.<br><br>Possible enhancement of porosity in the underlying lithologies. | Later cements #C7 and #D1 reduce and fill mold and vug porosity in the Canville limestone, Galesburg shale and Bethany Falls limestone.<br><br>Cement #C6 is restricted to the Canville limestone molds.<br><br>Ferroan calcite cement #C5 is truncated prior to the overlying saddle dolomite #D1 cement in the same pore space. | Burial Diagenesis<br><br>There appears to be no break in sedimentation and progressive burial of Canville limestone by the Stark shale and younger formations.<br><br>Prior to #C6 and #C7 calcite cementation, there must have been a dissolution event because these cements fill secondary porosity in the Canville limestone. | |
| **11) Cementation Event D:**<br><br>**Equant nonferroan #C6 calcite and ferroan #C7 calcite cementation in the Canville limestone, Galesburg shale and Bethany Falls limestone.**<br><br>***Reduction of Bethany Falls Limestone primary and secondary porosity.*** | Equant, nonferroan, calcite cement #C6 reduces and fills phylloid and mollusk molds in the Canville limestone only.<br><br>Equant, ferroan, nonluminescent calcite cement #C7 reduces and fills moldic porosity in the Canville limestone, Galesburg shale and upper one foot of the Bethany Falls limestone. | There is no evidence that there is a break in cementation between nonferroan calcite #C6 and ferroan calcite #C7 since they fill the same pore in the Canville limestone.<br><br>Ferroan saddle dolomite #D1 cement is observed adjacent to this cement but does not fill the same pore spaces. | Burial Diagenesis<br><br>There appears to be no break in sedimentation and progressive burial of Canville limestone by the Stark shale and younger formations. | This cementation event have very little impact on Bethany Falls limestone porosity reduction. |

Table 4.2 Bethany Falls limestone paragenesis continued.

| Paragenetic Event | Significant Features or Cements | Cross-cutting Observations | Interpreted Diagenetic Environment | Additional Comments |
|---|---|---|---|---|
| **12) Dissolution Event #4:**<br><br>**Creation of secondary porosity in the Canville limestone, Galesburg shale and Bethany Falls limestone.**<br><br>***Possible enhancement of primary and secondary porosity in the Bethany Falls limestone.*** | Ferroan saddle dolomite #D1 is observed in the Canville limestone, Galesburg shale and Bethany Falls limestone.<br><br>Dolomite #D1 overlies an etched ferroan calcite #C5 in Bethany Falls vug porosity. | Ferroan saddle dolomite #D1 cement is much more abundant in the Bethany Falls limestone than ferroan calcite #C7 cement and do not fill the same pore spaces. | Burial Diagenesis<br><br>There appears to be no break in sedimentation and progressive burial of Canville limestone by the Stark shale and younger formations. | Because ferroan saddle dolomite #D1 cement is observed adjacent to ferroan calcite #C7 cement but does not fill the same pore spaces, it is likely that a dissolution event opened up a new pore system prior to dolomite #D1 cementation. |
| **13) Cementation Event E:**<br><br>**Precipitation of ferroan saddle dolomite #D1 cement in the Canville limestone, Galesburg shale and Bethany Falls limestone.**<br><br>***Reduction of primary and secondary porosity in the Bethany Falls limestone.*** | Ferroan saddle dolomite #D1 cement is observed in the Canville limestone, Galesburg shale and Bethany Falls limestone.<br><br>Cement #D1 is observed in Bethany Falls primary and secondary porosity in the grainstone lithofacies.<br><br>This cement is also observed reducing secondary porosity in the Bethany Falls packstone and wackestone lithofacies. | Cement #D1 is the second cement that is present in both the Canville and Bethany Falls limestone.<br><br>Dolomite #D1 fills fractures and is truncated by fractures in the Bethany falls limestone.<br><br>This cement overlies ferroan calcite cement #C5 in vug and moldic pores in the Bethany falls limestone. | Burial Diagenesis<br><br>This cement reduces and is truncated by fractures. | Fracturing appears to have been a progressive throughout the rest of the burial history. Open fractures are observed in the regressive and transgressive limestone. |

Table 4.2 Bethany Falls limestone paragenesis continued.

| Paragenetic Event | Significant Features or Cements | Cross-cutting Observations | Interpreted Diagenetic Environment | Additional Comments |
|---|---|---|---|---|
| **14) Fracturing:**<br><br>***Enhancement of primary and secondary porosity and permeability in the Bethany Falls limestone.*** | Open fractures truncate all facrics and cements. | Fracturing is observed truncating and filled by saddle dolomite #D1 cements in the Bethany Falls limestone, Galesburg shale and Canville limestone. | Burial Compaction | |

Table 4.2 Bethany Falls limestone paragenesis continued.

A summary of the Bethany Falls limestone paragenetic events and identification of porosity and permeability development and reduction events are presented in graphical form in Figure 4.21.

Bethany Falls paragenesis suggest four dissolution events have enhanced Bethany Falls limestone reservoir porosity forming a complex pore system of primary and secondary porosity. The final cementation event, ferroan saddle dolomite, fills and reduces primary interparticle and secondary porosity in the Bethany falls grainstone lithofacies. This observation indicates that despite four major cementation events, primary interparticle porosity remains open and is a part of Collier Flats field effective porosity. Additionally, vertical fracturing enhances Bethany Falls limestone reservoir permeability.

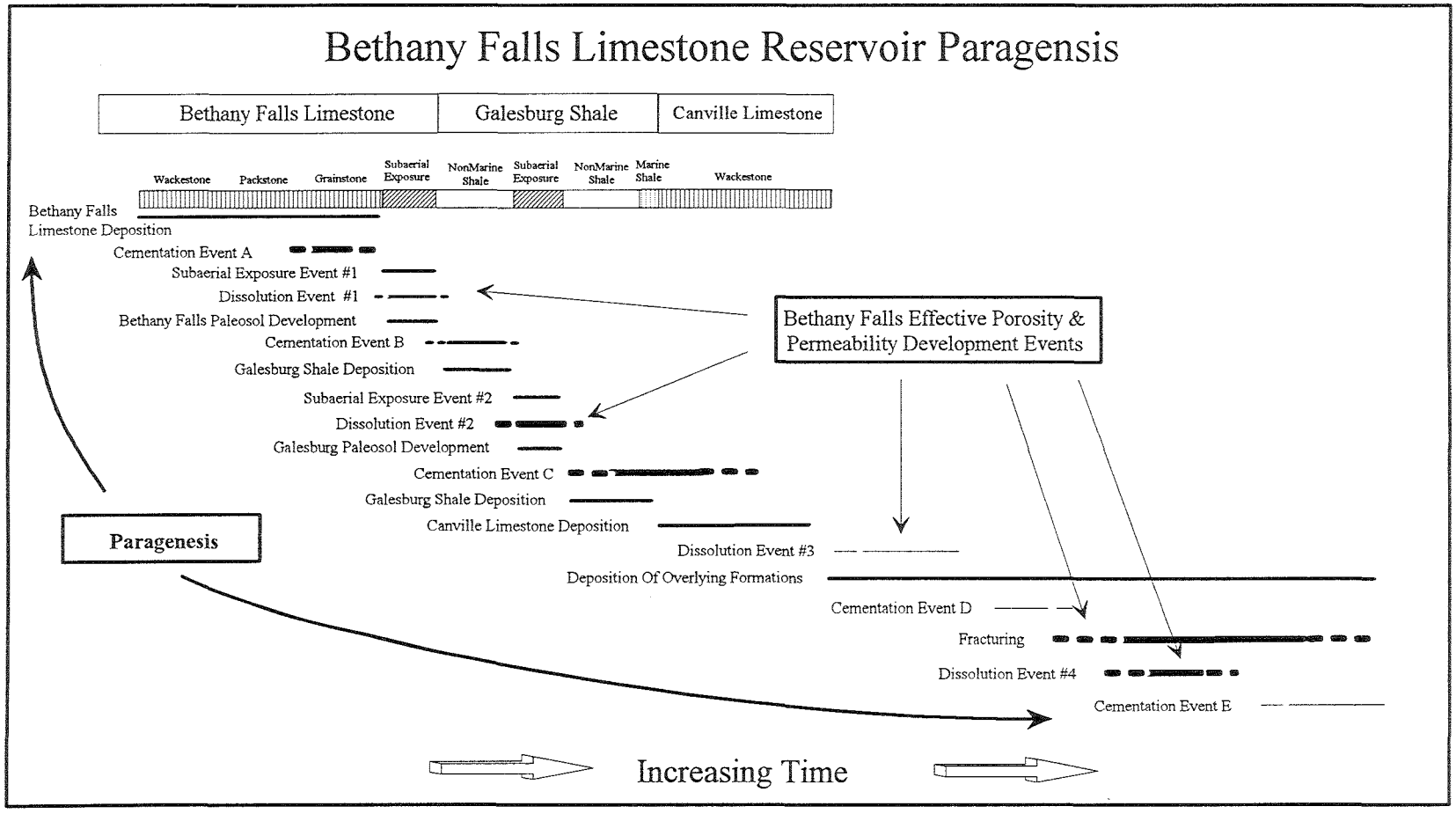


Figure 4.21 Bethany Falls limestone reservoir paragenesis.

## Integrated Bethany Falls Limestone Porosity and Permeability Model

### Bethany Falls Paragenesis And Core Analysis Integration

Quantitative whole core analysis, qualitative thin-section analysis, interpreted paragenetic events and depositional processes are used to create an integrated Bethany Falls limestone porosity and permeability model. Effective and closed pores consist of interparticle, moldic, vug, microvug and fracture pores. Effective porosity is present only in the grainstone lithofacies in the productive Lemon 5, 7 and 10 cores (low permeability cores). Effective porosity is developed in the grainstone, packstone and wackestone lithofacies in the remaining productive cores (high permeability cores). Permeability is also highly variable within and between these cored wells. The foundation for this integrated porosity and permeability model is the recognition and acceptance that overall average permeability for a core can be grouped into two porosity and permeability distributions (high and low permeability) related to depositional environment. Correlation of whole core analysis data with thin-section pore types estimates is used to verify the two porosity and permeability distributions. These porosity and permeability distributions are:

1) **Porosity & Permeability Distribution #1**, Rhoades 1, Lemon 7, Lemon 8 and Lemon 10 low permeability cores. These cores have moderate and high porosity grainstone intervals with low to zero permeability. Underlying mud supported lithologies are non-productive.
2) **Porosity & Permeability Distribution #2,** Lemon 5, Lemon 6, Lemon 11, Rhoades 2 and Rhoades 3 high permeability cores. These cores have high porosity and permeability developed in the grainstone and underlying mud supported lithologies. These cores also have moderate and high porosity grainstone intervals with low to zero permeability.

## Low Permeability Core Observations, Porosity & Permeability Distribution #1

Average porosity and horizontal permeability for low permeability cores are 14% and 3md respectively (Table 4.3). Additionally, many of these cored intervals show good porosity and no permeability indicating permeability heterogeneity exists within individual cores classified as high or low permeability. Individual cored intervals are correlated with thin-section samples noted on core descriptions in Appendix B. Thin-section estimates of open pore types and core-analysis porosity and permeability are presented in Figure 4.22. Relative percentages of these pore types are normalized to 100% and are presented in Table 4.4.

| CORE ANALYSIS DATA | | | | |
|---|---|---|---|---|
| LOW PERMEABLE CORES - Porosity/Permeability Distribution #1 | | | | |
| RHOADES 1 | | | | |
| | Depth | Horiz. k (md) | Vert. k (md) | Porosity (%) |
| | 4766-67 | 0 | 0 | 11.1 |
| | 4767-68 | 22.1 | 9.8 | 16.1 |
| | 4768-69 | 4.6 | 4.6 | 14.2 |
| | 4769-70 | 0 | 0 | 9.6 |
| | | | | |
| LEMON 7 | | | | |
| | Depth | Horiz. k | Vert. k | Porosity |
| | 4793-94 | 1 | 0 | 7.6 |
| | 4794-95 | 0 | 0 | 10.8 |
| | 4795-96 | 0 | 0 | 22.4 |
| | 4796-97 | 0 | 0 | 23.9 |
| | 4797-98 | 1 | 0 | 21.7 |
| | | | | |
| LEMON 8 | | | | |
| | Depth | Horiz. k | Vert. k | Porosity |
| | 4776-77 | 0 | 0 | 7.8 |
| | 4777-78 | 0.8 | 0 | 7.9 |
| | 4778-79 | 1.2 | 0.2 | 7.8 |
| | 4779-80 | 12.1 | 4.6 | 15.1 |
| | 4780-81 | 0 | 0 | 6.1 |
| | 4781-82 | 1 | 0 | 8.6 |
| | 4782-83 | 0 | 0 | 7.4 |
| | 4783-84 | 0 | 0 | 9.6 |
| | | | | |
| LEMON 10 | | | | |
| | Depth | Horiz. k | Vert. k | Porosity |
| | 4773-74 | 23 | 21.6 | 21.6 |
| | 4774-75 | 2 | 2.1 | 25 |
| | 4775-76 | 3 | 2.4 | 28.5 |
| | 4776-77 | 2.1 | 0.8 | 14.8 |
| | 4777-78 | 0 | 0 | 6.7 |
| | | | | |
| AVE | | 3 | 2 | 14 |
| STDEV | | 7 | 5 | 7 |

Table 4.3 Core analysis porosity and permeability data. Low permeability cores. "k" - refers to permeability in millidarcies.

Figure 4.22 illustrates low permeability core observations **(Porosity and Permeability Distribution #1)** from thin-sections with whole core porosity and permeability data. This correlation indicates the most significant pore types are vuggy, moldic and microvugular porosity. Thin section estimates for average moldic, vuggy and microvugular porosity are 39%, 13% and 44% of total porosity for low permeability cores respectively (Table 4.4).

Thin section pore type estimates clearly show samples that are exceptions to the calculated averages. These exceptions are possibly due to natural heterogeneity in biotic constituents in the Bethany Falls reservoir facies. For example, where crinoids bioclasts all primary porosity is filled with syntaxial cements and secondary porosity is absent. Additionally, any particular thin section of the reservoir facies are too small to be representative of the total variance in pore types.

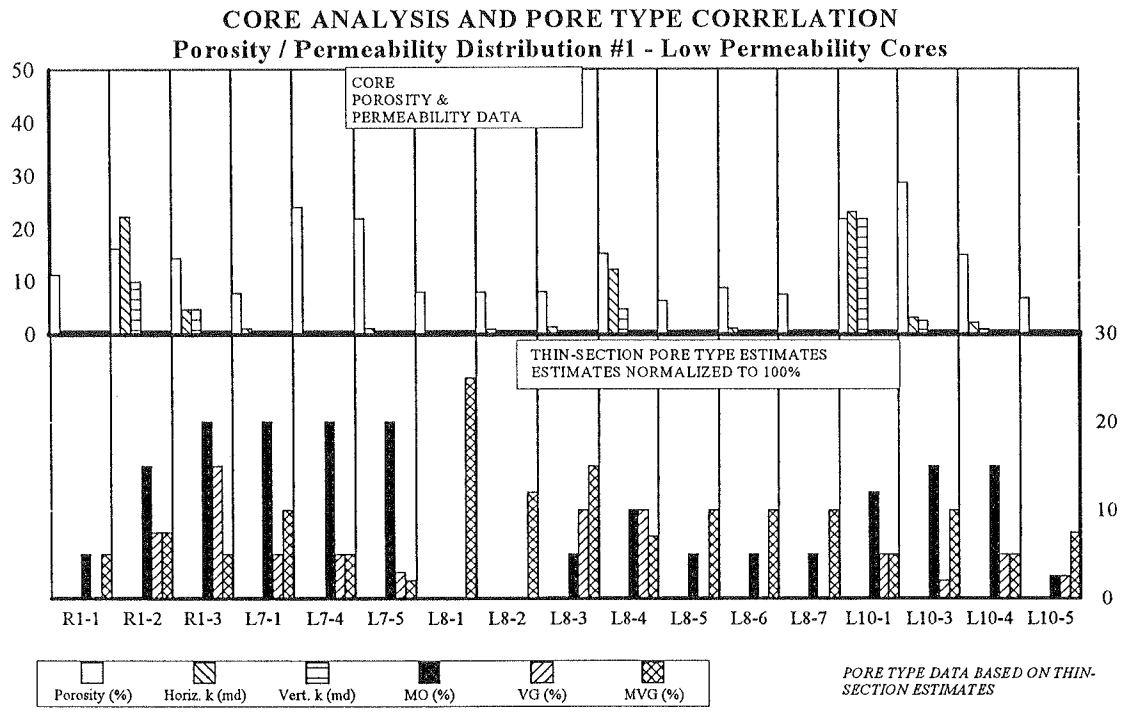


Figure 4.22 Core analysis and pore type estimates for low permeability cores.
This correlation illustrates the low vuggy pore percentage and high moldic porosity percentage ratio trend for low permeability cores in the Lemon Ranch and Rhoades leases of the Collier Flats field. There are exceptions to this trend possibly due to biotic heterogeneity in the Bethany Falls reservoir facies and thin section small sampling scale.

Porosity is in Percent.
Horiz K. is Horizontal permeability in millidarcies.
Vert. K. is Vertical permeability in millidarcies.
MO is moldic porosity percentage of total porosity.
VG is vug porosity percentage of total porosity.
MVG is microvug porosity percentage of total porosity.

| LOW PERMEABLE CORES<br>Porosity/Permeability Distribution #1 | | | | | | HIGH PERMEABLE CORES<br>Porosity/Permeability Distribution #2 | | | | |
|---|---|---|---|---|---|---|---|---|---|---|
| PORE TYPE DATA BASED ON THIN-SECTION ESTIMATES | | | | | | PORE TYPE DATA BASED ON THIN-SECTION ESTIMATES | | | | |
| RELATIVE PERCENTAGE OF PORE TYPES | | | | | | RELATIVE PERCENTAGE OF PORE TYPES | | | | |
| Sample # | MO | VG | MVG | BP | | | MO | VG | MVG | BP |
| | % | % | % | % | | Sample # | % | % | % | % |
| R1-1 | 50 | 0 | 50 | 0 | | R3-1 | 57 | 14 | 14 | 14 |
| R1-2 | 50 | 25 | 25 | 0 | | R3-2 | 46 | 18 | 28 | 9 |
| R1-3 | 44 | 33 | 11 | 11 | | R3-7 | 25 | 25 | 50 | 0 |
| L7-1 | 57 | 14 | 29 | 0 | | R3-10 | 27 | 0 | 73 | 0 |
| L7-4 | 67 | 17 | 17 | 0 | | R2-1 | 40 | 40 | 20 | 0 |
| L7-5 | 80 | 12 | 8 | 0 | | R2-2 | 40 | 40 | 20 | 0 |
| L8-1 | 0 | 0 | 100 | 0 | | R2-4 | 17 | 50 | 33 | 0 |
| L8-2 | 0 | 0 | 100 | 0 | | R2-5 | 17 | 50 | 33 | 0 |
| L8-3 | 17 | 33 | 50 | 0 | | R2-8 | 20 | 40 | 40 | 0 |
| L8-4 | 37 | 37 | 26 | 0 | | R2-9 | 25 | 25 | 50 | 0 |
| L8-5 | 33 | 0 | 67 | 0 | | L5-1 | 43 | 0 | 14 | 43 |
| L8-6 | 33 | 0 | 67 | 0 | | L5-3 | 43 | 0 | 14 | 43 |
| L8-7 | 33 | 0 | 67 | 0 | | L5-4 | 43 | 0 | 14 | 43 |
| L10-1 | 38 | 16 | 16 | 31 | | L6-3 | 35 | 25 | 25 | 15 |
| L10-3 | 52 | 7 | 34 | 7 | | L6-5 | 56 | 11 | 33 | 0 |
| L10-4 | 60 | 20 | 20 | 0 | | L6-8 | 17 | 50 | 33 | 0 |
| L10-5 | 20 | 20 | 60 | 0 | | L6-9 | 17 | 50 | 33 | 0 |
| AVE | 39 | 14 | 44 | 3 | | L11-1 | 31 | 41 | 29 | 0 |
| STDEV | 21 | 13 | 28 | 8 | | L11-3 | 50 | 0 | 50 | 0 |
| | | | | | | L11-4 | 20 | 60 | 20 | 0 |
| | | | | | | L11-5 | 17 | 0 | 83 | 0 |
| | | | | | | AVE | 33 | 26 | 34 | 8 |
| | | | | | | STDEV | 14 | 21 | 19 | 15 |

Table 4.4 Relative percentages of pore types identified in thin-section for low and high permeability cores.
MO - Moldic porosity, VG - Vuggy porosity, MVG - Microvug porosity, BP - Interparticle porosity, AVE - Average and STDEV - Standard Deviation. Sample numbers refer to individual cored intervals that correlate with thin-section data.

The location of low permeability cores are as follows:

- Location of low permeability cores are restricted to the eastern and western margins of Collier Flats production in the Lemon and Rhoades Leases in sections 13 and 14, T34N, R20W (Figure 3.5).

- These low permeability areas correlate with less than 6 feet of low gamma ray well log response (Figure 3.4).
- Net porosity thickness greater than 10% is less than 5 feet (Figure 3.4).
- Porosity and permeability development does not cross Bethany Falls grainstone lithofacies into the lower mud-supported lithologies (Figure 3.4).
- Lemon 7, 8 and 10 cores contain thick porous zones with thin permeability streaks typical of permeability heterogeneity within a individual well (Figure 3.5).

## High Permeability Core Observations, Porosity & Permeability Distribution #2

Average porosity and permeability for high permeability cores are 16% and 43 md respectively (Table 4.5). Many of these cored intervals show good porosity and permeability ranging from zero to several hundred milldarcies indicating permeability heterogeneity exists within individual cores classified as high permeability. Thin-section estimates of the relative percentage of open pore type and core analysis porosity and permeability are presented in Figure 4.23. Relative percentages of open pore types normalized to 100% are presented in Table 4.4.

Figure 4.23 illustrates high permeability core observations **(Porosity and Permeability Distribution #2)** from thin-sections with whole core porosity and permeability data. This correlation indicates the most significant pore types are vuggy, moldic and microvugular porosity. Thin section analysis indicates average moldic, vuggy and microvugular porosity is 33%, 26% and 34% of total porosity for high permeability cores respectively (Table 4.4). As with the low permeability core, thin section pore type estimates

clearly show samples that are exceptions to the calculated averages. These exceptions are also likely due to heterogeneity in the Bethany Falls reservoir facies and thin sections too small to be representative of the variance in pore types. However, there is an average of 13% more open vuggy porosity in these high permeability cores relative to the open vuggy porosity in the low permeability cores. Vug pores aid in connecting open moldic and microvug porosity.

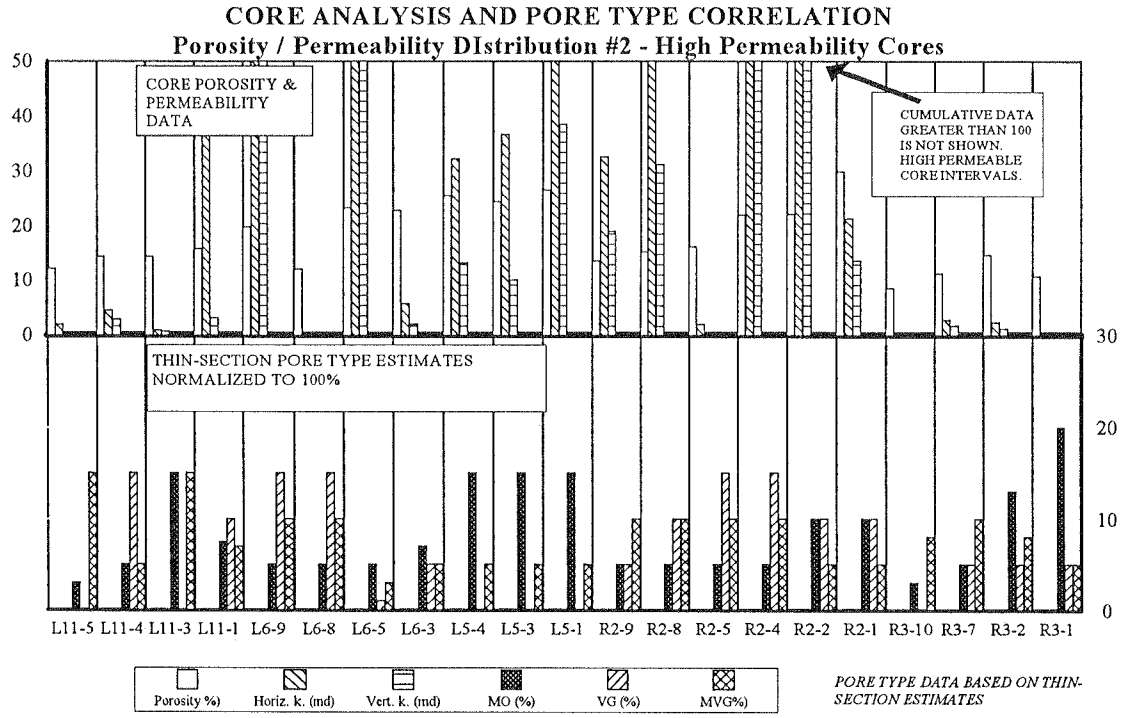


Figure 4.23 Core analysis and pore type correlation for high permeability cores.
This correlation illustrates the high vuggy pore percentage and lower moldic porosity percentage ratio relationship for high permeability cores in the Lemon Ranch and Rhoades leases of the Collier Flats field. There are exceptions to this trend due to heterogeneity in the Bethany Falls lithofacies. Porosity is in Percent.

Horiz K. is Horizontal permeability in millidarcies.
Vert. K. is Vertical permeability in millidarcies.
MO is moldic porosity percentage of total porosity.
VG is vug porosity percentage of total porosity.
MVG is microvug porosity percentage of total porosity.

| CORE ANALYSIS DATA | | | | |
|---|---|---|---|---|
| HIGH POROUS AND PERMEABLE CORES - Porosity / Permeability Distribution #2 | | | | |
| RHOADES 3 | | | | |
| | Depth | Horiz. k (md) | Vert. k (md) | Porosity (%) |
| | 4772-73 | 0 | 0 | 10.8 |
| | 4773-74 | 2.4 | 1.2 | 14.6 |
| | 4774-75 | 2.2 | 0.8 | 19.9 |
| | 4775-76 | 67.9 | 55.2 | 23.2 |
| | 4776-77 | 22.1 | 7.4 | 17.8 |
| | 4777-78 | 0 | 0 | 5.8 |
| | 4778-79 | 2.9 | 1.8 | 11.2 |
| | 4779-80 | 4.7 | 3 | 11.7 |
| | 4780-81 | 0 | 0 | 9.7 |
| | 4781-82 | 0 | 0 | 8.6 |
| | 4782-83 | 0 | 0 | 8.5 |
| RHOADES 2 | | | | |
| | Depth | Horiz. k | Vert. k | Porosity |
| | 4755-56 | 21.3 | 13.6 | 29.9 |
| | 4756-57 | 140 | 130 | 22.1 |
| | 4757-58 | 110 | 55.2 | 19.3 |
| | 4758-59 | 300 | 125 | 22 |
| | 4759-60 | 2.1 | 0 | 16.1 |
| | 4760-61 | 51.6 | 32.8 | 16.5 |
| | 4761-62 | 48.2 | 39.6 | 16.8 |
| | 4762-63 | 56.1 | 31.2 | 15.2 |
| | 4763-64 | 32.6 | 18.9 | 13.6 |
| | 4764-65 | 0 | 0 | 10.3 |
| LEMON 5 | | | | |
| | Depth | Horiz. k | Vert. k | Porosity |
| | 4784-85 | 77.8 | 38.5 | 26.5 |
| | 4785-86 | 0 | 0 | 10.2 |
| | 4786-87 | 36.6 | 10.1 | 24.4 |
| | 4787-88 | 32.2 | 13.2 | 25.5 |
| LEMON 6 | | | | |
| | Depth | Horiz. k | Vert. k | Porosity |
| | 4781-82 | 10.1 | 1 | 29.7 |
| | 4782-83 | 8 | 4.2 | 20.7 |
| | 4783-84 | 5.8 | 2.1 | 22.8 |
| | 4784-85 | 22.5 | 7.4 | 16.5 |
| | 4785-86 | 130 | 57 | 23.2 |
| | 4786-87 | 130 | 120 | 19.2 |
| | 4787-88 | 26.7 | 32.2 | 17.8 |
| | 4788-89 | 0 | 0 | 12 |
| | 4789-90 | 280 | 280 | 19.7 |
| | 4790-91 | 0 | 0 | 12.4 |
| | 4791-92 | 0 | 0 | 6.9 |
| LEMON 11 | | | | |
| | Depth | Horiz. k | Vert. k | Porosity |
| | 4758-59 | 43.8 | 3.2 | 15.8 |
| | 4759-60 | 125 | 62.7 | 15.6 |
| | 4760-61 | 1 | 0.8 | 14.4 |
| | 4761-62 | 4.6 | 3 | 14.4 |
| | 4762-63 | 2.1 | 0 | 12.2 |
| | 4763-64 | 0 | 0 | 7.7 |
| | | | | |
| | AVE | 43 | 27 | 16 |
| | STDEV | 70 | 53 | 6 |

Table 4.5 Core analysis porosity and permeability data. High permeable cores. "k" - refers to permeability in millidarcies.

Microvug porosity is observed in micritized allochem shell walls in the grainstone lithofacies and appears as a "moth-eaten" fabric in packstone and wackestone lithofacies.

The location of the high permeability cores correlate with:

- Areas in the Lemon and Rhoades leases where the Bethany Falls grainstone shoals are thicker than 6 feet.
- Net thickness of low gamma ray well log response (lowest 12 API Gamma Ray units) is more than 6 feet (Figure 3.4).
- Net porosity thickness with porosity greater than 10% is more than 5 feet thick (Figure 3.4).
- Core porosity and permeability development cross lithologic boundaries from the Bethany Falls grainstones down into the mud supported lithologies (Figure 3.4).

## Bethany Falls Limestone Reservoir Porosity and Permeability Model Summary

### Depositional Environment Component

Where Bethany Falls grainstone shoals are not present, porosity is generally very low and permeability is less than one millidarcy (Lemon 4 and Lemon 2x cores), leading to nonproductive wells. In cores where grainstone lithofacies are present, all other cored wells, porosity and permeability is present leading to productive wells. Thus, the presence of Bethany Falls grainstone lithofacies is essential for effective porosity and permeability development.

Areas with the thickest low gamma ray well log responses correlate with cores that are characterized as high permeability, *porosity and permeability distribution #2* (Lemon 6, Lemon 3, Rhoades 2 and Rhoades 3), and correspond to thick, greater than 5 feet, grainstone sand shoals. In these cores, high porosity and permeability is also observed in the packstone and wackestone lithologies below the grainstone lithofacies. Cores characterized as low permeability, *porosity and permeability distribution #1*, were recovered on the eastern, southern and western margins of the grainstone sand shoals in the Lemon and Rhoades leases and correlate with thin low gamma ray well log responses, less than 5 feet.

In high permeability cores, *porosity and permeability distribution #2*, moldic to vug pore type ratio average approximately 1.3 to 1. In the low permeability cores, *porosity and permeability distribution #1*, moldic to vug pore type ratio average approximately 2.8 to 1 (Table 4.4). The vug to moldic pore type ratio trends clearly has an effect on porosity and permeability.

It is likely that primary porosity in the Bethany Falls grainstone sand shoals provided a pathway for fluids undersaturated with respect to $CaCO_3$ to focus carbonate dissolution in the thicker portions of the carbonate sand shoals. The thicker portions of the carbonate sand shoals would have been a topographic high area where a freshwater lens would have been

present during subaerial exposure and meteoric diagenesis of the Bethany Falls limestone. Thus, the geometry of the Bethany Falls carbonate sand shoals, location of the freshwater lens and primary interparticle porosity likely influenced effective porosity development and creation of two porosity and permeability distributions.

### Dissolution Event 1: Creation of Bethany Falls Secondary Porosity in the Grainstone Lithofacies

Bethany Falls limestone paragenesis includes four dissolution events responsible for Bethany Falls limestone porosity formation. It is likely that the first dissolution event was related to subaerial exposure and meteoric diagenesis at the end of Bethany Falls limestone deposition. Dissolution Event #1 appears to have impacted only Bethany Falls limestone grainstone lithofacies. Cementation Event "B", the first cement to reduce secondary porosity in the Bethany Falls limestone, generally lines moldic and interparticle porosity in the Bethany Falls limestone grainstones. Galesburg shale deposition followed subaerial exposure and meteoric diagenesis indicating that Cementation Event "B" is also the result of meteoric diagenesis. Because Cementation Event "B" is present in only the Bethany Falls grainstone lithofacies, it is likely that the observed secondary porosity in the packstone and wackestone lithologies did not develop from Dissolution Event #1.

### Dissolution Event 2: Creation of Bethany Falls Secondary Porosity in the Grainstone, Packstone and Wackestone Lithofacies

Dissolution Event #2 is related to subaerial exposure and meteoric diagenesis during Galesburg shale deposition. Dissolution Event #2 created secondary porosity in the Bethany Falls grainstones and underlying packstone and wackestone lithologies. Cementation Event "C", which followed Dissolution Event #2, is a ferroan calcite cement that reduces and fills secondary porosity in the Galesburg shale paleosol, Bethany Falls primary and secondary porosity in the grainstones and secondary porosity in the underlying packstone and wackestone lithologies. Cementation Event "C" is also a meteoric cement because it formed during and

after Galesburg shale deposition and subaerial exposure. However, cement #C5 is truncated by a later dissolution event indicating a percentage of primary and secondary porosity must have remained open for the later diagenetic pore fluids.

### Dissolution Event 3: Minor Enhancement of Bethany Falls Secondary Porosity in the Grainstone Lithofacies?

Dissolution Event #3 is interpreted to have occurred after deposition of the overlying Canville limestone. Dissolution Event #3 is a major diagenetic event that created Canville limestone and Galesburg shale moldic porosity. However, it is only a minor event that created secondary porosity in the upper one foot of the Bethany Falls grainstone lithofacies.

Cementation Event "D" which followed Dissolution Event #3 consists of nonferroan calcite cement #C6 that reduces and fills moldic porosity in the Canville phylloid algal wackestones only. This cement is overlain by ferroan calcite cement #C7 that fills the same Canville limestone moldic pores and fractures. Cement #C7 is also observed filling Galesburg shale rhizoliths and moldic porosity in the upper one foot of the Bethany Falls grainstones. Cement #C7 has a strong ferroan stain and is observed filling fractures in the Canville limestone suggesting this cement was precipitated after burial and lithification of the Canville limestone. Because these two cements fill the same pores and there is no evidence that a dissolution event separates them they are lumped together as one cementation event.

Assuming the distribution of Cementation Event "D" cements reflects filling of pores created by Dissolution Event #3, it is likely that this dissolution event followed burial of the Canville limestone by the Stark Shale and overlying lithologies.. This dissolution event created moldic porosity in the Canville limestone that extended down into the Galesburg shale and the upper one foot of the Bethany Falls limestone. Thus, it is interpreted that Dissolution Event #3 is a minor Bethany Falls limestone diagenetic event that had a minor impact on Bethany Falls limestone reservoir.

### Dissolution Event 4: Creation of Additional Bethany Falls Effective Porosity In The Grainstone, Packstone and Wackestone Lithofacies

Dissolution Event #4 is interpreted to have occurred after deposition, burial and fracturing of the overlying Canville limestone and prior to ferroan saddle dolomite cementation, Cementation Event E. Ferroan saddle dolomite cements reduce pores created or modified by Dissolution Event #4. These pores include: (1) primary and secondary pores in the Bethany Falls grainstone lithofacies, (2) secondary pores in the Bethany Falls packstone and wackestone lithofacies, (3) secondary pores in the overlying Canville limestone and Galesburg shale and (4) fracture pores in the Bethany Falls limestone, Galesburg shale and Canville limestone. Based on the distribution of ferroan saddle dolomite, Dissolution Event #4 is very different from prior dissolution events because Dissolution Event #4 created or enhanced porosity in all the cored intervals. This dissolution event is interpreted to be responsible for a majority of Bethany Falls limestone reservoir effective porosity because saddle dolomite is the only cement that reduces effective porosity in the Bethany Falls limestone reservoir. There are several lines of evidence for a fourth dissolution event:

(1) Cement #C7 which fills secondary pores created by Dissolution Event #3 in the Canville limestone, Galesburg shale and upper one foot of the Bethany Falls grainstone lithofacies is not present in the lower portions of the Bethany Falls limestone.

(2) Cement #C7 is not overlain by dolomite #D1 in the same secondary pores. Both cements are the only cements observed in the Canville limestone, Galesburg shale and Bethany Falls limestone.

(3) Cementation Event E, ferroan saddle dolomite #D1, is observed overlying cement #C5 in the same vug pores in the Bethany Falls limestone. Additionally, cement #C7 is observed alone in secondary pores of the Bethany Falls limestone.

(4) Saddle Dolomite #D1 is the only cement observed reducing effective porosity. Effective porosity was identified as pores filled with blue epoxy in thin-sections.

It is likely that the higher vug to moldic porosity ratio observed in the high permeability cores of the Bethany Falls reservoir is the result of enhancement of primary porosity and pre-existing moldic and vug porosity caused by Dissolution Event #4. There are two possibilities as to why creation and enhancement of effective porosity would likely occur in the thickest portions of the Bethany Falls grainstone sand shoals: (1) the thickest areas of the Bethany Falls carbonate sand shoals developed over a flexural zone that would likely produce fractures along the crest of the plunging anticline structure forming a conduit for migration of burial diagenetic fluids and (2) a higher percentage of primary interparticle porosity was preserved in the thick carbonate sand shoals which provide a higher volume of pores for burial diagenetic fluid migration.

### Fracturing: Enhancement of Bethany Falls Permeability

Late stage fracturing caused by burial and compaction of the Bethany Falls limestone and formation of the Collier Flats field plunging anticlinal structure is a additional component to the late stage diagenetic fluids responsible for permeability enhancement in the Bethany Falls limestone reservoir. Fractures are filled by cements from Cementation Events "D" and "E". Open fractures are also observed truncating all cements and fabrics indicating fracturing occurred late in the diagenetic history of this reservoir. The impact of fracturing is quantified in core data because whole core analysis was used to obtain porosity and permeability data.

### Conclusions

These observations and interpretations will provide the criteria for classifying and subdividing the entire Collier Flats field into high and low permeable zones. Each of these zones will require individual porosity, permeability and water saturation correlations. These correlations will allow reservoir characterization of the Collier Flats field which is essential for evaluating enhanced oil recovery potential and simulating primary oil production.

| Reservoir Heterogeneity Type | Reservoir Continuity | Horizontal Sweep Efficiency | Vertical Sweep Efficiency | Residual Oil Saturation | Rock / Fluid Interaction |
|---|---|---|---|---|---|
| Sealing Fault | X | X | | | |
| Semi-sealing Fault | (X) | X | X | | |
| Non-Sealing Fault | (X) | X | X | | |
| Boundaries Genetic Units | X | X | X | | |
| Permeability Zonation Within Genetic Units | | (X) | X | (X) | |
| Baffles Within Genetic Units | | (X) | X | (X) | |
| Lamination | | (X) | (X) | X | |
| Cross-bedding | | | | | |
| Microscopic Heterogeneity | | | | X | (X) |
| Textural Types | | | | X | X |
| Mineralogy | | | | | X |
| Fracturing - Tight | | (X) | | X | |
| Fracturing - Open | | X | X | X | |
| X - Strong Effect<br>(X) - Moderate Effect | | | | | |

Table 5.1: Significance of Reservoir Heterogeneity Type (modified after Weber, 1986).

At some point during the development and management of an oil field, decisions are made on how to increase the life of a field through infill drilling, workovers, stimulation or implementing enhanced oil recovery technologies. Key to these activities is a reassessment of geological and engineering data to better understand and delineate reservoir heterogeneity. Reservoir heterogeneity is a possible cause for poor primary production performance and failure of enhanced oil recovery projects. Reservoir heterogeneity is controlled by geological processes. Thus, various types and scales of reservoir heterogeneity can be inferred through combining geologic and reservoir engineering data to develop an integrated reservoir model. For the purpose of this investigation, this process is referred to as a reservoir characterization.

Research conducted by the Tertiary Oil Recovery Project (TORP) on analogous carbonate reservoirs to that present in the Collier Flats field have documented that low waterflood sweep efficiency is a typical problem encountered by independent operators. Low sweep efficiency has led to bypassing of significant amounts of petroleum and reduction of the economic life of Kansas oil fields (Schoeling et al., 1988). The following reservoir characterization is an attempt to provide the operators of the Collier Flats field and TORP with the best possible information to assess the potential for implementing enhanced oil recovery technologies to prolong the economic life of Collier Flats field. Additionally, it is hoped that the methodology and results of this reservoir characterization can be applied to other analogous Lansing-Kansas City carbonate reservoirs.

## Reservoir Characterization Methodology

This reservoir characterization integrates depositional and diagenetic models with reservoir engineering data obtained from cores in the Collier Flats field. The objective of this reservoir characterization is to identify porosity and permeability distributions, revised water saturation data and reservoir heterogeneity. An accurate characterization of the porosity and permeability distribution is crucial to evaluating EOR potential and defining reservoir flow units for the Collier Flats field. In the Bethany Falls porosity and permeability development section, it is hypothesized that Bethany Falls limestone cores can be combined into two catagories, low and high average permeability, which are related to depositional and diagenetic processes:

- Low average permeability cores ***(Porosity and Permeability Distribution #1)*** are restricted to the margins of grainstone shoals where carbonate diagenesis is responsible for effective porosity development. The relative percentage of open moldic vuggy porosity average approximately 2.8 to 1.

- High average permeability cores *(Porosity and Permeability Distribution #2)* are restricted to the thickest portions of the grainstone shoals where carbonate diagenesis is responsible for a majority of effective porosity development. The relative percentage of open moldic to vuggy porosity average approximately 1.3 to 1.

These two porosity and permeability distributions are integrated with wireline well logs, production, drill stem tests and scout ticket data to identify trends and or relationships between general oil field data and the Collier Flats geological models. These correlations and relationships are used to verify and test the initial classification of all the wells in the Collier Flats field as either high or low average permeability based on the geologic models. Additionally, the cementation factor used in the Archie water saturation equation is modified to compensate for the high percentage of secondary porosity. This exercise will also better characterize Collier Flats pay-zone attributes leading to revised reserve estimates that will impact EOR economics. The following geologic and engineering data are integrated in this reservoir characterization:

| Geologic Data | Reservoir Engineering Data |
|---|---|
| • Paleogeography Model<br>• Depositional Model | • Core Analysis: Porosity, Permeability & Water saturation |
| • Diagenetic Model | • Reservoir Fluid Analysis |
| • Porosity and Permeability Development Model | • Drill Stem Test and Other Pressure Data<br>• Production |
| • Core Descriptions | • Reserves |
| • Well Logs | • Waterflood Feasibility Analysis |

Table 5.2: Reservoir characterization data sources.

## Geologic Criteria Used For Oil Well Classification As High or Low Permeability

The foundation for classifying Collier Flats oil wells as high or low permeability for this reservoir characterization is based on macroscopic observations of core analysis data correlated with well log data in the Lemon and Rhoades leases, sections 13 and 14, T34S, R20W (Figures 3.4 & 3.5). Core observations show oil wells with high permeability correlates with:

- a net thickness of lowest 12 API gamma-ray units (shoal water facies) greater than 6 feet,
- and net thickness of porosity greater than 10%, greater than 5 feet. (Figure 5.2).

This correlation shows that high porosity and permeability is confined to the thickest areas of the Bethany Falls grainstone shoals in the Lemon and Rhoades leases. Gamma-ray wireline well-log curves are presented with density porosity curves (Figures 5.3 & 5.4). The shape and deflection character of the gamma ray curves is used to corroborate initial classification of Collier Flats field oil wells based on gamma ray and density porosity isopach data (Figures 5.3 & 5.4). Net thickness of low gamma-ray facies, net thickness of porosity > 10% and gamma-ray log signatures provide quantitative criteria for classification of Collier Flats field oil wells as either high permeability wells (wells with high porosity and permeability, Table 4.5) or low permeability wells (wells with low to moderate porosity and low permeability, Table 4.3). This information is also correlated with the geologic models that interpret porosity and permeability development. Porosity and gamma-ray criteria used to classify Collier Flats oil wells are as follows:

| Porosity & Gamma Ray Criteria | High Permeability Oil Well | Low Permeability Oil Well |
|---|---|---|
| Net Thickness of Low Gamma-Ray Facies (Shoal Water Facies) | ≥6 feet of low gamma-ray facies (shoal water facies). | ≤6 feet of low gamma-ray facies (shoal water facies). |

Table 5.3: Porosity, gamma-ray and geologic criteria used to classify Collier Flats oil wells.

| Porosity & Gamma Ray Criteria | High Permeability Oil Well | Low Permeability Oil Well |
|---|---|---|
| Net Thickness of Porosity Greater Than 10% | ≥5 feet of Porosity > 10% | ≤ 5 feet of Porosity > 10% |
| Gamma-Ray Log Signatures | 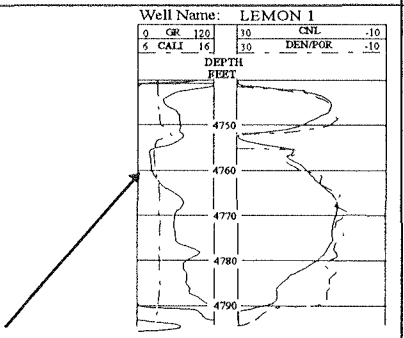 Strong relative deflection to low gamma-ray values (0-30 API). | 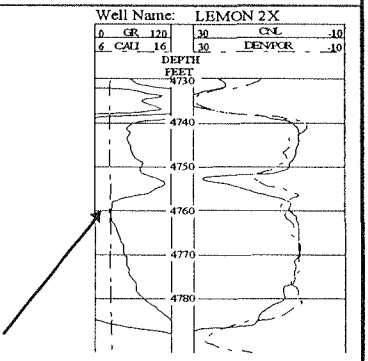 Minor deflection to low gamma-ray values (0-30 API). |
| Geologic Depositional Model | Located in the center portion of the clean carbonate sand shoals. | Located at the margins of the clean carbonate sand shoals. |
| Geologic Diagenetic Model | The thickest portions of the clean carbonate sand shoals were areas of intense carbonate dissolution and creation of secondary effective porosity. Moldic to vug porosity ratio is nearly 1.3:1. The higher percentage of vuggy porosity increases overall permeability. | The margins of the clean carbonate sand shoals were areas of carbonate dissolution and creation of secondary effective porosity. Moldic to vug porosity ratio is greater than 2.8:1. The higher percentage of moldic porosity decreases overall permeability. |

Table 5.3 Porosity, gamma-ray and geologic criteria used to classify Collier Flats oil wells (cont.).

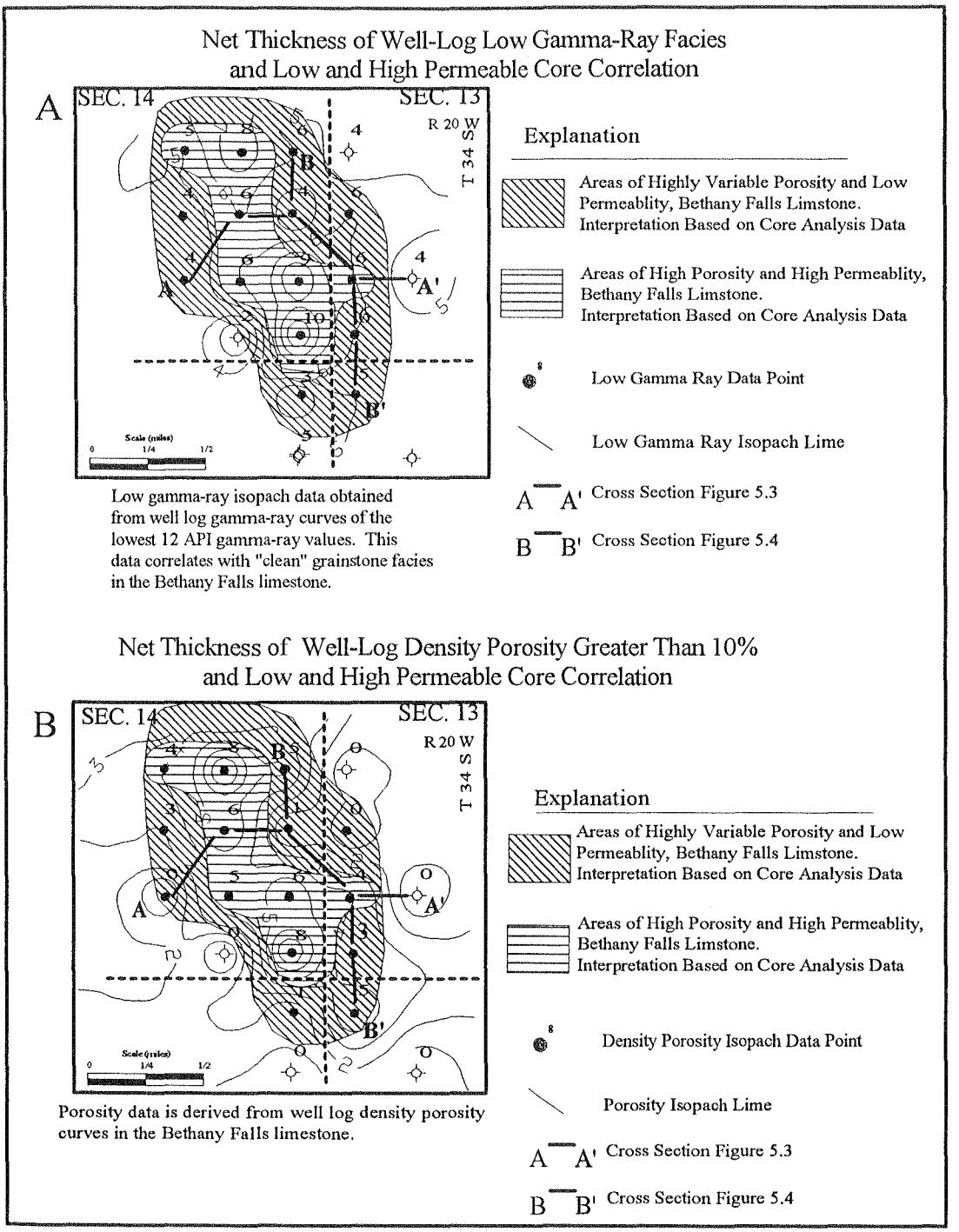


Figure 5.2 Correlation of core analysis data with: A) net thickness of the lowest 12 API gamma-ray units "Low Gamma Ray Facies" isopach map and B) net thickness of density porosity greater than 10% isopach map.

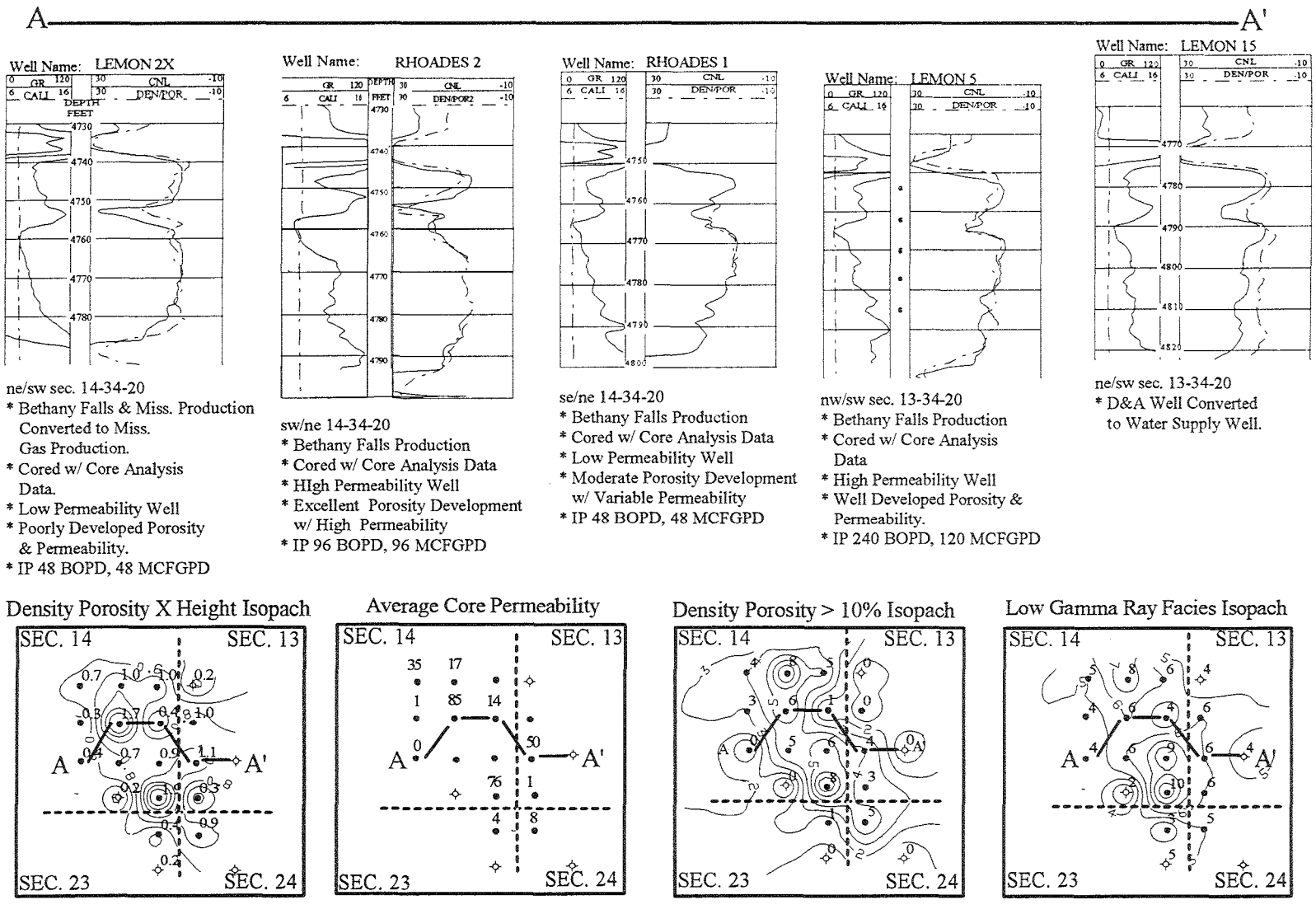


Figure 5.3 Correlation of Bethany Falls limestone gamma-ray log signatures with isopach maps of density porosity, core analysis permeability and net thickness of low gamma-ray facies. Well developed porosity and permeability correlate with low gamma-ray values that coincide with the thickest Bethany Falls grainstone lithofacies.

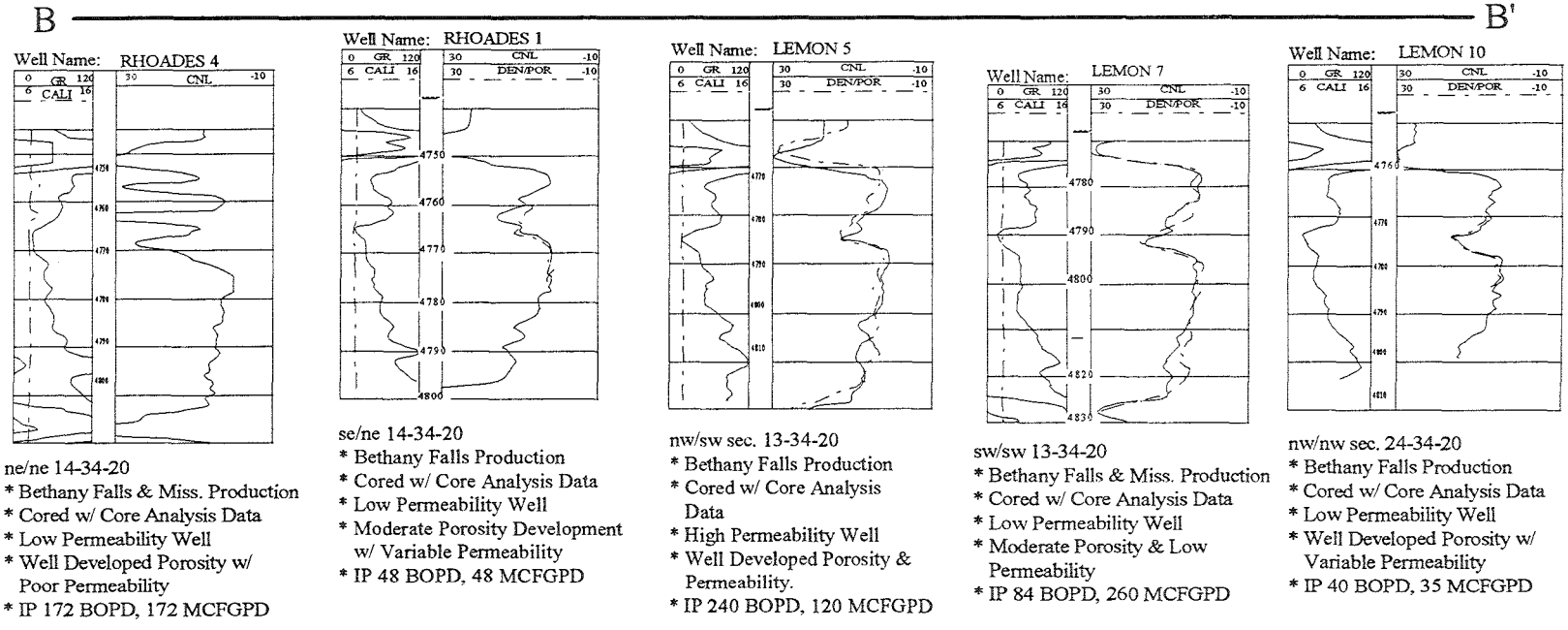


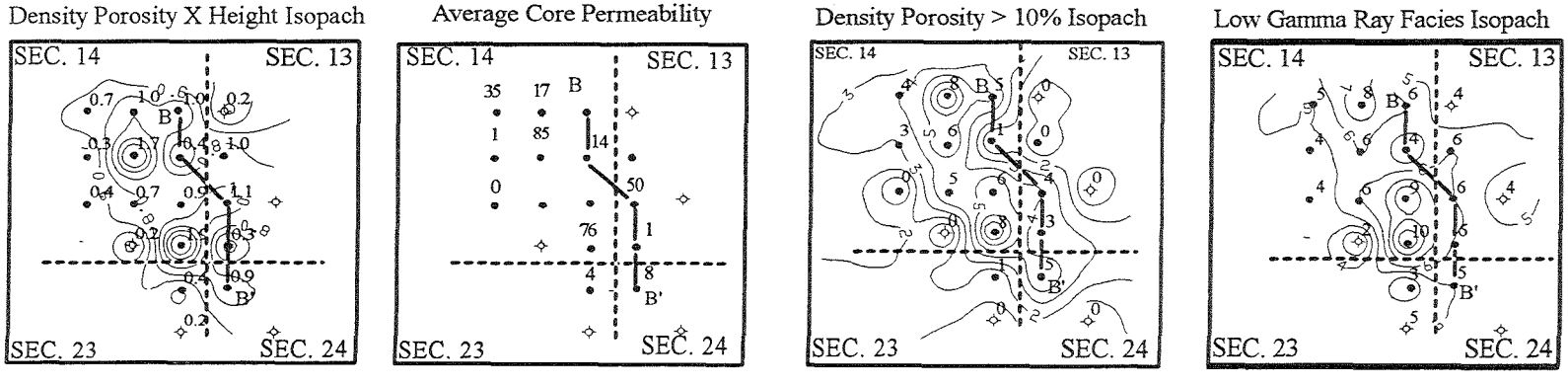


Figure 5.4 Correlation of Bethany Falls limestone gamma-ray log signatures with isopach maps of density porosity, core permeability and net thickness of low gamma-ray facies. Poorly developed porosity and permeability correlate with low gamma-ray values that coincide with thinner Bethany Falls grainstone lithofacies.

## Porosity-Permeability Correlation

### Introduction

In the Bethany Falls Limestone porosity and permeability development section of this thesis, core is characterized as either high or low permeability based on thin-section descriptions, core analysis, depositional and diagenetic models. Low permeability cores ***(Porosity and Permeability Distribution #1)*** are Bethany Falls oolitic and mixed oolitic-bioclastic grainstones restricted to the margins of the grainstone sand shoals. The relative percentage of moldic to vuggy porosity average approximately 2.8 : 1.

High permeability cores ***(Porosity and Permeability Distribution #2)*** are Bethany Falls oolitic and mixed oolitic and bioclastic grainstones and underlying packstones restricted to the thickest portions of the grainstone sand shoals. The relative percentage of moldic to vuggy porosity average approximately 1.3 : 1. In both high and low permeability cores, vugs and natural fracturing are present enhancing permeability. In general, high permeability cores show a higher relative percentage of vugs that connect moldic porosity.

### Porosity-Permeability Distribution #1

Cored wells included in the low permeability porosity / permeability distribution #1 are the Lemon 7, Lemon 8, Lemon 9, Lemon 10 and Rhoades 1. The Lemon 2x and Lemon 4 cores were not included in the calculations because these cores are non-permeable and non-productive. Figure 5.5 illustrates the relationship between porosity and permeability with a linear regression line. Porosity and permeability frequency histograms are presented to show porosity and permeability data distribution (Figures 5.6, 5.7).

Whole core analysis horizontal permeability data for these low permeability wells clearly show how tight these porous intervals are with only six permeability data values over 3 md. Porosity and permeability histograms are clearly non-normal and regression analysis results in a low correlation coefficient (Figures 5.5-5.7). Therefore, the porosity and permeability relationship

for low permeability cores are intended to estimate overall average permeability for a oil well in the Collier Flats Oilfield.

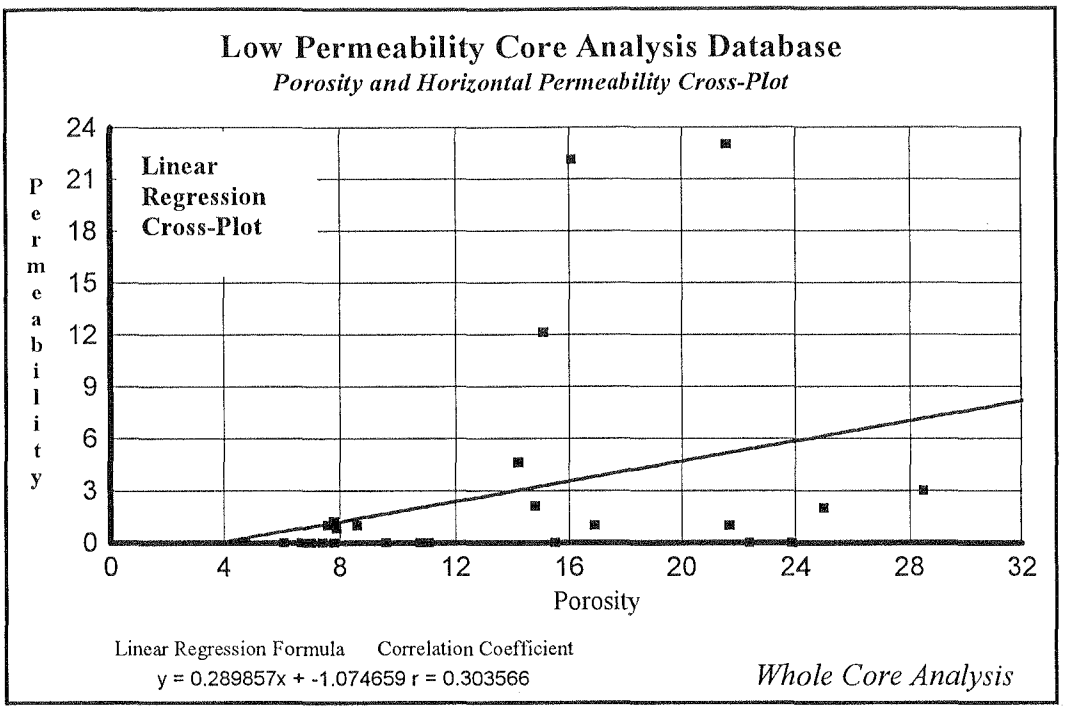


Figure 5.5 Porosity and Permeability Distribution #1 (Low Permeability Wells).

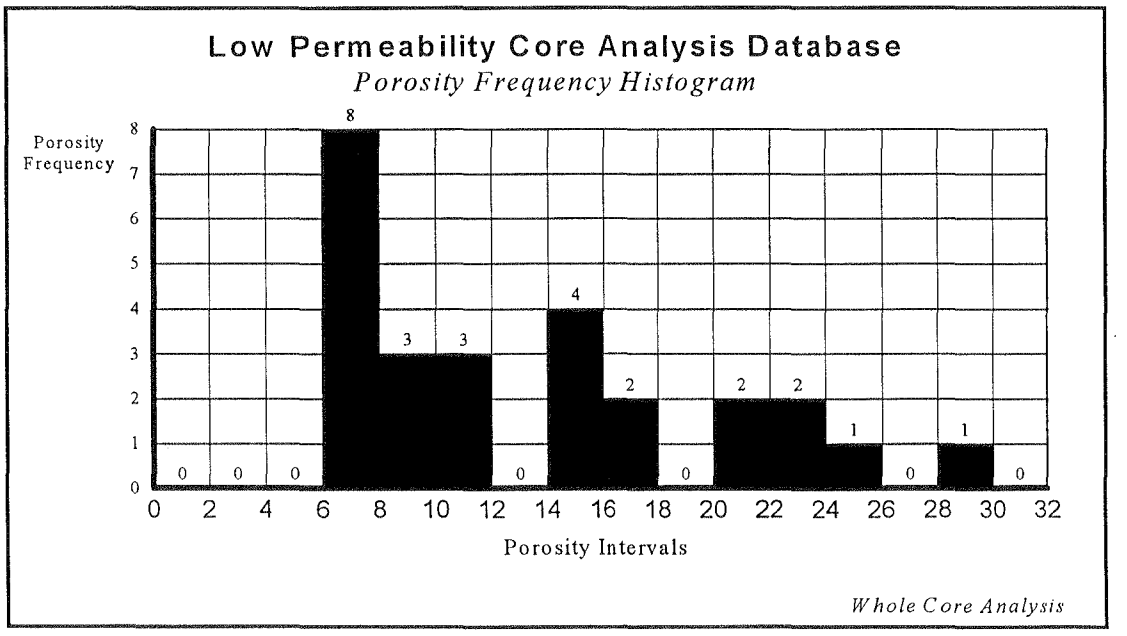


Figure 5.6 Low Permeability Core Analysis Database (Porosity Frequency Histogram).

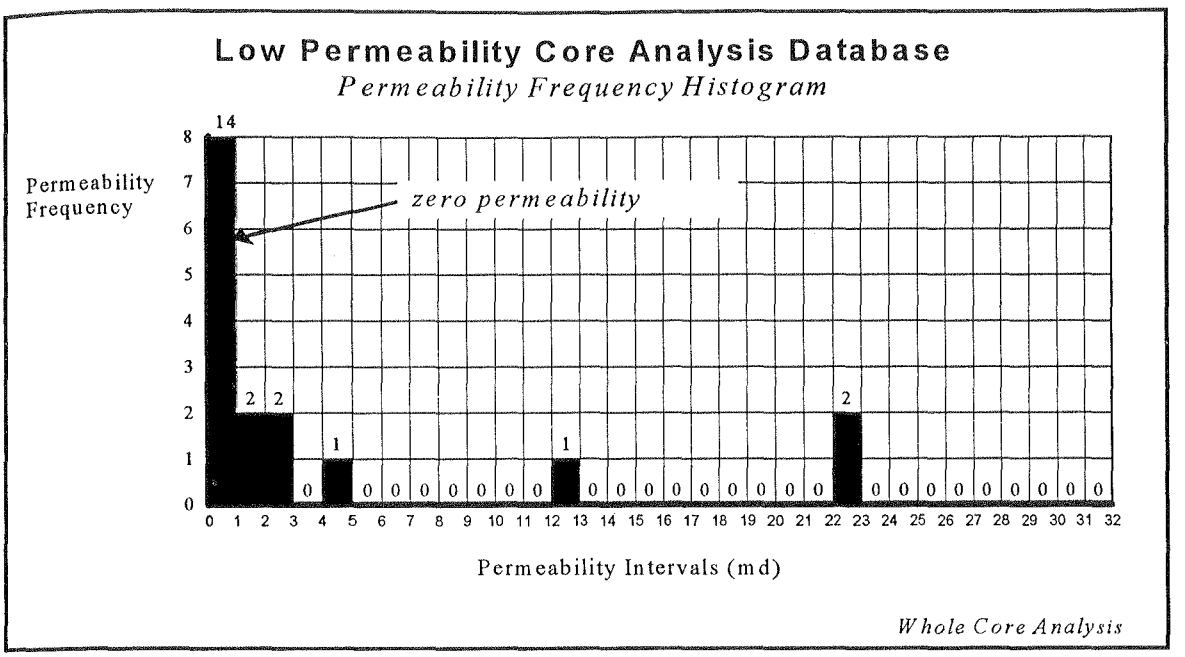


Figure 5.7 Low Permeability Core Analysis Data (Horizontal Permeability Frequency Histogram).

Horner analysis permeability calculations for low permeability productive wells average 2-3 md. Effective porosity begins at eight percent which corresponds to several 1 md permeability intervals. Equation 5.1 describes the linear regression line of core porosity and horizontal permeability in Figure 5.5. This relationship is used in the "Reservoir Characterization Results" section to calculate average horizontal permeability using well-log based density porosity data for wells classified as low permeability in the Collier Flats Oilfield.

**Equation 5.1 Low Permeability Core (Linear Regression Equation)**

**Permeability = (0.289857 * Porosity ) - 1.074659**

Vertical and horizontal permeability correlation show a nearly one to one relationship indicating that in this part of the reservoir, permeability is homogeneous (Figure 5.8).

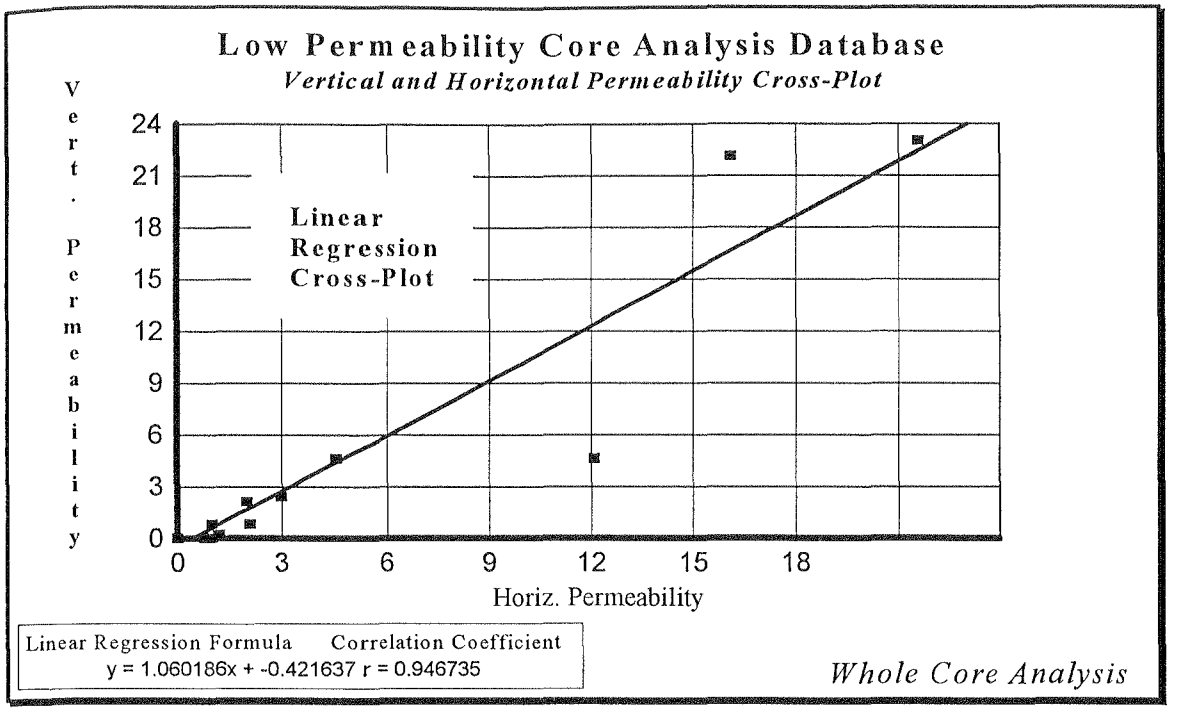


Figure 5.8 Low Permeability Core Analysis Data (Horizontal and Vertical Permeability Correlation)

**Porosity-Permeability Distribution #2**

Wells included in the high permeability *porosity and permeability distribution #2* are the, Lemon 5, Lemon 6, Lemon 11, Rhoades 2 and Rhoades 3. There are two issues that will impact this porosity-permeability correlation:

- Oomoldic porosity has been identified in the oolitic grainstone lithofacies that cap the regressive Bethany Falls limestone. Based on limited whole core analysis data and thin-section observations, these intervals are typically very porous (greater than 20%) with low permeability due to a lack of vuggy porosity (Tables 5.4 and 5.5).
- In the other Bethany Falls reservoir facies, there is a higher overall percentage of vuggy porosity and natural fractures enhance permeability.

Generally a linear regression line is used to characterize porosity and permeability relationships in reservoir engineering studies. However, the Lemon 6 and Rhoades 2 cores show that as porosity increases permeability decreases in the oomoldic intervals of the Bethany Falls reservoir.

| Lemon 6 Core Porosity and Permeability Characterization | | | | | | | | |
|---|---|---|---|---|---|---|---|---|
| Depth | Porosity % | Horz. K-md | Vert. K-md | [MO] % | [VUG] % | [BC] % | [BP] % | Lithologic Description |
| 4781-82 | 29.7 | 10.1 | 1 | | | | | Oolitic Grainstone |
| 4782-83 | 20.7 | 8 | 4.2 | | | | | |
| 4783-84 | 22.8 | 5.8 | 2.1 | 35 | 25 | 25 | 15 | Mixed Oolitic & Bioclastic Grainstone |
| 4784-85 | 16.5 | 22.5 | 7.4 | | | | | Bioclastic Grainstone |
| 4785-86 | 23.2 | 130 | 57 | 56 | 11 | 33 | 0 | |
| 4786-87 | 19.2 | 130 | 120 | | | | | |
| 4787-88 | 17.8 | 26.7 | 32.2 | | | | | Fossiliferous Packstone |
| 4788-89 | 12 | 0 | 0 | | | | | Fossiliferous Wackestone |
| 4789-90 | 19.7 | 280 | 280 | 17 | 50 | 33 | 0 | Peloidal Packstone |
| 4791-91 | 12.4 | 0 | 0 | | | | | Fossiliferous Wackestone |

Table 5.4 Lemon 6 core porosity and permeability characterization.

Pore type relative percentages are based on thin section estimates. Oolitic intervals at the top of the Bethany Falls limestone are very porous but with low permeability due to a higher relative percentage of oomoldic porosity.

| Rhoades 2 Core Porosity and Permeability Characterization | | | | | | | | |
|---|---|---|---|---|---|---|---|---|
| Depth | Porosity % | Horz. K-md | Vert. K-md | [MO] % | [VUG] % | [BC] % | [BP] % | Lithologic Description |
| 4755-56 | 29.9 | 21.3 | 13.6 | 40 | 40 | 20 | 0 | Oolitic Grainstone |
| 4756-57 | 22.1 | 140 | 130 | 40 | 40 | 20 | 0 | Oolitic and Bioclastic Grainstone |
| 4757-58 | 19.3 | 110 | 55.2 | | | | | |
| 4758-59 | 22 | 300 | 125 | 17 | 50 | 33 | 0 | |
| 4759-60 | 16.1 | 2.1 | 0 | | | | | Fossiliferous Packstone |
| 4760-61 | 16.5 | 51.6 | 32.8 | | | | | |
| 4761-62 | 16.8 | 48.2 | 39.6 | | | | | |
| 4762-63 | 15.2 | 56.1 | 31.2 | 20 | 40 | 40 | 0 | |
| 4763-64 | 13.6 | 32.6 | 18.9 | 25 | 25 | 50 | 0 | Fossiliferous Wackestone |
| 4764-65 | 10.3 | 0 | 0 | | | | | |

Table 5.5 Rhoades 2 core porosity and permeability characterization.

Pore type relative percentages are based on thin section estimates. Oolitic intervals at the top of the Bethany Falls limestone are very porous but with low permeability due to a higher relative percentage of moldic porosity.

Permeability reduction in these highly porous oolitic intervals can be explained by the observed higher oomoldic to vug pore type ratio observed in thin section.

Porosity in oolitic grainstones of the Drum Limestone in Montgomery County Kansas in places exceed 50%. However, due to poorly connected oomoldic porosity, permeability for these oolitic grainstones are less than 0.5 millidarcy (Stone, 1984). In the case of the Bethany Falls reservoir, it is likely that fracturing and vuggy porosity may connect oomolds and their relative abundance is responsible for variable permeability (although low in general) in these oomoldic intervals. Thus, the Bethany Falls limestone reservoir porosity-permeability relationship can not be characterized using a single regression correlation. Figure 5.9 illustrates the relationship between porosity and permeability using a 4th order polynomial regression correlation.

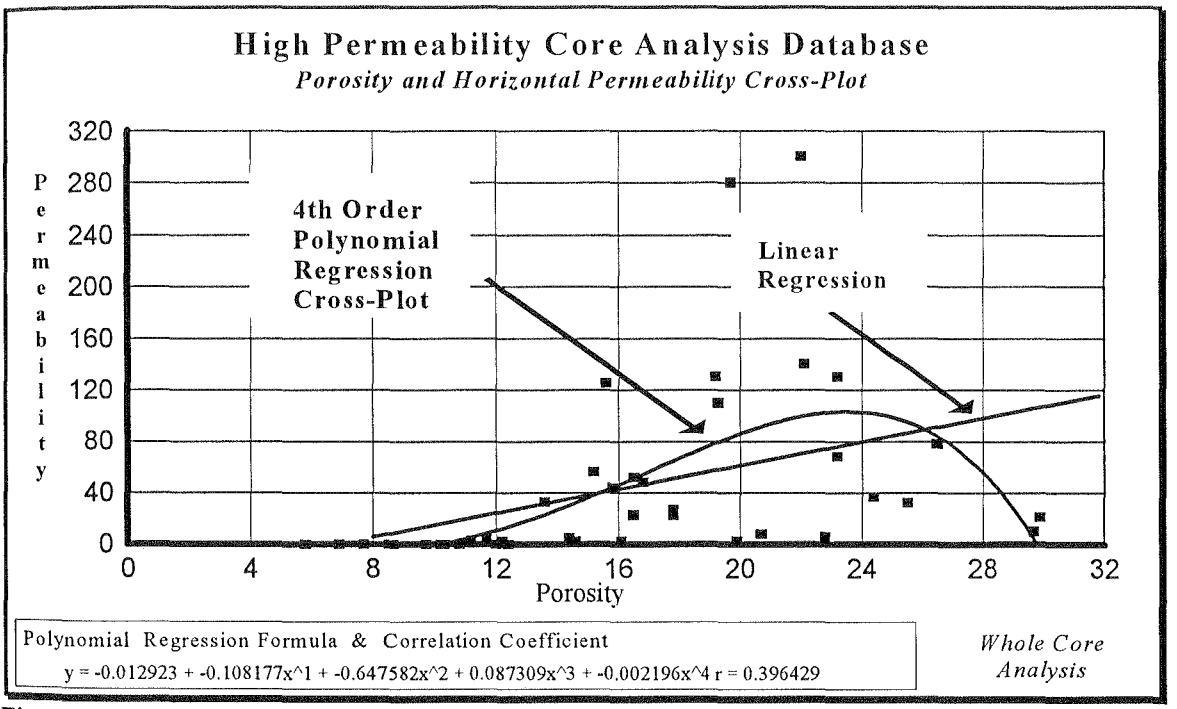


Figure 5.9 Porosity and Permeability Distribution #2 (High Permeability Wells). Two regression lines are plotted: 1) 4th Order Polynomial and 2) Linear regression.

A linear regression line is also presented in Figure 5.9, (y = -4.495523x - 31.1850 r=0.45) shows that between 24 to 30 % porosity, permeability increases from approximately 80 to 110 millidarcies. The 4th order polynomial regression correlation shows that permeability decreases in the 24-30% porosity range from approximately 105 to 10 millidarcies. Correlation coefficients for both regression lines are nearly identical and show that neither correlation is valid statistically. The permeability histogram also shows a non-normal distribution and regression analysis results in

a low correlation coefficient (Figure 5.11). Therefore, the porosity and permeability relationship for high permeability cores are intended to estimate overall average permeability for a oil well in the Collier Flats Oilfield.

**Equation 5.2 High Permeability Core (4th Order Polynomial Regression Equation)**

$$\text{Permeability} = -0.012923 + (-0.108177 * \phi) + (-0.647582 * \phi^2) + (0.087309 * \phi^3) + (-0.002196 * \phi^4)$$

$\phi$ = Porosity

Unfortunately, core is unavailable for the only two wells (Christian 1-11 and 2-11) where well-log density porosity in the upper 3 and 5 feet of the Bethany Falls limestone exceed 30%. Application of the proposed 4th order polynomial porosity-permeability regression equation results in negative permeability data indicating no permeability. There are two ways to resolve this issue:

- Because no core data are available with porosity greater than 30%, intervals with porosity greater than 30% are set aside with no permeability data.
- These two wells are located in an area were the net thickness low gamma ray facies and net thickness of porosity greater than 10% are the thickest in the field. It is likely that the upper few feet with porosity greater than 30% is a "clean" oolitic grainstone with oomoldic porosity. Based on the Lemon 6 core, permeability of the oolitic grainstone interval at the top of the Bethany Falls limestone (29% porosity and 10 md permeability). Thus, 10 md is used for intervals where porosity exceeds 30% for these two wells.

The second option is used to resolve this issue for these two wells.

Permeability derived from Horner analysis calculations tend to support this correlation since DST permeability values averaged over an entire porous interval range between 20 and 60 md (Tables 5.15-5.16). Effective porosity begins at 10 percent in the high permeability core data compared to 8 percent in low permeable cores. Vertical and horizontal permeability correlation shows vertical permeability is less than horizontal permeability in this part of the reservoir (Figure 5.12). This indicates that natural fracturing is not a dominate component of permeability. Equation 5.2 describes the 4th order polynomial regression line of core porosity and horizontal permeability in Figure 5.9. This relationship is used in the "reservoir characterization results" section to calculate average horizontal permeability using well-log based density porosity data for wells classified as high permeability in the Collier Flats field.

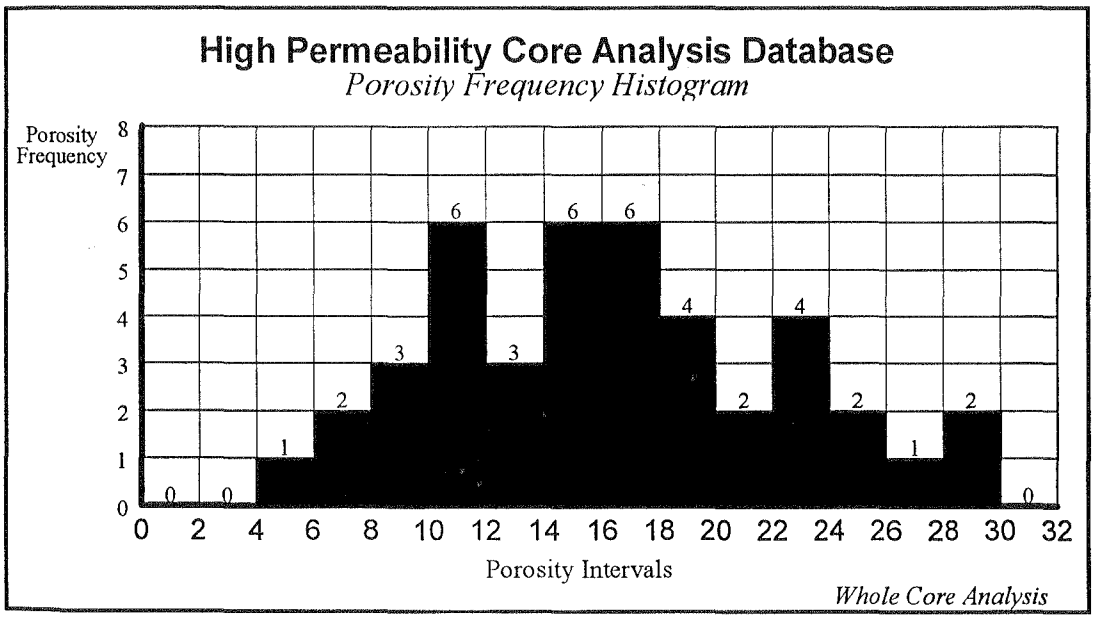


Figure 5.10 High Permeability Core Analysis Data (Porosity Frequency Histogram).

The two Collier Flats field porosity-permeability distributions, supported by Drill Stem test analysis, show that there is a considerable permeability contrast between producing wells within a single genetic unit. The permeability contrast can be classified as a Type 3 reservoir heterogeneity, (Figure 5.1), that will impact horizontal and vertical sweep efficiency along with residual oil saturation (Weber, 1986).

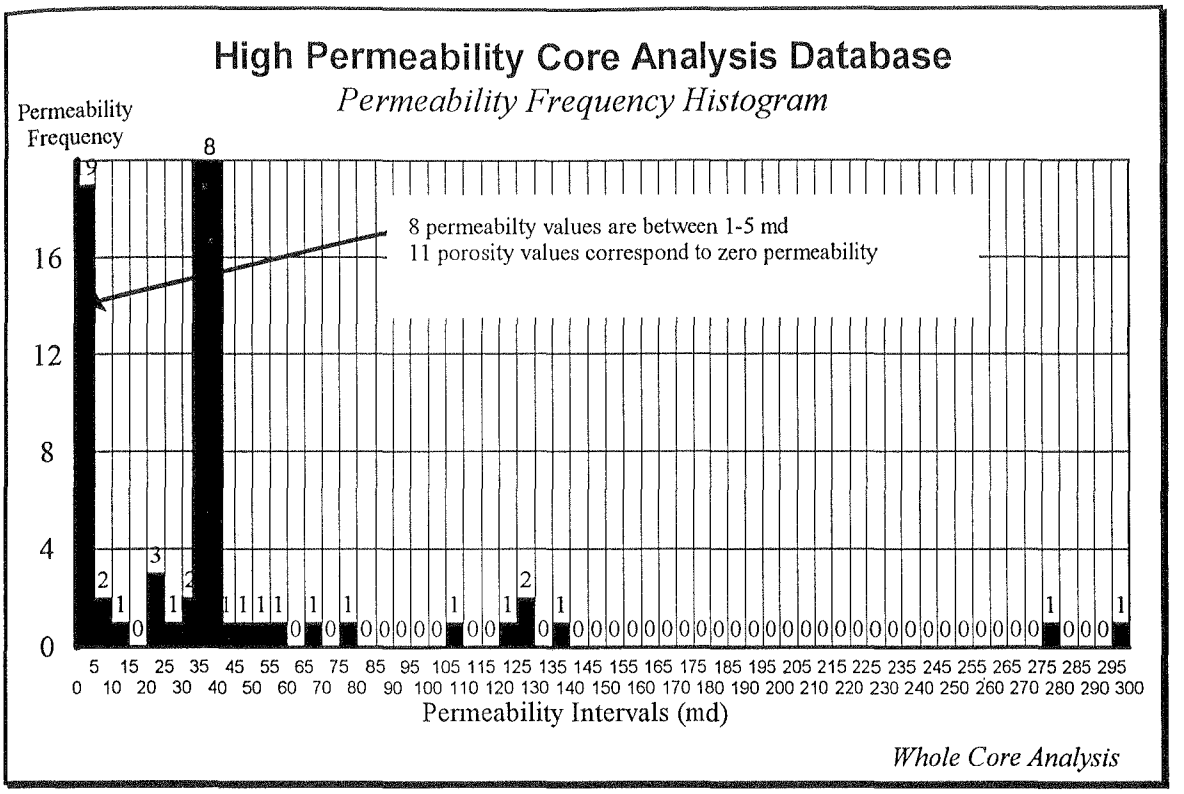


Figure 5.11 High Permeability Core Analysis Data (Permeability Frequency Histogram).

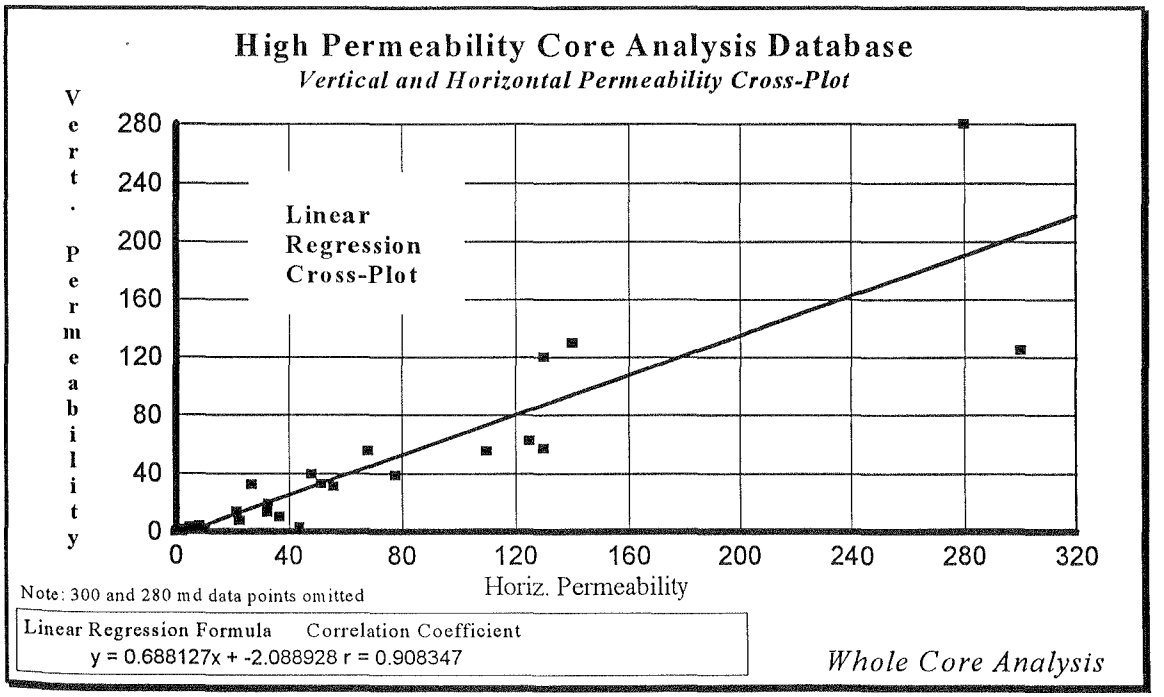


Figure 5.12 High Permeability Core Analysis Data (Vertical and Horizontal Permeability Correlation).

Additionally, since the permeability contrast is related to the relative abundance of vug and moldic porosity it can also be classified as a Type 6 reservoir heterogeneity that will impact residual oil saturation and rock fluid interactions (Figure 5.1).

### Conclusions

Statistically, the proposed porosity and permeability correlations for low and high permeability wells are not valid. Frequency histogram data clearly show non-normal permeability distributions and low regression analysis correlation coefficients. However, classification of core as low and high permeability is based on depositional and diagenetic geologic models which is the first step in an attempt to characterize Collier Flats Oilfield porosity and permeability on a fieldwide scale. Therefore, the proposed porosity and permeability relationships are intended to characterize porosity and permeability on the genetic unit scale and not the inter-well or microscopic scale.

## Water Saturation Characterization

### Introduction

Water saturation is typically calculated with the Archie (1942) water saturation equation using log derived porosity and a measurement of formation resistivity. Asquith (1985) demonstrated that pore geometry affects the flow of electrical current through a rock and the Archie equation cementation exponent can be modified to account for fracture, intergranular, intercrystalline, moldic and vuggy pore types (Figure 5.13).

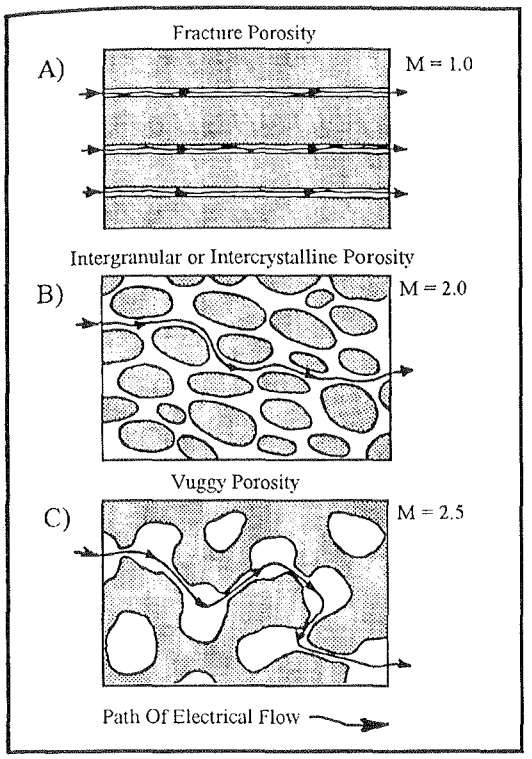


Figure 5.13 Correlation of Cementation Exponent with Pore Types (Modified After Asquith, 1985).

The fundamental difference between the two porosity-permeability distributions is based on the relative percentage of moldic and vuggy porosity. Thus, determination of appropriate cementation factors for the Collier Flats Field will be essential to calculate accurate water saturation data.

### Determination of Cementation Exponents

A Pickett plot of the log of porosity versus the log of deep resistivity ($R_{ILD}$, $R_{LLD}$ or $R_{Guard}$) is used in an attempt to identify cementation exponents for the two porosity-permeability distributions. To construct a valid Pickett plot, there must be a well where 100% of the pore space is filled with connate water (water-wet well below the oil-water contact). Unfortunately, only 13 wells in the Collier Flats Field produce water from the Bethany Falls reservoir zone.

The Petro 11-1 and 11-3 wells were selected for Pickett plots since they both produced oil and water, were logged using the same well log suites, appeared to displayed a distinct water-oil contact, and are classified as a high and low permeability wells.

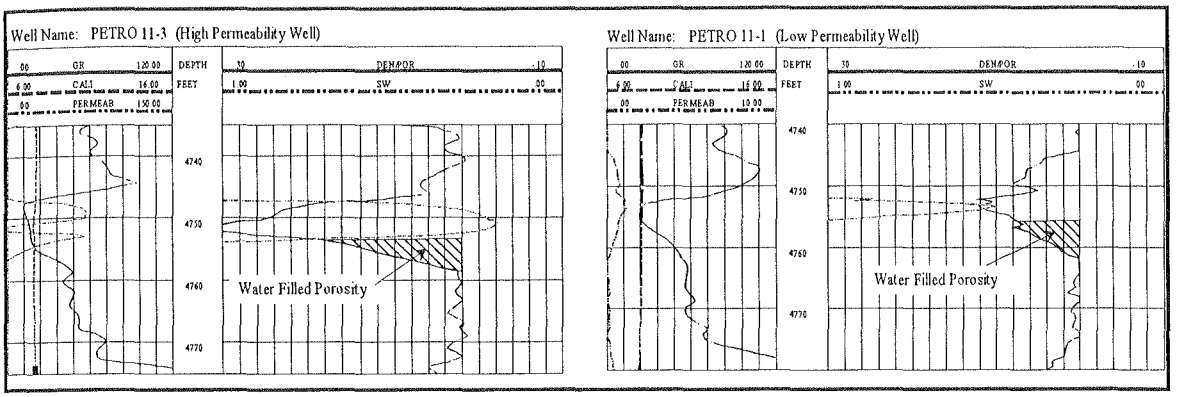


Figure 5.14 Oil Wells With Distinct Oil-Water Contacts Used For Pickett Plots of Porosity Versus Resistivity.
Petro 11-1 Initial Production, 57 BOPD and 96 BWPD. Petro 11-3 Initial Production, 400 BOPD and 100 BWPD. Preliminary water saturation data was calculated to show where the potential oil/water contact is located.

A Pickett crossplot is based on the following data: formation resistivity ($R_{ILD}$), porosity, water saturation and cementation exponent "m". On a Pickett plot, a porous zone with constant water resistivity, cementation exponent and 100% water saturation will plot along a straight line if pore type does not change as porosity varies and there is no residual oil impacting resistivity measurements. The straight line trend represents water filled porosity and the slope of the straight line is equal to the cementation exponent (Asquith, 1982). This straight line should pass through the most south-western data points which should be water filled porosity (Asquith, 1982).

The Terra Sciences TLOG module was used to construct the Pickett plots for both wells since the software can interactively generate a 100% water filled porosity-resistivity line based on a cementation factor and formation water resistivity (Figure 5.15 - 5.16). The 100% water filled porosity-resistivity lines for various cementation factors can then be compared with measured deep formation resistivity $R_{ild}$ (Figure 5.15 - 5.16).

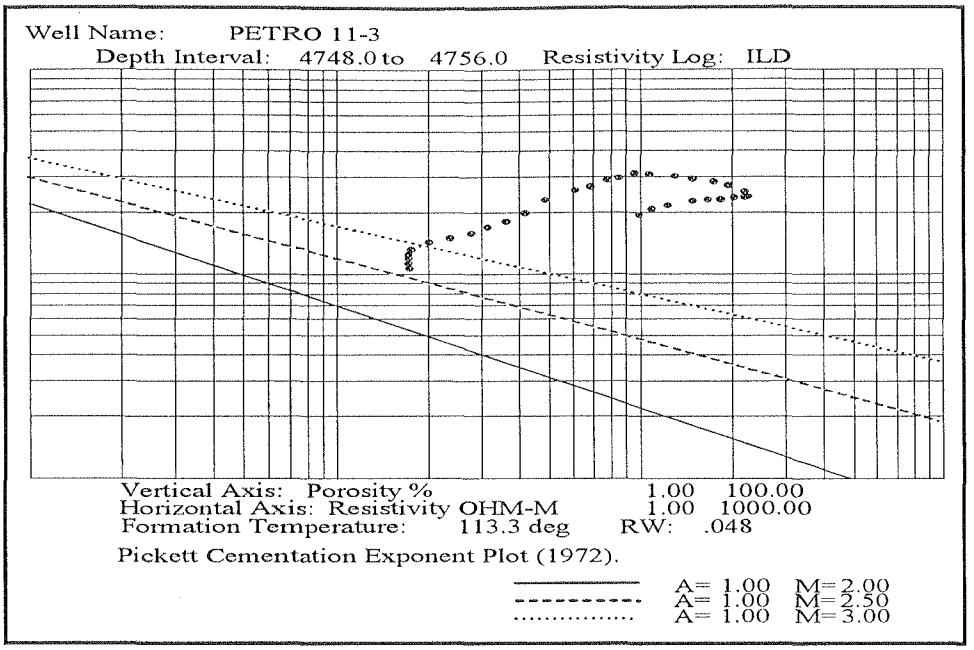


Figure 5.15 Petro 11-3 Pickett Crossplot (High Permeability Well).

Petro 11-3 and 11-1 Pickett plots use the following data: density porosity, deep induction resistivity and 0.044 ohms-meter @ 125° F formation water resistivity[5.1] corrected to formation temperature. Unfortunately, the shape of the Pickett plots indicate the lowest resistivity is likely associated with residual oil saturation since the lowest resistivity do not represent 100% water filled porosity (Watney, 1997, personal communication). Both porosity-resistivity plots do not show a well defined water-line. Porosity filled with 100% connate water should plot parallel to the theoretical water-lines based on cementation factors.

Since Pickett plots based on wells with the best potential for determining a cementation exponent (Petro 11-1 and 11-3) appear to be invalid for this purpose in the Collier Flats Field. Pickett plots are still useful in oil zones to examine conditions approaching irreducible water saturation and evidence for transition zones.

5.1 Formation Water Resistivity is obtained from Henderson & Company Waterflood Feasibility Study for the Lemon Ranch and Rhoades Leases, 1981.

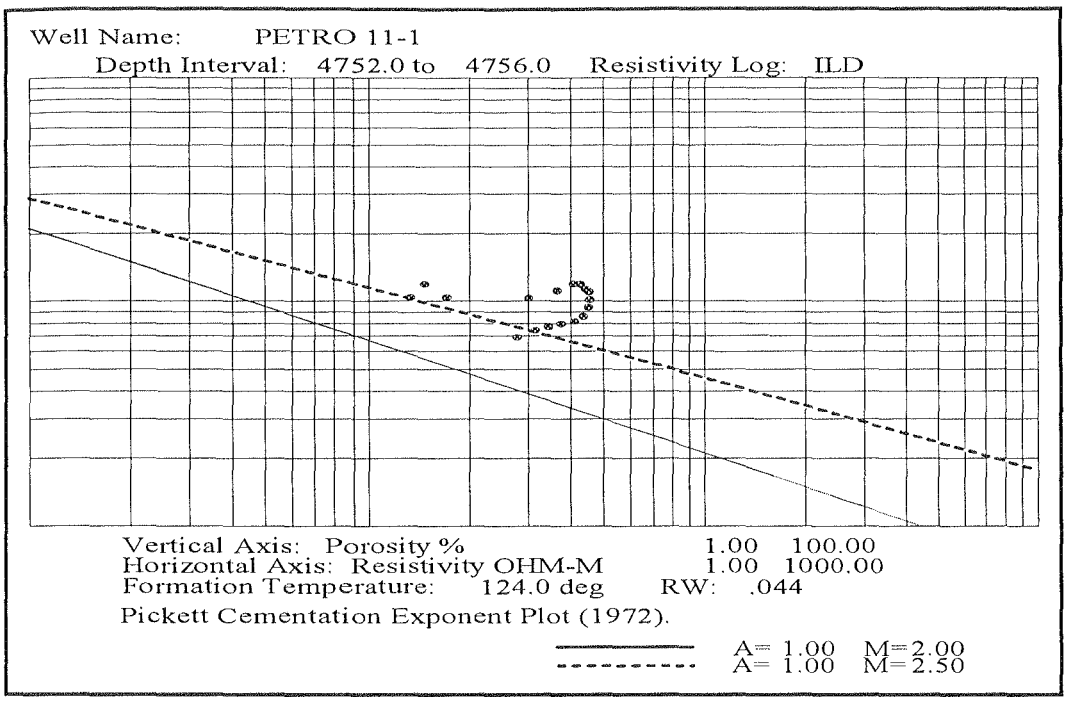


Figure 5.16 Petro 11-1 Pickett Crossplot (Low Permeability Well).

### Core Analysis Water Saturation Data

By the time a core sample has reached a laboratory for analysis, it has undergone significant changes from its original undisturbed state in the reservoir. First, drilling fluids usually invade a portion of the core and secondly; confining pressure is reduced when the core is brought to the surface. Water based coring fluids were used to obtain the Lemon and Rhoades cores which generally increase water saturation and lower hydrocarbon saturation (Gatlin, 1960, Core Lab, 1976) (Figure 5.17). Figure 5.17 illustrate the major process that occur in a core for the three phases when it is brought to the surface for an oil productive formation cored with water based mud.

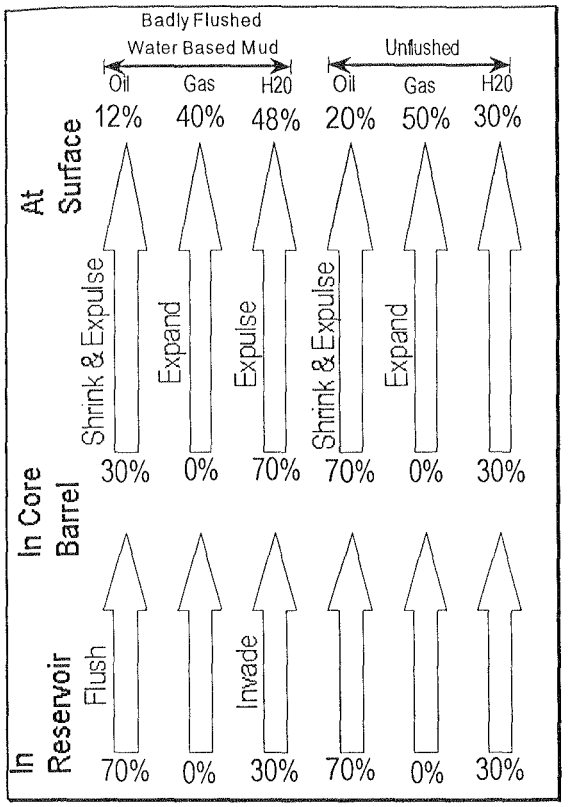


In the best case scenario, unflushed core water saturation will be the same at the surface and the reservoir. In a badly flushed core, surface calculated water saturation data can be misleading. An indicator of invasion and flushing is caliper curve data that identifies mudcake buildup on the borehole walls. Assuming minor invasion, the value of core analysis water saturation data is it will provide an upper limit on estimates of water saturation using the Archie water saturation equation.

Figure 5.17 Typical Fluid Contents From Reservoir Conditions to Surface, Oil Productive Reservoir, (Core Labs, 1976).

### Cementation Exponent Evaluation

Theoretical water saturation data for low and high permeability cores were calculated using core porosity, well-log derived deep induction resistivity and various cementation exponents m=2.0, 2.5 and 3.0) (Table 5.6). This data was then compared with core analysis water saturation data. This exercise is an attempt to determine if the 2.0 cementation exponent used in the Archie water saturation equation needs adjustment to better characterize water saturation in the Bethany Falls limestone reservoir.

| Low Perm. Wells | Core Porosity | Sw m=2.0 | Sw m=2.5 | Core Sw |
|---|---|---|---|---|
| **Lemon 10** | 22 | 10 | 15 | 17 |
| *No Caliper* | 25 | 10 | 14 | 18 |
| *Data* | 19 | 8 | 12 | 13 |
| | 15 | 15 | 25 | 34 |
| Lem 10 Ave. | 20 | 11 | 17 | 21 |
| **Lemon 7** | 11 | 35 | 60 | 58 |
| *0.1"* | 22 | 13 | 19 | 34 |
| *Mudcake* | 24 | 11 | 15 | 26 |
| *Minor* | 22 | 11 | 16 | 31 |
| *Invasion* | 22 | 11 | 16 | 31 |
| Lem 7 Ave. | 20 | 16 | 25 | 36 |
| **Rhoades 1** | 11 | 20 | 35 | 31 |
| *0.25-0.33"* | 16 | 13 | 20 | 19 |
| *Mudcake* | 14 | 15 | 25 | 18 |
| *Modest* | 10 | 29 | 51 | 27 |
| *Invasion* | 10 | 33 | 59 | 27 |
| Rho1 Ave. | 12 | 22 | 38 | 24 |

| High Perm. Wells | Core Porosity | Sw m=2.0 | Sw m=2.5 | Sw m=3.0 | Core Sw |
|---|---|---|---|---|---|
| **Rhoades 3** | 11 | 21 | 37 | 65 | 34 |
| *0.25-.033"* | 15 | 17 | 28 | 46 | 27 |
| *Mudcake* | 20 | 12 | 20 | 30 | 32 |
| | 23 | 11 | 16 | 23 | 22 |
| *Invasion* | 18 | 16 | 25 | 39 | 19 |
| | 11 | 25 | 43 | 75 | 27 |
| | 12 | 23 | 40 | 68 | 25 |
| | 10 | 31 | 55 | 98 | 27 |
| Rho3 Ave. | 15 | 20 | 33 | 56 | 27 |
| **Rhoades 2** | 30 | 5 | 6 | 8 | 15 |
| *0.1-0.2"* | 22 | 7 | 10 | 15 | 22 |
| *Mudcake* | 19 | 8 | 12 | 18 | 24 |
| *Modest* | 22 | 7 | 11 | 16 | 19 |
| *Invasion* | 16 | 11 | 17 | 27 | 24 |
| | 17 | 9 | 14 | 23 | 28 |
| | 17 | 12 | 18 | 29 | 25 |
| Rho2 Ave. | 20 | 10 | 13 | 24 | 23 |
| **Lemon 6** | 30 | 6 | 8 | 11 | 30 |
| *0.1"* | 21 | 7 | 11 | 16 | 28 |
| *Mudcake* | 23 | 8 | 11 | 16 | 27 |
| *Minor* | 17 | 11 | 17 | 26 | 40 |
| *Invasion* | 23 | 8 | 11 | 16 | 19 |
| | 19 | 9 | 14 | 21 | 21 |
| | 18 | 12 | 18 | 27 | 25 |
| | 12 | 14 | 24 | 41 | 20 |
| | 20 | 15 | 22 | 33 | 19 |
| | 12 | 25 | 42 | 71 | 23 |
| Lem6 Ave. | 20 | 12 | 18 | 28 | 25 |

Table 5.6 Summary of calculated water saturation data based on various cementation exponent data.

Water saturation values derived from low permeability cores with Porosity and Permeability Distribution #1 average approximately 24% (Table 5.6). There appears to be some invasion in the cores based on the caliper data over the cored intervals (Table 5.6). This indicates that the 24% core analysis average water saturation can be considered as the upper limit of water saturation at reservoir conditions.

Water saturation calculations based on a 2.5 cementation factor for the low permeable cores (Table 5.6) results in values that are 4-9% less than those of core analysis. The exception is the Rhoades 1 core where all calculated water saturation data using m=2.5 is greater than the core analysis results.

For porous zones in the Rhoades 1 core (greater than 10%), the calculated water saturation values using m=2.5 are only a few percentage points above the core analysis values. The bottom two feet of the Rhoades 1 core show calculated water saturation values too high even using a conventional cementation factor of m=2.0. Thus, all calculated water saturation data for this core are likely biased high. Potential errors in measured deep induction resistivity data can be attributed to mud filtrate invasion effects indicated by the presence of a 0.25-0.33" mudcake.

Water saturation calculations based on a cementation factor of m=2.0 for the low permeable cores (Table 5.6) results in values that are 10-20% less than those of core analysis. Based on water saturation data from the Lemon 10 and Lemon 7 core, the 2.5 cementation factor proposed for the low permeable cores appears to be a good approximation of the upper limit of actual reservoir water saturation based on a good agreement with core analysis water saturation data.

Water saturation measured in high permeability cores also average 25%. There appears to be some invasion in the cores based on the caliper data over the cored intervals. This indicates that a core analysis average water saturation value of 25% is actually a little less at reservoir conditions. Thus as in the low permeability core example, 25% water saturation is also a good approximation of the upper limit that can be used to constrain the Archie based water saturation calculation.

Analysis of well-logs derived water saturation data in high permeable cores using a 3.0 cementation factor appears to produce satisfactory water saturation values in intervals with porosity greater than 19% (Table 5.6).

In intervals with porosity less than 19% for the high permeability cores Rhoades 2 and Lemon 6 cores, well-log based calculations of water saturation values using a 2.5 cementation factor generally agree with core analysis based water saturation.

The Rhoades 3 core is an exception where all intervals with less than 20% porosity have well-log calculated water saturations that exceed core analysis results by 20-40%. Water saturation calculated using a 2.0 cementation factor are actually closer to the results from core analysis. Thus, it is likely that all calculated water saturation data for this core is likely biased high. As with the Rhoades 1 core, potential errors in measured deep induction resistivity data can be attributed to mud filtrate invasion effects.

It has been documented that the pore system in the Bethany Falls reservoir consists of moldic, vug, microvug and interparticle porosity. Since the Archie equation uses a cementation factor of 2.0 which is based on interparticle porosity, this cementation factor must be adjusted to compensate for the moldic and vug dominated pore system in the Bethany Falls limestone reservoir. Table 5.6 shows that using the 2.5 cementation factor for intervals where porosity is less than 20% and a 3.0 cementation factor for intervals with porosity greater than 20% is a good approximation of the upper limits of the Bethany Falls limestone reservoir water saturation.

## Core Porosity and Well Log Porosity Correlation

Application of the porosity-permeability and water saturation models require accurate porosity data. Since core data are not available for the entire Field, the only other source for porosity data is wireline well log density, neutron and sonic. In the Collier Flats Field, the following wireline well logging companies have logged wells; Dresser Atlas, Schlumberger, Wellex, Gearhart and Petro. These companies typically used compensated neutron and density wireline logs in the more recent wells which provide the best possible porosity data.

In older wells, neutron logs were run which typically recorded formation responses in API neutron units that were not converted into limestone porosity units. Sonic porosity data is only available for a few wells. Density wireline logs record API density units which is always converted to and presented as bulk density (grams per cubic centimeter). Thus, density data presents the most consistent Field wide porosity data source.

Wireline density logs measure bulk density while neutron logs measure fluid filled porosity (Dresser Atlas, 1974; Schlumberger, 1984). Bulk density is converted to density porosity using the following equation: $\phi_D = (\rho_{ma} - \rho_b / \rho_{ma} - \rho_f)$ where $\rho_{ma}$ = matrix density, $\rho_b$ = bulk density from density log and $\rho_f$ = pore fluid density (Dresser Atlas, 1974; Schlumberger, 1984). Compensated density data are corrected for mud cake density and bore-hole rugosity as the log is run. Additionally, a density correction curve shows the amount of correction that is applied to the raw bulk density data. Porosity data derived from the density porosity is total porosity including effective and noneffective porosity as with core porosity data. In the case of the Collier Flats Field, noneffective porosity may include oomoldic porosity. Thus, density porosity is analogous to whole core analysis porosity data since whole core analysis also measures total porosity.

Wireline neutron logs measure fluid filled porosity including water, hydrocarbons and gas. Compensated neutron logs have been designed such that environmental effects such as hole size, mud weight, mud cake, stand-off and reservoir fluids are greatly reduced. Older conventional and sidewall epithermal neutron logs need environmental corrections and some type of conversion from API neutron units to limestone porosity. Additionally, neutron logs are affected by lithology, light hydrocarbons or gas filled porosity. Thus, there are many more uncertainties involved using neutron logs alone to determine an accurate porosity value.

Neutron logs were only used when density porosity was not available. Calibration tails and repeat sections are usually appended to the final log run so they can be compared with the final log data. Porosity variations greater than 3% between the repeat section and the final logging data indicate problems with a logging tool and questionable data. Figures 5.18 and 5.19 illustrate porosity logs with poor and good matches between the calibration tails and the final well log data.

Correlation of density and neutron porosity data with core analysis porosity data clearly show the impact of improperly run, calibrated and/or witnessed wireline logging. Initial correlation of wireline and core porosity data show 4-6% lower values for the wireline density porosity data (Lemon 5,6,7,10,11, Rhoades 2,1) (Appendix B). Lemon 2x,4,8 and Rhoades 3 show a good correlation between density porosity and core analysis porosity (Appendix B). Calibration tails showed a good match between initial and final well log runs. For Lemon 5,6,7 and Rhoades 1,2, core analysis porosity data is 3-5% higher than density porosity data (Appendix B). Calibration tails showed a poor match between initial and final well log runs.

A correlation between whole core porosity and wireline density porosity is not possible due to the poor density porosity log quality where core is available. It is important to note where core is available (Lemon and Rhoades leases), density porosity log quality was generally poor. These wells were all logged by Welex. Because a valid correlation of core porosity with density porosity is not possible, density porosity data is used for the porosity-permeability and water saturation correlation in areas without core.

### Well Log Normalization

Poor correlation between core and density porosity data calls for some type of log normalization using statistical methods to correct errors caused by inaccurate tool calibration and variations of log data between service companies (Hunt E., Aly A. and Pursell D., 1996).

Prior to performing any type of log normalization, well log database editing is required. Well log database editing includes 1) identifying and performing depth corrections to individual well log curves and 2) performing environmental corrections.

The presence of the Stark Shale above the reservoir zone, allows for depth corrections since the gamma ray, density, neutron and resistivity curves all have a predictable reaction to the shale lithologies. Environmental corrections were performed on all resistivity well log suites (Schlumberger, Dresser Atlas, Welex and Gearhart) using Terrastation TLOG modules which account for borehole size, rugosity, mud weight, mud filtrate resistivity, mud salinity, temperature and tool standoff. The only exceptions are pre 1970's electric logs that consist of deep guard or laterologs and Welex deep guard logs where no charts were available to perform environmental corrections.

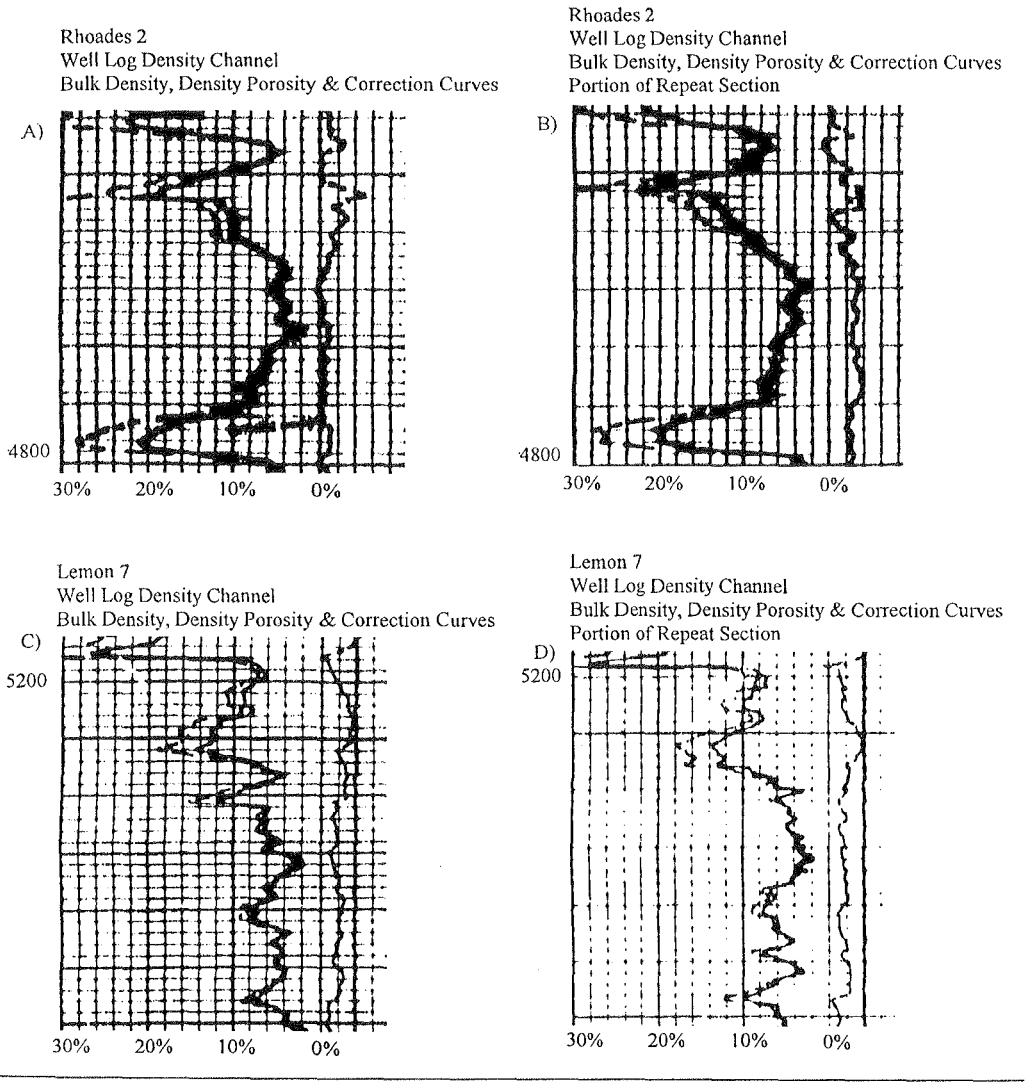


Figure 5.18 Examples of bulk density and density porosity curves and repeat sections over the same intervals. Inital logging repeat sections do not correlate with final wireline log data. These types of errors lead to questioning of the density porosity data.

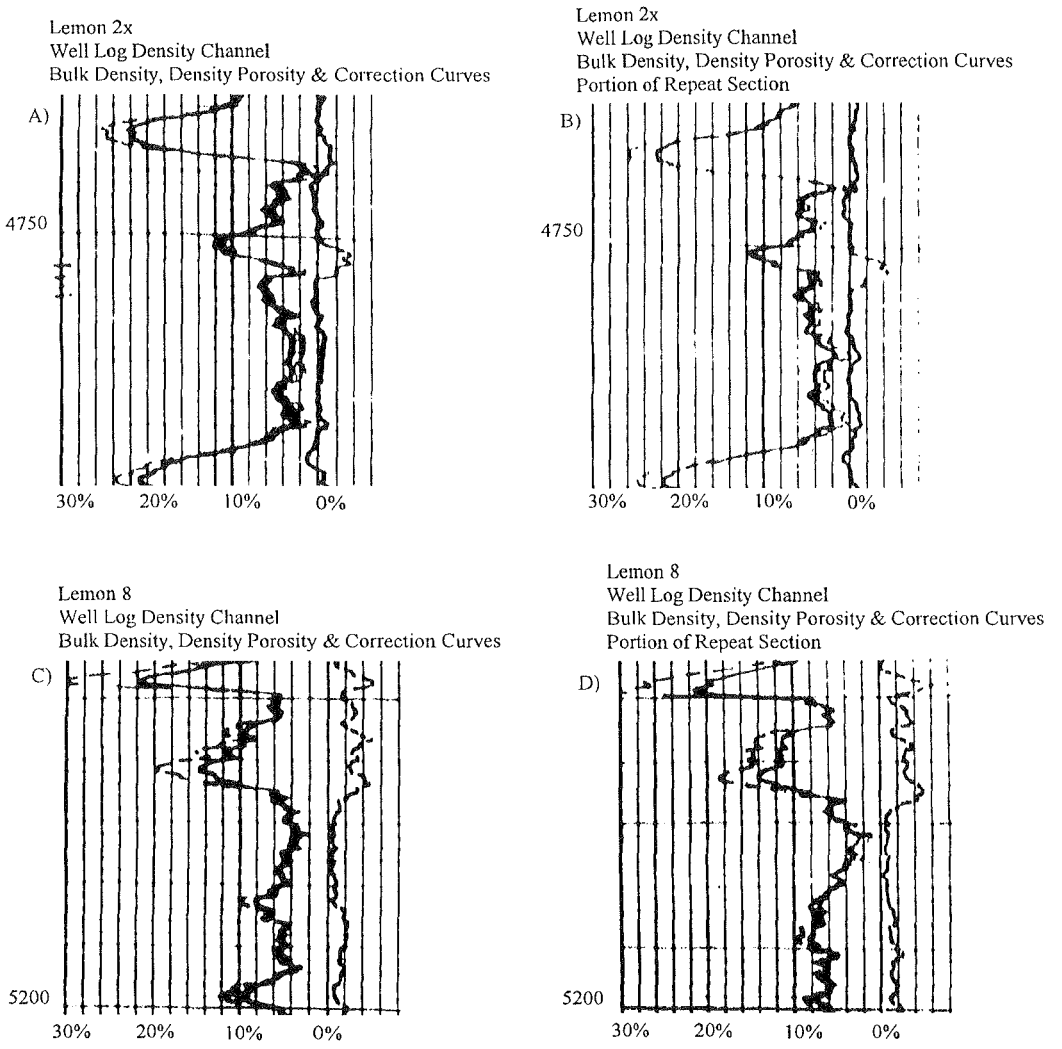


Figure 5.19 Examples of bulk density and density porosity curves and repeat sections over the same intervals. Initial logging repeat section does correlate with the final log data.

## Drill Stem Test Pressure Data

### Pressure Data Sources And Initial Observations

Core analysis data clearly demonstrate a significant contrast in permeability exists in the Bethany Falls limestone reservoir. This contrast should be detected by reservoir performance data including pressure transient tests and initial oil flow rates. Reservoir performance can be assessed through:

- Initial Fluid Production (IPOIL & IPGAS),
- Drillstem Test shut-in pressure data (ISIP & FSIP),
- Drillstem Test flow pressures,
- and drilling characteristics such as lost circulation and drilling breaks.

This information can further corroborate initial geologic classification of Collier Flats Field oil wells. Initial fluid production, transient pressure data and drilling characteristics are available from these sources:

- Scout Ticket data,
- 14 wells with complete DST test data
- drillers logs and reports.

Drill Stem Tests (DST) record pressure build-up responses in the well bore which can provide valuable information on formation parameters that are used to assess potential for future production. Pressure build-up analysis and DST chart analysis were performed when the data was available. However, complete DST pressure data including pressure charts are unavailable for most wells. Initial and final shut-in pressure data are reported on scout tickets and exist for a majority of oil wells in the Collier Flats Field. This data was used to investigate its potential to test initial geologic classification of the oil wells in the Collier Flats Field.

The following initial oil production (IPOIL) and final shut-in pressure (FSIP) are correlated with core data and well logs for the Lemon and Rhoades leases:

| High Permeability Oil Wells (based on geologic criteria) | | | | | | Low Permeability Oil Wells (based on geologic criteria) | | | | | |
|---|---|---|---|---|---|---|---|---|---|---|---|
| **Well Name** | **ipoil bopd** | **ffp psig** | **fsip psig** | **ave $\phi$3** | **ave (k)[4]** | **Well Name** | **ipoil bopd** | **ffp psig** | **fsip psig** | **ave $\phi$3** | **ave (k)[4]** |
| LEMON 1 | 288 | 455 | 1833 | 15[5] | 24[6] | LEMON 7 | 84 | 77 | 1695 | 16 | 1 |
| LEMON 5 | 240 | 68 | 1700 | 22 | 35 | LEMON 10 | 40 | 117 | 1524 | 22 | 8 |
| LEMON 6 | 264 | 243 | 1741[1] | 19 | 61 | LEMON 8 | 115 | 67 | 1498 | 10 | 4 |
| LEMON 3 | 170 | 85 | 1737[1] | 15[5] | 32[6] | RHOADES 1 | 48 | 50 | 1495 | 14 | 8 |
| RHOADES 3 | 156 | 140 | 1689[1] | 16 | 17 | RHOADES 4 | 172 | 237 | 1735 | 16 | 2 |
| RHOADES 2 | 96 | 554 | 1693 | 19 | 79 | LEMON 2-X | 48 | 208 | 779 | 7 | 1 |
| LEMON 11 | 2[2] | 160 | 1823 | 14[5] | 30[6] | HACKN'Y 2-13 | 76 | 88 | 1415 | 24[5] | 2[6] |
| | | | | | | LEMON 1-26 | 9 | 252 | 1404 | 11[5] | 1[6] |
| | | | | | | LEMON 9 | 216 | 21 | 1737 | 16[5] | 1[6] |
| average | 177 | 244 | 1745 | 17 | 40 | average | 90 | 124 | 1476 | 15 | 3 |
| | | | | | | | | | | | |

1 - ISIP (initial shut-in pressure data)
2 - gas cap well (excluded from average and std. deviation computations)
3 - weighted average (2 foot intervals) of core porosity data
4 - weighted average (2 foot intervals) of core horizontal permeability data
5 - weighted average (2 foot intervals) of well-log derived porosity data
6 - weighted average (2 foot intervals) of well-log derived permeability data

Table 5.7 Initial oil production (IPOIL), final shut-in pressure (FSIP), final flowing pressure (FFP), porosity ($\phi$), permeability (k) are correlated with core data and well logs for the Lemon and Rhoades leases.

Final shut-in pressure for high permeability wells average 1749 psi which is significantly different from the 1457 psi average for low permeability wells. Unfortunately, DST build-up data for the cored wells are unavailable to verify if FSIP and IPOIL are related to permeability.

Horner (1951) developed the basic equation (Equation 5.3) used for analysis of drillstem test data. The equation relates pressure behavior in an infinite, homogeneous, one well reservoir containing a fluid of small constant compressibility. These assumptions have been applied to newly completed oil reservoirs above the bubble point and expressed in oil field

units of pounds per square inch gauge (psig) , stock tank barrels per day (STB/D), centipoise (cp.), millidarcy (md), feet (ft) and minutes (t).

Equation 5.3 Horner Equation

$$p_{ws} = p_i - 162.6\frac{quB}{kh}\log\left(\frac{t + \Delta t}{\Delta t}\right)$$ from Horner, 1951.

$p_{ws}$ = formation pressure during build - up (psig)

$p_i$ = shut - in reservoir pressure (psig)

q = average production rate (stock tank barrels / day)

u = oil viscosity (centipoise)

B = formation volume factor (reservoir barrels / stock tank barrels)

k = permeability (milldarcies)

h = net DST zone (feet)

t = flowing time (minutes)

Dt = shut - in time (minutes)

The Horner equation can be simplified to equation 5.4 where "M" is defined as the slope of a straight line that describes "$P_{ws}$" versus "log (t + Δt / Δt) on semi-log paper.

Equation 5.4: Horner Equation Modification

$$p_{ws} = p_i - M\log\left(\frac{t + \Delta t}{\Delta t}\right)$$ from Horner, 1951.

where M = 162.6 QuB / kh and

the slope of the line in (psi / cycle)

on a semi - log plot.

Once "M" is identified from a semi-log plot, permeability is derived by rearranging the equation as follows: k h = ((162.6 Q u B) / M) and solving for "k". In the Collier Flats Field, there are 14 wells where complete DST data are available including wells previously classified as low and high permeability wells. Drill Stem Test pressure analysis on those 14 wells shows that Final Shut In Pressure (FSIP) is can be related to permeability and supports the initial oil well classification based on the geologic models.

## Drillstem Test Analysis

Drillstem tests are essentially a temporary open hole completion of a potential reservoir to determine the possibility of commercial production by virtue of the fluids recovered and observed flow rates. In addition to a sample of reservoir fluids and their flow rates, static bottom hole pressure, flowing bottom hole pressure and short term pressure transient data are obtained from the drillstem test. The testing procedure records the following pressure data as a function of time: 1)initial hydrostatic mud pressure, 2)first initial flowing pressure, 3) first final flowing pressure, 4) initial shut-in pressure, 5) second initial flowing pressure, 6) second final flowing pressure, 7) final shut-in pressure and 8) final hydrostatic mud pressure (Figure 5.20). These pressures and recovered fluids are typically recorded on scout ticket forms and are available for a majority of the wells in the Collier Flats Field. There are 14 wells with complete Drill Stem Test data that include pressure data as a function of time describing pressure changes during first and second flow periods and pressure buildup between points (three & four) and points (six & seven) (Figure 5.20). Transient pressure data allows Drill Stem Test analysis using the Horner Method to calculate permeability and evaluate pressure data (Appendix D). Unfortunately, none of the wells with DST data have core data (Figure 5.21).

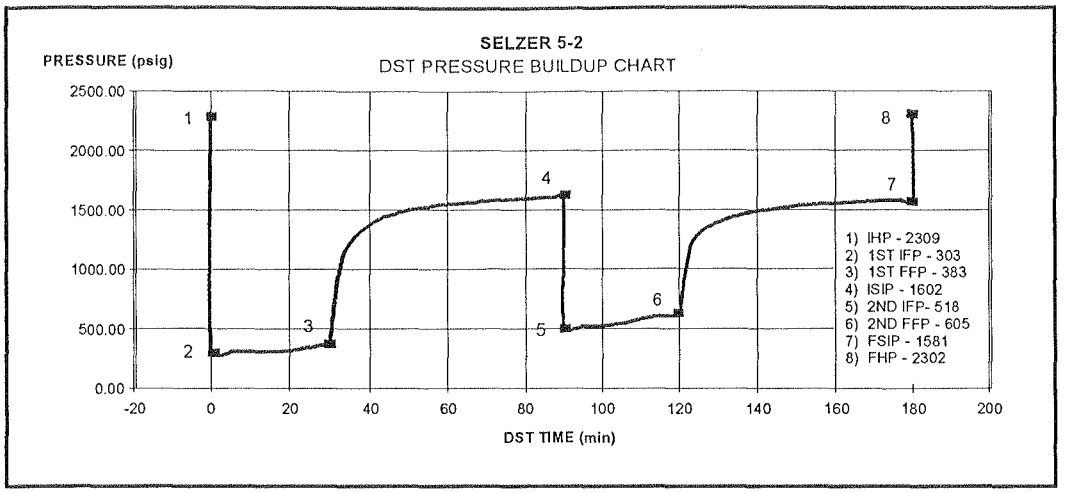


Figure 5.20 DST Pressure Buildup Chart displaying reported pressure data.

### Horner Analysis Methodology: Selzer 1-35 DST Data

The first step in the Horner analysis is to construct a Horner plot to determine the slope of a line that describes initial and final pressure buildup data versus Horner time on a semi-log plot. Horner time, (tp +Δt/Δt), is calculated individually for the initial and final pressure buildup data. Horner time for the initial buildup plot is calculated as follows: tp = first flow period time and Δt = is the time interval between initial pressure buildup measurements. Horner time for the final buildup is calculated as follows: tp = second flow period time and Δt = is the time interval between final pressure buildup measurements (Figure 5.22).

Several pieces of information are obtained from a Horner Plot: 1) "M"; slope of the final pressure buildup use to calculate permeability, 2) "Pi" an estimate of initial reservoir pressure and 3) "P1 hr" an estimate of the pressure 1 hour into the final buildup used in calculating wellbore damage (Figure 5.22). The second step in the Horner analysis is to calculate an average production rate based on the fluids recovered during the DST test. Table 5.8 shows DST data and methodology used to calculate average fluid production rate.

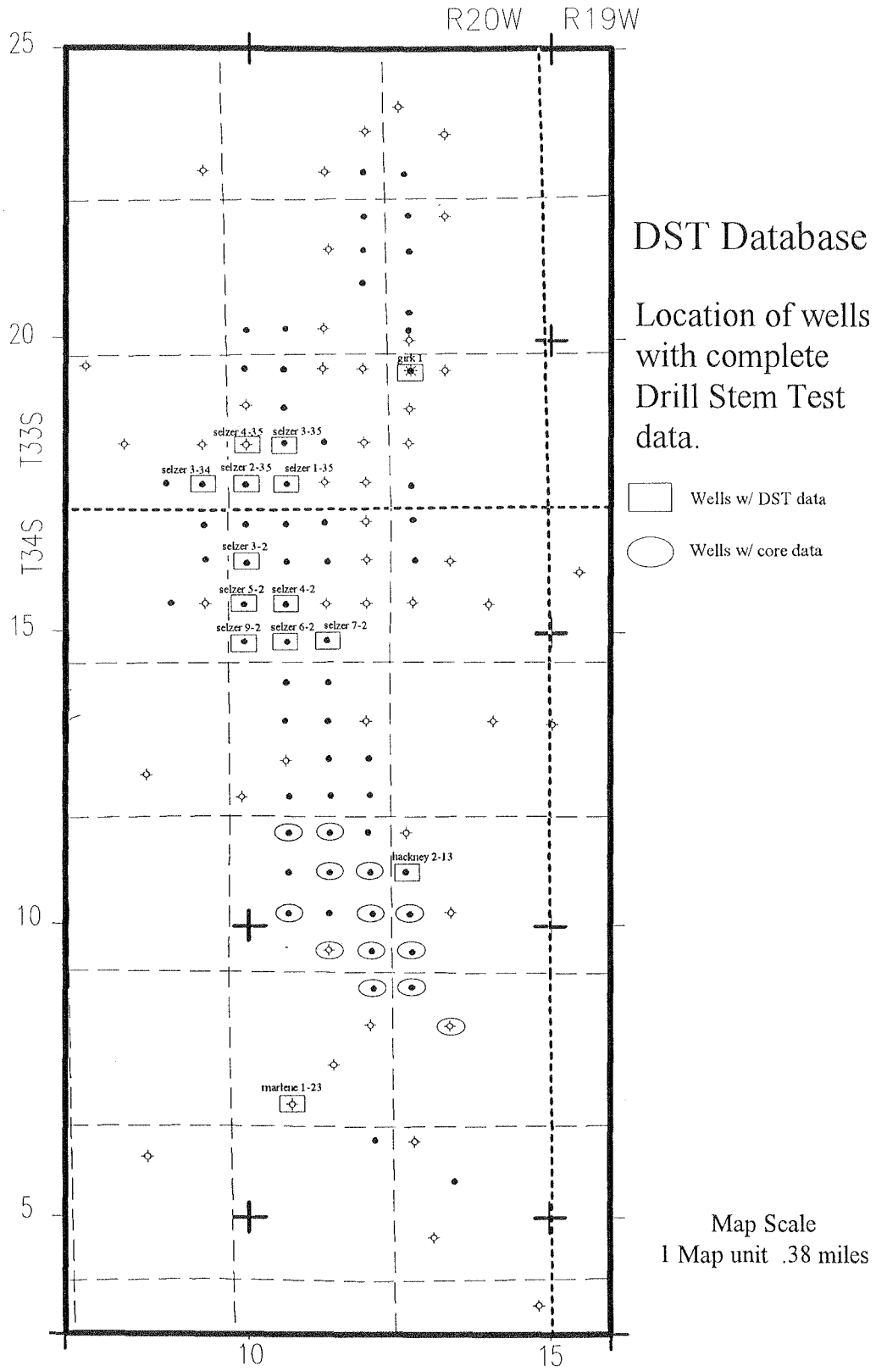


Figure 5-21 Drill Stem Test database and well location map.

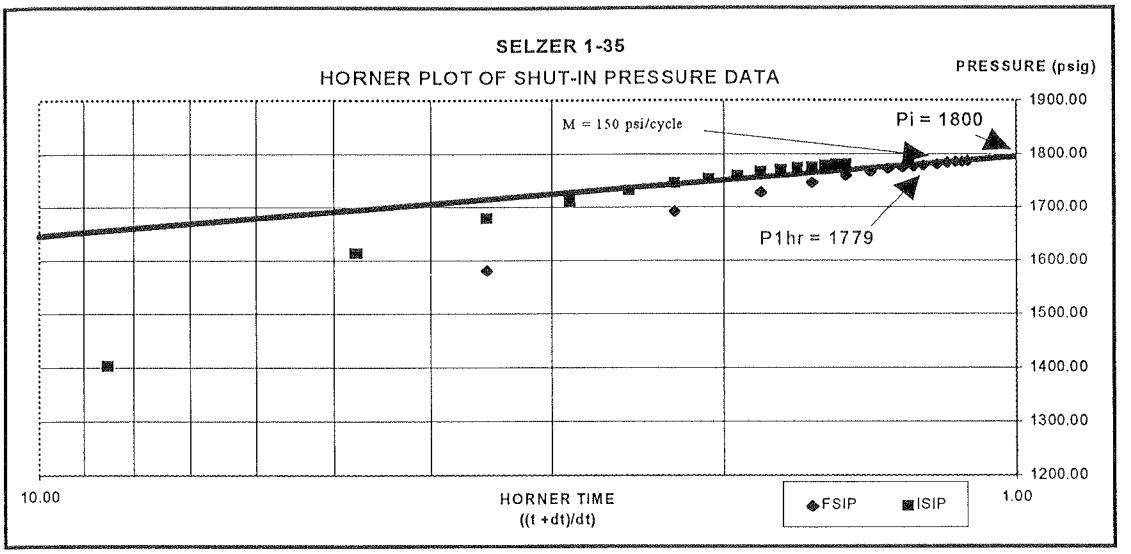


Figure 5.22 Sample Horner Plot of initial and final pressure build-up data.

| Selzer 1-35 DST Average Fluid Production Rate Calculation | | |
|---|---|---|
| **Data Type** | **Data Value** | **Data Source** |
| Drill Collar Length | 510 ft. | DST Header |
| Drill Collar I.D. | 2.25 in. | DST Header |
| Drill Collar Volume | 0.0049 bbl./ft. | Halliburton Cementing Table |
| Drill Pipe Length | 4183 ft. | DST Header |
| Drill Pipe I.D. | 3.8 in. | DST Header |
| Drill Pipe Volume | 0.0142 bbl./ft. | Halliburton Cementing Table |
| Total Flowing Time - "T" | Initial Flow 30 min; Final Flow 15 min | DST Header |
| Total Fluid Recovery | 120 ft. ogcm & 1500 ft. go = 1620 ft. of fluid | DST Recovery Section |
| Fluid recovered in drill collar | 510 ft. * 0.0049 bbl./ft. = 2.5 bbls. | |
| Fluid recovered in drill pipe | 1110 ft * 0.0142 bbl./ft. = 15.8 bbls. | |
| Total Fluid Rate (BFPD) | [2.5 bbls. + 15.8 bbls.]*[1440 (min/day) / 45 min. (Total Production Time)]= 585 BFPD | |

Table 5.8 Average Fluid Production Rate Calculation.

Calculation of average fluid production rate is at best an approximation due to many factors including; errors in measurements of flow-period length, drill collar measurements, types of fluids recovered and decompression of fluids in the well bore from hydrostatic (2268 psig) to reservoir pressures (1800 psig).

| Selzer 1-35 DST Average Permeability Calculation | | |
|---|---|---|
| **Data Type** | **Data Value** | **Data Source** |
| Average Fluid Production Rate "Q" | 585 BFPD | Average fluid production rate calculation. |
| Oil Viscosity "μ" | 0.389 centipoise @ 1695 psig and 125 F▪ | Henderson & Co. 1981. |
| Formation Volume Factor "B" | 1.49 RB/STB @ 1695 psig and 125 F▪ | Henderson & Co. 1981. |
| Slope of FSIP Buildup "M" | 150 psi./cycle | Horner Plot. |
| DST Interval (porous interval) "h" | 12 ft. | Well log analysis |
| Average Permeability "k" | [(162.6 * 585 BOPD * .52 cp. * 1.49 (RB/STB))/ (150 (psi/cycle)* 12 ft)] = 31 md. | |

Table 5.9 Average permeability calculation.

The third step in the Horner analysis is a calculation of permeability based on equation 5.4 $k = [(162.6\ Q\mu B)/(Mh)]$ (Table 5.9).

Henderson & Company performed a waterflood feasibility study on the Lemon Ranch and Rhoades leases in 1981. This study included calculating a formation volume factor and oil viscosity based on a reservoir fluid analysis of the Lemon 6 well. This data is used in all DST calculations. Calculation of permeability is fairly straight forward, however, interpretation of the results is complicated by variations in build-up time, wellbore damage and improvement effects.

Wellbore damage and improvement effects are expressed in terms of a "skin factor" "S" which is positive for wells with formation damage and negative for improvement in the wellbore. The skin factor can vary from -5 for a fractured well and $+\infty$ for a damaged well (Earlougher, 1977).

The skin factor of 5.95 indicates that there is well bore damage that inhibits flow into the wellbore (Table 5.10). Wellbore damage impacts Horner permeability and average oil production rate calculations by reducing total feet of reservoir fluids recovered during the DST flow periods.

| Selzer 1-35 DST Skin Factor Calculation | | |
|---|---|---|
| **Data Type** | **Data Value** | **Data Source** |
| FSIP @ 1 hour - $P_{1hr}$ | 1779 psig | Extrapolated from Horner straight line. |
| FSIP @ $\Delta t = 0$ - $P_{wf}$ | 344 psig | DST Data |
| Slope of Horner Line - M | 150 psi/cycle | Extrapolated from Horner straight line. |
| Second Flow Production Time - Tp | 0.25 hours | DST Data |
| Horner Permeability - k | 31 md | DST Ave. Perm. Calculation |
| Porosity - $\phi$ | 0.25 | Log Analysis |
| Oil Viscosity - $\mu$ | 0.389 cp | Henderson & Co., 1981 |
| Oil Compressibility - Cr | 1.39E-05 | Henderson & Co., 1981 |
| Well Bore Radius - $Rw^2$ | 0.33 ft. | DST Data |
| Skin Factor - s<br>s = 5.95 | $s = 1.1513 * \left[ \frac{p_{1hr} - p_{wf(\Delta t = 0)}}{M} + log\left(\frac{t_p + 1}{t_p}\right) - log\left(\frac{k}{\phi \mu c_t r_w^2}\right) + 3.2275 \right]$ | |

Table 5.10 Selzer 1-35 DST Skin Factor Calculation.

### Discussion of Selzer 1-35 DST Analysis Example

Drillstem test analysis data provide an opportunity to test initial classification of the Selzer 1-35 and others as high or low permeability oil wells based on the geologic models and well log signatures. However, bad hole conditions, tool malfunctions and inaccurate flow measurements can render DST data questionable to unusable. It is therefore important to perform DST quality checks. Hydrostatic pressure calculations, theoretical flow recovery calculations, DST chart characteristics and remarks noted on the DST forms are used to quality check DST data.

| Selzer 1-35 DST Hydrostatic Pressure Quality Check Calculation | | | |
|---|---|---|---|
| **Data Type** | **Data Value** | | **Data Source** |
| DST Gauge Depth | 4772 | ft | DST Header |
| Mud Weight | 9.2 | lb/gal | DST Header |
| (lb/cu ft) to (lb/gal) conversion | 7.4805 | (lb/cu ft)/(lb/gal) | Conversion Tables |
| Water Density | 62.3664 | lb / cu ft | Conversion Tables |
| Water Gradient | 0.4331 | psi/ ft | Conversion Tables |
| Hydrostatic Pressure Equation | = (Gauge Depth)*(Mud wt)* 7.4805 * (.4331 / 62.3664) | | |
| Calculated hydrostatic pressure | 2280 | psig | Equation |
| Initial Hydrostatic Pressure | 2255 | psig | DST Header |
| Final Hydrostatic Pressure | 2268 | psig | DST Header |

Table 5.11 Selzer 1-35 DST Hydrostatic Pressure Quality Check Calculation.

The first test of DST data is a simple calculation of hydrostatic pressure which should identify DST tool leaks. Table 5.11 shows the data and equation used to calculate DST hydrostatic pressure. The difference between Selzer 1-35 calculated and measured hydrostatic pressures is approximately 1 percent. The difference between initial and final measured hydrostatic pressure is also approximately 1 percent. Deviations in the range of 0.5 to 1 percent are indicative of good DST pressure data (Earlougher, 1977).

Table 5.12 shows the data and equation used to calculate theoretical fluid recoveries based on final flow pressures. This information can be compared to actual DST recovered fluids to get a feel for well bore damage and fluid recovery.

| Selzer 1-35 DST Theoretical Fluid Recovery Calculations | | | |
|---|---|---|---|
| **Data Type** | **Data Value** | | **Data Source** |
| First Final Flow Pressure | 280 | psig | DST Header |
| Mud Weight | 9.2 | lb/gal | DST Header |
| (lb/cu ft) to (lb/gal) conversion | 7.4805 | (lb/cu ft)/(lb/gal) | Conversion Tables |
| Water Density | 62.3664 | lb / cu ft | Conversion Tables |
| Water Gradient | 0.4331 | psi/ ft | Conversion Tables |
| Theoretical first Flow Fluid Recovery (mud only) | = (1st Flow Pres)/[(Mud wt)* 7.4805 * (0.4331 / 62.3664)] | | |
| **Calculated Theoretical First Flow Fluid Recovery (mud only)** | 585 | ft of mud | Equation |

Table 5.12 Selzer 1-35 DST Theoretical Fluid Recovery Calculations.

| Data Type | Data Value | | Data Source |
|---|---|---|---|
| Second Final Flow Pressure | 344 | psig | DST Header |
| Oil Weight | 6.68 | lb/gal | Based on (0.8 g/cm^3 oil specific gravity) *(8.345405 (gm/cm) / (lb/gal)) conversion |
| (lb/cu ft) to (lb/gal) conversion | 7.4805 | (lb/cu ft)/(lb/gal) | Conversion Tables |
| Water Density | 62.3664 | lb / cu ft | Conversion Tables |
| Oil Gradient | 0.35 | psi/ ft | Conversion Tables |
| Theoretical Second Flow Fluid Recovery (oil only) | = (2nd Flow Pres)/[(oil wt)* 7.4805 * (0.35 / 62.3664)] | | |
| **Calculated Theoretical Second Flow Fluid Recovery (oil only)** | 1240 | ft of oil | Equation |

Table 5.12 Cont.: Selzer 1-35 DST Theoretical Fluid Recovery Calculations.

In the Selzer 1-35 DST test header, only 120 feet of oil and gas cut mud was reported and a "well flowed oil" notation. Assuming that the first flow period flowed 585 feet of mud and the second flow period flowed 1240 feet of oil totaling 1825 feet of fluids, a reported value of 120 feet of oil and gas cut mud appears very questionable. In a drilling report on the Selzer 1-35, it is noted that 1500 ft of gassy oil was reversed out of the pipe for a total of 1620 feet of reservoir fluids.

A third way to check DST data is visual inspection of DST charts. Good DST charts typically have the following characteristics:

- pressure base line is straight,
- recorded initial and final hydrostatic pressures are nearly identical and are consistent with depth and mud weight,
- and flow and pressure build-up pressures plot as a smooth curve (Earlougher, 1977).

Earlougher (1977) published fourteen DST charts that illustrate the effects of bad hole conditions, tool malfunctions and other difficulties on DST pressure charts.

In the case of the Selzer 1-35 oil well, conventional analysis of DST pressure data can be used to test the geologic models for the Collier Flats Field used to classify oil wells as either high or low permeability (Table 5.14). The Selzer 1-35 oil well is located in an area where the net feet of porosity greater than 10% is seven feet and net thickness of low gamma-ray facies is six feet. Additionally, porosity appears to cross lithologic boundaries from the "clean" grainstones down into the mud supported lithologies defined by gamma-ray well log signatures. Using the high permeability porosity-permeability correlation (Equation 5.2), average permeability for a seven foot interval of porosity greater than 10% is estimated at 58 md. A 10% porosity cutoff is used since whole core analysis data show effective porosity begins at 10%. Horner permeability is calculated as 31 md with a skin factor of 5.95 indicating that there is some well bore damage that reduces average permeability for the well. Calculated hydrostatic pressures, theoretical fluid recoveries and visual inspection of the DST pressure chart all indicate that the DST pressure data is sound. Initial oil production was 241 BOPD with 385 MCFPD of associated gas from a perforated interval of 4758 to 4763 feet. Selzer 1-35 production data is reported by lease with three other wells. Therefore, production data can not be used as an additional independent reservoir performance criteria to test geologic interpretations due to this commingling of production.

**Discussion of Other DST Results**

Initial classification of the 14 wells with DST data is presented in Tables 5.13 and 5.14 with their locations presented in Figure 5.21. Additionally, Collier Flats Field net feet of porosity greater than 10%, (Figure 5.23), and net feet of low gamma-ray facies (Figure 5.24) isopach maps are referenced to aid in the discussion of DST analysis results.

| Initial Geologic Classification of Wells W/ DST Data (Low Permeability Oil Wells) | | | | | | |
|---|---|---|---|---|---|---|
| Well Name | IPOIL | IPGAS | LOW-GR | POR >10% | AVE-POR | Well Location Relative To Sand Shoals |
| Marlene 1-23 | 0 | 0 | 4 | 2 | 11 | Well located south of the southern margin of carbonate sand shoal. |
| Girk 1 | 54 | 160 | 4 | 3 | 12 | Well located on the southern margin of northern carbonate sand shoal behind main sand shoal. |
| Selzer 3-2 | 123 | 192 | 5 | 3 | 12 | Well located in the main carbonate sand shoal between thicker more porous zones. |
| Selzer 9-2 | 7 | N/A | 5 | 6 | 14 | Well located on the seaward margin of main carbonate sand shoal. |
| Selzer 3-34 | 280 | 450 | 6 | 4 | 17 | Well located on the seaward margin of main sand shoal. |
| Selzer 4-35 | 0 | 0 | 5 | 2 | 15 | Well located on the seaward margin of main carbonate sand shoal. |
| Selzer 2-35 | 0 | 0 | 5 | 4 | 17 | Well located in the main carbonate sand shoal. |
| Hackney 2-13 | 76 | N/A | 5 | 4 | 24 | Well located leeward margin of main carbonate sand shoal. |

Table 5.13 Initial Classification of Wells W/ DST Data (Low Permeability Oil Wells).

| Initial Geologic Classification of Wells W/ DST Data (High Permeability Oil Wells) | | | | | | |
|---|---|---|---|---|---|---|
| Well Name | IPOIL | IPGAS | LOW-GR | POR >10% | AVE POR | Well Location Relative To Sand Shoals |
| | BOPD | MCFPD | Net Ft. | Net Ft. | | |
| Selzer 4-2 | 113 | 195 | 6 | 8 | 17 | Well located in the thickest area of main carbonate sand shoal. |
| Selzer 5-2 | 113 | 120 | 10 | 10 | 21 | Well located in the thickest area of main carbonate sand shoal. |
| Selzer 6-2 | 292 | 200 | 6 | 11 | 20 | Well located in the thickest area of main carbonate sand shoal. |
| Selzer 7-2 | 90 | 121 | 6 | 6 | 21 | Well located in the thickest area of main carbonate sand shoal. |
| Selzer 1-35 | 241 | 385 | 6 | 7 | 25 | Well located in the thickest area of main carbonate sand shoal. |
| Selzer 3-35 | 9 | N/A | 6 | 6 | 15 | Well located in the thickest area of main carbonate sand shoal. |

Table 5.14 Initial Classification of Wells W/ DST Data (High Permeability Oil Wells).

Initial classification of the 14 wells with DST pressure data is based entirely on depositional and diagenetic geologic models, well log analysis and well log curve character. Figure 5.25 is a histogram that summarize DST pressure data for the 14 wells in question. Tables 5.15 and 5.16 summarize DST Horner calculations.

| DST Horner Calculation Summary (Low Permeability Oil Wells) | | | | |
|---|---|---|---|---|
| **Well Name** | **Horner Perm. md** | **Calc. Perm. md** | **Skin** | **Comments** |
| Marlene 1-23 | 1.28 | 2.1 | -4.14 | Good shows w/ froggy oil recovered. Completed in Mississippian. Negative skin indicates permeability may be fractures. No drilling report. No vuggy porosity reported. |
| Girk 1 | 6.17 | 2.1 | 12.88 | Initial completion in Toronto. Recompleted in Bethany Falls. Put on pump to complete. No vuggy porosity reported. |
| Selzer 3-2 | 2.71 | 1.8 | -1.59 | Completed as a flowing oil well. Permeability my be enhanced from fractures. Vuggy porosity is reported. |
| Selzer 9-2 | 0.11 | 3.1 | -2.96 | Reacidized, very gassy well, put on pump to complete. Permeability may be enhanced by fractures. Vuggy porosity reported. |
| Selzer 3-34 | 2.91 | 4.1 | -0.43 | Completed as a flowing well and dual completion. Good vuggy porosity reported. |
| Selzer 4-35 | 3.96 | 2.4 | 18.86 | Not completed in Bethany Falls. Minor vuggy porosity reported. |
| Selzer 2-35 | 0.23 | 2.9 | 36.88 | Completed in Stark Shale. Vuggy porosity reported. |
| Hackney 2-13 | 18.73 | 37 | 1.83 | Good vuggy and crystalline porosity reported. No drilling and completion reports. |

Table 5.15 DST Horner Calculation Summary (Low Permeability Oil Wells).

Correlation of interpreted low permeability wells with DST permeability calculations, initial production and DST pressure data indicate general agreement with the initial geologic classification. Generally, little or no vuggy porosity is reported by the DST operators which agrees with the interpretation of a moldic to vuggy porosity ratio of 2.8 : 1 or higher in the low permeability and non-productive cores.

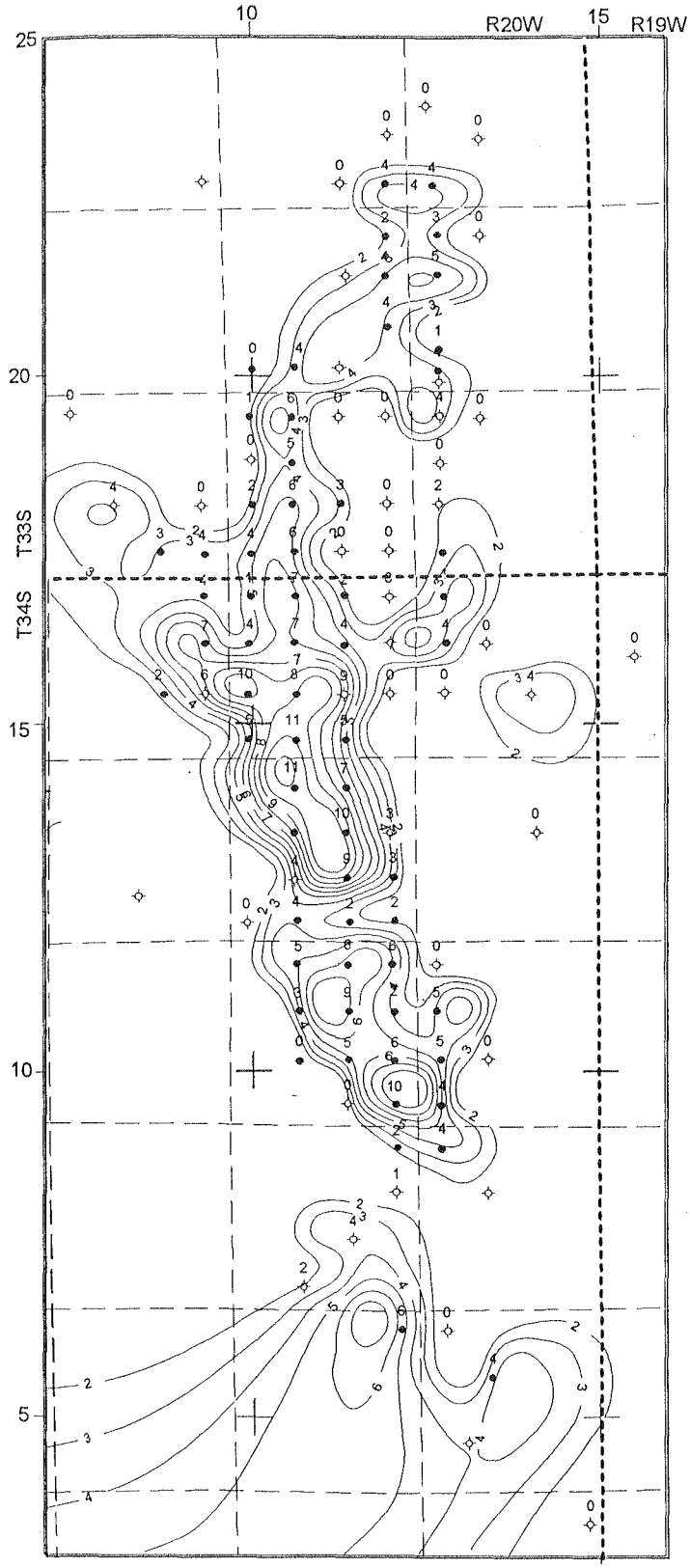


Net Thickness Of Porosity Greater Then 10 % In The Bethany Falls Limestone

(Porosity Data Based On Wireline Well Log Density Porosity Data)

Map Scale
1 Map Unit = 0.38 Mi.
Contour Interval = 1 Ft.

Figure 5.23 Net feet of porosity greater than 10%, Bethany Falls limestone.

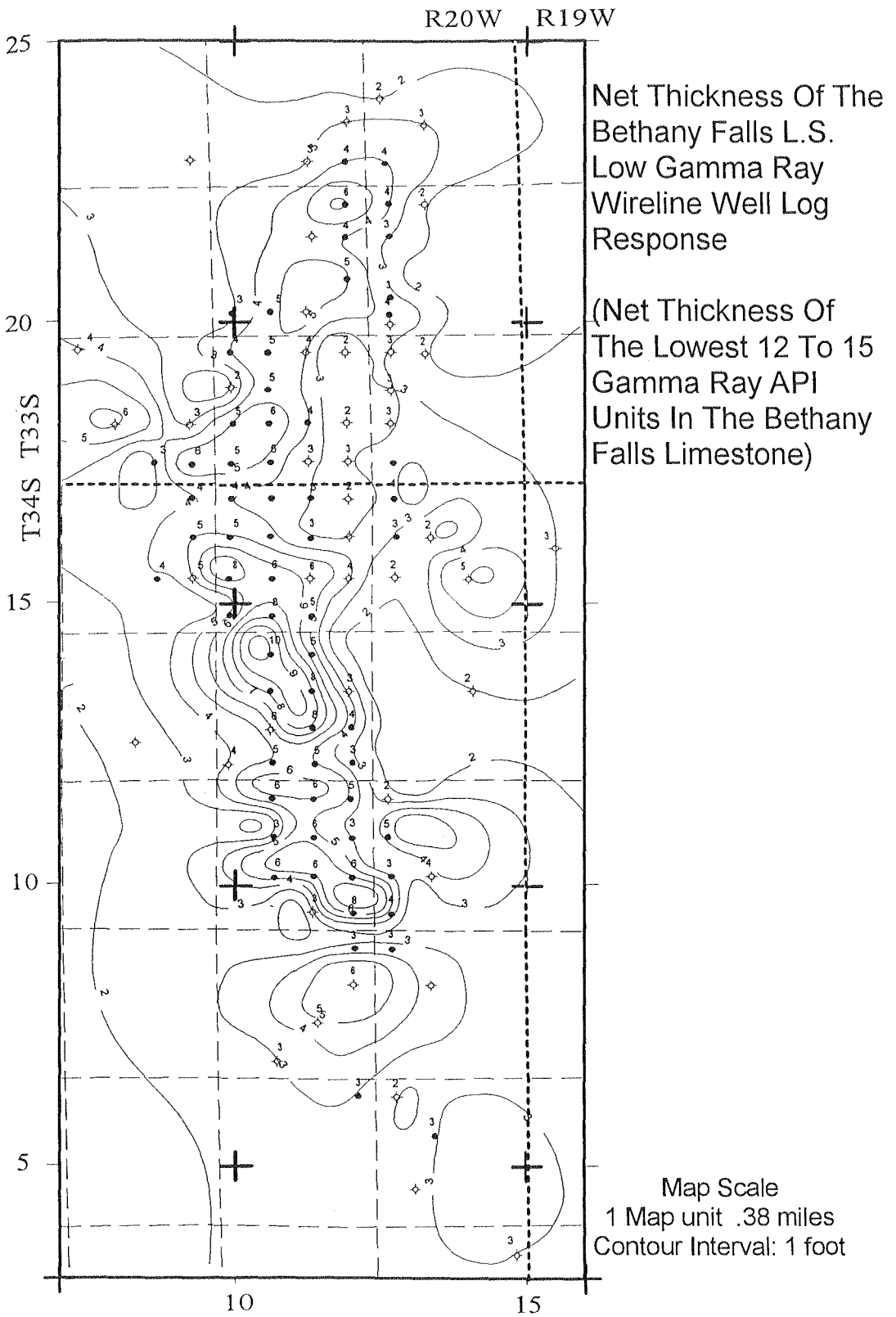


Figure 5-24 Net feet of low gamma-ray facies (net thickness of the lowest 12 API units), Bethany Falls limestone.

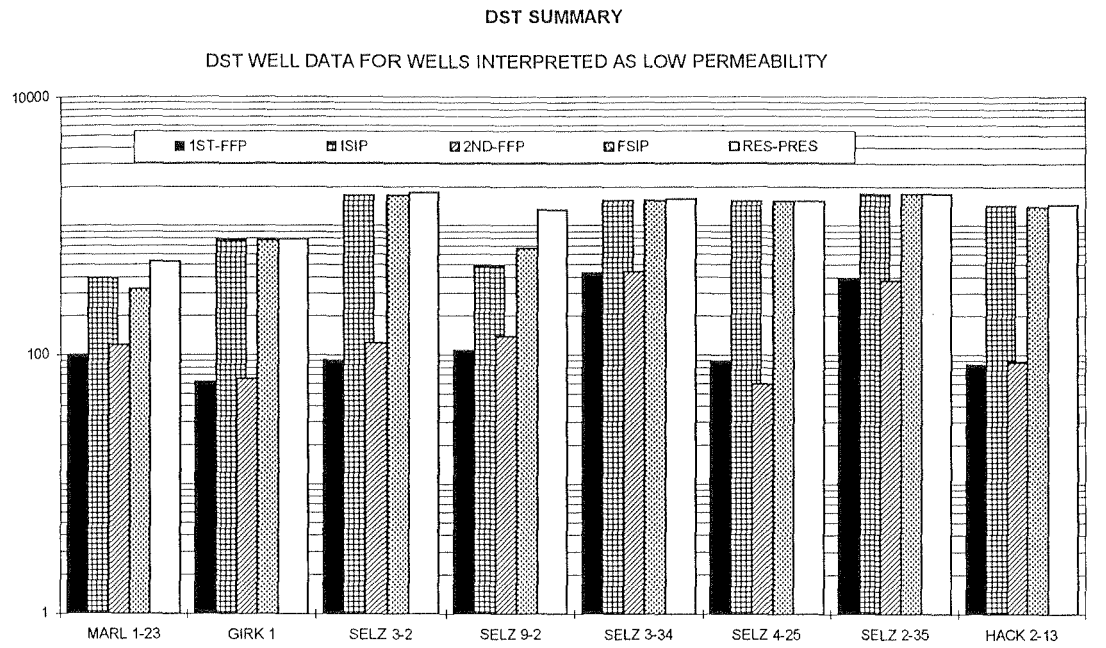


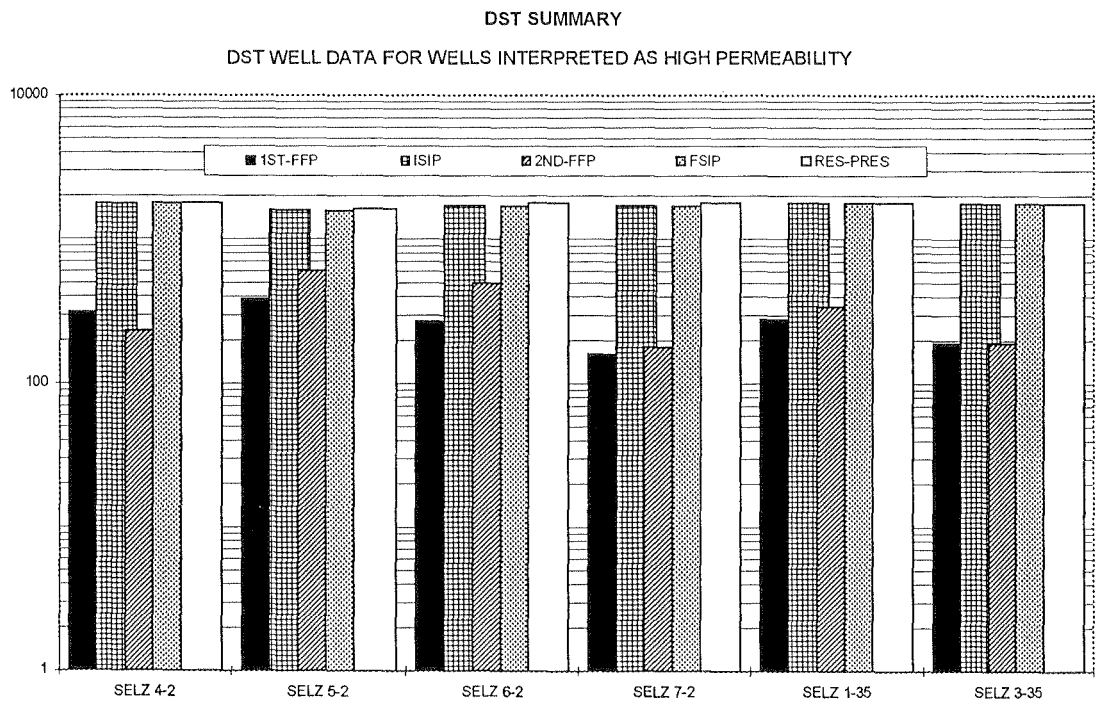


Figure 5.25 DST pressure data summary.

| DST Horner Calculation Summary (High Permeability Oil Wells) | | | | |
|---|---|---|---|---|
| Well Name | Horner Perm. md | Calc. Perm. md | Skin | Comments |
| Selzer 4-2 | 55.0 | 35 | 33.7 | Good vuggy , oolitic, oomoldic porosity reported. Flowing oil well on completion. Dual completion. |
| Selzer 5-2 | 23.3 | 61 | -1.84 | Good vuggy, oolitic, oomoldic porosity reported. Flowing oil well on completion. |
| Selzer 6-2 | 12.8 | 53 | -2.12 | Good vuggy, oolitic, oomoldic porosity reported. Flowing oil well on completion. |
| Selzer 7-2 | 8.1 | 51 | -1.43 | No vuggy porosity reported. Flowing oil well on completion. |
| Selzer 1-35 | 30.6 | 58 | 5.57 | Good vuggy, oolitic, oomoldic porosity reported. No drilling or completion report. |
| Selzer 3-35 | 0.3 | 36 | 69.26 | No vuggy porosity reported. Very gassy well. |

Table 5.16 DST Horner Calculation Summary (High Permeability Oil Wells).

Average initial and final flowing pressures are generally less than 150 psig (Figure 5.25) However, there are likely exceptions to the observed DST pressure trends, gamma ray well log trends, porosity greater than 10% isopach trends and well locations relative to depositional environment trends used to classify well locations as high or low permeability for the purposes of this reservoir characterization. These exceptions can be attributed to:

- The general trend of 6 feet of low gamma-ray facies and 5 feet of porosity greater than 10% not always work to differentiate low and high permeable wells. Subaerial exposure at the end of Bethany Falls deposition may have led to erosion of the upper portions of the generally permeable grainstone lithofacies (i.e. Hackney 2-13). Hackney 2-13 falls just below the borderline used to identify high permeability wells in terms of thickness of low gamma ray facies and thickness of porosity greater than 10% cutoffs used to classify wells as high or low permeability wells (Table 5.13). The Hackney 2-13 well averages 24 percent porosity over a four foot interval with DST permeability calculated as 18.73 md and a skin factor of 1.83 indicating that permeability may be even higher. Based on DST results, this well should use the high permeability porosity-permeability correlation #2 to

calculate permeability. As a result of this exception to the low gamma-ray and net feet of porosity greater than 10% criteria, it is realized that high average porosity, strong deflection of the gamma-ray curve to low gamma-ray values and good initial production are also indicative of high permeability wells. This example shows the value of these additional geologic and engineering criteria when considering borderline wells.

- Initial and final flowing pressure are generally less than 100 psig. However, DST flowing pressures for Selzer 3-34 and Selzer 2-35 wells are greater than 150 psig. In the case of the Selzer 3-34 well, a negative skin factor indicates natural fracturing. For the Selzer 2-35 wells, a high positive skin factor may explain the poor fluid recovery and anomalous flowing pressure.
- Natural fractures are observed in core and consequently may impact DST pressure build-up, fluid recovery, permeability calculations and initial production. A negative skin factor typically indicates a fractured well (Earlougher, 1977).
- Low initial production is not diagnostic of low permeability wells. Selzer 3-34 and Selzer 3-2 high initial production may be the result of natural fractures inferred from a negative skin factor.

Correlation of interpreted high permeability wells with DST permeability calculations, initial production and DST pressure data indicate general agreement with the initial geologic classification. Generally, vuggy porosity is reported which agrees with the interpretation of a moldic to vuggy porosity ratio of 1.3 : 1 or more in the high permeability productive cores. Average initial and final flowing pressures are generally more than 150 psig (Figure 5.25). Initial shut-in, final shut-in and initial reservoir pressure identified from the Horner plot are remarkably consistent. However, there are exceptions which can be attributed to:

- Horner permeability for the Selzer 3-35 is calculated at 0.3 md with a skin factor of 69.26. The high skin factor may be a result of low oil volume and high gas production. Two

million cubic feet of gas per day with only 2 feet of clean oil was reported on the DST test. No gas measurements were made for the initial production data.

- Horner permeability for the Selzer 7-2 is calculated at 8.08 md with a skin factor of -1.43. The low calculated Horner permeability may be related to no vuggy porosity reported in the drilling summary. The negative skin factor indicate that natural fracturing may play a role in oil production.

In general, permeability calculations based on DST pressure data appear to verify that a permeability contrast in these wells exists which lends supports to the previously developed Collier Flats Field geologic models.

Drill Stem Test analysis clearly illustrates that strict use of initial oil production, DST shut-in and buildup pressure reported on scout tickets can not be relied on to verify initial geologic classification of the wells in the Collier Flats Field. However, these types of pressure and production data can aid in classification of Collier Flats Field oil wells in borderline cases and test initial classification.

# Reservoir Characterization Results

## Collier Flats Field Reservoir Data (Porosity, Permeability, Water Saturation)

The preceding sections of this reservoir characterization present the correlations (porosity / permeability and cementation factor) necessary to begin the Collier Flats field reservoir characterization. The following steps were followed to calculate porosity, permeability and water saturation data for the Collier Flats field:

1) Well log data were digitized into TerraSciences, Inc., Terrastation TLOG modules for analysis.

2) Well log data were quality checked against original logs and printed using TLOG modules to verify digitizing accuracy.

3) Standard company borehole or environmental corrections (Dresser Atlas, Schlumberger, Wellex, Gearhart) were performed on the well log resistivity data using Terrastation TLOG modules.

4) True Formation Resistivity (Rt) was calculated from company tornado charts using Terrastation TLOG modules, or a deep resistivity curve was used for Rt (i.e. Guard, Deep Induction or Laterolog).

5) Selection of the porosity/permeability model (low or high permeability).

6) Water saturation data was calculated using the Archie equation in the Terrastation TLOG modules. The following data was using in the Archie equation:

    a) Formation water resistivity (Rw) of 0.044 ohms @ 125 degrees F.;

    b) density porosity ($\phi_D$) if available;

    c) True formation resistivity data (Rt);

    d) Cementation factor (m) of 2.5 or 3.0;

    e) Saturation exponent (n) of 2.0;

    f) and formation factor / porosity constant "a" is 1.0.

7) Permeability was calculated using the low or high permeability porosity/permeability correlation equation 5.1 or 5.2 in the Terrastation TLOG module.

8) Well log data with water saturation and permeability were printed using TLOG modules to present results.

9) Well Name, Well-ID, Gamma Ray, Porosity, Water saturation and Permeability data in one foot intervals through the Bethany Falls limestone *(8% porosity was used as a lower cutoff value for potential pay)* was converted into ASCII text files using Terrastation TerraLOAD modules and compiled in Excel 5.0 spreadsheets (Table 5.17).

| WELL NAME | WELL-ID | DEPTH | GAMMA-RAY (API) | POROSITY (%) | WAT-SAT (%) | PERM (md) |
|---|---|---|---|---|---|---|
| LEMON 6 | 55.00 | 4780.00 | 30 | 30 | 30 | 10.0 |
| | | 4781.00 | 25 | 21 | 28 | 8.0 |
| | | 4782.00 | 24 | 23 | 27 | 5.8 |
| | | 4783.00 | 24 | 17 | 40 | 22.5 |
| | | 4784.00 | 25 | 23 | 19 | 130 |
| | | 4785.00 | 28 | 19 | 21 | 130 |
| | | 4786.00 | 31 | 18 | 25 | 26.7 |
| | | 4787.00 | 36 | 12 | 20 | 0.00 |
| | | 4788.00 | 42 | 20 | 19 | 280 |
| | | 4789.00 | 48 | 12 | 23 | 0.00 |

Table 5.17 Terrastation TLOG one foot average of reservoir data example.

Each productive well in the Collier Flats field with Terrastation well log data was written to a Excel 5.0 spreadsheet and the gamma ray, porosity, water saturation and permeability data was averaged over two foot intervals (Table 5.18). Two foot averages of the TLOG data were used because the vertical resolution for density logs is approximately 15"; 24" for Neutron logs and 20" for Gamma Ray logs (Hunt, E., Aly,A., and Pursell, D, 1996).

| WELL NAME | WELL-ID | INTERVAL THICK. (ft) | GAMMA-RAY (API) | POROSITY (%) | WAT-SAT (%) | PERM (md) |
|---|---|---|---|---|---|---|
| LEMON 6 | 55.00 | 2 | 27 | 25 | 29 | 9 |
| | | 2 | 24 | 20 | 34 | 14 |
| | | 2 | 26 | 21 | 20 | 130 |
| | | 2 | 34 | 15 | 22 | 13 |
| | | 2 | 45 | 16 | 21 | 140 |

Table 5.18 Two foot averages of Lemon 6 Terrastation TLOG reservoir data.

When two foot interval averaging of well log data was complete, an average for the entire porous interval was computed for gamma ray, porosity, water saturation and permeability data (Table 5.19). This data is mapped using PCMS mapping software and used to characterize genetic unit scale reservoir heterogeneity.

## Mapping Collier Flats Field Reservoir Data

Figures 5-26 through 5.34 are a series of maps that summarize Collier Flats Field reservoir data including the PCMS generated grids used to generate contour line data. Grids of reservoir elevation data, porosity, permeability and water saturation are presented since this information is typically used in reservoir simulators. A moving least square algorithm using the following data:

| | |
|---|---|
| Minimum X Coordinate ..... | 6.5 |
| Maximum X Coordinate ..... | 18.2 |
| Minimum Y Coordinate ..... | 2.6 |
| Maximum Y Coordinate ..... | 27.3 |
| X Direction Gridding Interval .... | 0.65 |
| Y Direction Gridding Interval .... | 0.65 |
| Number Of Grid Rows ..... | 39 |
| Number Of Grid Columns ..... | 19 |
| Number Of Z-Value Nodes..... | 741 |
| Number Of ZNON Nodes..... | 0 |
| Value of ZNON..... | -999999 |
| Data collection radius (REACH).... | 20.00 |

constructed the grids by interpolating between individual well data. The gridded data was then contoured by PCMS.

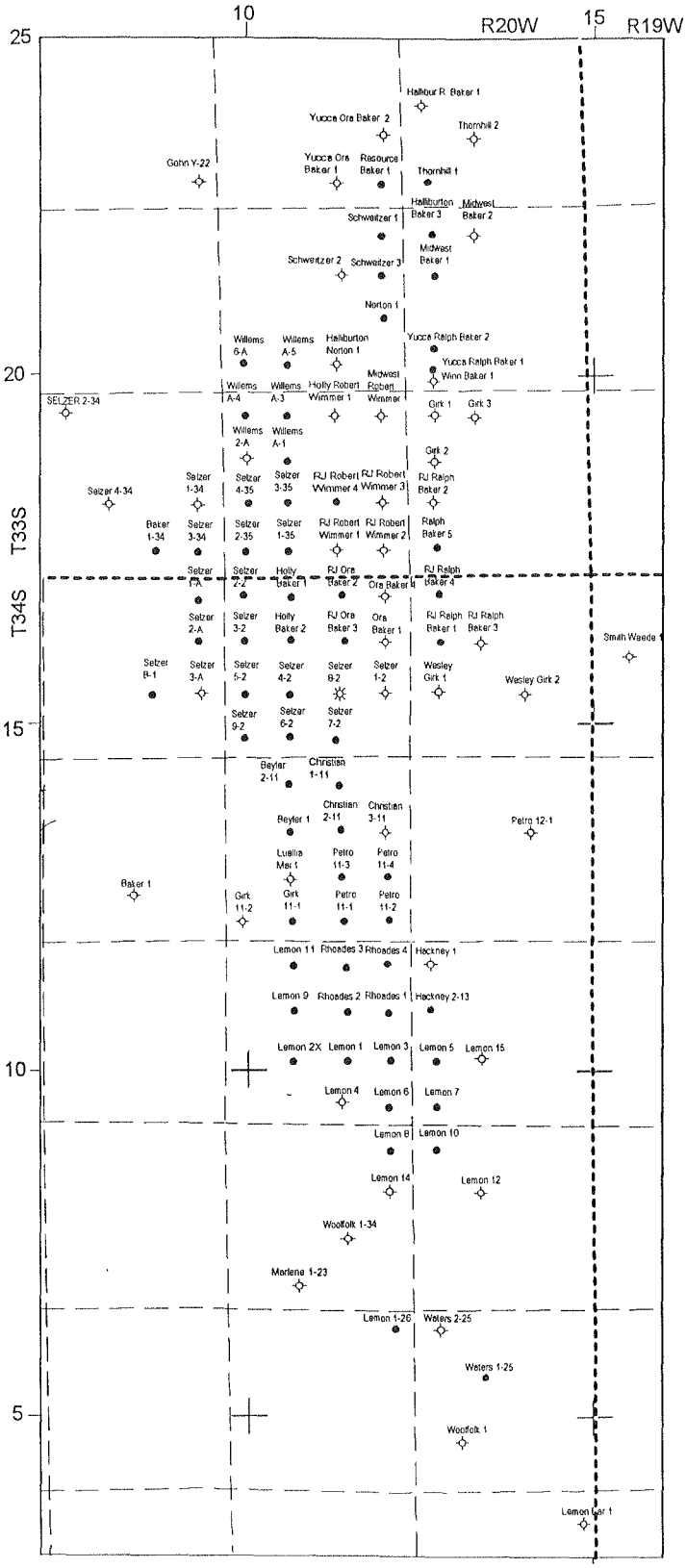


Figure 5-26 Collier Flats Field, Reservoir Characterization Well Location Database Map.

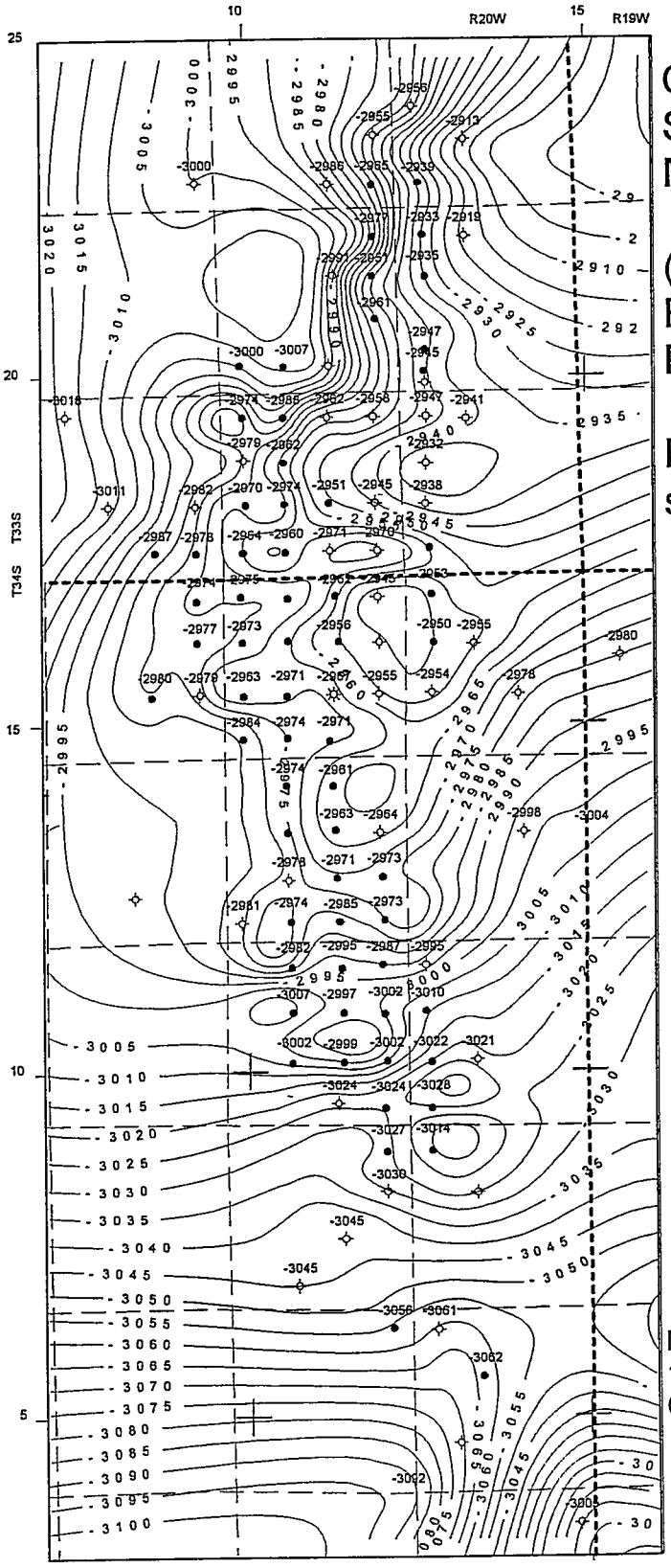


Collier Flats Field Structure Contour Map

(Top of the Bethany Falls Limestone Pay Zone)

Elevation data is sub-sea.

Map Scale
1 Map Unit = 0.38 Mi.
Contour Interval = 5 feet

Figure 5-27 Collier Flats Field, Structure Contour Map.

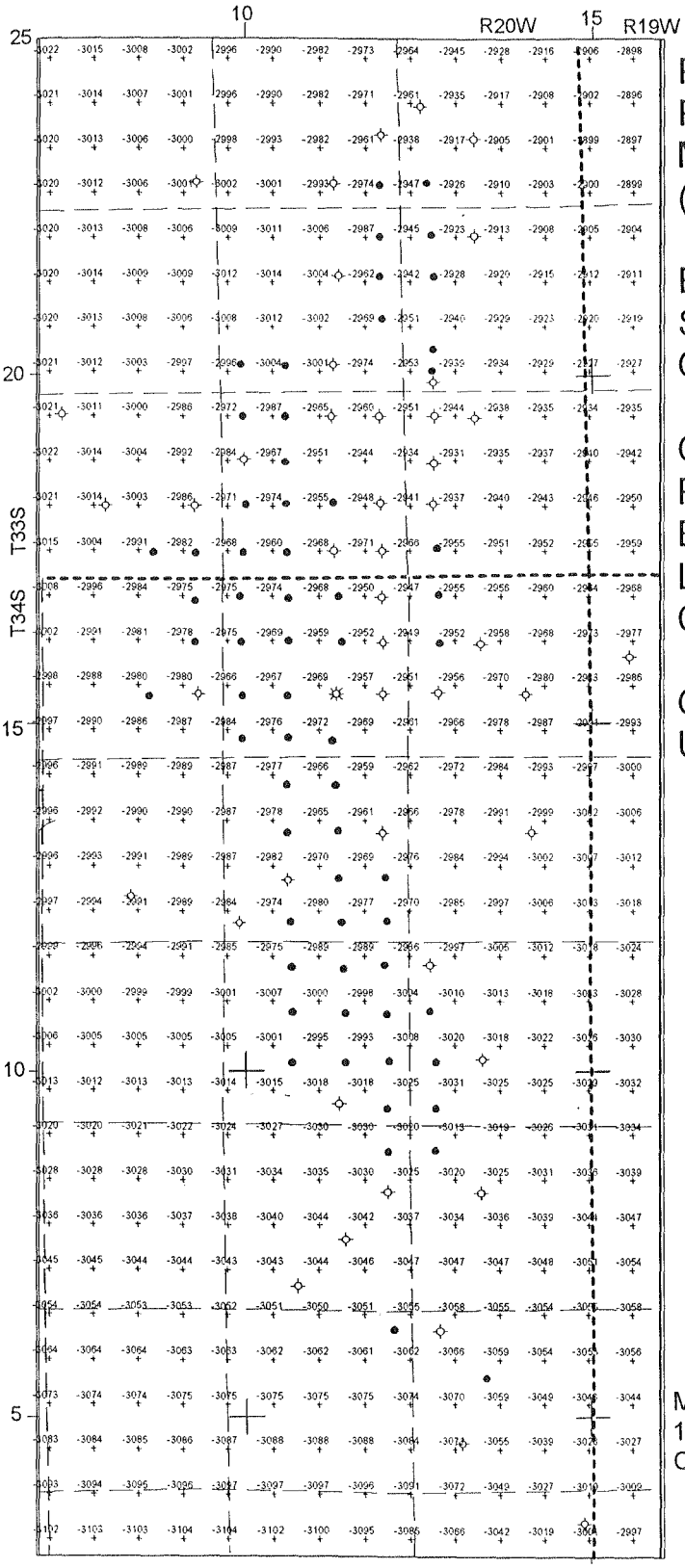


Petrospec Personal Computer Mapping System (PCMS) Software

Bethany Falls L.S. Structure Grid Data File

Grid File Is Used By PCMS To Create Bethany Falls Limestone Structure Contour Map

Grid spacing 0.65 Map Units = 0.25 mi.

Map Scale
1 Map Unit = 0.38 Mi.
Contour Interval = 5 feet

Figure 5-28 Collier Flats Field, Structure Grid.

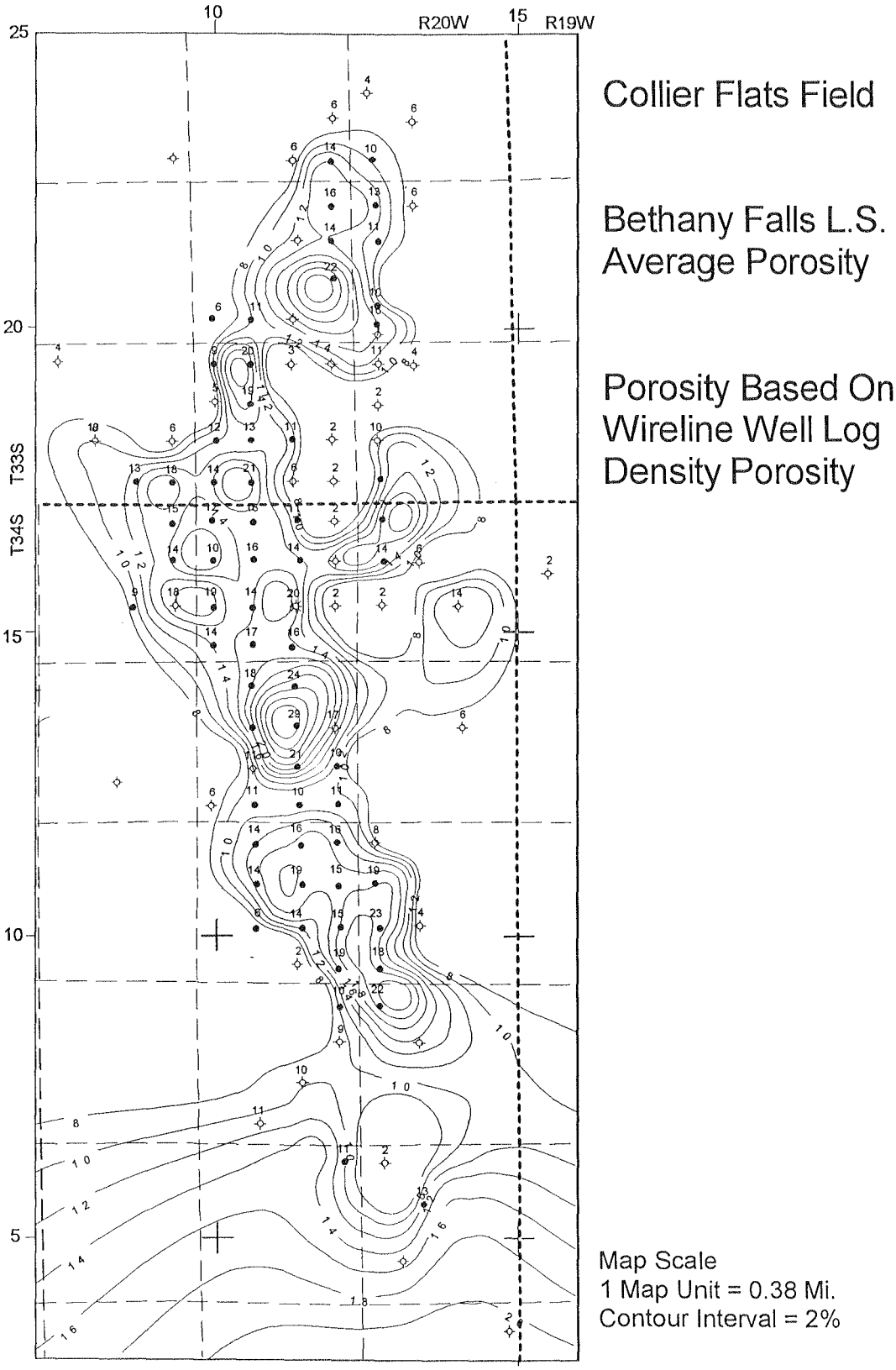


Figure 5-29 Collier Flats Field, Bethany Falls limestone average porosity isopach map.

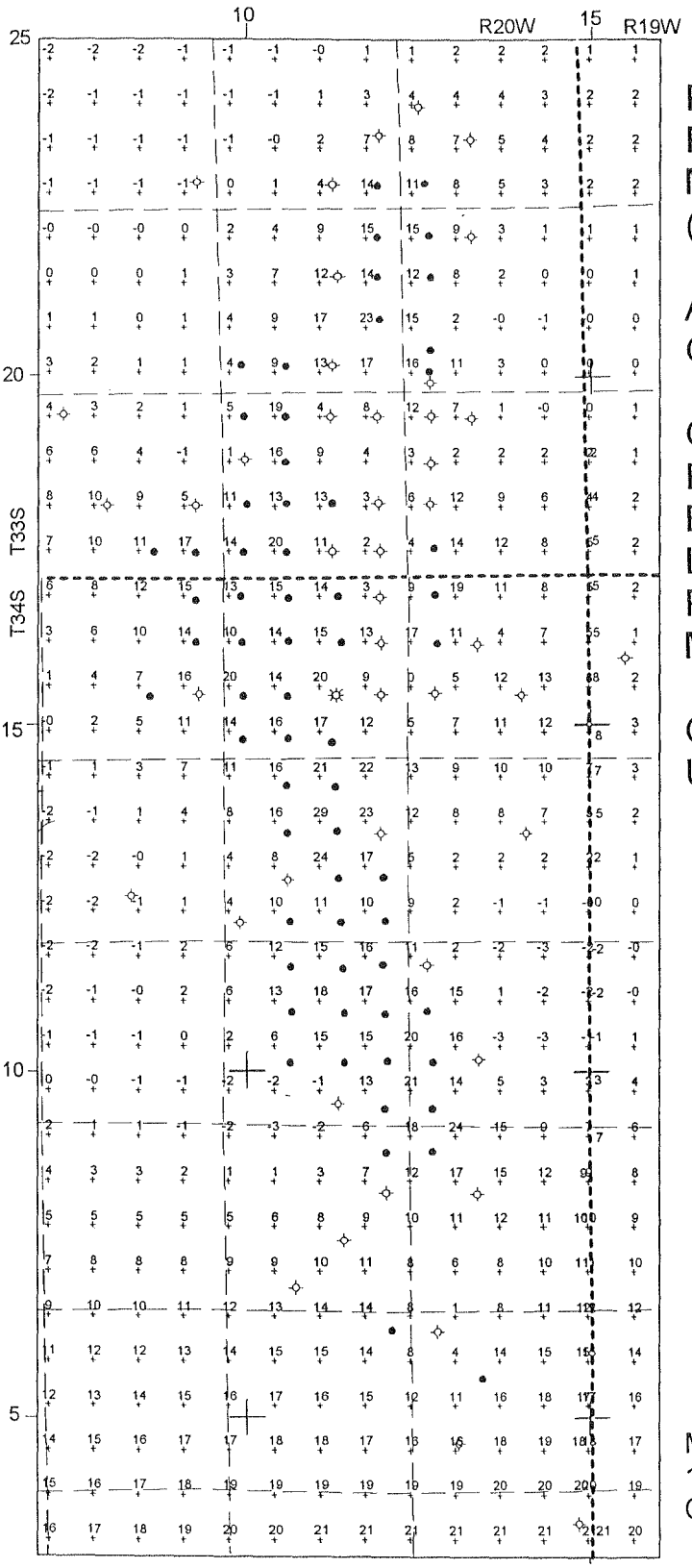


Petrospec Personal Computer Mapping System (PCMS) Software

Average Porosity Grid Data File

Grid File Is Used By PCMS To Create Bethany Falls Limestone Average Porosity Contour Map

Grid spacing 0.65 Map Units = 0.25 mi.

Map Scale
1 Map Unit = 0.38 Mi.
Contour Interval = 2%

Figure 5-30 Collier Flats Field, Bethany Falls limestone average porosity grid.

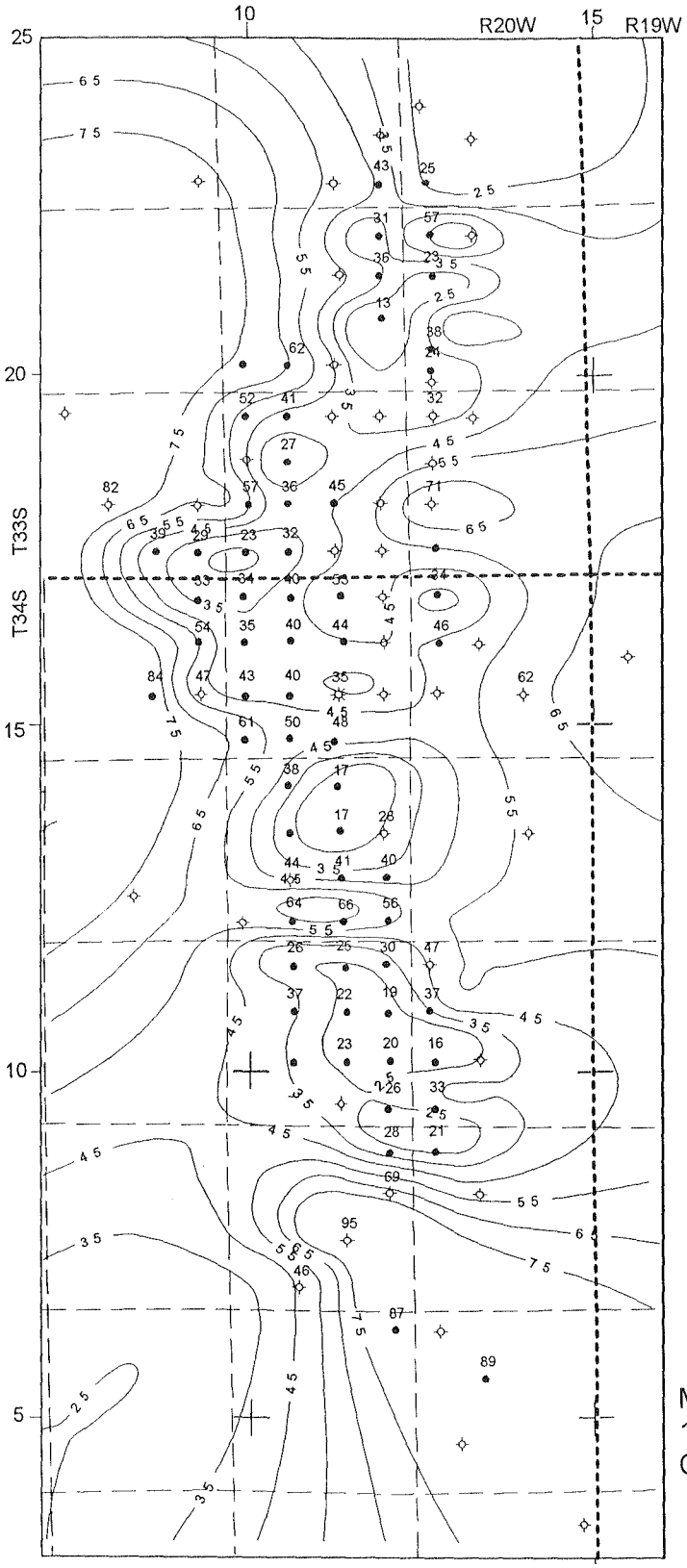


Figure 5-31 Collier Flats Field, Bethany Falls limestone average water saturation isopach map.

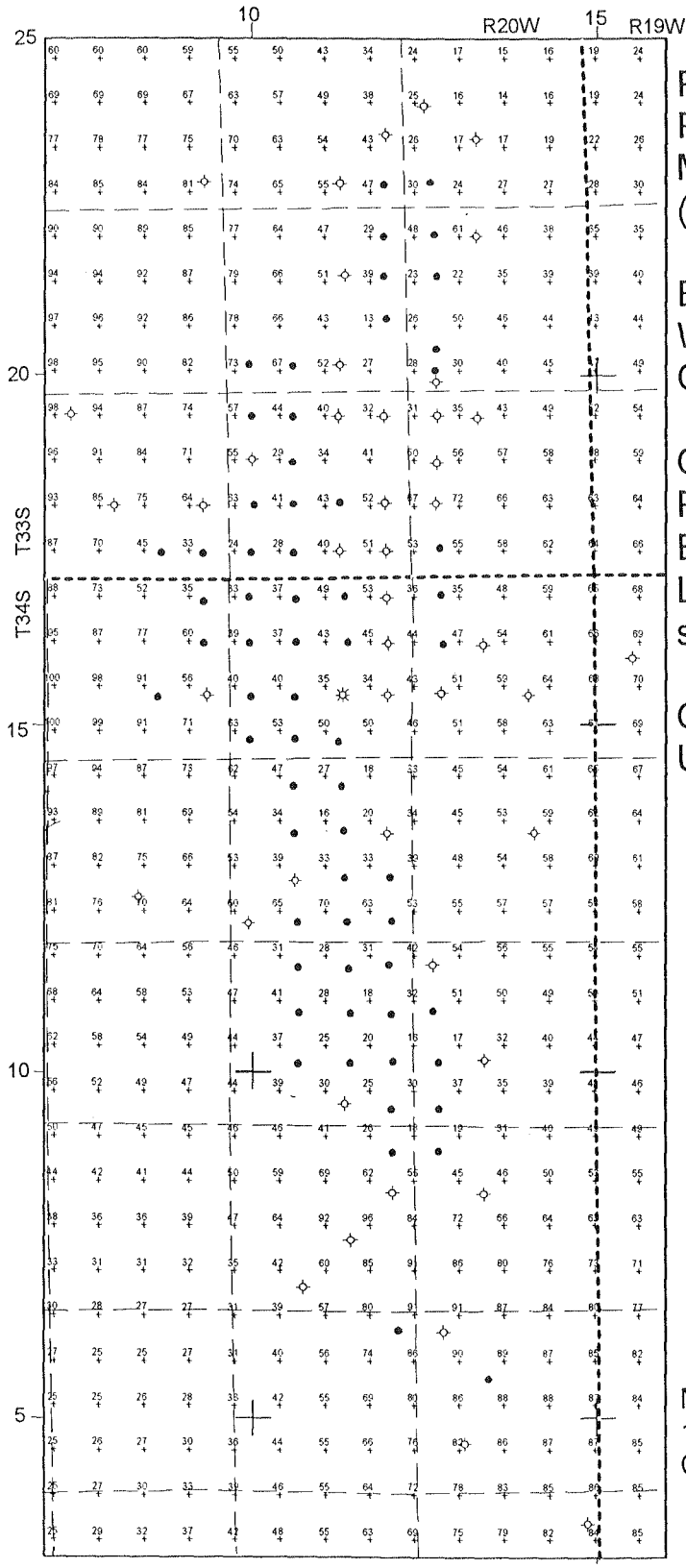


Figure 5-32 Collier Flats Field, Bethany Falls limestone average water saturation grid.

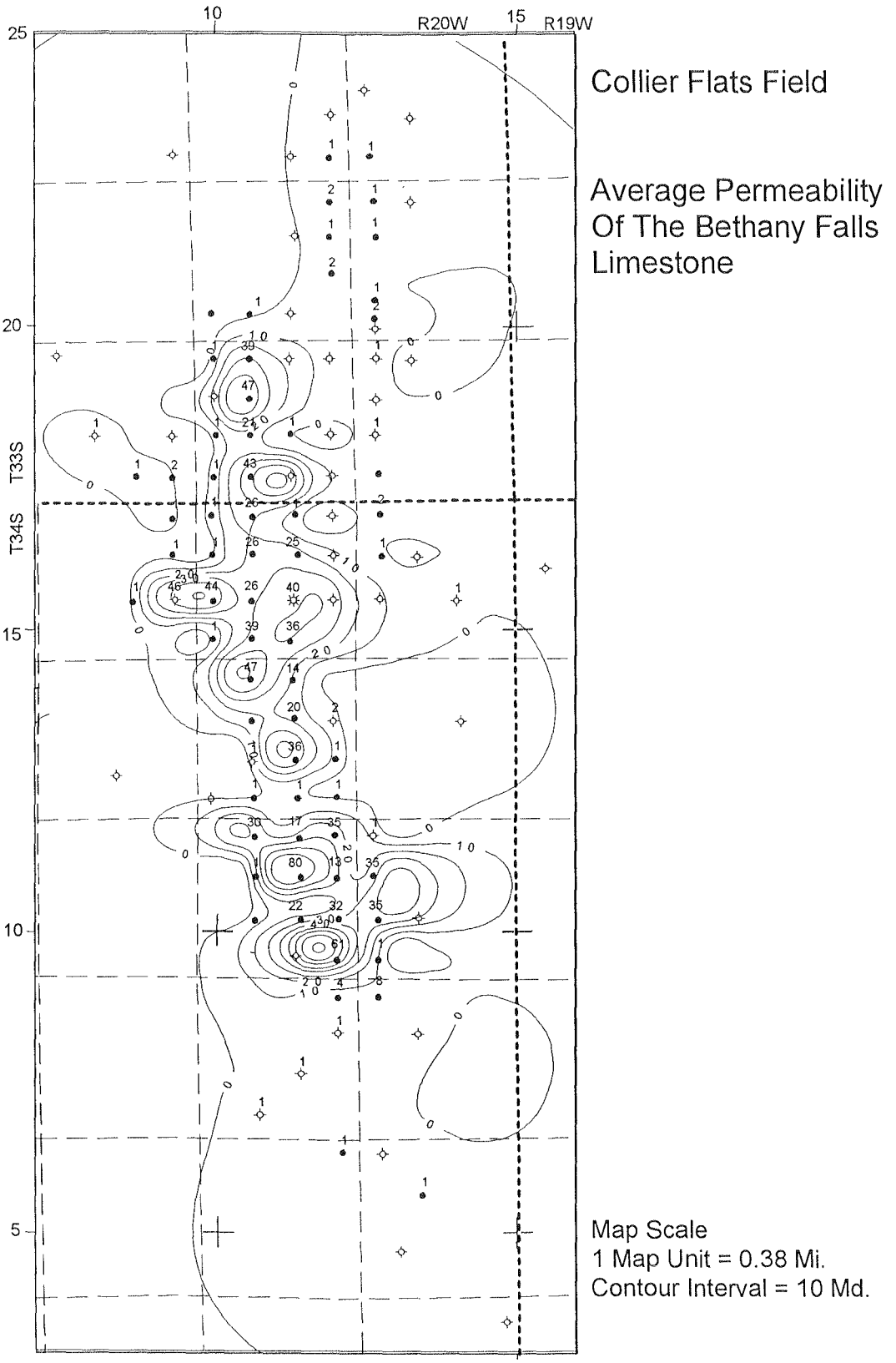


Figure 5-33 Collier Flats Field, Bethany Falls limestone average horizontal permeability isopach map.

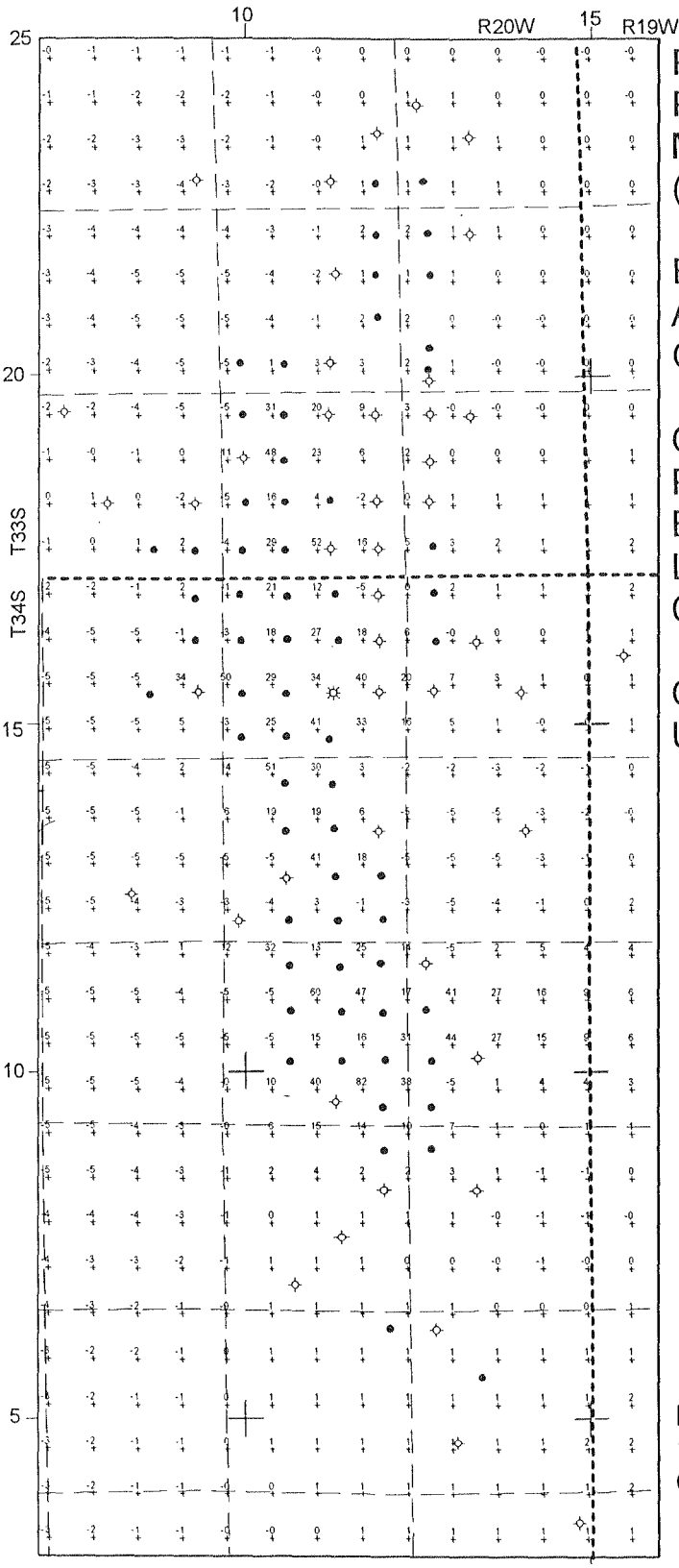


Figure 5-34 Collier Flats Field, Bethany Falls limestone average horizontal permeability grid.

### Collier Flats Field Pay Identification Procedure

Collier Flats field pay is defined using the following data: porosity greater than 8%, porosity that is permeable, porosity with less than 75% water saturation and porosity confined to the Bethany Falls limestone. Core analysis data shows that Bethany Falls limestone with 8% porosity is permeable. A one foot interval with 8% porosity is used as the lower cutoff for pay. Core analysis also demonstrates that porosity greater than 25% consist of low permeability oomoldic grainstones. One foot intervals with greater than 75% water saturation are deemed water wet and nonproductive. Thus, porous one foot intervals with less than 75% water saturation are considered productive. Pay thickness is identified for each productive well and mapped based on the above pay criteria. Non-pay zones are also identified and mapped. This information is used to characterize genetic unit and microscopic scale reservoir heterogeneity.

### Mapping Collier Flats Field Reservoir Data

Figures 5-35 through 5.38 are a series of maps that summarize Collier Flats Field Pay data, including the PCMS generated grids used to generate contour line data. Collier Flats Field pay and non-pay grids are presented since this information is typically used in reservoir simulators. A moving least square algorithm using the following data:

| | |
|---|---|
| Minimum X Coordinate ..... | 6.5 |
| Maximum X Coordinate ..... | 18.2 |
| Minimum Y Coordinate ..... | 2.6 |
| Maximum Y Coordinate ..... | 27.3 |
| X Direction Gridding Interval .... | 0.65 |
| Y Direction Gridding Interval .... | 0.65 |
| Number Of Grid Rows ..... | 39 |
| Number Of Grid Columns ..... | 19 |
| Number Of Z-Value Nodes..... | 741 |
| Number Of ZNON Nodes..... | 0 |
| Value of ZNON..... | -999999 |
| Data collection radius (REACH).... | 20.00 |

constructed the grids by interpolating between individual well data. The gridded data was then contoured using the PCMS mapping software.

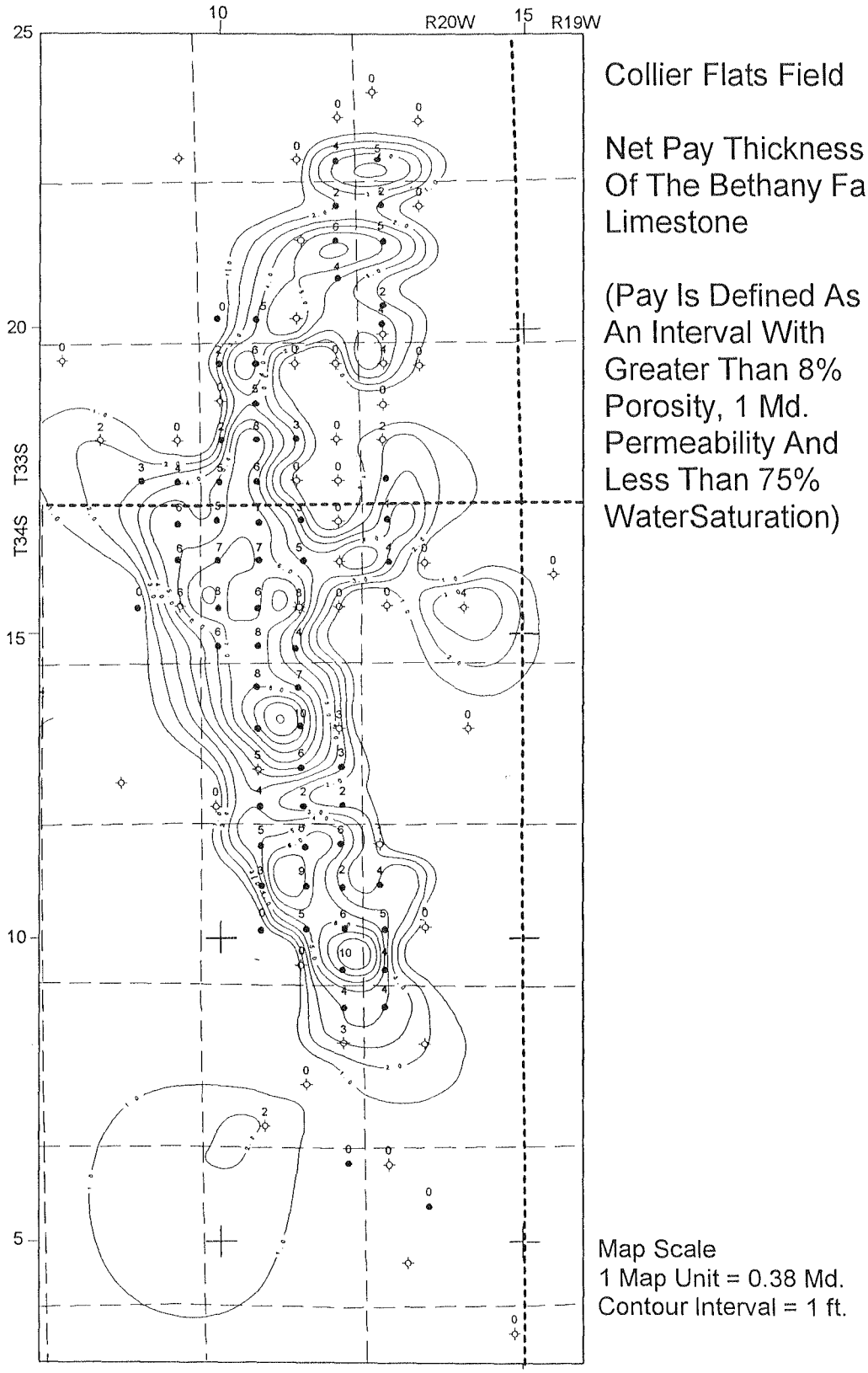


Figure 5-35 Collier Flats Field, Bethany Falls limestone net pay thickness isopach map.

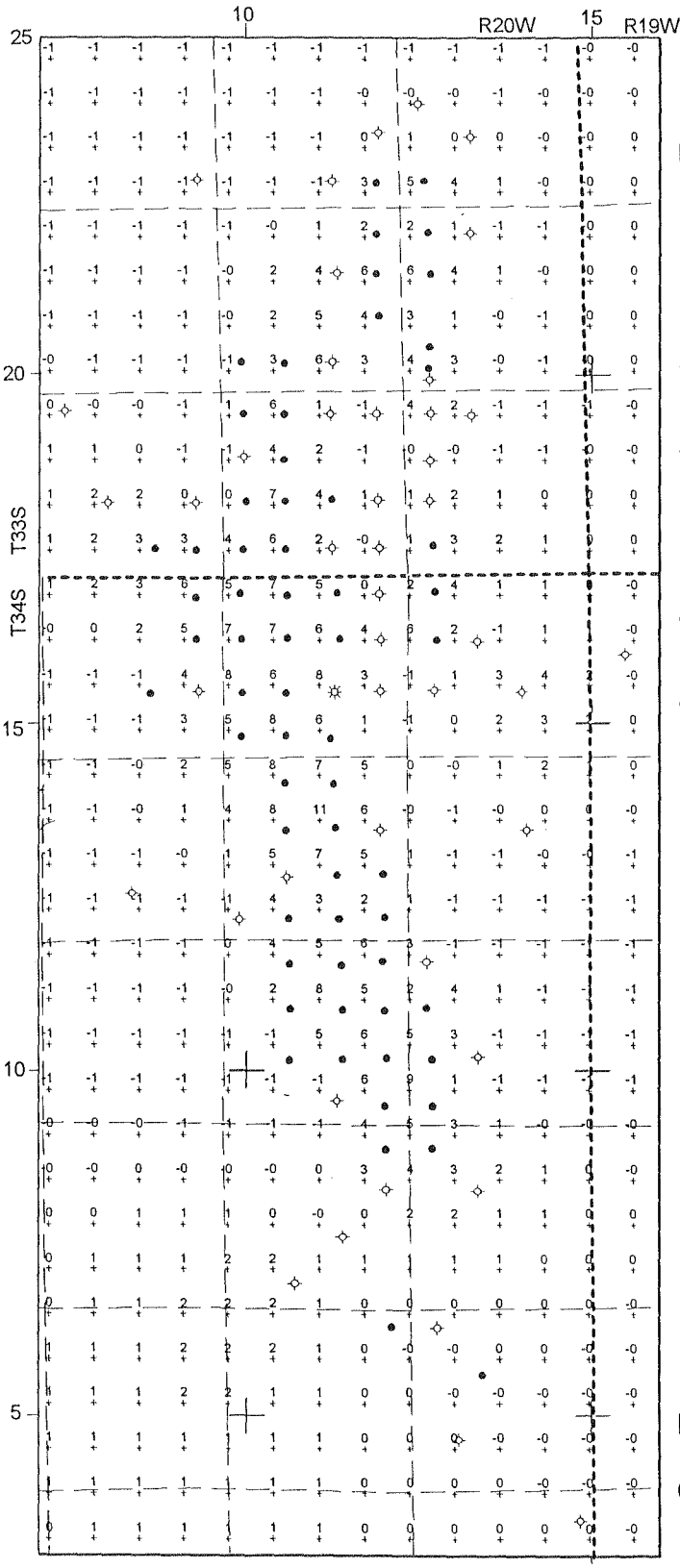


Petrospec
Personal Computer
Mapping System
(PCMS) Software

Bethany Falls L.S.
Pay Thickness
Grid Data File

Grid File Is Used By
PCMS To Create
Bethany Falls
Pay Thickness
Contour Map

Grid spacing 0.65 Map
Units = 0.25 mi.

Map Scale
1 Map Unit = 0.38 Md.
Contour Interval = 1 ft.

Figure 5-36 Collier Flats Field, Bethany Falls limestone net pay thickness grid.

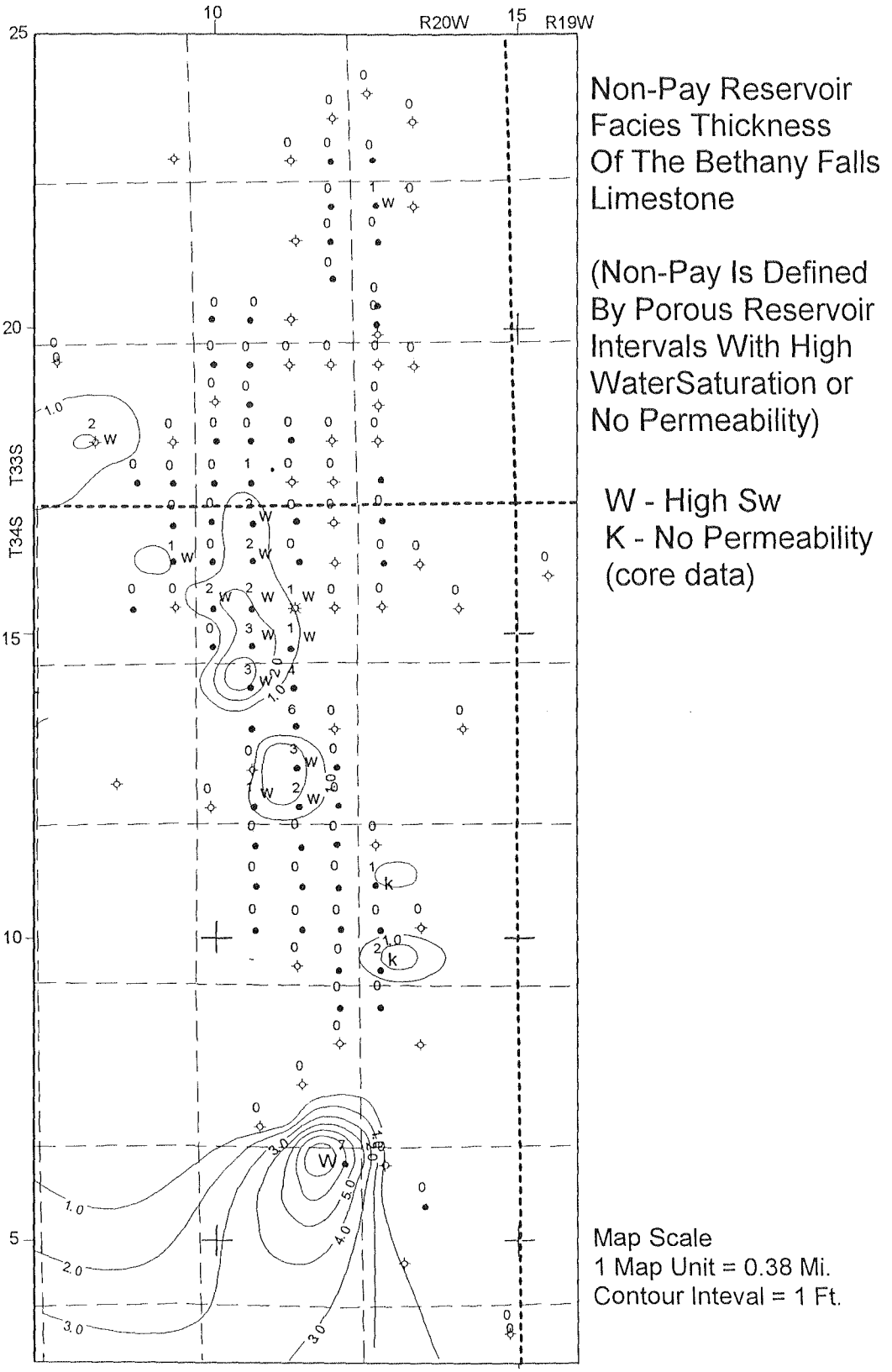


Figure 5-37 Collier Flats Field, Bethany Falls limestone nonpay reservoir thickness isopach map.

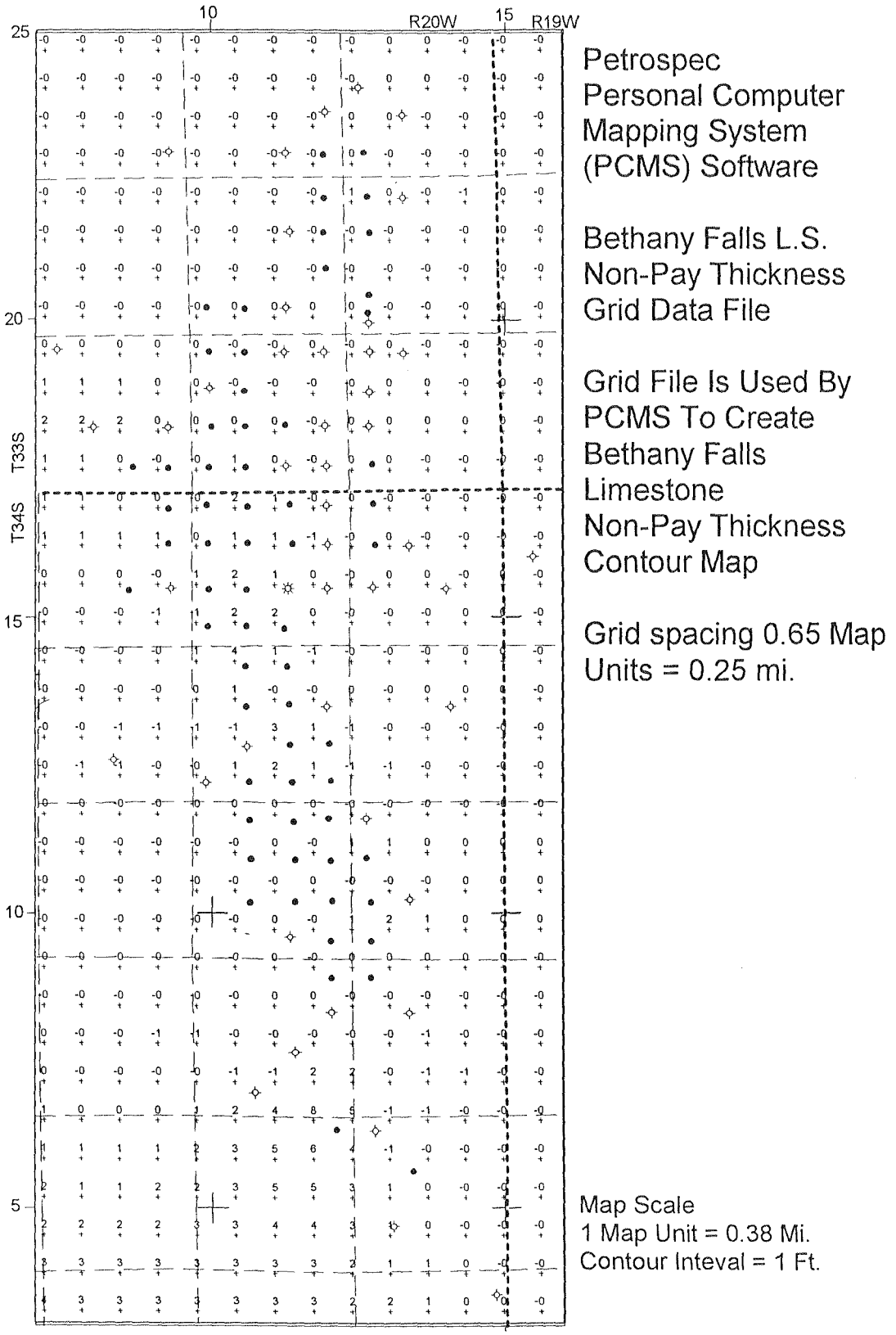


Figure 5-38 Collier Flats Field, Bethany Falls limestone nonpay thickness grid.

## Estimation of Collier Flats Field Oil Reserves

### Original Oil In Place and Estimated Ultimate Recoverable Reserves

Reserve data including ultimate recoverable reserves for primary and secondary recovery production is essential to evaluate enhanced oil recovery economics. The Henderson & Company waterflood feasibility study estimated an additional 21% of the Lemon Ranch and Rhoades leases wells original oil in place (OOIP) can be recovered by waterflooding. Reserve data for the Lemon and Rhoades leases was compared with production data since these leases were water flooded in 1983 after the Henderson & Company report was written.

An estimate of OOIP for each productive well was attempted using the volumetric methodology and the following equation:

Equation 5.5 $$N = \frac{7{,}758 * V_o * \phi * (1 - S_w)}{B_o}$$

$N$ = reservoir oil originally in place (STB)
$7{,}758$ = number of barrels per acre foot
$V_o$ = net pay volume of the oilbearing zone (40 acre – ft)
$B_o$ = formation volume factor (1.49 RB/STB)
$S_w$ = water saturation fraction
$\phi$ = porosity fraction

For each two foot interval, OOIP, primary depletion drive estimated ultimate recovery (EUR-Primary) and secondary waterflood estimated ultimate recovery (EUR-Secondary) was calculated and tabulated for each well in Excel 5.0 spreadsheets. Based on the 1981 Henderson & Company waterflood feasibility study for the Lemon Ranch and Rhoades leases, a 15% recovery factor for OOIP is used to estimate production during the primary straight depletion drive production period (EUR Primary column, Table 5.19).

| WELL NAME | WELL ID # | INTERVAL THICK. (ft) | GR (API) | POR (%) | Sw | K (md) | OOIP 40 acre (STB) | EUR Primary (STB) | EUR Secondary (STB) |
|---|---|---|---|---|---|---|---|---|---|
| LEMON 6 | 55.00 | 2 | 27 | 25 | 29 | 9 | 74,317 | 11,794 | 27,423 |
| | | 2 | 24 | 20 | 34 | 14 | 54,307 | 8,619 | 20,039 |
| | | 2 | 26 | 21 | 20 | 130 | 70,468 | 11,183 | 26,003 |
| | | 2 | 34 | 15 | 22 | 13 | 48,224 | 7,653 | 17,795 |
| | | 2 | 45 | 16 | 21 | 140 | 52,882 | 8,392 | 19,513 |
| SUM ⇒ | | 10 | | | | | 300,197 | 47,641 | 110,773 |
| AVERAGE ⇒ | | | 31 | 19 | 26 | 61 | | | |

Table 5.19: Two foot averages of Lemon 6 Terrastation TLOG reservoir data with two foot interval estimates of Original Oil In Place (OOIP) and Estimated Ultimate Recovery (EUR) for primary and secondary recovery phases.

A 36% recovery factor of OOIP is used to estimate oil production from a secondary waterflood production phase (EUR Secondary), Table 5.19. Total reserve estimates for OOIP, EUR 15% and EUR 36% was summed over the pay interval.

## Assessment of Enhanced Oil Recovery (EOR) Incremental Recovery (Lemon and Rhoades Leases)

### Introduction

Collier Flats Field production data is typically reported to the state by lease (Figure 5.39-5.40). Lease production data averages production from high and low permeability wells. Thus, decline curve analysis of lease production data can identify average recovery factors for the field. The Lemon and Rhoades leases were waterflooded beginning in 1983 and provide an opportunity to estimate incremental enhanced oil recovery due to waterflooding a portion of the Collier Flats field. Decline curve analysis of the Lemon and Rhoades lease production data provides an opportunity to evaluate the 1981 Henderson & Company 15% primary oil recovery factor and 36% EOR oil recovery factor with a 21% incremental enhanced oil recovery factor. A good estimate of incremental oil production is essential to assess EOR economics for waterflooding additional Collier Flats acreage.

### Lemon and Rhoades Pre-Waterflood Production (Primary Production)

Monthly oil and gas production was entered from the Lemon and Rhoades leases into a spreadsheet and graphed using Excel's graphing software. Excel was used to perform decline curve analysis on the production data. Lemon and Rhoades "Pre-EOR" lease oil production is presented in Figures 5.41-5.42. Excel was used to calculate an "Exponential Regression Correlation Curve" which is overlain on the production data. This regression curve is used to approximate a "Constant Percentage Decline Curve" for decline curve analysis. From a Constant Percentage Decline Curve, a Nominal Monthly Decline Rate can be calculated since the decline rate is constant. Equations 5.5 through 5.10 are used in this decline curve analysis.

Equations 5.5 and 5.8:

Lemon Ranch Primary Oil Production Exponential Decline Curve Equation

$y = 11{,}465 * e^{-0.0798 * x}$

Lemon Ranch EOR Oil Production Exponential Decline Curve Equation

$y = 1409 * e^{-0.0345 * x}$

Rhoades Primary Oil Production Exponential Decline Curve Equation

$y = 4023 * e^{-0.125 * x}$

Rhoades EOR Oil Production Exponential Decline Curve Equation

$y = 1591 * e^{-0.0544 * x}$

See Figures 5.43 – 5.44 for explanation.

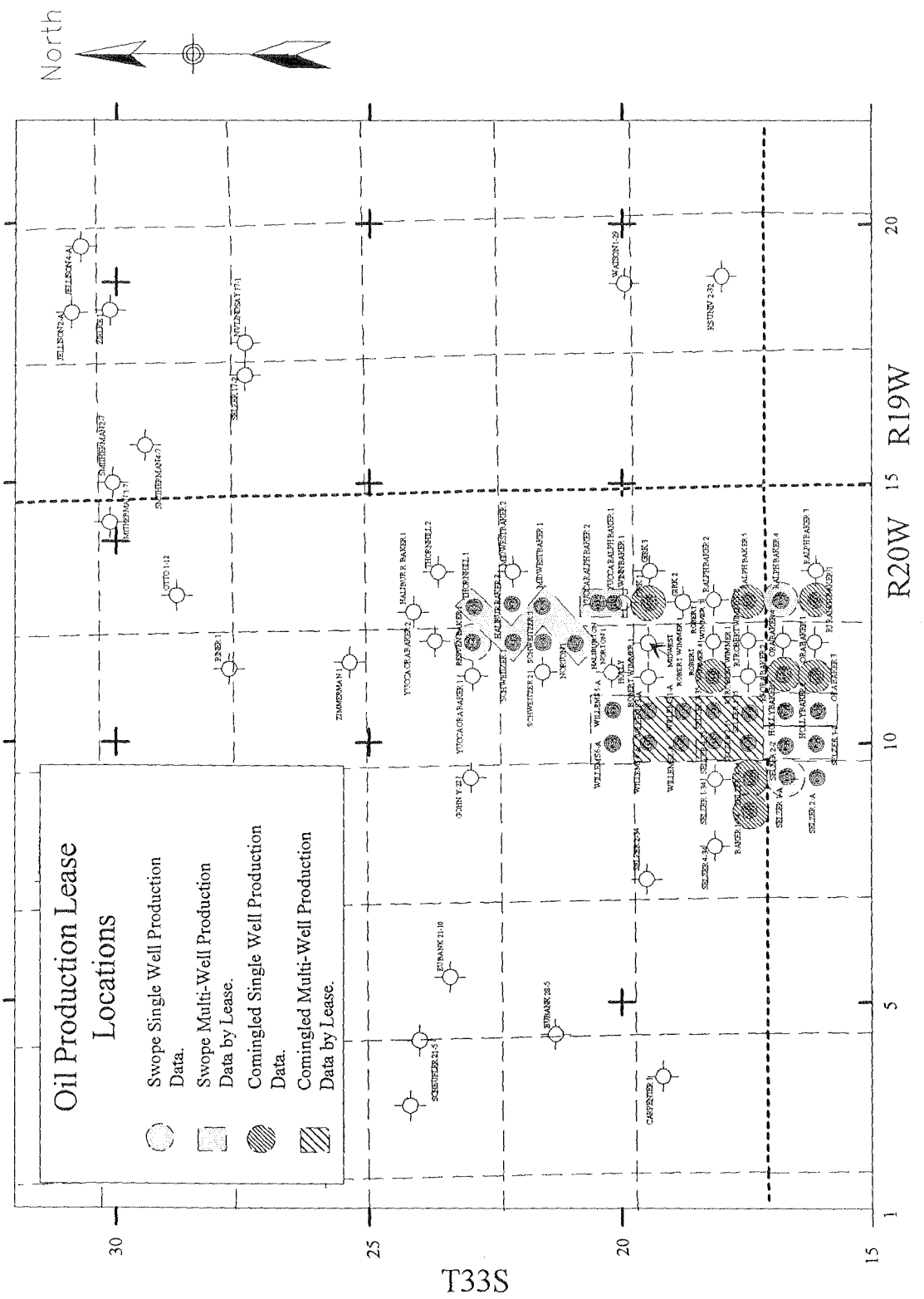


Figure 5-39 Collier Flats Field, production lease boundaries map (northern 1/2 of field).

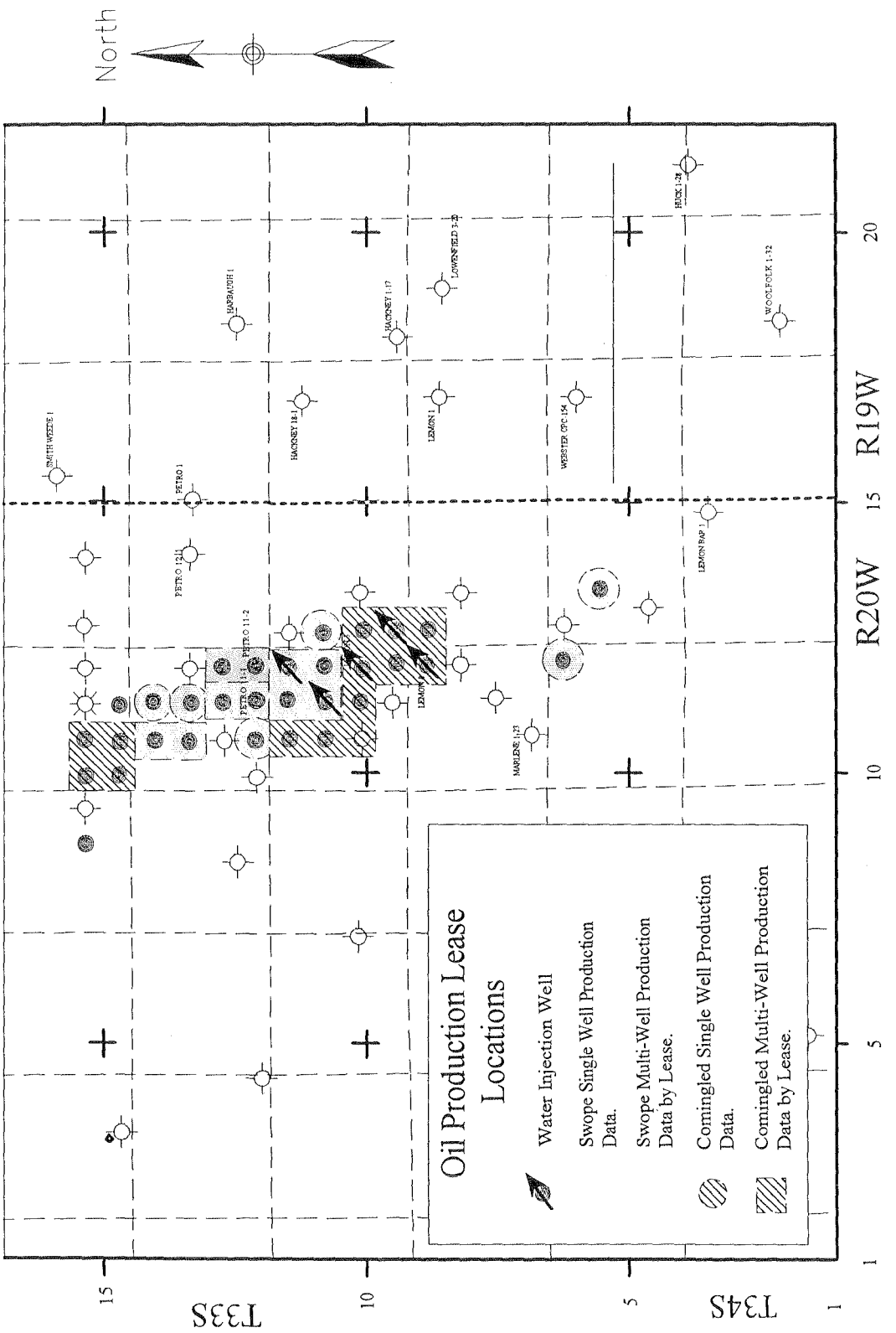


Figure 5-40 Collier Flats Field, production lease boundaries map (southern 1/2 of field).

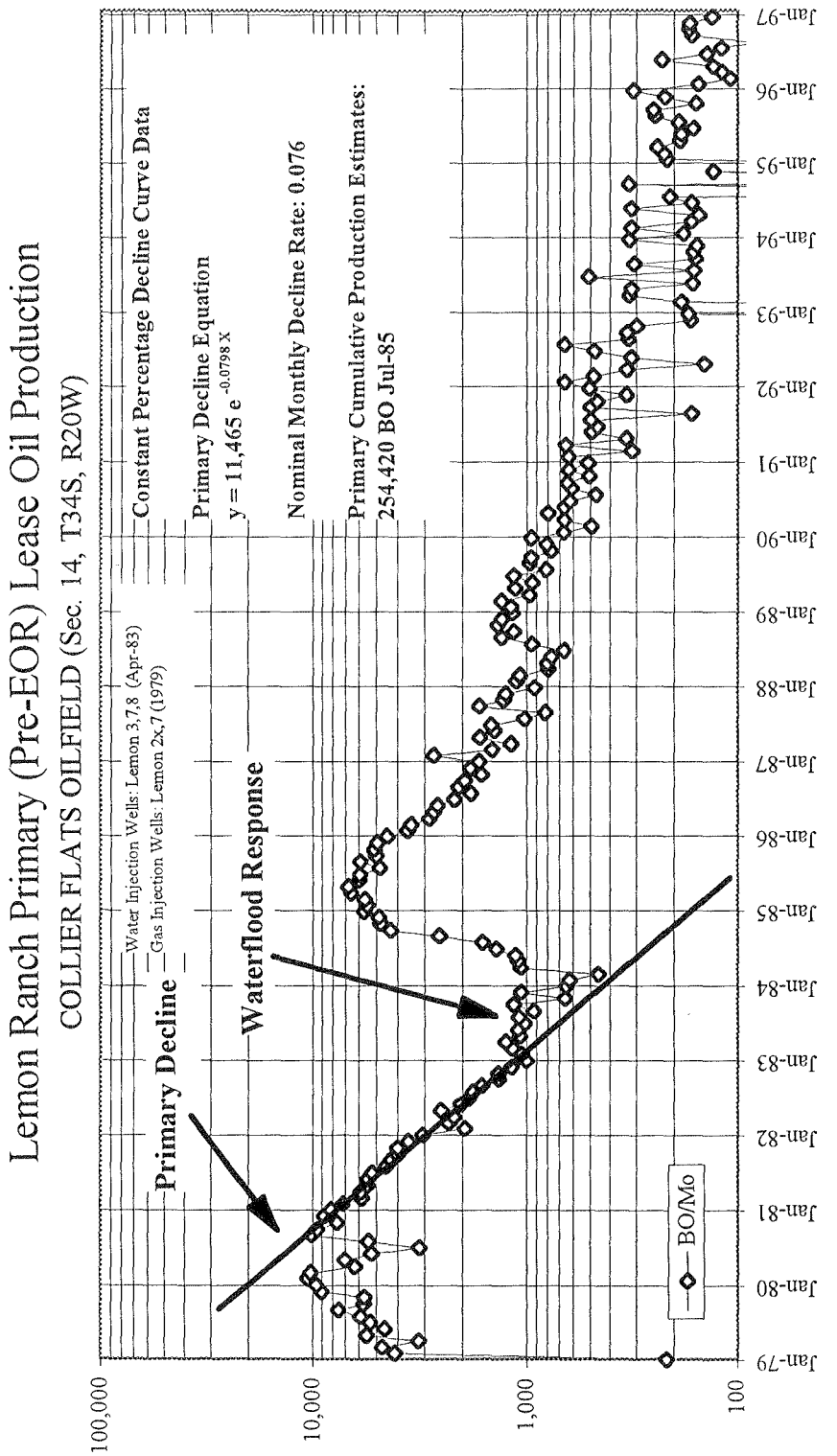


Figure 5-41 Lemon primary (Pre-EOR) lease production w/ decline curve overlay.

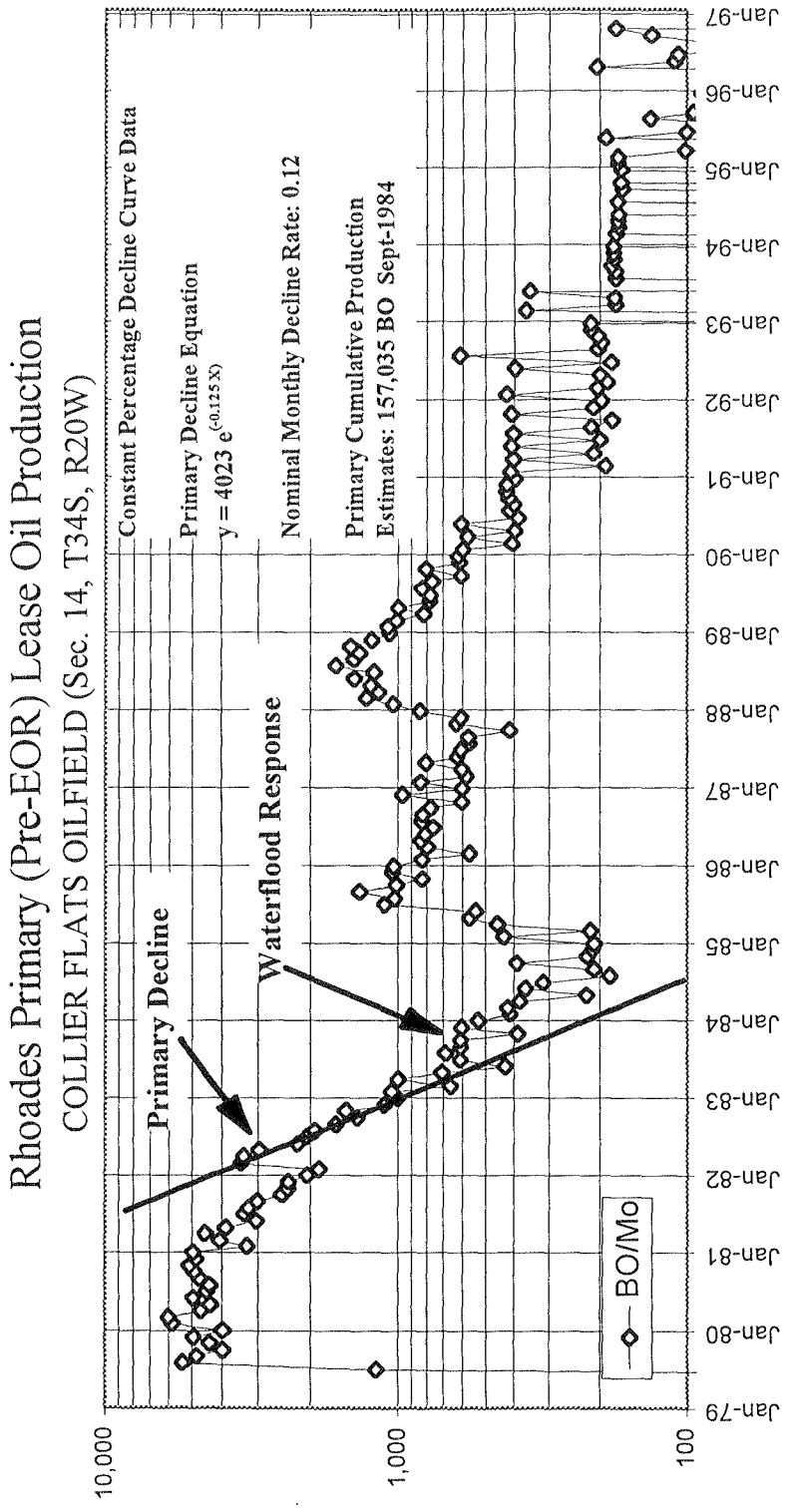


Figure 5-42 Rhoades primary (Pre-EOR) lease production w/ decline curve overlay.

Equation 5.9:

Nominal Decline Rate

$$a = \frac{dq / dt}{q}$$

$dq = q_i - q_{1\,month}$

$q_i$ = initial oil production (STB/Mo)

$q_{1\,month}$ = oil production 1 month after $q_i$ (STB/Mo)

$dt$ = 1 month

$q = q_i$

Equation 5.10:

Cumulative Production Estimates

$$N_p = \frac{q_i - q_f}{a}$$

$q_i$ = initial monthly production (STB / Mo)

$q_f$ = final monthly production (economic limit) (STB/Mo)

a = Nominal Decline Rate

$N_P$ = Cumulative Oil Production (STB)

Primary (Pre-EOR) lease production for the Lemon and Rhoades leases (Table 5.20) was calculated as follows:

Step 1) Calculate a constant percentage decline curve using Excel;

Step 2) Use primary decline curve equations 5.5 and 5.6 to calculate production after 1 month;

Step 3) Calculate a Nominal Decline Rate using equation 5.9;

Step 4) Calculate Primary Pre-EOR Production ($N_p$) using Equation 5.10 and $q_f$ = 100 STB/mo.

The 100 BOPM economic limit for reserve estimates is an arbitrary value. Accurate economic limits for these leases will require acquiring economic data for the individual leases.

| | Lemon Ranch Lease Data<br>10 Wells | Rhoades Lease Data<br>4 wells |
|---|---|---|
| Primary Decline Curve | $y = 11465 * e^{-0.0798 * x}$ | $y = 4023 * e^{-0.125 * x}$ |
| $q_i$ | 11465 STB / Mo. | 4023 STB / Mo. |
| $q_{1\ Month}$ | 10585 STB / Mo. | 3550 STB / Mo. |
| Primary Nominal Decline Rate | 0.076 STB / Mo. | 0.12 STB / Mo. |
| $q_f$ (economic limit) | 100 STB / Mo. | 100 STB / Mo. |
| Estimated Primary Cumulative Production | 254,420 STB on Jul-85 | 157,035 STB on Sept-84 |

Table 5.20 Decline Curve Analysis; Lemon and Rhoades Lease Primary Estimated Cumulative Production.

### Lemon and Rhoades Lease Primary & EOR Production

The same decline curve analysis procedure used to determine Primary Pre-EOR production was used to calculate Lemon and Rhoades Lease Primary & EOR waterflood production (Figures 5.43 - 5.44).

| | Lemon Ranch Lease Data<br>10 Wells | Rhoades Lease Data<br>4 wells |
|---|---|---|
| EOR Decline Curve | $y = 1409 * e^{-0.0345 * x}$ | $y = 1591 * e^{-0.0544 * x}$ |
| qi | 1409 STB / Mo. | 1591 STB / Mo. |
| $q_{1\ month}$ | 1361 STB / Mo. | 1506 STB / Mo. |
| EOR Nominal Decline Rate | 0.067 STB / Mo. | 0.053 STB / Mo. |
| $q_f$ (economic limit) | 100 STB / Mo. | 100 STB / Mo. |
| Estimated Primary & EOR Cumulative Production | 446,506 STB on Nov-95. | 225,185 STB on May-93 |

Table 5.21 Decline Curve Analysis; Lemon and Rhoades Lease Primary & EOR Estimated Cumulative Production.

The difference between primary oil production estimates and primary plus EOR production estimates is incremental EOR production due to waterflooding. Although waterflooding began in 1983, in 1988 a change occurred in the waterflood operation that increased oil production in both the Lemon and Rhoades leases.

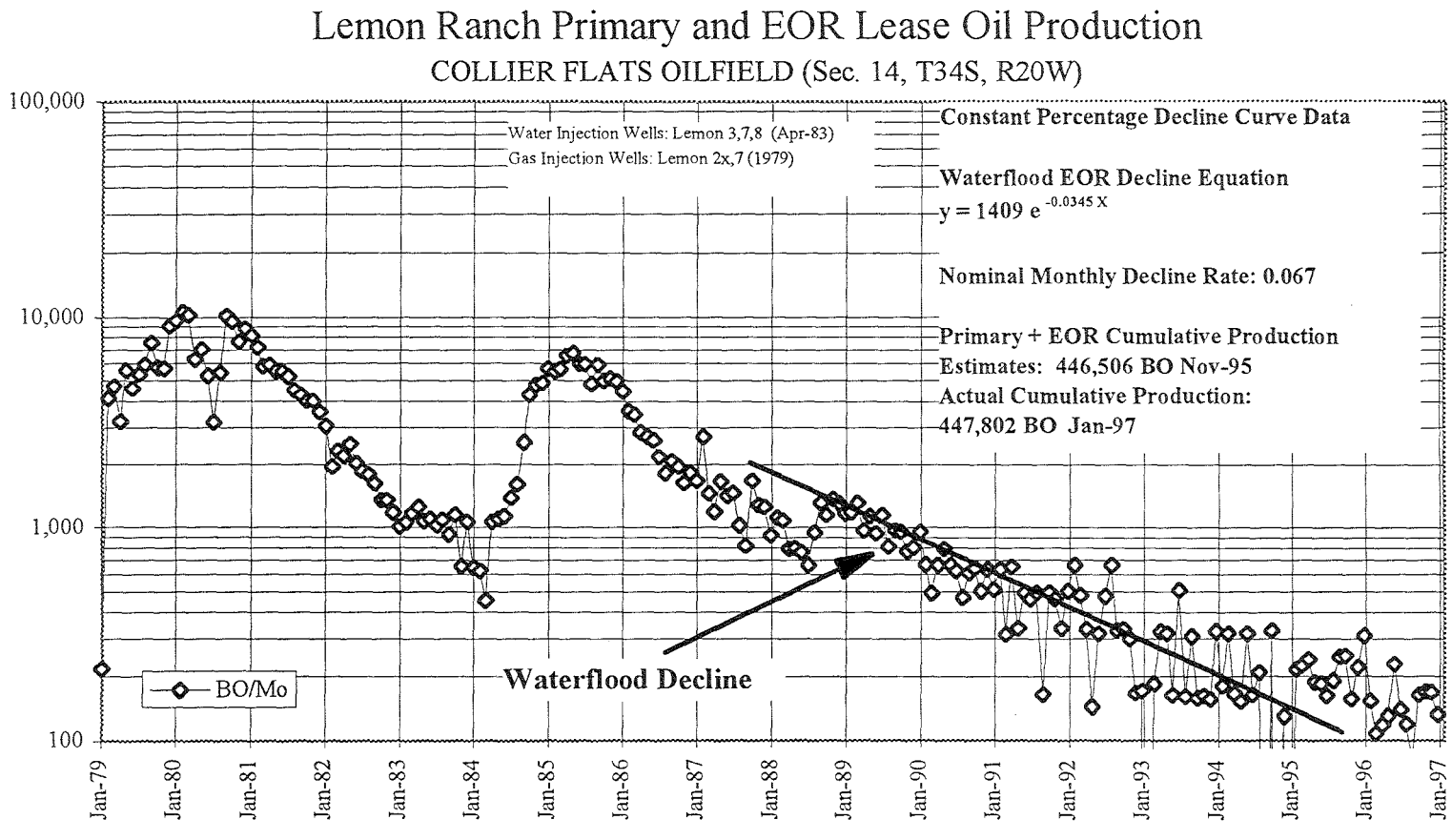


Figure 5-43 Lemon primary and EOR lease production w/ EOR decline curve overlay.

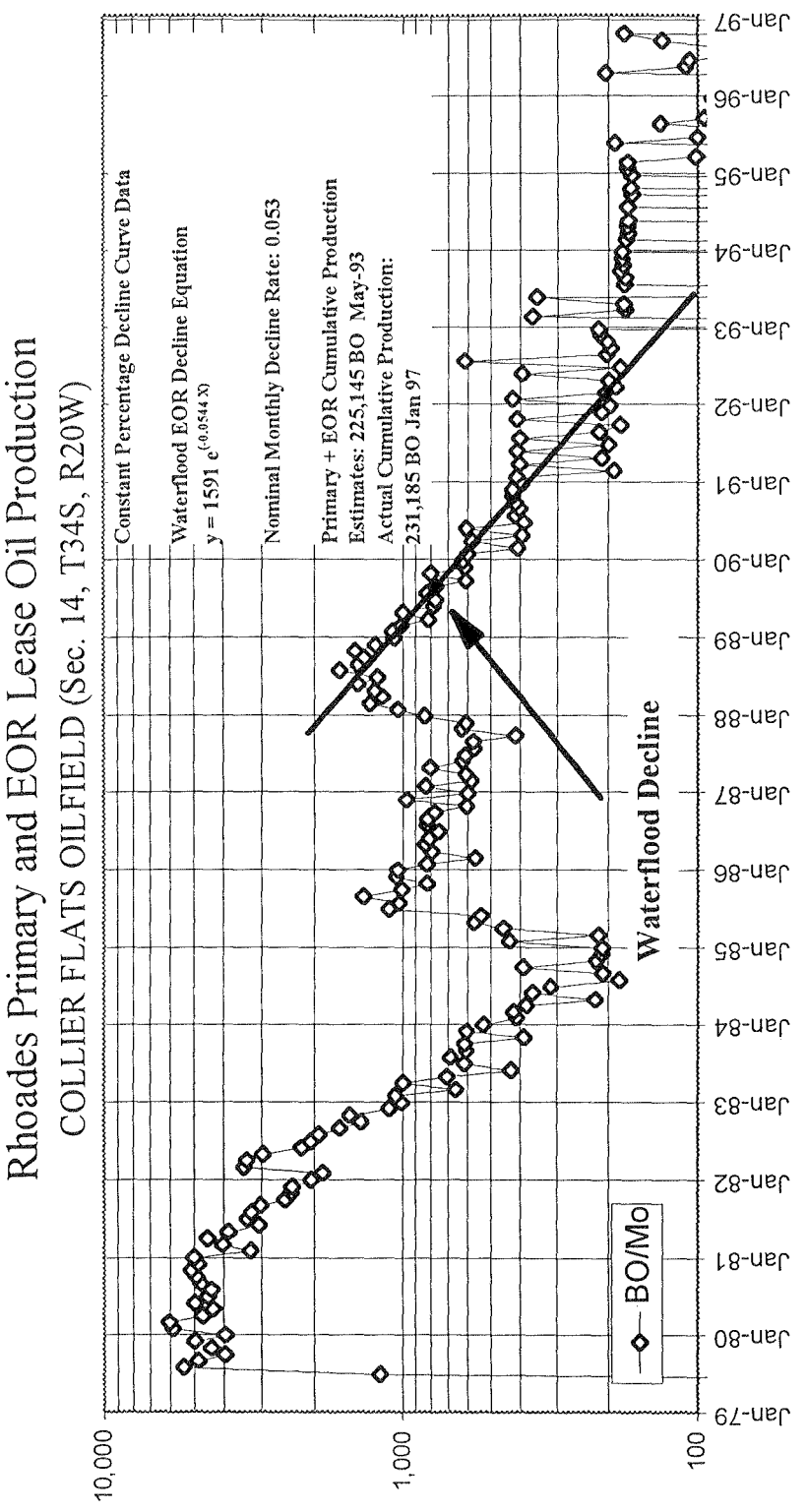


Figure 5-44 Rhoades primary and EOR lease production w/ EOR decline curve overlay.

Waterflood EOR decline equations were calculated after this event. Estimated EOR decline is more dramatic than actual decline due to periodic shut-in of the producing wells since 1993 prolonging production. Original Oil In Place (OOIP) data from well-log analysis data is summed for the 4 wells in the Rhoades lease and 10 wells in the Lemon lease (Appendix E) to complete the Lemon and Rhoades reserve database for this exercise. OOIP for the Lemon lease is approximately 1,243,000 STB and 627,000 STB for the Rhoades lease.

### Lemon and Rhoades Lease Incremental EOR Production

The best possible data to assess incremental waterflood EOR production in the Collier Flats Field is from decline curve analysis of primary and waterflood oil production data. Incremental waterflood EOR production for the Lemon lease is approximately 192,000 STB of OOIP or 16% and 68,100 STB of OOIP or 11% for the Rhoades lease. Combining both recovery factors, 13% appears to be a good approximation for both leases.

Comparing decline curve analysis production estimates with primary and EOR production estimates from well-log analysis based on the 1981 Henderson & Company Waterflood Feasibility Study, indicate that the Henderson and Company total EOR oil recovery estimates agree with actual production trends. However, decline curve analysis revealed a 13.5% waterflood EOR incremental oil recovery factor compared to 21% recovery factor cited in the Henderson and Company report. Both methods indicate that incremental oil recovery due to waterflooding merits waterflooding additional Collier Flats field acreage if the procedure is economic.

| Estimated Oil Reserve Data and Source | Lemon Ranch Lease Data 10 Wells | Rhoades Lease Data 4 wells |
|---|---|---|
| OOIP - (Well Log Analysis) | 1,243,000 STB | 627,000 STB |
| Primary Production (Decline Curve Analysis) | 254,420 STB | 157,035 STB |
| Total Cumulative Production (Decline Curve Analysis) | 446,506 STB | 225,145 STB |
| Actual Cumulative Production (P.I.) | 447,802 STB | 231,185 STB |
| Incremental Oil Production (Decline Curve Analysis) | 192,086 STB | 68,110 STB |
| Primary Production Recovery Factor (Decline Curve Analysis) | 20% | 25% |
| Primary + EOR Production Recovery Factor (Decline Curve Analysis) | 36% | 36% |

| | | |
|---|---|---|
| Incremental EOR Recovery Factor (Decline Curve Analysis) | 16% | 11% |
| OOIP - Volumetric (Henderson & Co. Waterflood Feasibility Study, 1981) | 1,800,000 STB | |
| OOIP - Material Balance (Henderson & Co. Waterflood Feasibility Study, 1981) | 3,450,000 STB | |
| OOIP - Summary (Henderson & Co. Waterflood Feasibility Study, 1981) | 2,500,000 STB | |
| Primary Production Recovery Factor (Henderson & Co. Waterflood Feasibility Study, 1981) | 15% of 2.5 MMBO = 375,000 STB | |
| Primary Production Recovery Factor (Decline Curve Analysis) | 22.5% of 2.5 MMBO = 562,500 STB | |
| Incremental EOR Recovery Factor (Decline Curve Analysis ) | 13.5% of 2.5 MMBO = 338,250 STB | |
| Incremental EOR Recovery Factor (Henderson & Co. Waterflood Feasibility Study, 1981) | 21% of 2.5 MMBO = 525,000 STB | |
| Primary + EOR Production Recovery Factor (Henderson & Co. Waterflood Feasibility Study, 1981) | 36% of 2.5 MMBO = 900,000 STB | |

Table 5.22 Summary of recovery factors, decline curve analysis production estimates and OOIP data for the Lemon and Rhoades leases.

## Collier Flats Field Reservoir Heterogeneity

Identification and classification of Collier Flats field reservoir heterogeneity is based on a reservoir heterogeneity classification and its impact on production performance proposed by Weber, 1986 (Figure 5.1 and Table 5.1). Weber, 1986, related seven heterogeneity types with their impact on fluid flow which is the bottom line for reservoir engineers. Identification of Collier Flats field reservoir heterogeneity is based on geologic models and reservoir characterization aspect mapping (pay, porosity, water saturation and permeability).

### Collier Flats Field Microscopic Reservoir Heterogeneity

#### Type 6 Microscopic Textural Reservoir Heterogeneity

In the section on Bethany Falls porosity and permeability development, it is hypothesized that two porosity and permeability distributions are related to depositional and diagenetic processes. The foundation for this distinction is the relative percentage between moldic and vuggy porosity. Low permeability cores ***(Porosity and Permeability Distribution #1)*** are restricted to the margins of grainstone shoals which were impacted by four dissolution events that created Bethany Falls limestone effective porosity.

The relative percentage of moldic porosity to vuggy porosity is more than 2.8 : 1. High permeability cores ***(Porosity and Permeability Distribution #2)*** are restricted to the thickest portions of the grainstone shoals which were impacted by four dissolution events that created Bethany Falls limestone effective porosity. The relative percentage of moldic porosity to effective vuggy porosity is nearly 1.3 : 1.

According to Weber's 1986 reservoir heterogeneity classification, the observed Collier Flats field microscopic heterogeneity is a Type 6, Textural Type Heterogeneity which will impact residual oil saturation and/or rock/fluid interactions (Table 5.1). The method used to relate porosity, deep induction resistivity and water saturation for this heterogeneity type is a modification of the cementation exponent used in the Archie equation.

## Collier Flats Field Macroscopic Reservoir Heterogeneity

### Type 2 Genetic Unit Reservoir Heterogeneity

General geologic mapping using net porosity and low gamma ray facies were used to identify genetic unit (carbonate sand shoals) scale reservoir heterogeneity. Genetic unit scale reservoir heterogeneity define reservoir continuity within an oil field. However, permeability barriers within genetic units are possible. For the Collier Flats field, porosity times height, isoporosity thickness mapping, average porosity and net thickness of porosity greater than 10% are used to define Type 2 Genetic Unit reservoir heterogeneity (Figures 5.45-5.47).

In all three figures, non-productive wells separate Type 2 Genetic Units 2, 3 and 4. The boundary between Type 2 Genetic Units 1 and 2 are based on a decrease in isoporosity, porosity and net thickness of porosity greater than 10%. Additionally, this non-productive area also correlates with lower permeability that creates a permeability contrast between Type 2 Genetic Units 1 and 2.

### Type 3 Permeability Zonation Within Genetic Unit Reservoir Heterogeneity

Type 3 reservoir heterogeneity is defined by permeability mapping. Figure 5.48 illustrates permeability contrasts within Genetic Units 1 and 2. Figure 5.49 also illustrates the location and thickness of low permeability zones that cap the Bethany Falls limestone reservoir due to very high porosity and low permeability oomoldic porosity observed in core. The significance of this type of heterogeneity is it will impact fluid flow within the reservoir, however, it does not form a barrier within the genetic units.

### Type 7 Fracture Reservoir Heterogeneity

Characterizing this type of reservoir heterogeneity is difficult since the cores were not oriented to identify fracture azimuths. However, since whole core analysis was performed to determine porosity, permeability and fluid saturations, the impact of fractures has been averaged into these reservoir characteristics. Unfortunately, distinguishing the impact of the fractures alone is not possible.

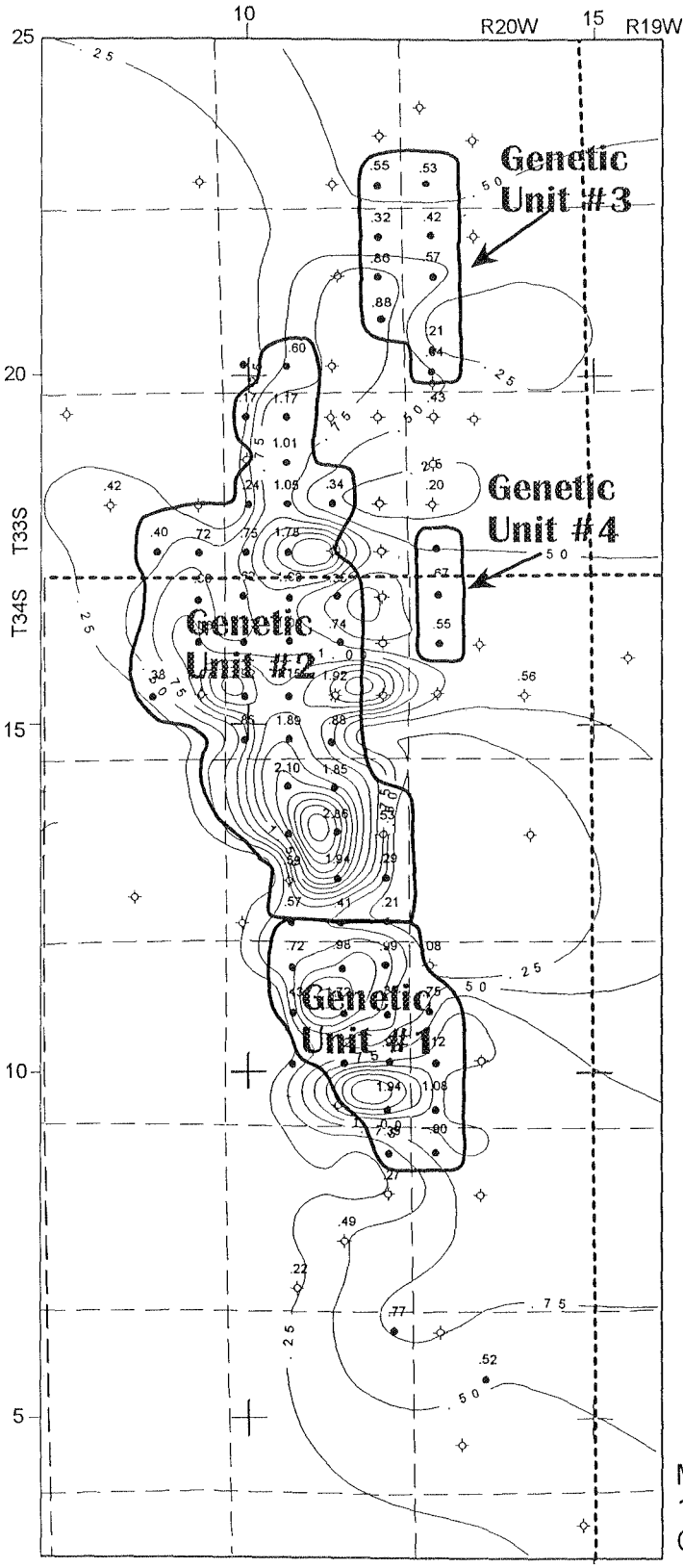


Figure 5-45 Bethany Falls limestone isoporosity map with Type 2 Reservoir Heterogeneity Genetic Unit Boundaries.

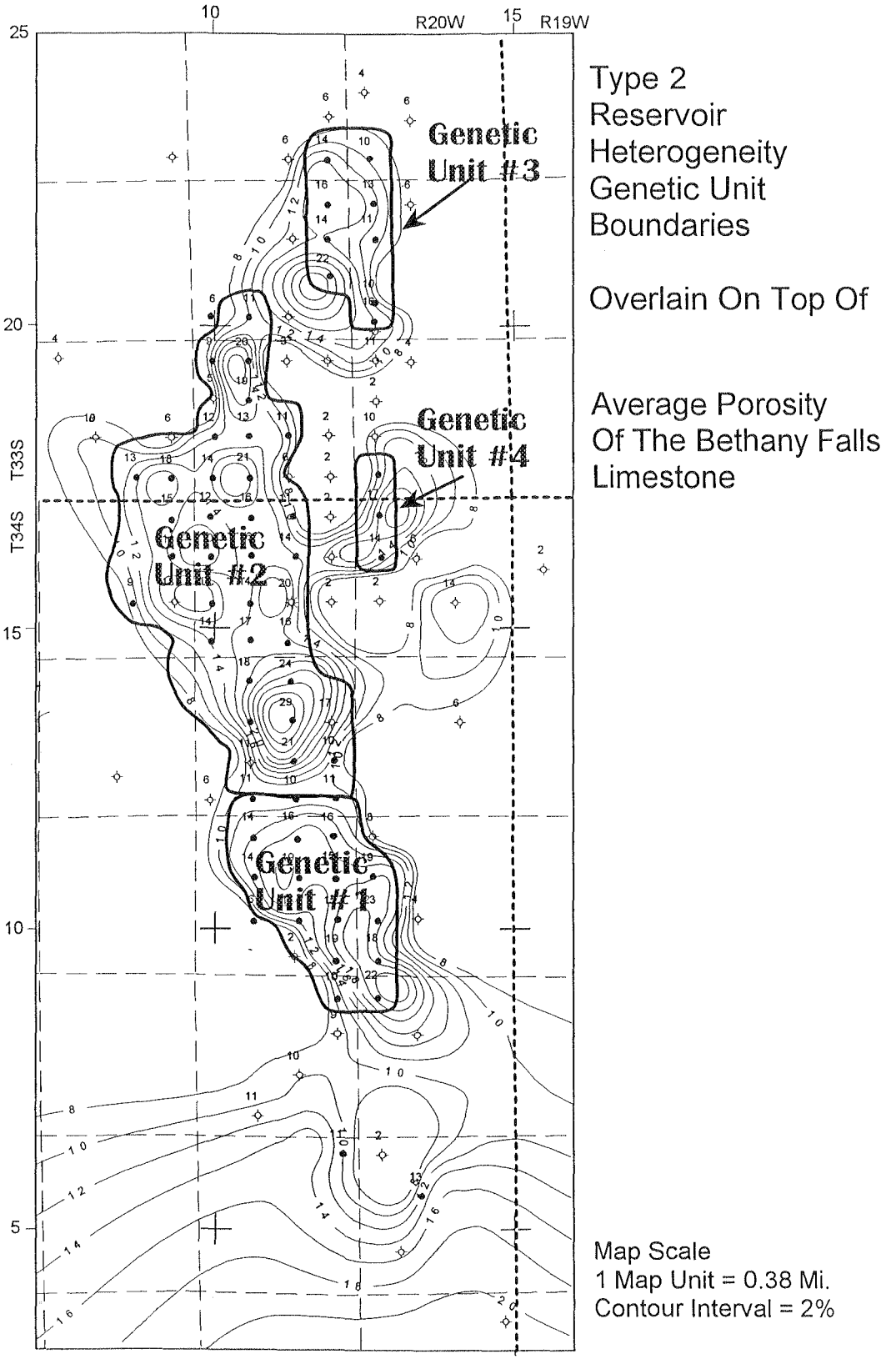


Figure 5-46 Bethany Falls limestone average porosity isoapch map with Type 2 Reservoir Heterogeneity Genetic Unit Boundaries.

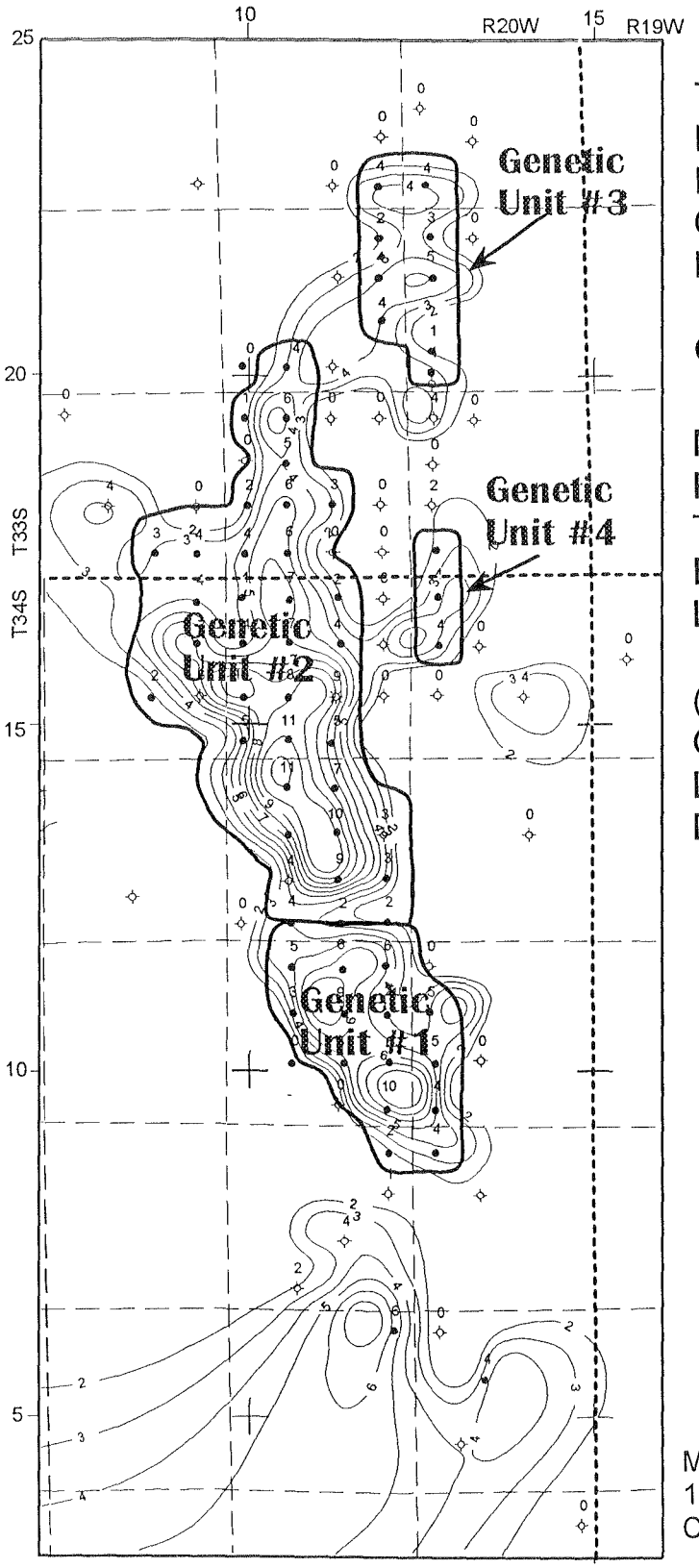


Type 2 Reservoir Heterogeneity Genetic Unit Boundaries

Overlain On Top Of

Net Thickness Of Porosity Greater Then 10 % In The Bethany Falls Limestone

(Porosity Data Based On Wireline Well Log Density Porosity Data)

Map Scale
1 Map Unit = 0.38 Mi.
Contour Interval = 1 Ft.

Figure 5-47 Bethany Falls limestone net thickness of porosity > 10% isoapch map with Type 2 Reservoir Heterogeneity Genetic Unit Boundaries.

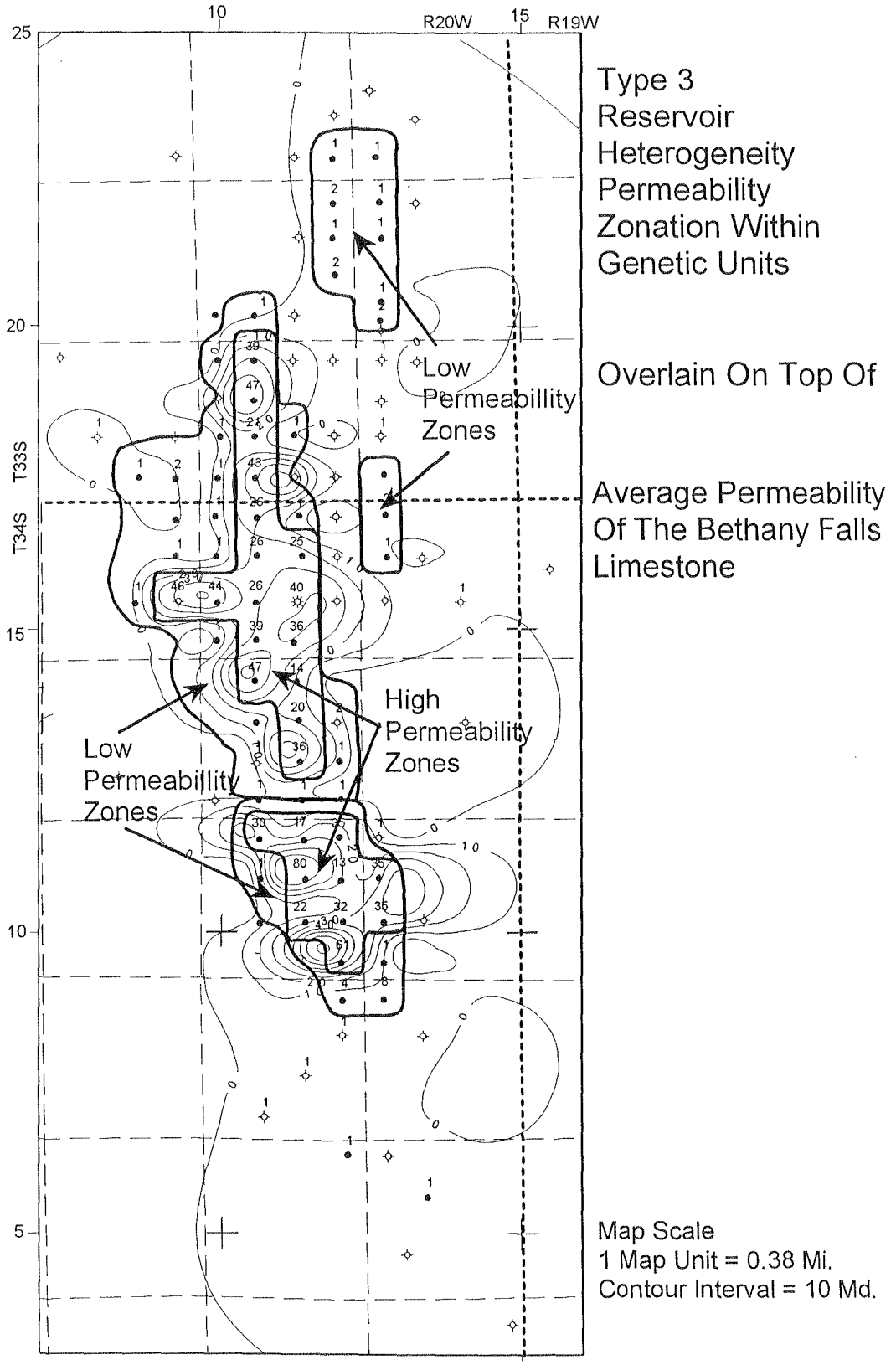


Figure 5-48 Bethany Falls limestone average permeability contour map with Type 3 Reservoir Heterogeneity Permeability Zonation Within Genetic Units.

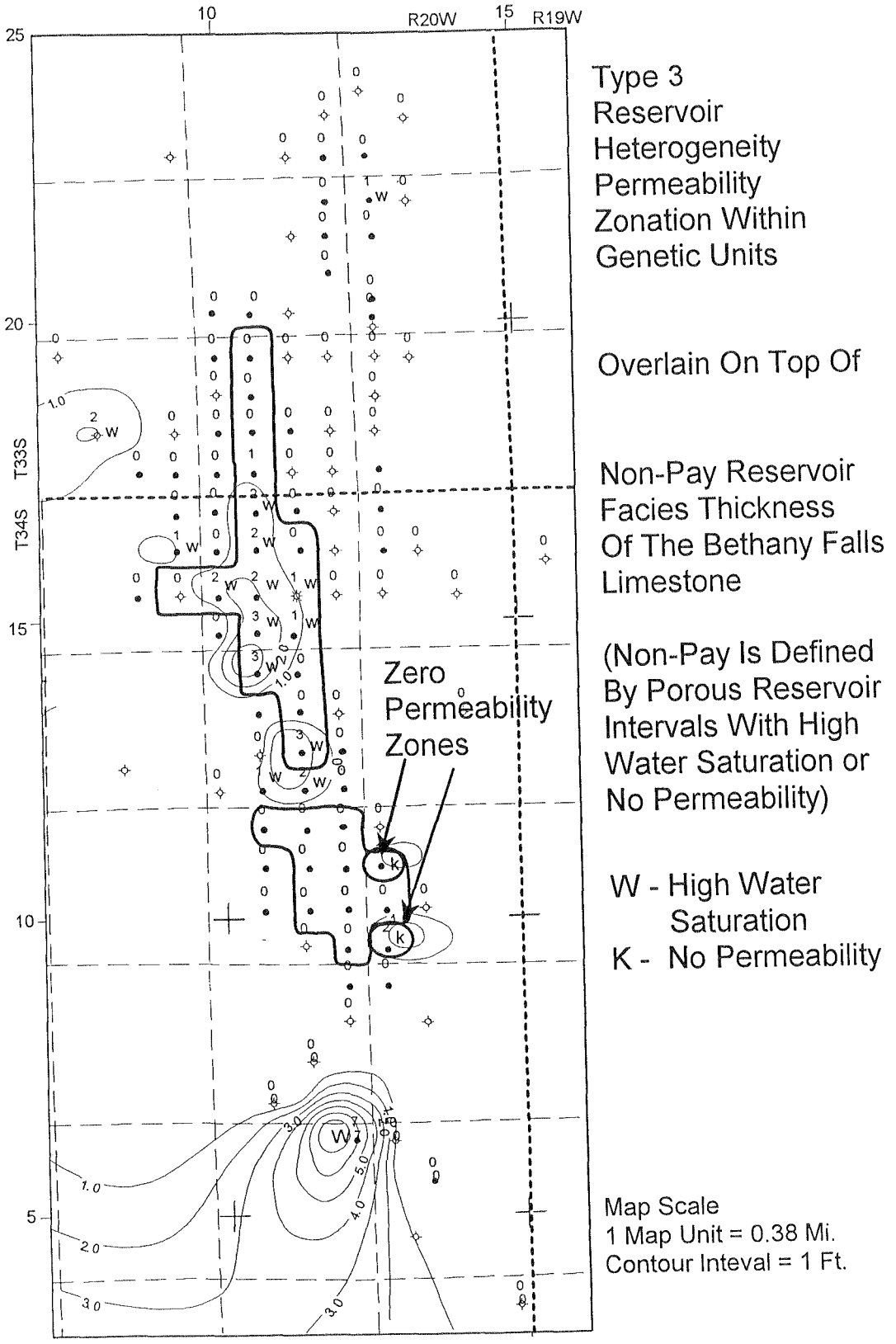


Figure 5-49 Bethany Falls limestone nonpay contour map with Type 3 Reservoir Heterogeneity Permeability Zonation Within Genetic Units (High Permeability Zones).

## Collier Flats Field EOR Potential

This exercise in identifying and classifying reservoir heterogeneity is intended to provide Tertiary Oil Recovery Project (TORP) engineers and scientists with the best possible geologic and engineering data to simulate reservoir flow mechanics and processes. This information may also be used by TORP to justify further EOR research in the Collier Flats field. Current operators and royalty interest owners interested in implementing enhanced oil recovery technologies to prolong the economic life of this field can refer to this reservoir characterization for unitization purposes. Based on this reservoir characterization, Genetic Unit #2 would be a good candidate for additional study by TORP (Figure 5.50).

There are thirty seven productive wells in Genetic Unit #2 with approximately 4,700,000 STB of Original Oil In Place. Assuming the recovery estimates based on decline curve analysis of the Lemon and Rhoades leases are correct, a 23% primary recovery during initial production and a 36% recovery factor during waterflooding, incremental oil production would be approximately 661,000 STB or 13% incremental oil recovery (Table 5.23).

| Genetic Unit #2 Well Name | OOIP (STB) | EUR 15% (STB) | EUR 36% (STB) | Incremental Oil (STB) |
|---|---|---|---|---|
| Baker 1-34 | 50,950 | 11,719 | 18,801 | 7,082 |
| Beyler 1 | 271,422 | 62,427 | 100,155 | 37,728 |
| Beyler 2-11 | 271,422 | 62,427 | 100,155 | 37,728 |
| Christian 1-11 | 311,015 | 71,534 | 114,394 | 43,231 |
| Christian 2-11 | 474,246 | 113,728 | 174,997 | 68,731 |
| Christian 3-11 | 79,883 | 18,373 | 29,477 | 11,104 |
| Girk 11-1 | 41,054 | 9,443 | 15,149 | 5,707 |
| Holly Baker 1 | 131,813 | 30,316 | 48,639 | 18,322 |
| Holly Baker 2 | 131,813 | 30,316 | 48,639 | 18,322 |
| Luellia Mai | 68,743 | 15,811 | 25,366 | 9,555 |
| Petro 11-1 | 21,543 | 4,955 | 7,949 | 2,994 |
| Petro 11-2 | 19,695 | 4,530 | 7,267 | 2,738 |
| Petro 11-3 | 223,824 | 51,480 | 82,591 | 31,112 |
| Petro 11-4 | 36,433 | 8,380 | 13,444 | 5,064 |
| RJ Ora Baker 2 | 34,898 | 8,026 | 12,877 | 4,851 |
| Rj Ora Baker 3 | 86,163 | 19,817 | 31,794 | 11,977 |

Table 5.23 Reserve calculations for Genetic Unit #2. Collier Flats Field.

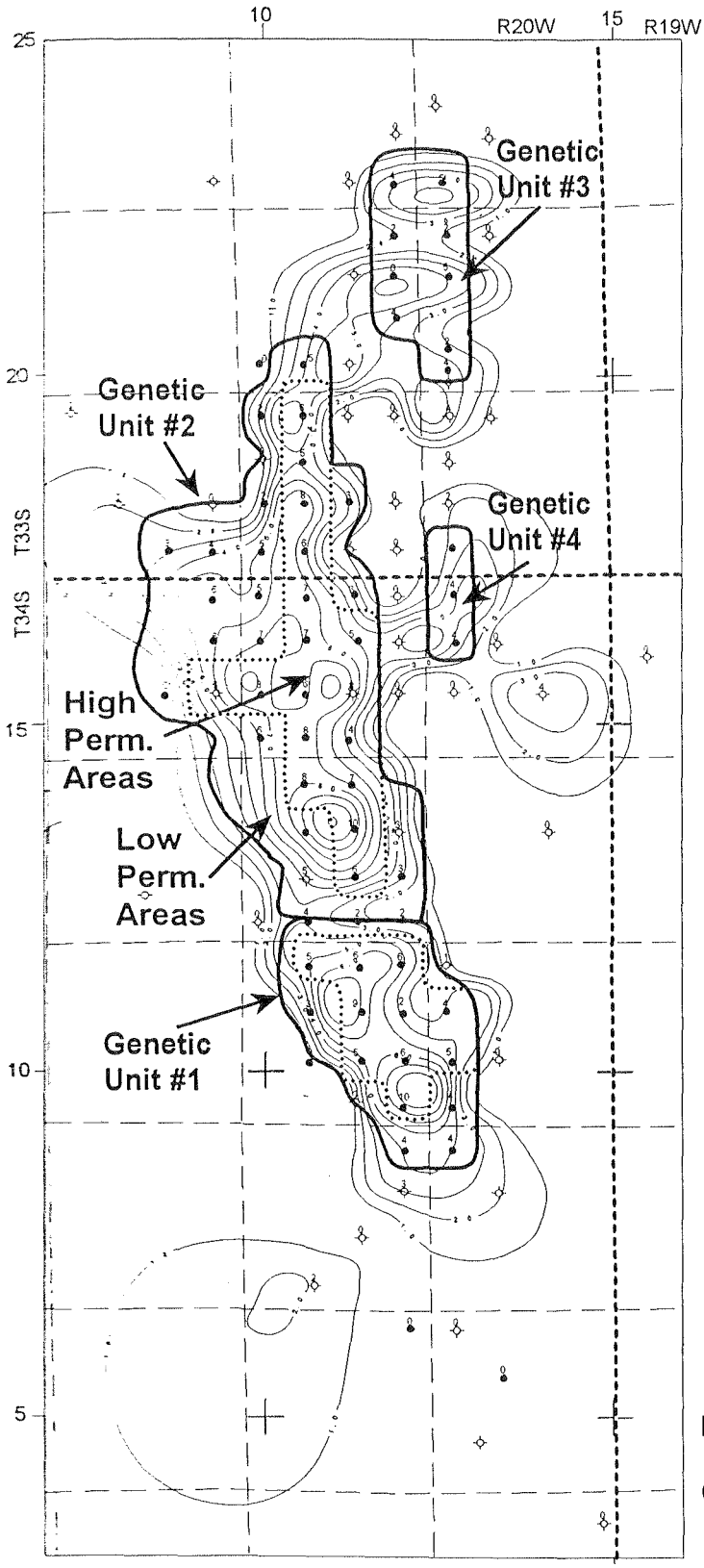


Figure 5-50 Collier Flats Field Reservoir Heterogeneity Summary Diagram.

| Genetic Unit #2 Well Name | OOIP (STB) | EUR 23% (STB) | EUR 36% (STB) | Incremental Oil (STB) |
|---|---|---|---|---|
| RJ Robert Wimmer 4 | 38,470 | 8,848 | 14,195 | 5,347 |
| Selzer 1-35 | 235,693 | 54,209 | 86,971 | 32,761 |
| Selzer 1-a | 125,429 | 28,849 | 46,283 | 17,435 |
| Selzer 2-2 | 85,208 | 19,598 | 31,442 | 11,844 |
| Selzer 2-35 | 120,830 | 27,791 | 44,586 | 16,795 |
| Selzer 2-a | 100,015 | 23,003 | 36,906 | 13,902 |
| Selzer 3-2 | 97,406 | 22,403 | 35,943 | 13,539 |
| Selzer 3-34 | 106,035 | 24,388 | 39,127 | 14,739 |
| Selzer 3-35 | 139,590 | 29,711 | 47,667 | 17,956 |
| Selzer 3-a | 118,351 | 27,221 | 43,672 | 16,451 |
| Selzer 4-2 | 131,813 | 30,317 | 48,639 | 18,322 |
| Selzer 4-35 | 21,525 | 4,951 | 7,943 | 2,992 |
| Selzer 5-2 | 215,586 | 49,585 | 79,551 | 29,966 |
| Selzer 6-2 | 181,682 | 41,787 | 67,041 | 25,254 |
| Selzer 7-2 | 92,146 | 21,194 | 34,002 | 12,808 |
| Selzer 8-2 | 255,362 | 58,733 | 94,229 | 35,495 |
| Selzer 9-2 | 68,295 | 16,034 | 25,723 | 9,690 |
| Willems 1-a | 152,792 | 35,142 | 56,380 | 21,238 |
| Willems 3-a | 144,341 | 33,198 | 53,262 | 20,063 |
| Willems 4-a | 17,337 | 3,987 | 6,397 | 2,410 |
| Willems 5-a | 47,730 | 10,978 | 17,612 | 6,634 |
| | | | | |
| sum | 4,750,553 | 1,095,209 | 1,749,265 | 661,887 |

## Bethany Falls Limestone Reservoir Conclusions

The main producing interval of the Collier Flats Oilfield is the Upper Pennsylvanian (Missourian) Bethany Falls limestone. Reservoir lithologies of the Bethany Falls limestone consist of fossiliferous wackestones, peloidal and fossiliferous packstones, oolitic-bioclastic grainstones and oolitic grainstones capped by a paleosol. The main grainstone reservoir lithofacies was deposited on a paleotopographic high on the northern Anadarko shelf of Kansas. The paleotopographic high focused wave and current energy to form regressive carbonate grainstone sand shoals with a north-south marine sand belt morphology.

The distribution and reservoir porosity type is controlled by a complex diagenetic overprint. There were four dissolution and five cementation events. The first two dissolution and

the first three cementation events are attributed to meteoric diagenesis, subaerial exposure and paleosol formation after Bethany Falls limestone deposition and during Galesburg shale deposition. The final two dissolution and the last two cementation events are related to burial diagenesis and occurred after Canville limestone deposition, burial and fracturing.

Bethany Falls limestone reservoir lithofacies consist of fossiliferous wackestones, peloidal and fossiliferous packstones, mixed bioclastic-oolitic grainstones and oolitic grainstones where the carbonates sand shoals are thickest. On the margins of the carbonate sand shoals, effective porosity is only observed in the grainstone lithofacies.

Porosity in the Bethany Falls reservoir averages 17.4 percent and ranges from 8-30 percent. Permeability averages 43 millidarcies and is very heterogeneous ranging from zero to 300 milladarcies in the porous Bethany Falls reservoir facies. Primary interparticle, moldic, vug, microvug and fracture pores are observed in all the Bethany Falls limestone lithofacies. However, the dominant effective pores are vug and moldic connected by natural fractures. Effective porosity and fracturing was focused preferentially in the center and thickest portions of the Bethany Falls carbonate sand shoals by late burial-related fluid migration in preserved primary and secondary pores connected by fractures caused by differential subsidence along an underlying flexural zone.

Correlation of core descriptions and quantitative analyses with depositional and diagenetic models led to characterization of the Collier Flats Field cores as high or low permeability. Two porosity and permeability equations based on high and low permeability cores are used to characterize permeability.

Evaluation of the Collier Flats Oilfield water saturation data was necessary because a majority of the Bethany Falls effective porosity is secondary. Two cementation factors were used to calculate Bethany Falls reservoir water saturation. When porosity is less than 20%, a 2.5 cementation factor was used to calculate water saturation. When porosity is greater than 20%, a 3.0 cementation factor was used to calculate water saturation.

Four types of reservoir heterogeneity are present in the Collier Flats Oilfield based on the Weber (1986) reservoir heterogeneity classification:

- Type 2 Genetic Unit
- Type 3 Permeability Zonation
- Type 6 Microscopic Textural and
- Type 7 Fracture.

The Collier Flats Oilfield Type 2 and Type 3 reservoir heterogeneity can be mapped. Type 2 Genetic Unit reservoir heterogeneity can be subdivided into four genetic units separated by non-productive wells and Type 3 reservoir heterogeneity, Permeability Zonation (Figure 5-50). The largest genetic unit, Genetic Unit #2, is approximately four miles long and one mile wide and contains a high permeability zone approximately 1/2 mile wide and four mile long trending north south along the eastern margin of known production. A low permeability zone exists between Genetic Units #1 and #2 which is due to lower porosity, thinner reservoir facies and lower permeability.

# References


**Alpay, A.O., 1972, A Practical Approach To Defining Reservoir Heterogeneity**: Journal of Petroleum Technology 24, July 1972, p. 841-848.

**Anchor Bay, 1990, Operator of the Lemon, Rhoades and Petro Leases, Collier Flats Field**: personal communication.

**Asquith, G.B., 1984, Depositional And Diagenetic History Of The Upper Chester (Mississippian) Oolitic Reservoirs, North-Central Beaver County, Oklahoma**, in Hyne, N.J., ed., Limestone Of The Midcontinent: Tulsa Geological Society, Special Publication No. 2, p. 87-92.

**Asquith, G.B., 1985, Handbook Of Log Evaluation Techniques For Carbonate Reservoirs**: AAPG Methods In Exploration Series No. 5, 47 p.

**Ball, M.M., 1967, Carbonate Sand Bodies Of Florida And The Bahamas**: Journal Of Sedimentary Petrology Vol.37, No. 2, p. 556-591.

**Baars, D.L., Watney, W.L., Steeples, D.W., and Brostuen, E.A., 1989, Petroleum: A Primer For Kansas**: Kansas Geological Survey, Educational Series 7, 40 p.

**Bateman, R.M., 1985, Open Hole Log Analysis And Formation Evaluation**: International Human Resources Development Corporation, p. 63-70 and 519-534.

**Bathurst, R.G.C., 1975, Carbonate Sediments And Their Diagenesis, Chapter 3, Recent Carbonate Environments 1: General Introduction And The Great Bahama Bank**, in Developments In Sedimentology, Bathurst R.G.C. ed.: Elsevier Science Publishing Co. Inc., New York, N.Y., p. 93-145.

**Bathurst, R.G.C., 1975, Carbonate Sediments And Their Diagenesis**: New York, Elsevier, 2nd Edition, 658 p.

**Bradley, H.B., 1987, Petroleum Engineering Handbook**, in Bradley, H.B. ed., Petroleum Engineering Handbook: SPE, 1,200 p.

**Brown, H.A., 1984, Lansing-Kansas City Carbonate Reservoirs Of Haskell County, Kansas**, in Hyne, N.J., ed., Limestone Of The Midcontinent: Tulsa Geological Society, Special Publication No. 2, p. 75-85.

**Brown, L.F., 1979, Deltaic Sandstone Facies Of The Mid-Continent**, in Hyne, N.J., ed., Pennsylvanian Sandstones Of The Mid-Continent: Tulsa Geological Society, p. 35-63.

**Chang, M.M., Maerefat, N.L., and Tomutsa, M.M., 1986, Evaluation And Comparison Of Residual Oil Saturation Determination Techniques:** 6th SPE/DOE Symposium On Enhanced Oil Recovery, p. 491-512.

**Chenoweth, P.A., 1979, Geological Prospecting For Mid-Continent Sandstones**, in Hyne, N.J., ed., Pennsylvanian Sandstones Of The Mid-Continent: Tulsa Geological Society, p. 13-33.

**Choquette, P.W., and Pray, L.C., 1970, Geological Nomenclature And Classification Of Porosity In Sedimentary Carbonates**: Am. Association Of Petroleum Geologists Bulletin, Vol. 54, No., p. 207-250.

**Core Laboratories Inc., 1982, Reservoir Fluid Study, KRM Petroleum Corp., Selzer No. 3-2, Comanche County Kansas**: Core Laboratories, 11p.

**Core Laboratories Inc., 1976, A Course In The Fundamentals Of Core Analysis**: Core Labs, 72 p.

**Coveney, R.M., 1985, Temporal And Spacial Variations In Pennsylvanian Black Shale Geochemistry**, in Recent Interpretations Of Late Paleozoic Cyclothems, Proceeding Of The Third Annual Meeting And Field Trip Conference: Mid-Continent Section, SEPM, p. 247-266.

**Crawford, M.L., 1981, Phase Equilibra In Aqueous Fluid Inclusions**, in MAC Short Course In Fluid Inclusions: Hollister And Crawford eds., Chapter 4, p. 75-100.

**Davies, G.R., 1970, Carbonate Bank Sedimentation, Eastern Shark Bay, Western Australia**: AAPG Mem., 13, p. 85-168.

**Dickson, J.A.D., 1965, A Modified Staining Technique For Carbonates In Thin Section**: Nature Vol. 205, p. 587.

**Dravis, J.J., 1977, Rapid And Widespread Generation Of Recent Ooid Hardgrounds On A High Energy Bahamian Bank Platform**: JSP, Vol. 49, p. 195-208.

**Dresser Atlas, 1974, Well Logging And Interpretation Techniques**: Dresser Atlas, 200 p.

**Dresser Atlas, 1982, Well Logging And Interpretation Techniques**: Dresser Atlas, 211 p.

**Dunham, R.J., 1962, Classification Of Carbonate Rocks According To Depositional Texture**, in W.E. Ham, ed., Classification Of Carbonate Rocks: AAPG Mem., 1, p.108-121.

**Enos, P., 1974, Surface Sediment Facies Of The Florida-Bahamas Plateau**: Geological Society Of America Map, 5 p.

**Enos, P., 1977, Quaternary Sedimentation In The South Florida, Part I, Holocene Sediment Accumulations Of The South Florida Shelf Margin**: Geological Society Of America Mem., 147.

**Earlougher, R.C., 1977, Advances In Well Test Analysis, Nomograph Volume 5**: American Institute Of Mining, Metalurigical And Petroleum Engineers Inc., p. 90-103.

**Esteban, M., Klappa, C.F., 1983, Subaerial Exposure Environment**, in Scholle, P.A., Bebout, D.G., and Moore, C.H., Carbonate Depositional Environments: AAPG Mem. 33, p.1-95.

**Fairchild, I.J., 1983, Chemical Controls Of Cathodoluminescence Of Natural Dolomites And Calcite**: New Data And Review: Sedimentology Vol. 30, p.579-583.

**Folk, R.L., 1965, Some Aspects Of Recrystallization In Ancient Limestones**, in Pray, L.C., and Murray, R.C., eds., Dolomitization And Limestone Diagenesis - A Symposium: SEPM Spec. Publ., 13, p. 14-48.

**Gatlin, C., 1960, Petroleum Engineering, Drilling A Well Completions**: Prentice-Hall, Inc., p. 172-180.

**Goldstein, R.H., 1986, Reequilibration Of Fluid Inclusions In Low Temperature Calcium-Carbonate Cement**: Geology, Vol. 14, p. 792-795.

**Goldstein, R.H., Carlson, R.H., Bowman, M.W., and Anderson, J.A., 1989, Diagenetic Responses To Sea-Level Change-Integration Of Field, Stable Isotopes, Paleosol, And Cement Stratigraphy Research To Determine History And Magnitude Of Sea-Level Fluctuation**: in Franseen, E.K., and Watney, W.L., ,eds., Sedimentary Modeling: Computer Simulation Of Depositional Sequences: Kansas Geological Survey, Subsurface Geology Vol. 12, 88p.

**Goldstein, R.H., 1991, Practical Aspects Of Cement Stratigraphy With Illustrations From Pennsylvanian Limestone And Sandstone, New Mexico And Kansas**, in Barker, C.E., and Kopp, O.C., eds., Luminescence Microscopy and Spectroscopy: Qualitative and Quantitative Applications: SEPM Short Course 25, p. 123-132.

**Goldstein, R.H., and Reynolds, T.J., 1991, Systematics Of Fluid Inclusions In Diagenetic Minerals, Notes For A Short Course.**, University Of Kansas, Dept. Of Geology. 78 p.

**Halley, R.B., Harris, P.M., and Hine, A.C., 1983, Bank Margin Environment**, in Scholle, P.A., Bebout, D.G., and Moore, C.H., Carbonate Depositional Environments: AAPG Mem. 33, p.464-506.

**Halliburton, 1995, Halliburton Cementing Tables**: Halliburton, 240 p.

**Harris, P.M., 1979, Facies Anatomy And Diagenesis Of A Bahamian Ooid Shoal**, in Ginsburg, R.N. ed.,: Sedimenta VII, p. 113-150.

**Harris, P.M., Kendall, C., and Lerche, I, 1985, Carbonate Cementation - A Brief Review**, in Schneidermann, Nahum, and Harris, P.M., eds., Carbonate Cements: SEPM Spec. Publ., 36, p. 79-95.

**Heckel, P.H., 1977, Origin Of Phosphatic Black-Shale Facies In Pennsylvanian Cyclothems Of The Mid-Continent North America**: AAPG Bull. Vol. 61, p. 1045-1068.

**Heckell, P.H., 1979, Pensylvanian Cyclic Platform Deposits Of Kansas And Nebraska, Guidebook**: Kansas State Geological Survey, Guidebook Series #4, 79 p.

Heckel, P.H., 1980, **Paleogeography Of The Eustatic Model For Deposition Of Midcontinent Upper Pennsylvanian Cyclothems**, in Paleozoic Paleogeography Of The West-Central United States: Fouche, T.D. and Magathan, E.R., eds.: Rocky Mountain Section, SEPM, Rocky Mountain Paleogeography Symposium 1, p. 197-216.

Heckel, P.H., 1983, **Diagenetic Model For Carbonate Rocks In Midcontinent Pennsylvanian Eustatic Cyclothems**: Journal Of Sedimentary Petrology, Vol. 53, p. 535-553.

Heckel, P.H., 1984, **Factors In Mid-Continent Pennsylvanian Limestone Deposition**, in Hyne, N.J., ed., Limestone Of The Midcontinent: Tulsa Geological Society, Special Publication No. 2, p. 25-50.

Heckel, P.H., 1985, **Current View Of Midcontinent Pennsylvanian Cyclothems**, in Recent Interpretations Of Late Paleozoic Cyclothems, Proceeding Of The Third Annual Meeting And Field Trip Conference: Mid Continent Section, SEPM, p. 1-22.

Helander, D.P., 1983, **Fundamentals Of Formation Evaluation**: Oil And Gas Consultants International, p. 13-28.

Henderson & Company Petroleum Services, 1981, **Waterflood Feasibility Study, Lemon Ranch Field, Swope Limestone Reservoir, Comanche County Kansas**: Henderson & Company, 150 p.

Hine, A.C., Wilber, R.J., and Neumann, A.C., 1971, **Carbonate Sand Bodies Along Contrasting Shallow-Bank Margins Facing Open Seaways, Northern Bahamas**: AAPG Bull., Vol. 65, p. 261-290.

Hine, A.C., 1977, **Lily Bank, Bahamas History Of An Active Oolite Shoal**: JSP Vol. 47, p. 1554-1581.

Hine, A.C., and Neumann, H., 1977, **Shallow Carbonate Bank Margin Growth And Structure, Little Bahama Bank**: AAPG Bulletin., Vol. 61, p. 376-406.

Honarpour, M.M., Szpakiewicz, M.J., Schatzinger, R.A., Tomusta, L., and Carrol, H.B., 1988, **Integrated Geological/Engineering Model For Barrier Island Deposits In The Bell Creek Field, Montana**: Proceedings of 8th SPE/DOE Symposium On Enhanced Oil Recovery, p. 491-512.

Horner, P.R., 1951, **Pressure Build-Up In Wells**: Preceedings, Third World Petroleum Congress, The Hague (1951), Sec. II, p. 503-523.

Houseknecht, D.W., 1986, **Evolution From Passive Margin to Foreland Basin, The Atoka Formation Of The Arkoma Basin, South-Central, U.S.A.**: Spec. Pubs. Int. Ass. Sediment, Vol. 8, p. 327-345.

Hunt, E., 1996, **Fundamentals Of Well Log Analysis, Parts I-V**,: 6/96 - 12/96: World Oil.

Imbre, J., and Buchanan, H., 1965, Sedimentary Structures In Modern Carbonate Sands Of The Bahamas: SEPM Spec. Publ. No. 12, p. 149-172.

James, N.P., and Choquette, P.W., 1983, Diagenesis 9 - Limestones - The Meteoric Diagenetic Environment: Geoscience Canada Vol. 11, No. 4, p. 162-190.

Kerans, C., 1989, Karst-Controlled Reservoir Heterogeneity And An Example From The Elllenburger Group (Lower Ordovician) Of West Texas, Report Of Investigations No. 186: Bureau Of Economic Geology, University Of Texas, p. 1-40.

Kluth, C.F., 1986, Plate Tectonics Of The Ancestral Rocky Mountains, in Peterson, J.A., ed., Paleotectonics And Sedimentation In The Rocky Mountain Region, U.S.: AAPG Mem. 41, p. 353-369.

Kumar, Naresh, and Slatt, R.M., 1984, Submarine Fan And Slope Facies Of Tonkawa (Missourian - Virgillian) Sandstones In Deep Anadarko Basin: AAPG Bull., Vol. 689, p. 1839-1856.

Lasseter, T.J., Waggoner, J.R., and Lake, L.W., 1986, Reservoir Heterogeneity And Their Influence On Ultimate Recovery, in Reservoir Characterization: Academic Press, p. 545-561.

LeJune, N.F., 1979, Geological And Petrophysical Report On The Collier Flats Pool: KRM internal report, 58 p.

Lindberg, C.A., 1979, Depositional Environment And Diagenesis Of The Swope Limestone Formation Pennsylvanian In The KRM Lemon Wells, Comanche County Kansas: KRM internal report, 45 p.

Longman, M.W., 1980, Carbonate Diagenetic Textures From Nearshore Diagenetic Environments: AAPG Bulletin Vol. 64, No. 4, p. 461-485.

Machel, H.G., Mason, R.A, Mariano, A.N., and Mucci, A, 1991, Causes And Emission Of Luminescence In Calcite And Dolomite, in Barker, C.E., and Kopp, O.C., eds., Luminescence Microscopy and Spectroscopy: Qualitative and Quantitative Applications: SEPM Short Course 25, p. 37-58.

Mannhard, G.W., and Busch, D.A., 1974, Stratigraphic Trap Accumulations In Southernwestern Kansas And Northwestern Oklahoma: AAPG Bulletin vol. 58, p. 447-463.

McCartney Engineering, Inc., 1990, Estimated Reserves And Future Net Revenue: PETX Petroleum Corp., 194 p.

Merriam, D.F., 1963, The Geologic History Of Kansas: Kansas Geological Survey Bulletin 162: University Of Kansas Publications, 225 p.

Meyers, W.J., 1991, **Calcite Cement Stratigraphy: An Overview**, in Barker, C.E., and Kopp, O.C., eds., Luminescence Microscopy and Spectroscopy: Qualitative and Quantitative Applications: SEPM Short Course 25, p. 133-148.

Moore, R.C., 1936, **Stratigraphic Classification Of The Pennsylvanian Rock Of Kansas**: Kansas Geological Survey Bull. 22, p. 1-256.

Moore, R.C., 1949, **Divisions Of The Pennsylvanian System In Kansas**: Kansas Geological Survey Bull. 83, 203 p.

Moore, R.C., 1964, **Paleoecological Aspects Of Kansas Pennsylvanian And Permian Cyclothems**, in Symposium On Cyclic Sedimentation: KGS Bull. 169, Vol. 1, p. 287-380.

Moore, G.E., 1979, **Pennsylvanian Paleogeography Of The Southern Mid-Continent**, in Hyne N.J., ed., Pennsylvanian Sandstones Of The Midcontinent: Tulsa Geological Soc. Spec. Pub. 1, p. 2-12.

Morris, C.H., and Druckman, Y., 1981, **Burial Diagenesis And Porosity Evolution, Upper Jurassic Smackover, Arkansas And Louisiana**: AAPG Bulletin Vol. 65, P.597-628.

Morrow, D.W., 1982, **Diagenesis 2. Dolomite - Part 2 Dolomitization Models And Ancient Dolostones**: Geoscience Canada Vol. 9, No. 2, p. 96-107.

Mossler, J.H., 1971, **Diagenesis And Dolomitization Of The Swope Formation (Upper Pennsylvanian) Southeast Kansas**: Journal Of Sedimentary Petrology, Vol. 41, No. 4, p. 962-970.

Mossler, J.H., 1973, **Carbonate Facies Of The Swope Limestone Formation (Upper Pennsylvanian) Southeast Kansas**: Kansas Geological Survey, Bulletin 206, Part 1. p. 3-17.

Payton, C.E., 1966, **Petrology Of The Carbonate Members Of The Swope And Dennis Formations (Pennsylvanian), Missouri and Iowa**: Journal Of Sedimentary Petrology, Vol. 36, No. 2, p. 576-601.

Pierson, B.J., 1981, **The Control Of Cathodoluminescence In Dolomite By Iron And Manganese**: Sedimentology, Vol. 28, p. 601-610.

Prather, B.E., 1984, **Deposition And Diagenesis Of An Upper Pennsylvanian Cyclothem From The Lansing-Kansas City Groups Hitchcock County, Nebraska**, in Hyne, N.J., ed., Limestone Of The Midcontinent: Tulsa Geological Society, Special Publication No. 2, p. 393-419.

Purdy, E.G., 1962, **Recent Calcium Carbonate Facies Of The Great Bahama Bank 1. Petrography And Reaction Groups**: Journal Of Geology Vol. 71, p. 334-355.

Purdy, E.G., 1963, Recent Calcium Carbonate Facies Of The Great Bahama Bank; Petrography And Reaction groups, Sedimentary Facies: Jour. Geology, Vol. 71, p.334-355, 472-497.

Purser, B.H., 1973, Regional Sedimentation Along The Trucial Coast In The Persian Gulf, Holocene Carbonate Sedimentation And Diagenesis In A Shallow Epicontinental Sea: New York Springer - Verlag Pub., p. 211-231.

Rascoe, B., Jr., 1962, Regioanl Stratigraphic Analysis Of Pennsylvanian And Permian Rocks In Western Mid-Continent, Colorado, Kansas, Oklahoma and Texas: AAPG Bulletin vol. 46, p. 1345-1370.

Rascoe, B. Jr., and Adler, F.J., 1983, Permo-Carboniferous Hydrocarbon Accumulations, Midcontinent, U.S.A.: AAPG Bull. Vol. 67, p. 979-1001.

Reeder, R.J., 1991, AN Overview Of Zoning In Carbonate Minerals, . in Barker, C.E., and Kopp, O.C., eds., Luminescence Microscopy and Spectroscopy: Qualitative and Quantitative Applications: SEPM Short Course 25, p. 77-82.

Roedder E., 1984, Fluid Inclusions, in Reviews In Mineralogy Vol. 12: Ribbe, P.H. ed., Mineralogical Society Of America, Chapters 1-12, p. 1-336.

Rupee, S.C., Candor, H.S., 1988, Effects Of Facies And Diagenesis On Reservoir Heterogeneity: Me San Andrews Field, West Texas, Report Of Investigations No. 178: Bureau Of Economic Geology, University Of Texas, p. 1-64.

Russell, K., 1981, Geological Heterogeneity's Important To Future Enhanced Recovery In Carbonate reservoirs Of The Upper Ordovician Red River Formation At Cabin Creek Field, Montana: Proceedings, Second Joint SPE/DOE Symposium On Enhanced Oil Recovery, p. 403-417.

Schoeling, L.G., Green, D.W., and Willhite, G.P., 1988, Introducing EOR Technology To Independent Operators: Proceedings of 8th SPE/DOE Symposium On Enhanced Oil Recovery, p. 863-872.

Scholle, P.A., and Halley, R.B., 1985, Burial Diagenesis: Out Of Sight, Out Of Mind: SEPM Spec. Publ. 36, p. 309-330.

Selley, R.C., 1985, Elements Of Petroleum Geology: W.H. Freeman And Company, 450 p.

Silvester, R.S., 1981, Enhanced Oil Recovery - A Literature Review: British Hydromechanics Research Association, 76 p.

Stone, W.P., 1984, Origin And Evolution Of Oolite In The Drum Limestone (Pennsylvanian, Missourian), Montgomery County , Kansas, in Hyne, N.J., ed., Limestone Of The Midcontinent: Tulsa Geological Society, Special Publication No. 2, p. 51-74.

Szpakiewicz, M.J., McGee, K., and Sharma, B., 1986, **Geological Problems Related to Characterization Of Clastic Reservoirs For Enhanced Oil Recovery**: 6th SPE/DOE Symposium On Enhanced Oil Recovery, p. 97-118.

**Thompson, R.S., and Wright, J.D., 1985, Oil Property Evaluation:** Second edition Thompson-Wright Associates, p 4.1-5.52.

**Wanless, H.R., and Shepard, F.P., 1936, Sea-Level And Climatic Changes Related To Late Paleozoic Cycles**: GSA Bull., Vol. 47, No. 8, p. 1177-1206.

**Watney, W.L., 1980, Cyclic Sedimentation Of The Lansing And Kansas City Groups (Missourian) In Northwestern Kansas And Southwestern Nebraska - A Guide For Petroleum Exploration**: KGS Bull. 220, 72 p.

**Watney, W.L., 1983, Carbonate Dominated Shelf Cycles In The Late Pennsylvanian Of Midcontinent-Intrabasinal And Extrabasinal Controls On Sedimentation And Early Diagenesis**: AAPG Bull. Vol. 67, No. 3, p. 567.

**Watney, W.L., 1984, Recognition Of Favorable reservoir Trends In Upper Pennsylvanian Cyclic Carbonates In Western Kansas**, in Hyne, N.J., ed., Limestone Of The Midcontinent: Tulsa Geological Society, Special Publication No. 2, p. 201-245.

**Watney, W.L., 1985, Evaluation Of The Significance Of Tectonic, Sedimentary Control Versus Eustatic Control Of Upper Pennsylvanian Cyclothems In The Western Midcontinent, in Recent Interpretations Of Late Paleozoic Cyclothems**: Proceeding Of The Third Annual Meeting And Field Trip Conference, Mid Continent Section, SEPM, p. 105-140.

**Watney, W.L., 1985, Swope Limestone (K-Zone) In central And Southwestern Kansas, The Role Of Core In Understanding reservoir Development And Mechanisms responsible For Cyclic Sedimentation**, in Core Studies In Kansas, Sedimentology And Diagenesis Of Economically Important Rock Strata In Kansas: Adkins-Heljeson, M.D., ed.: Kansas Geological Survey, Subsurface Geology Series 6. P. 102-119.

**Watney, W.L., and French, J., 1988, Characterization Of Carbonate reservoirs In The Lansing-Kansas City Groups (Upper Pennsylvanian) In The Victory Field, Haskell County**, in Goolsby, S.M., and Longman, M.W., eds., Occurrence And Petrophysical Properties Of Carbonate Reservoirs In The Rocky Mountain Region: 1988 Carbonate Symposium, Rocky Mountain Association Of Geologists, p. 27-46.

**Watney, W.L., and French, J., 1988, Missourian (Upper Pennsylvanian) Lansing and Kansas City Groups In The Kansas City Area - Mixed Carbonate Clastic Sequences**: Kansas Geological Survey Open File No. 8841, 60 p.

**Watney, W.L., French, J., and Franseen, E.K., 1989, Guidebook For A Field Conference On Sequence Stratigraphy Interpretations And Modeling Of Cyclothems In The Upper Pennsylvanian (Missourian) Lansing And Kansas City Groups In Eastern Kansas**: in Kansas Geological Society 41st Annual Field Trip. 209 p.

**Watney, W.L., West, R., Maples, C., and Denham, P, 1991, Upper Pennsylvanian (Virgillian And Missourian) Cyclothems In The Lawrence, Kansas Area**, in Mid-Continent Meeting Of Predictive Stratigraphic Analysis (PSA) Workshop: Kansas Geological Survey Open File Report 91-22, 127 p.

**Weber, K.J., 1986, How Heterogeneity Affects Oil Recovery**, in Reservoir Characterization: Academic Press, p. 487-544.

**Willhite, G.P., 1986, The Role Of Geology In Waterfloods**, in Waterflooding: Society Of Petroleum Engineers, 2nd Edition, p. 225-301.

# Appendix A

# Collier Flats Field
# Wireline Well Log Database

Wells Listed In Alphabetical Order

# WELL LOG DATABASE

| | | | | | | |
|---|---|---|---|---|---|---|
| | WELL LOGS DIGITIZED IN TERRALOG DATABASE | | LOG TYPES | | | |
| | SEPT. 19, 1993 | | GR | GAMMA RAY | | |
| | | | D | DENSITY | | |
| | WELLS SORTED IN ALPHABETIC ORDER | | N | NEUTRON | | |
| | | | SONIC | SONIC | | |
| | | | ACOUS | ACOUSTIC | | |
| | | | D.I. | DUAL INDUCTION | | |
| | | | GUARD | GUARD | | |
| | | | LAT | LATEROLOG | | |
| | | | FOC | FOCUSED LATEROLOG | | |
| | | | SFL | SPHERICALLY FOCUSED | | |
| WELLID | WELLNAME | OPERATOR | LOCATION | DATE | LOGCOMPANY | LOGTYPES |
| 129 | BAKER 1-34 | KRM | 250'E OF C-SW-SE;34-33S-20W | 7/25/82 | DRESSER | GR;D;N;D.I.FOC |
| 107 | BEYLER 2-11 | KRM | NE-NW;11-34S-20W | 2/28/82 | DRESSER | GR;D;N;D.I.FOC |
| 87 | CHRISTAIN 1-11 | KRM | NW-NE;11-34S-20W | 12/31/81 | DRESSER | GR;D;N;D.I.FOC |
| 86 | CHRISTIAN 2-11 | KRM | SW-NE;11-34S-20W | 3/10/82 | DRESSER | GR;D;N;D.I.FOC |
| 64 | CHRISTIAN 3-11 | KRM | 140'SW OF C-SE-NE;11-34S-20W | 5/2/82 | DRESSER | GR;D;N;D.I.FOC |
| 138 | CIMMARON B-1 | DONALD SLAWSON | C-N/2-SW-NE;33-34S-20W | 9/28/78 | DRESSER | GR;D;N |
| 139 | EUBANK 21-10 | SAMUEL GARY | NW-SE;21-33S-20W | 4/9/82 | SCHLUMBERGER | GR;D;N;D.I.SFL |
| 142 | EUBANK 28-5 | SAMUEL GARY | SW-NW;28-33S-20W | 12/13/81 | SCHLUMBERGER | GR;D;N;D.I.SFL |
| 40 | GIRK 1 | KRM | NW-NW;36-33S-20W | 9/25/80 | DRESSER | GR;D;N;LAT |
| 122 | GIRK 11-1 | INTERNORTH | SE-SW;11-34S-20W | 8/30/80 | GEARHART | GR;D;N;D.I.LAT |
| 101 | GIRK 11-2 | NORTEX | SW-SW;11-34S-20W | 4/12/80 | SCHLUMBERGER | GR;D;N;D.I.LAT |
| 43 | GIRK 2 | KRM | SW-NW;26-33S-20W | 12/30/80 | DRESSER | GR;D;N;D.I.FOC |
| 29 | GIRK 3 | KRM | NE-NW;36-33S-20W | 3/10/81 | DRESSER | GR;D;N;D.I.FOC |
| 127 | GOHN Y-22 | KRM | SE-SE;22-33S-20W | 1/19/81 | DRESSER | GR;D;D.I.FOC |
| 49 | HACKNEY 1 | KRM | NW-NW;13-34S-20W | 7/25/80 | WELEX | GR;D;N;GUARD |
| 50 | HACKNEY 2-13 | KRM | SW-NW;13-34S-20W | 10/27/81 | DRESSER | GR;D;N;D.I.FOC |
| 48 | HALIBUR BAKER 3 | HALIBURTON | NW-NW;25-33S-20W | 6/16/84 | WELEX | GR;N;GUARD |
| 53 | HALIBUR R. BAKER 1 | HALIBURTON | SW-NW;24-33S-20W | 10/27/70 | WELEX | GR;N;GUARD |
| 95 | HOLLY ROBERT WIMMER 1 | HOLLY ENERGY | NW-NE;35-33S-20W | 5/31/82 | DRESSER | GR;D;N;D.I.FOC |
| 80 | KRM LEMON 1 | KRM | NW-SE;14-34S-20W | 12/14/78 | WELLEX | GR;D;N;GUARD |
| 54 | LEMON 1-26 | KRM | NE-NE;26-34S-20W | 7/12/82 | DRESSER | GR;D;N;D.I.FOC |
| 39 | LEMON 10 | KRM | NW-NW;24-34S-20W | 11/19/79 | WELEX | GR;D;N |
| 57 | LEMON 14 | KRM | SE-NE;23-34S-20W | 4/25/81 | DRESSER | GR;D;N;D.I.FOC |
| 26 | LEMON 15 | KRM | NE-SW;13-34S-20W | 12/18/81 | DRESSER | GR;D;N;D.I.FOC |
| 98 | LEMON 2-X | KRM | NE-SW;14-34S-20W | 3/28/79 | WELEX | GR;D;N;GUARD |
| 82 | LEMON 4 | KRM | SW-SE;14-34S-20W | 4/18/79 | WELEX | GR;D;N;GUARD |
| 41 | LEMON 5 | KRM | NW-SW;13-34S-20W | 4/28/79 | WELEX | GR;D;N;GUARD |
| 55 | LEMON 6 | KRM | SE-SE;14-34S-20W | 5/9/79 | WELEX | GR;D;N;GUARD |
| 38 | LEMON 7 | KRM | SW-SW;13-34S-20W | 5/22/79 | WELEX | GR;D;N;GUARD |
| 56 | LEMON 8 | KRM | NE-NE;23-34S-20W | 6/5/79 | WELEX | GR;D;N;GUARD |
| 100 | LEMON 9 | KRM | SE-NW;14-34S-20W | 8/23/79 | WELEX | GR;D;N;GUARD |
| 22 | LEMON BAR 1 | M.B. ARMER | SW-NW;15-34S-20W | 4/4/55 | SCHLUMBERGER | GR;LAT |
| 106 | LUELLA MAI 1 | AMERADA HUBER | NE-SW;11-34S-20W | 11/23/63 | SCHLUMBERGER | GR;SONIC;LAT |
| 96 | MARLENE 1-23 | KRM | SE-SW;23-34S-20W | 3/1/84 | DRESSER | GR;D;N;D.I.FOC |
| 51 | MIDWEST BAKER 1 | MIDWEST | SW-NW;25-33S-20W | 9/5/70 | DRESSER | GR;N;LAT |
| 30 | MIDWEST BAKER 2 | MIDWEST OIL | NE-NW;25-33S-20W | 10/3/70 | DRESSER | GR;N;LAT;ACOUS |
| 69 | MIDWEST NORTON 1 | MIDWEST OIL | NE-SE;26-33S-20W | 8/14/70 | DRESSER | GR;N;ACOUS;LAT |
| 74 | MIDWEST ROBERT WIMMER 1 | MIDWEST OIL | NE-NE;35-33S-20W | 12/23/70 | DRESSER | GR;N;LAT |
| 91 | ORA BAKER 3 | R.J. PATRICK | 150'W OF C-SW-NE;2-34S-20W | 2/25/82 | GEARHART | GR;D;N;D.I.LAT |
| 66 | ORA BAKER 4 | R.J. PATRICK | 150'W OF C-NE-NE;2-34S-20W | 3/18/82 | GEARHART | GR;D;N;D.I.LAT |
| 78 | PETRO 11-1 | INTERNORTH | SW-SE;11-34S-20W | 7/18/81 | SCHLUMBERGER | GR;D;N;D.I.SFL |
| 59 | PETRO 11-2 | INTERNORTH | SE-SE;11-34S-20W | 9/29/81 | SCHLUMBERGER | GR;D;N;D.I.SFL |
| 83 | PETRO 11-3 | NORTEX | NW-SE;11-34S-20W | 2/22/82 | SCHLUMBERGER | GR;D;N;D.I.SFL |
| 61 | PETRO 11-4 | INTERNORTH | NE-SE;11-34S-20W | 4/18/82 | GEARHART | GR;D;N;D.I.LAT |
| 23 | PETRO 12-1 | INTERNORTH | 150'W OF C-SW-NE;12-34S-20W | 2/10/82 | SCHLUMBERGER | GR;D;N;D.I.SFL |
| 88 | R.J. ORA BAKER 2 | R.J. PATRICK | 150'W OF C;NW-NE;2-34S-20W | 11/24/81 | GEARHART | GR;D;N;D.I.LAT |
| 44 | R.J.RALPH BAKER 2 | R.J. PATRICK | 1980' FS/L, 660'FW/L;36-33S-20W | 3/27/81 | GEARHART | GR;D;N;D.I.LAT |
| 28 | RALPH BAKER 3 | R.J. PATRICK | SE-NW;1-34S-20W | 8/21/81 | GEARHART | GR;D;N;D.I.LAT |
| 37 | RALPH BAKER 4 | PATRICK | NW-NW-NW;1-34S-20W | 1/18/85 | GEARHART | GR;D;N;D.I.LAT |
| 73 | RESVEN BAKER 1 | RESOURCE VENTURES | SE-SE;23-33S-20W | 6/12/84 | GREAT GUNS | GR;D;N;D.I. |
| 60 | RHOADES 1 | KRM | SE-NE;14-34S-20W | 6/17/79 | WELEX | GR;D;N;GUARD |
| 81 | RHOADES 2 | KRM | SW-NE;13-34S-20W | 6/28/79 | WELEX | GR;D;N;GUARD |
| 79 | RHOADES 3 | KRM | C-NW-NE;14-34S-20W | 12/21/79 | WELEX | GR;N;D;GUARD |
| 35 | RJ RALPH BAKER 1 | PATRICK | SW-NW;1-34S-20W | 10/3/80 | GEARHART | GR;D;N;D.I.LAT |
| 92 | RJ ROBERT WIMMER 1 | R.J. PATRICK | 682'FS/L-1951'FE/L;35-33S-20W | 3/18/81 | GEARHART | GR;D;N;D.I.LAT |
| 67 | ROBERT WIMMER 2 | R.J. PATRICK | SE-SE;35-33S-20W | 12/23/81 | GEARHART | GR;D;N;D.I.LAT |
| 70 | ROBERT WIMMER 3 | R.J. PATRICK | 150'S OF C-NE-SE;35-33S-20W | 3/7/82 | GEARHART | GR;D;N;D.I.LAT |
| 94 | ROBERT WIMMER 4 | R.J. PATRICK | 150'NW OF SE1/4;35-33S-20W | 3/30/82 | GEARHART | GR;D;N;D.I.LAT |
| 144 | SCHEUFLER 21-5 | SAMUEL GARY | SW-NW;21-33S-20W | 6/2/81 | SCHLUMBERGER | GR;D;N;D.I.SFL |
| 71 | SCHWEITZER 1 | HALIBURTON | 100'N OF C-NE-NE;26-33S-20W | 4/29/70 | WELEX | GR;ACOUS;GUARD |
| 85 | SCHWEITZER 2 | HALIBURTON | 150'E OF C-SW-NE;26-33S-20W | 9/13/70 | WELEX | GR;N |
| 72 | SCHWEITZER 3 | HALIBURTON | SE-NE;26-33S-20W | 8/26/84 | WELEX | GR;N;GUARD |

WELL LOG DATABASE

| WELLID | WELLNAME | OPERATOR | LOCATION | DATE | LOGCOMPANY | LOGTYPES |
|---|---|---|---|---|---|---|
| 65 | SELZER 1-2 | KRM | NE-SE;2-34S-20W | 2/13/81 | DRESSER | GR;D;D.I.FOC |
| 128 | SELZER 1-34 | KRM | NE-SE;34-33S-20W | 10/12/81 | WELEX | GR;D;N;D.I.GUARD |
| 109 | SELZER 1-35 | KRM | SE-SW;35-33S-20W | 2/25/81 | DRESSER | GR;D;N;D.I.FOC |
| 125 | SELZER 1-A | CITIES SERVICES | 100'N OF-C;NE-NE;3-34S-20W | 1/15/81 | DRESSER | GR;D;N;LAT |
| 120 | SELZER 2-2 | KRM | NW-NW;2-34S-20W | 5/9/81 | PETRO-LOG | GR;D;N;GUARD |
| 135 | SELZER 2-34 | KRM | NW-NW;34-33S-20W | 2/5/82 | DRESSER | GR;D;N;D.I.FOC |
| 116 | SELZER 2-35 | KRM | SW-SW;35-33S-20W | 6/2/81 | DRESSER | GR;D;N;D.I.FOC |
| 124 | SELZER 2-A | CITIES SERVICES | SE-NE;3-34S-20W | 4/18/82 | DRESSER | GR;D;N;D.I.FOC |
| 117 | SELZER 3-2 | KRM | SW-NW;2-34S-20W | 5/22/81 | PETRO-LOG | GR;D;N;GUARD |
| 126 | SELZER 3-34 | KRM | SE-SE;34-33S-20W | 2/18/82 | DRESSER | GR;D;N;D.I.FOC |
| 110 | SELZER 3-35 | KRM | NE-SW;35-33S-20W | 6/23/81 | DRESSER | GR;D;N;D.I.FOC |
| 123 | SELZER 3-A | CITIES SERVICES | NE-SE;3-34S-20W | 4/28/82 | DRESSER | GR;D;N;D.I.FOC |
| 105 | SELZER 4-2 | KRM | NE-SW;2-34S-20W | 6/12/81 | DRESSER | GR;D;N;D.I.FOC |
| 133 | SELZER 4-34 | KRM | NE-SW;34-33S-20W | 12/1/82 | DRESSER | GR;D;N;D.I.FOC |
| 114 | SELZER 4-35 | KRM | NW-SW;35-33S-20W | 12/2/81 | DRESSER | GR;D;N;D.I.FOC |
| 121 | SELZER 5-2 | KRM | NW-SW;2-34S-20W | 12/15/81 | DRESSER | GR;D;N;D.I.FOC |
| 104 | SELZER 6-2 | KRM | SE-SW;2-34S-20W | 9/22/81 | DRESSER | GR;D;N;D.I.FOC |
| 89 | SELZER 7-2 | KRM | SW-SE;2-34S-20W | 11/20/81 | DRESSER | GR;D;N;D.I.FOC |
| 90 | SELZER 8-2 | KRM | NW-SE;2-34S-20W | 10/2/81 | DRESSER | GR;D;N;D.I.FOC |
| 119 | SELZER 9-2 | KRM | SW-SW;2-34W-20W | 2/16/82 | DRESSER | GR;D;N;D.I.FOC |
| 130 | SELZER B-1 | CITIES SERVICES | 100'E OF C-NW-SE;3-34S-20W | 2/20/82 | GEARHART | GR;D;N;D.I.LAT |
| 52 | THORNHILL 1 | HALIBURTON | SW-SW;24-33S-20W | 9/29/70 | WELEX | GR;N;GUARD |
| 31 | THORNHILL 2 | HALIBURTON | NE-SW;24-33S-20W | 10/11/70 | WELEX | GR;N;GUARD |
| 25 | WATERS 1-25 | KRM | NW-NW;25-34S-20 | 11/7/81 | DRESSER | GR;D;N;D.I.FOC |
| 34 | WATERS 2-25 | KRM | SE-NW;25-34S-20W | 3/21/82 | DRESSER ATLAS | GR;D;N;D.I.FOC |
| 36 | WESLEY GIRK 1 | PATRICK | NW-SW;1-34S-20W | 1/4/81 | GEARHART | GR;D;N;D.I.LAT |
| 24 | WESLEY GIRK 2 | R.J. PATRICK | NW-SE;1-34S-20W | 8/11/81 | GEARHART | GR;D;N;D.I.LAT |
| 112 | WILLEMS 1-A | TEXAS OIL & GAS | SE-NW;35-33S-20W | 9/30/81 | SCHLUMBERGER | GR;D;N;D.I.SFL |
| 115 | WILLEMS 2-A | TXO PRODUCTION | SW-NW;35-33S-20W | 1/15/82 | SCHLUMBERGER | GR;D;N;D.I.SFL |
| 111 | WILLEMS 3-A | TEXAS OIL & GAS | 660'FNL-1980'FWL;35-33S-20W | 12/10/81 | SCHLUMBERGER | GR;D;N;D.I.SFL |
| 118 | WILLEMS 4-A | TXO PRODUCTION | 660'FNL-660'FWL;35-33S-20W | 2/18/82 | SCHLUMBERGER | GR;D;N;D.I.SFL |
| 97 | WILLEMS 5-A | TXO PRODUCTION | 660'FSL-1980'FWL;26-33S-20W | 6/15/82 | GEARHART | GR;D;N;D.I.LAT |
| 113 | WILLEMS 6 | TXO PRODUCTION | 660'FSL-660'FWL;26-33S-20W | 7/14/82 | SCHLUMBERGER | GR;N |
| 76 | WOOLFOLK CPC-134 | CIMMARRON PETROLEUM | NW-SE;23-34S-20W | 1/24/80 | SCHLUMBERGER | GR;D;N;LAT |
| 93 | YUCCA ORA BAKER 1 | YUCCA PETROLEUM | SW-SE;23-33S-20W | 9/11/70 | WELEX | GR;N;GUARD |
| 68 | YUCCA ORA BAKER 2 | YUCCA PETROLEUM | 150' SE OF C-NE-SE;23-33S-20W | 12/3/70 | WELEX | GR;N;GUARD |
| 47 | YUCCA RALPH BAKER 1 | YUCCA PETROLEUM | 150'N-C;25-33S-20W | 10/23/70 | WELEX | GR;N;GUARD |
| 46 | YUCCA RALPH BAKER 2 | YUCCA PETROLEUM | 920'FSL-760'FWL;25-33S-20W | 7/26/78 | WELEX | GR;ACOUS;GUARD |
| | | | | | | |
| | TOTAL | 100 | | | | |

# Appendix B

# Collier Flats Field
# Core Database

Core Descriptions
Core & Well Log Correlations
Core Porosity/Permeability To Open Pore Type Correlations

Lemon & Rhoades Leases
Sections 13,14, 23 & 24
T34S, R20W

Wells Listed In Alphabetical Order

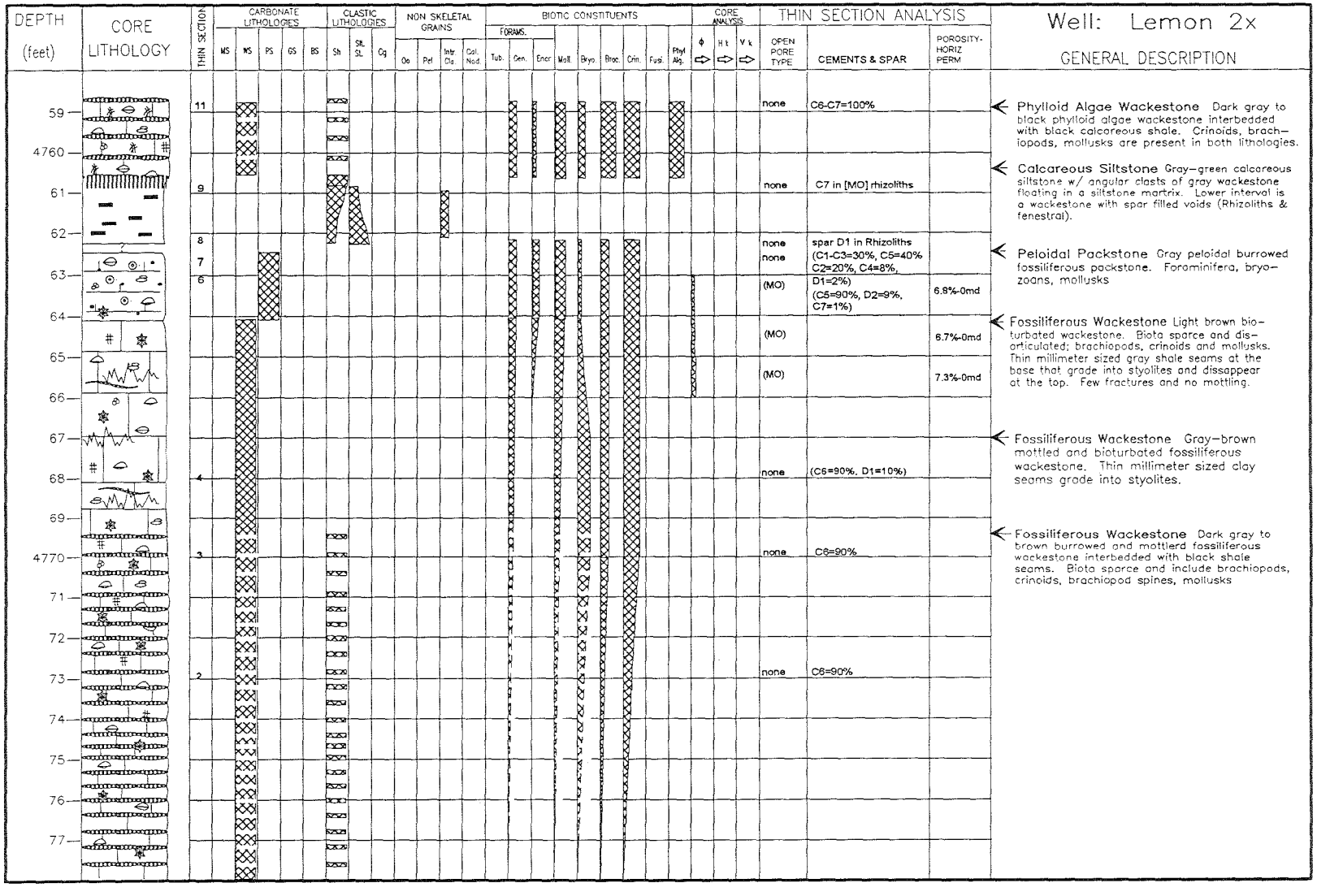


Well: Lemon 2x

GENERAL DESCRIPTION

**Phylloid Algae Wackestone** Dark gray to black phylloid algae wackestone interbedded with black calcareous shale. Crinoids, brachiopods, mollusks are present in both lithologies.

**Calcareous Siltstone** Gray-green calcareous siltstone w/ angular clasts of gray wackestone floating in a siltstone martrix. Lower interval is a wackestone with spar filled voids (Rhizoliths & fenestral).

**Peloidal Packstone** Gray peloidal burrowed fossiliferous packstone. Foraminifera, bryozoans, mollusks

**Fossiliferous Wackestone** Light brown bioturbated wackestone. Biota sparce and disarticulated; brachiopods, crinoids and mollusks. Thin millimeter sized gray shale seams at the base that grade into styolites and dissappear at the top. Few fractures and no mottling.

**Fossiliferous Wackestone** Gray-brown mottled and bioturbated fossiliferous wackestone. Thin millimeter sized clay seams grade into styolites.

**Fossiliferous Wackestone** Dark gray to brown burrowed and mottlerd fossiliferous wackestone interbedded with black shale seams. Biota sparce and include brachiopods, crinoids, brachiopod spines, mollusks

Well Name: LEMON 2X

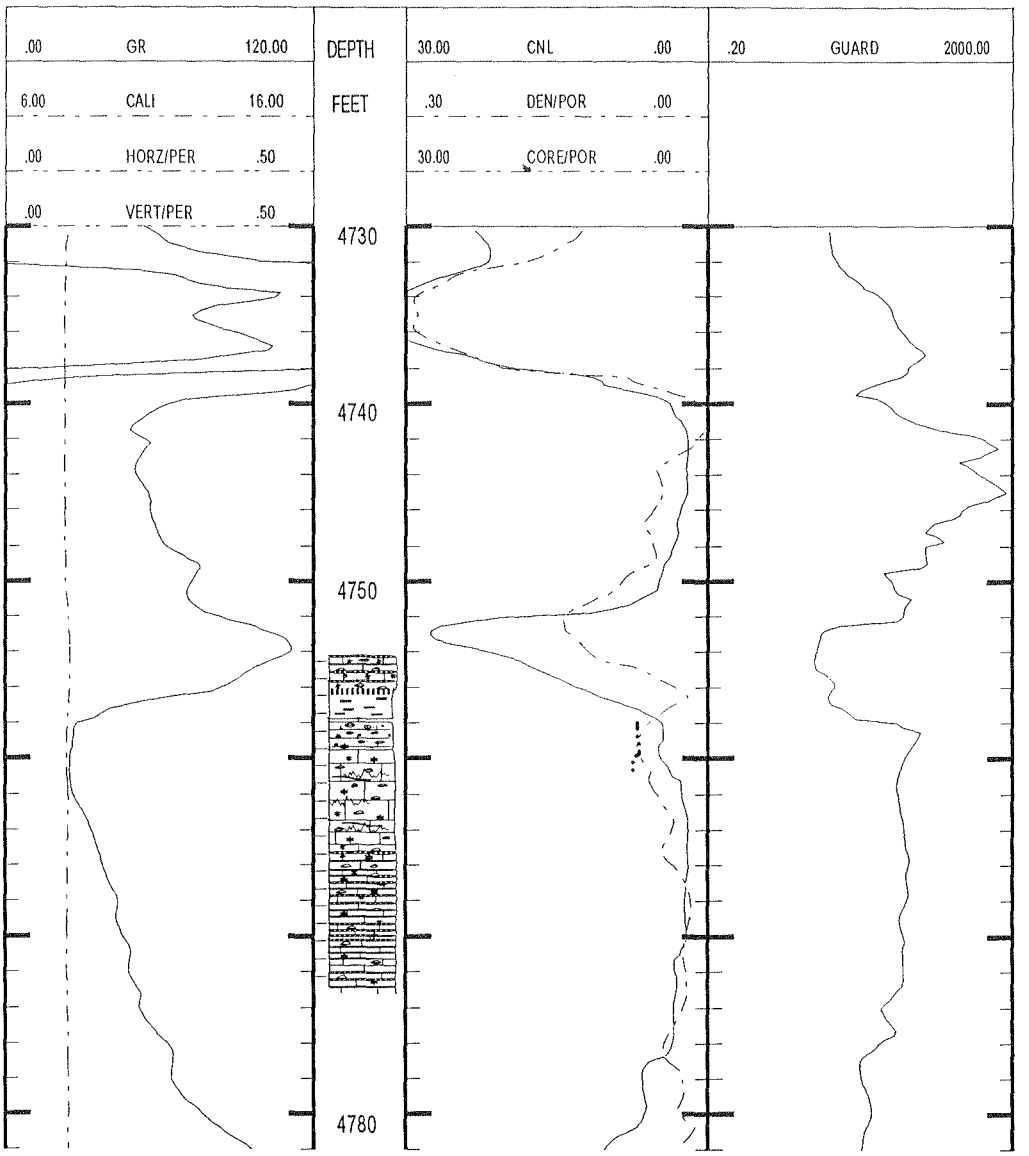


Lemon 2x: Initial Production 48 BOPD, 48 MCFGPD (5/1/79) from Perfs: 4755 to 4760'

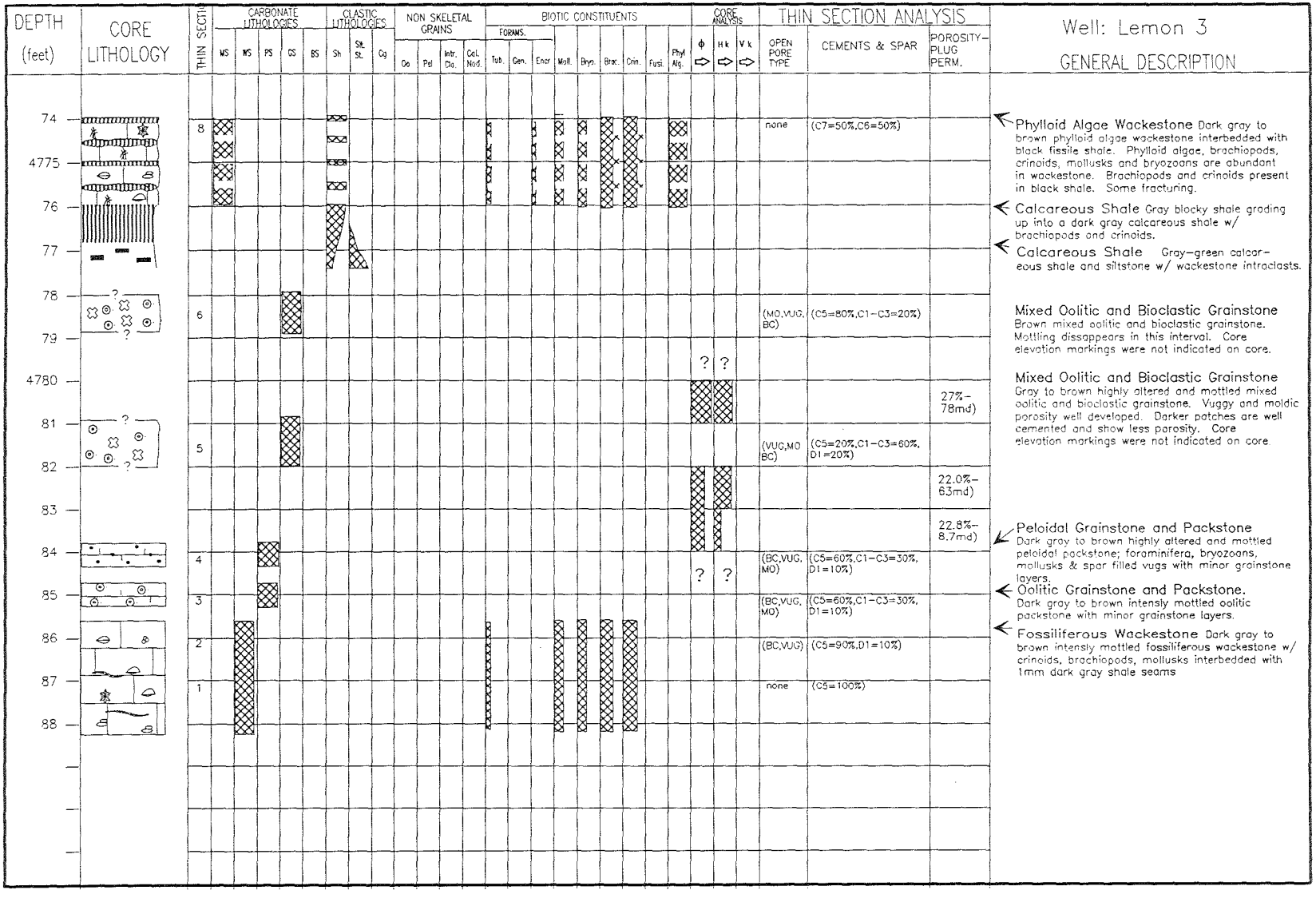


Well: Lemon 3

GENERAL DESCRIPTION

**Phylloid Algae Wackestone** Dark gray to brown phylloid algae wackestone interbedded with black fissile shale. Phylloid algae, brachiopods, crinoids, mollusks and bryozoans are abundant in wackestone. Brachiopods and crinoids present in black shale. Some fracturing.

**Calcareous Shale** Gray blocky shale grading up into a dark gray calcareous shale w/ brachiopods and crinoids.

**Calcareous Shale** Gray-green calcareous shale and siltstone w/ wackestone intraclasts.

**Mixed Oolitic and Bioclastic Grainstone** Brown mixed oolitic and bioclastic grainstone. Mottling dissappears in this interval. Core elevation markings were not indicated on core.

**Mixed Oolitic and Bioclastic Grainstone** Gray to brown highly altered and mottled mixed oolitic and bioclastic grainstone. Vuggy and moldic porosity well developed. Darker patches are well cemented and show less porosity. Core elevation markings were not indicated on core.

**Peloidal Grainstone and Packstone** Dark gray to brown highly altered and mottled peloidal packstone; foraminifera, bryozoans, mollusks & spar filled vugs with minor grainstone layers.

**Oolitic Grainstone and Packstone.** Dark gray to brown intensly mottled oolitic packstone with minor grainstone layers.

**Fossiliferous Wackestone** Dark gray to brown intensly mottled fossiliferous wackestone w/ crinoids, brachiopods, mollusks interbedded with 1mm dark gray shale seams

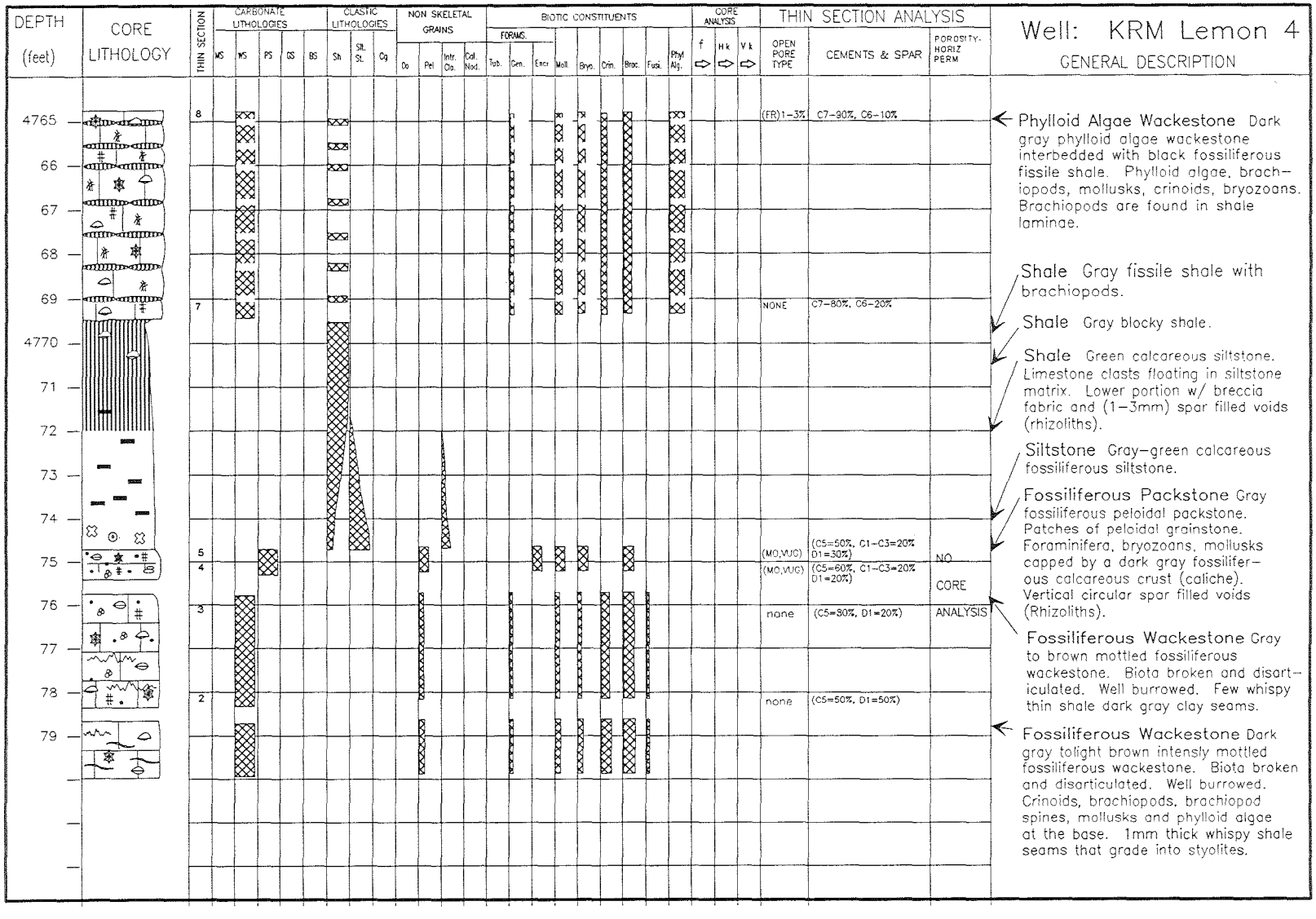


Well: KRM Lemon 4

GENERAL DESCRIPTION

**Phylloid Algae Wackestone** Dark gray phylloid algae wackestone interbedded with black fossiliferous fissile shale. Phylloid algae, brachiopods, mollusks, crinoids, bryozoans. Brachiopods are found in shale laminae.

**Shale** Gray fissile shale with brachiopods.

**Shale** Gray blocky shale.

**Shale** Green calcareous siltstone. Limestone clasts floating in siltstone matrix. Lower portion w/ breccia fabric and (1-3mm) spar filled voids (rhizoliths).

**Siltstone** Gray-green calcareous fossiliferous siltstone.

**Fossiliferous Packstone** Gray fossiliferous peloidal packstone. Patches of peloidal grainstone. Foraminifera, bryozoans, mollusks capped by a dark gray fossiliferous calcareous crust (caliche). Vertical circular spar filled voids (Rhizoliths).

**Fossiliferous Wackestone** Gray to brown mottled fossiliferous wackestone. Biota broken and disarticulated. Well burrowed. Few whispy thin shale dark gray clay seams.

**Fossiliferous Wackestone** Dark gray to light brown intensly mottled fossiliferous wackestone. Biota broken and disarticulated. Well burrowed. Crinoids, brachiopods, brachiopod spines, mollusks and phylloid algae at the base. 1mm thick whispy shale seams that grade into styolites.

Well Name: LEMON 4

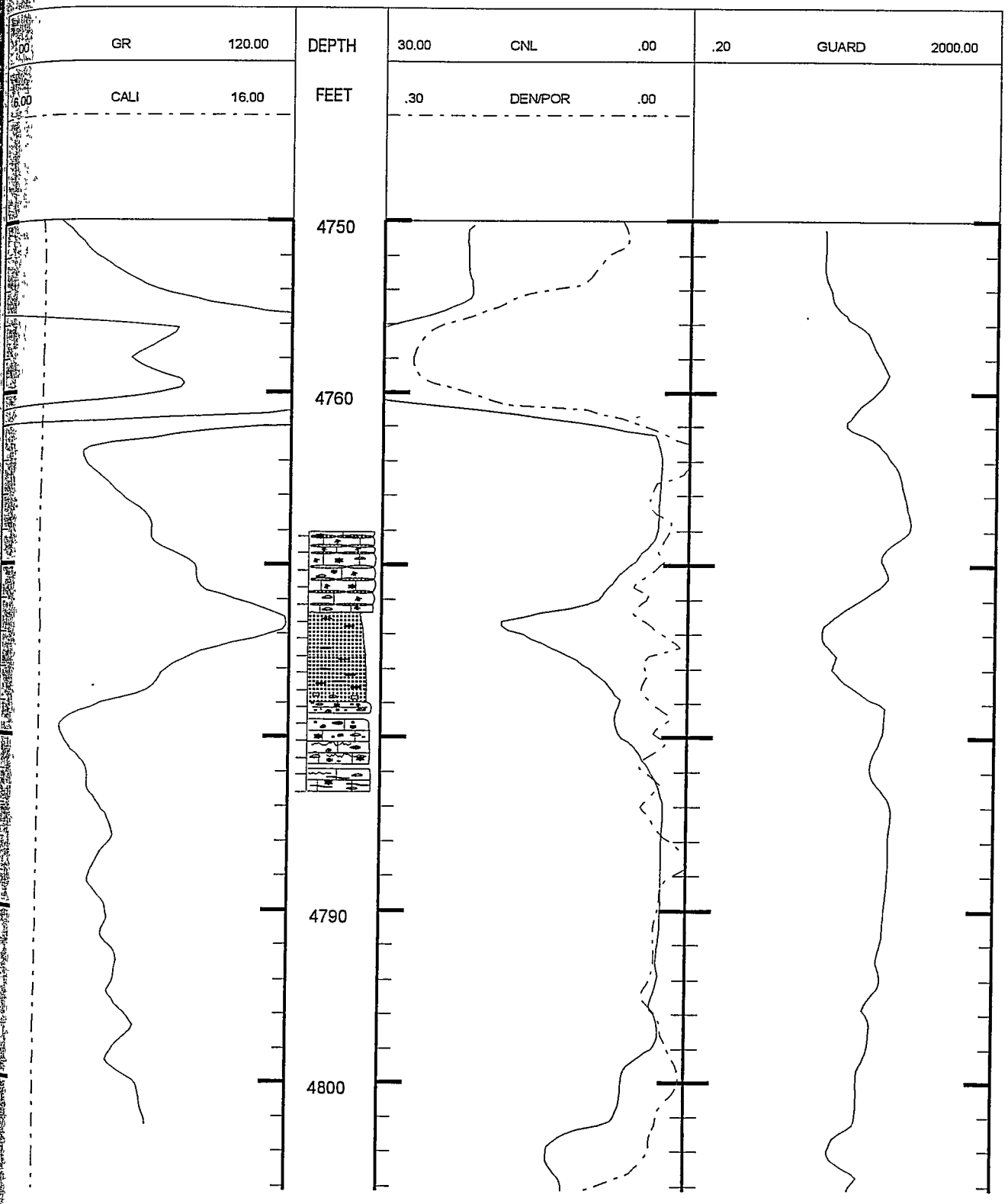


Lemon 4: Initial Production D&A (4/20/79)

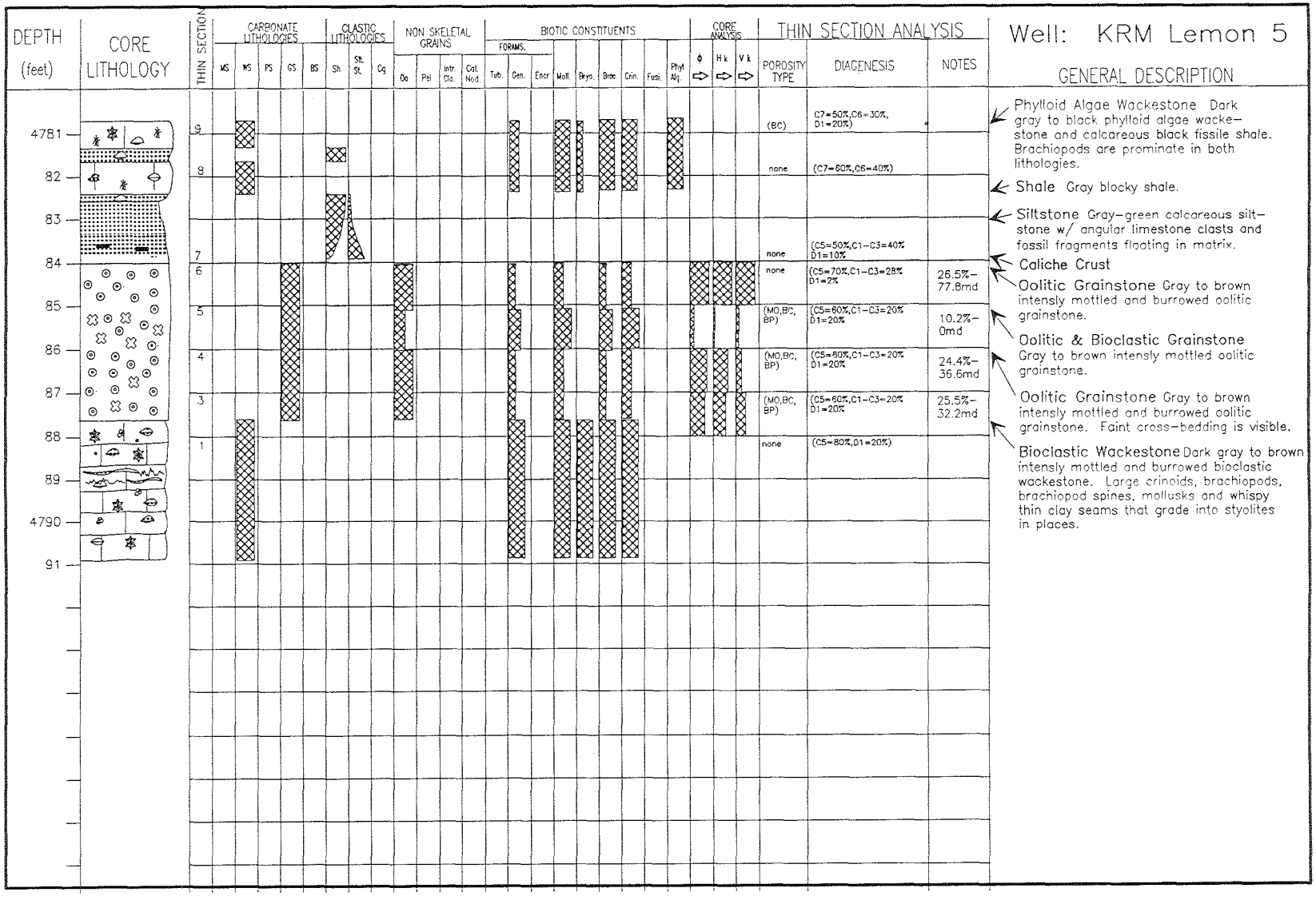
DEPTH (feet)
CORE LITHOLOGY
THIN SECTION
CARBONATE LITHOLOGIES
MS
WS
PS
GS
BS
CLASTIC LITHOLOGIES
Sh
Slt. St.
Cg
NON SKELETAL GRAINS
Oo
Pel
Intr. Cla.
Coal Nod.
BIOTIC CONSTITUENTS
FORAMS.
Tub.
Cen.
Encr
Moll.
Bryo.
Broc.
Crin.
Fusi.
Phyl Alg.
CORE ANALYSIS
ϕ
H k
V k
THIN SECTION ANALYSIS
POROSITY TYPE
DIAGENESIS
NOTES
Well: KRM Lemon 5
GENERAL DESCRIPTION
4781
82
83
84
85
86
87
88
89
4790
91
9
8
7
6
5
4
3
1
(BC)
none
none
none
(MO,BC, BP)
(MO,BC, BP)
(MO,BC, BP)
none
(C7=50%,C6=30%, D1=20%)
(C7=80%,C6=40%)
(C5=50%,C1-C3=40% D1=10%
(C5=70%,C1-C3=28% D1=2%
26.5%-77.8md
(C5=60%,C1-C3=20% D1=20%
10.2%-0md
(C5=60%,C1-C3=20% D1=20%
24.4%-36.6md
(C5=60%,C1-C3=20% D1=20%
25.5%-32.2md
(C5=80%,D1=20%)
Phylloid Algae Wackestone Dark gray to black phylloid algae wacke-stone and calcareous black fissile shale. Brachiopods are prominate in both lithologies.
Shale Gray blocky shale.
Siltstone Gray-green calcareous silt-stone w/ angular limestone clasts and fossil fragments floating in matrix.
Caliche Crust
Oolitic Grainstone Gray to brown intensly mottled and burrowed oolitic grainstone.
Oolitic & Bioclastic Grainstone Gray to brown intensly mottled oolitic grainstone.
Oolitic Grainstone Gray to brown intensly mottled and burrowed oolitic grainstone. Faint cross-bedding is visible.
Bioclastic Wackestone Dark gray to brown intensly mottled and burrowed bioclastic wackestone. Large crinoids, brachiopods, brachiopod spines, mollusks and whispy thin clay seams that grade into styolites in places.

Well Name: LEMON 5

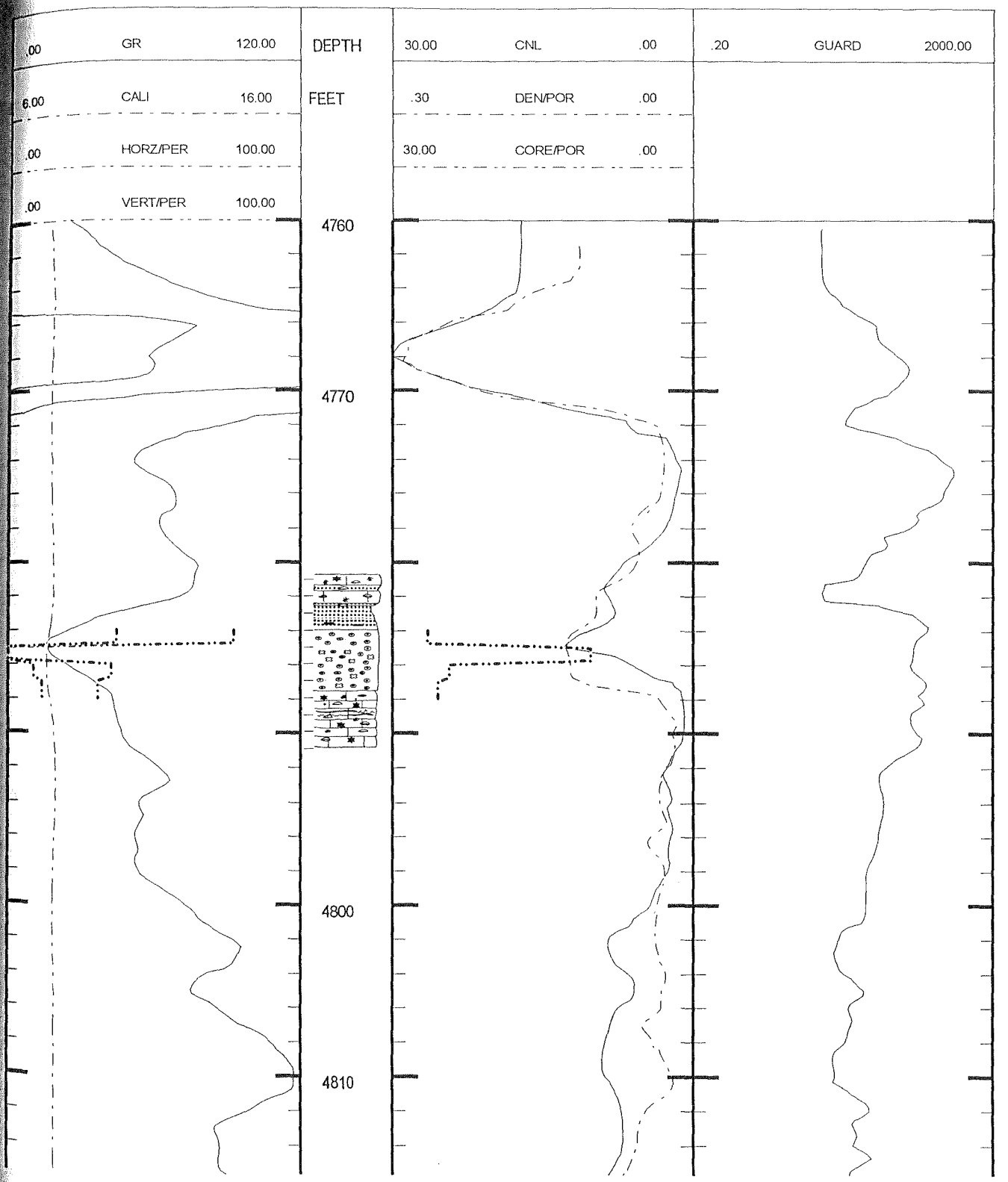


Lemon 5: Initial Production 240 BOPD, 120 MCFGPD (5/5/79) from Perfs: 4782-4787'

# LEMON 5

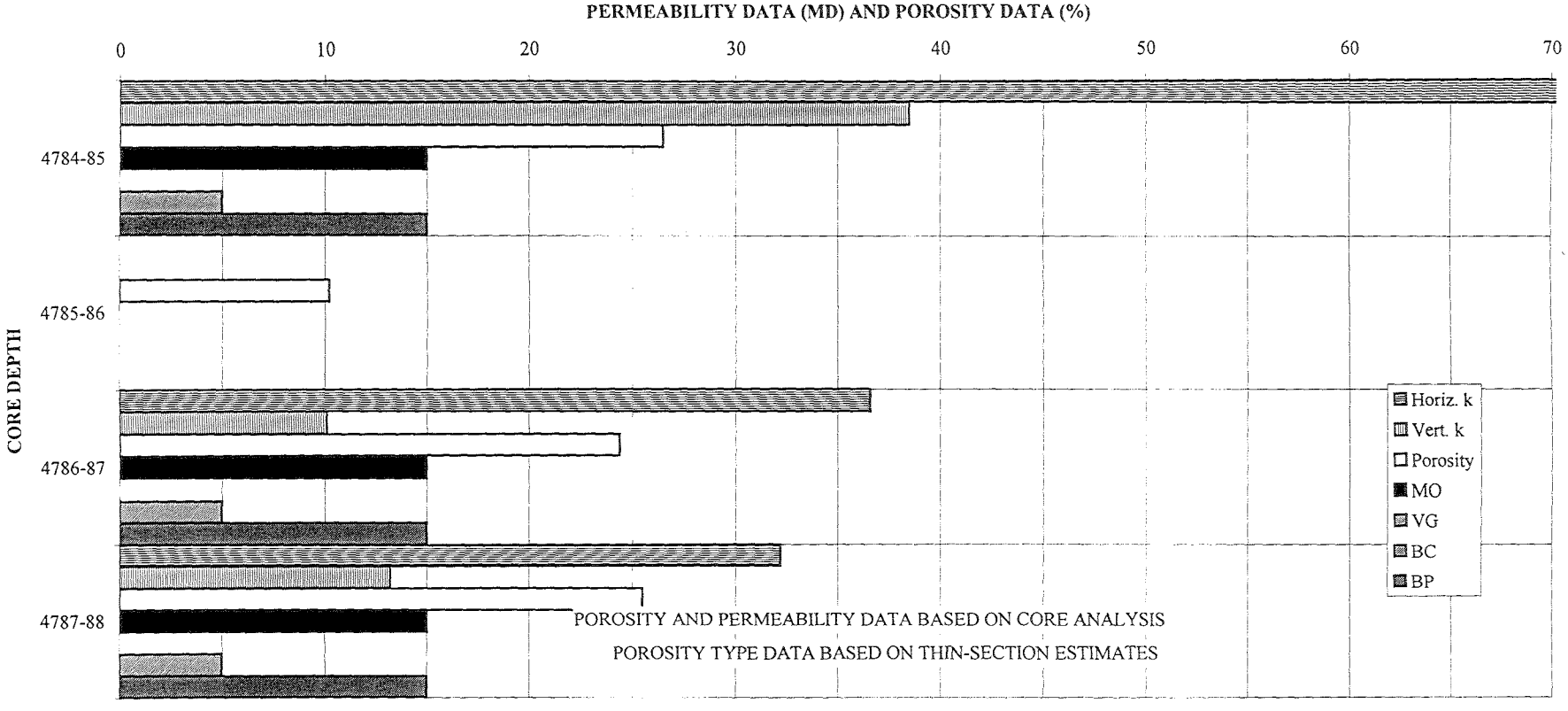
PERMEABILITY DATA (MD) AND POROSITY DATA (%)
0
10
20
30
40
50
60
70
CORE DEPTH
4784-85
4785-86
4786-87
4787-88
Horiz. k
Vert. k
Porosity
MO
VG
BC
BP
POROSITY AND PERMEABILITY DATA BASED ON CORE ANALYSIS
POROSITY TYPE DATA BASED ON THIN-SECTION ESTIMATES

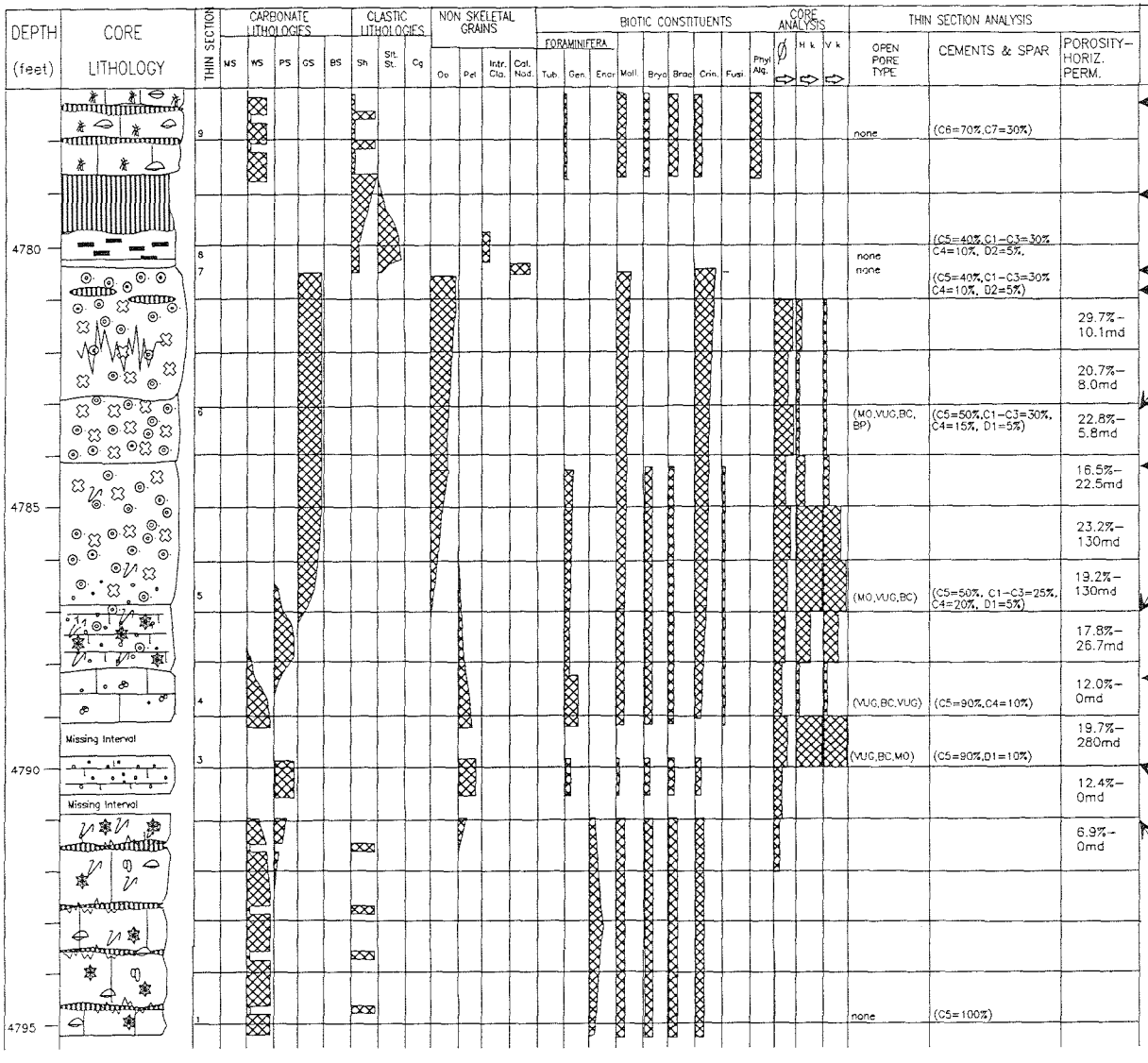


# Well: KRM Lemon 6

## GENERAL DESCRIPTION

**Phylloid Algae Wackestone** Dark grey to brown phylloid algae wackestone interbedded with black fissile calcareous shale. Phylloid algae, brachiopods, mollusks, crinoids, and bryozoans are abundant in the wackestone. Crinoids and brachiopods are present in the black fissile shale.

**Calcareous Shale** Grey-green calcareous shale and siltstone. Angular intraclasts of lime mudstone (w/ spar filled root molds) floating in a calcareous siltstone matrix. Calcareous siltstone grades up into calcareous shale.

**Caliche Crust**

**Oolitic Grainstone** Dark grey to brown oolitic grainstone. Ooids uniform in size (1/2 to 3/4 mm) with faint crossbedding of thin layers of crinoidal and molluskan grainstones. Vertical and horizontal fractures, styolites, and mottling.

**Mixed Oolitic-Bioclastic Grainstone** Brown layered oolitic and bioclastic grainstone. Strong cross-bedding expressed between the layered oolites and bioclasts. Oolites and bioclasts much larger than overlying oolitic grainstone. Mottling is related to cross-bedding. Oolite bioclasic ratio approximately 50 : 50.

**Bioclastic Grainstone** Dark grey to brown extremely mottled bioclastic grainstone with minor oolitic grainstone layers. Mottling is linear and follows well developed crossbedding. Large cm. sized vugs are filled with a coarse spar. Bioclasts oriented parallel to crossbedding. Bioclasts much larger than the overlying oolitic and mixed oolitic grainstones.

**Fossiliferous Packstone** Dark grey to brown extremely mottled fossiliferous packstone. Mottling is intense including cm. sized vugs filled with a coarse spar. Crossbedding dissappears and mottling appears to be related to burrowing. Packstone fabric is observed in t the dark grey mottles and packstone-wackstone fabric is expressed in the lighter colored burrowd areas.

**Fossiliferous Wackestone** Dark grey to brown intensly mottled foraminiferal wackestone. Mottling is intense including mm-cm sized vugs filled with coarse spar. Mottling appears to be related to borrowing. Dark grey areas are un-altered foraminiferal wackestone. Brown areas contain broken and altered bioclasts in a wackstone matrix. Vugs cut both fabrics.

**Peloidal Packstone** Dark grey to brown intensly mottled peloidal packstone. Mottling is intense including cm size vugs filled with coarse spar. Original packstone fabric appears to be burrowed to produce the randomally oriented wackestone (vs) grain supported packstone fabric.

**Fossiliferous Wackestone** Dark grey to brown mottled crinoidal, brachiopod wackestone. Mottling increases in intensity upward in the unit while thin mm-cm shale seams increase toward the base. Contact between mottling is gradational with large unaltered crinoids and brachiopods in the darker colored matrix. Smaller broken and abraded bioclasts are present in the lighter colored mottling. Mottling appears to be related to burrowing.

# Well Name: LEMON 6

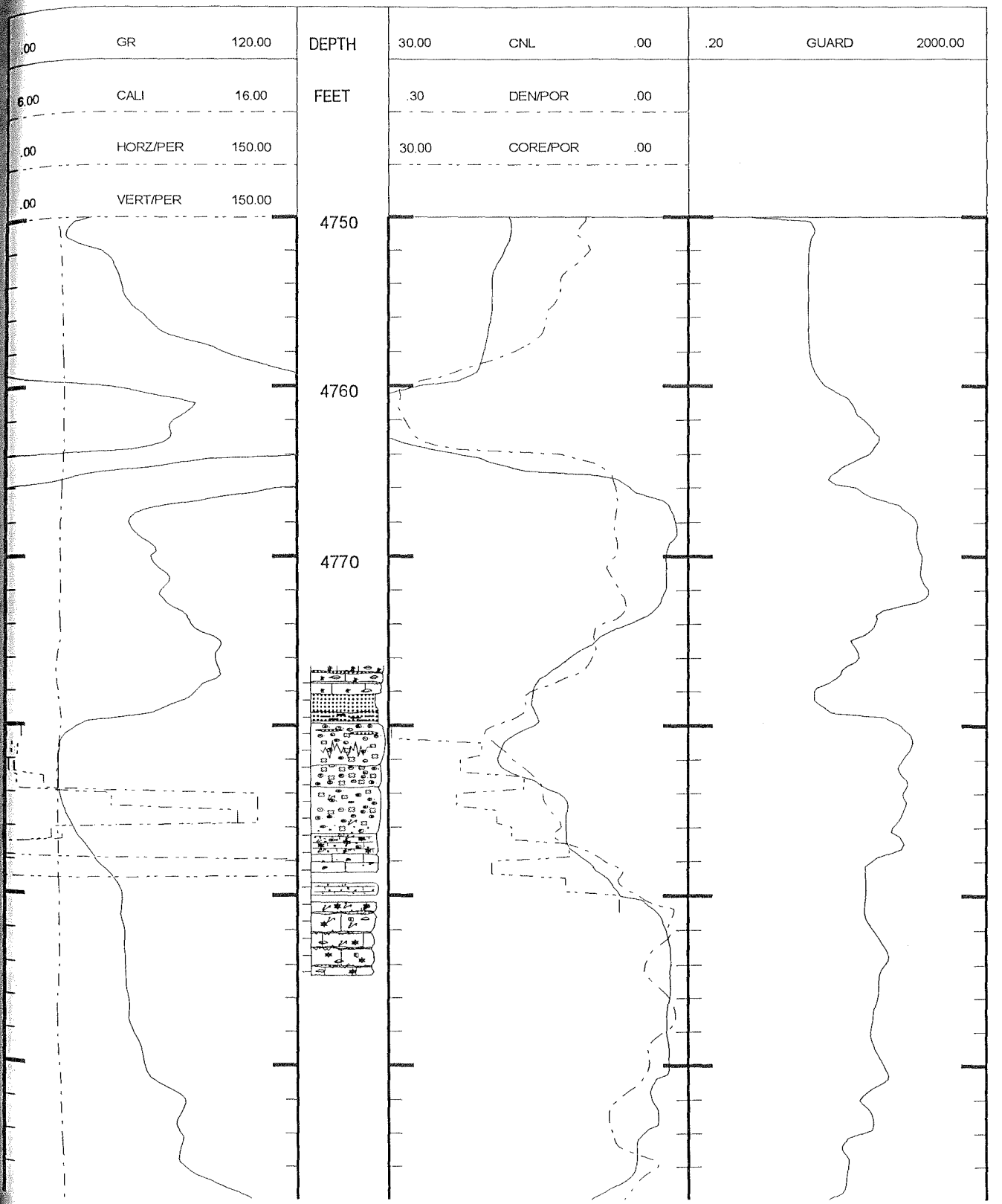


Lemon 6: Initial Production 264 BOPD, 132 MCFGPD (5/17/79) from Perfs: 4778-4788'

# LEMON 6

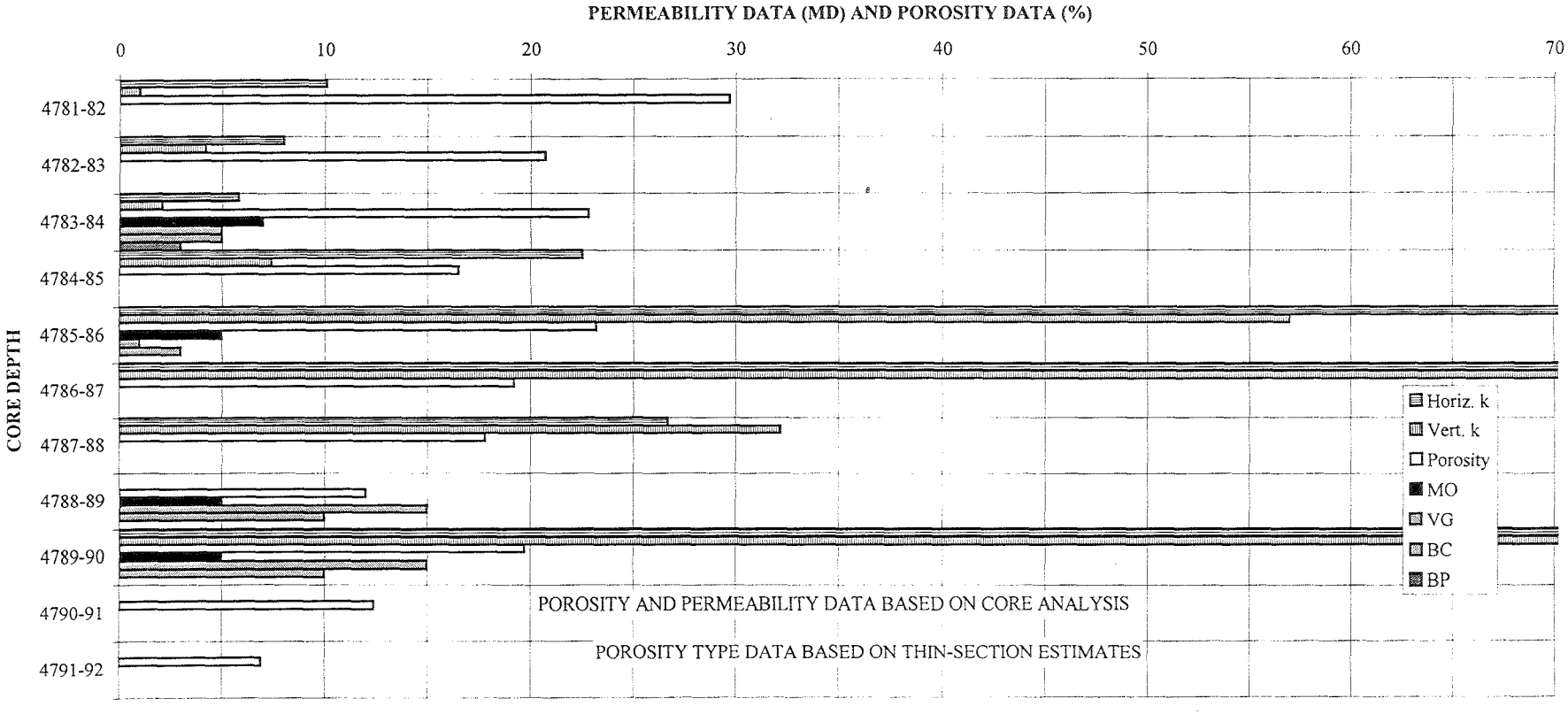
PERMEABILITY DATA (MD) AND POROSITY DATA (%)
0
10
20
30
40
50
60
70
CORE DEPTH
4781-82
4782-83
4783-84
4784-85
4785-86
4786-87
4787-88
4788-89
4789-90
4790-91
4791-92
Horiz. k
Vert. k
Porosity
MO
VG
BC
BP
POROSITY AND PERMEABILITY DATA BASED ON CORE ANALYSIS
POROSITY TYPE DATA BASED ON THIN-SECTION ESTIMATES

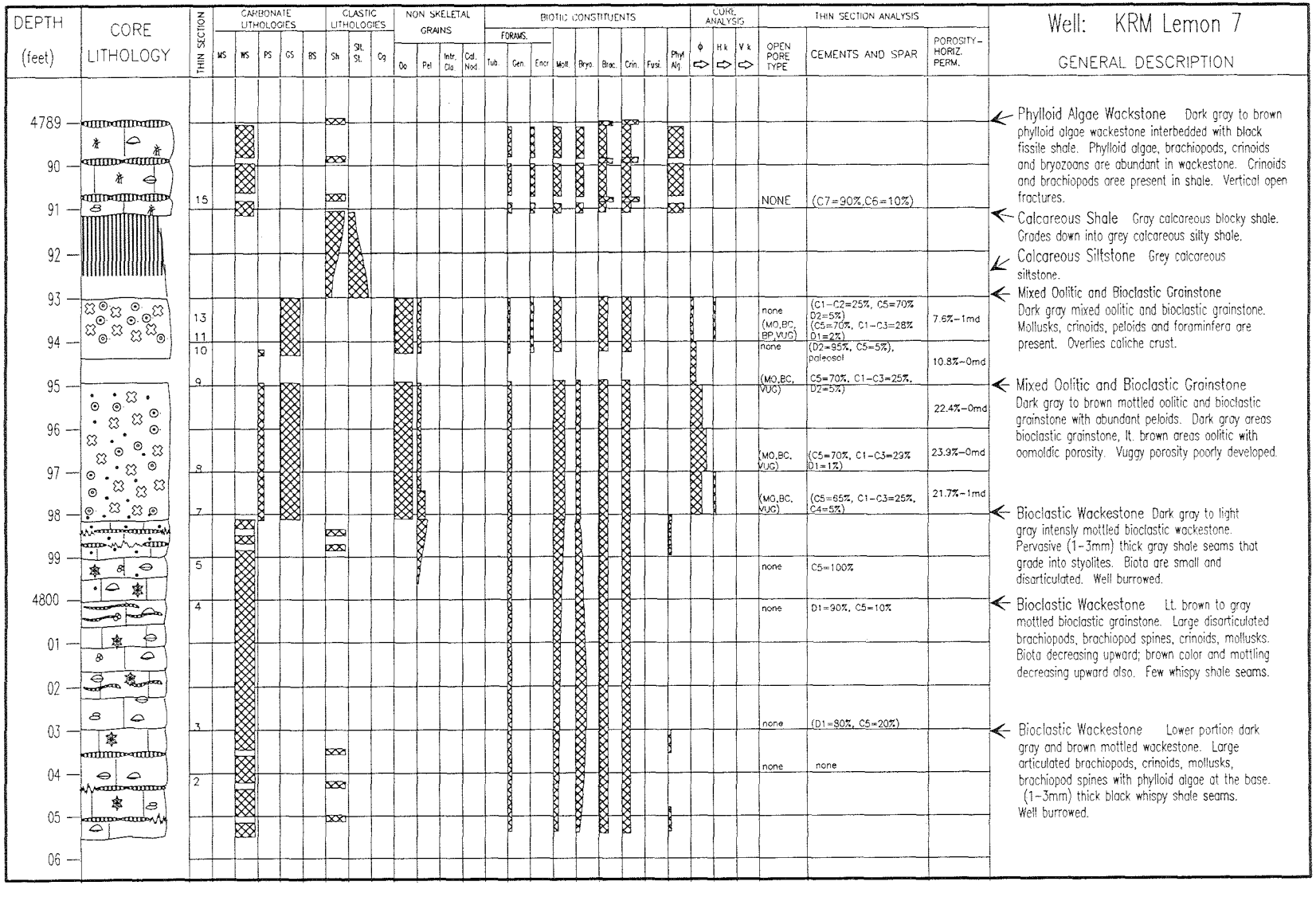


Well: KRM Lemon 7

GENERAL DESCRIPTION

**Phylloid Algae Wackstone** Dark gray to brown phylloid algae wackestone interbedded with black fissile shale. Phylloid algae, brachiopods, crinoids and bryozoans are abundant in wackestone. Crinoids and brachiopods aree present in shale. Vertical open fractures.

**Calcareous Shale** Gray calcareous blocky shale. Grades down into grey calcareous silty shale.

**Calcareous Siltstone** Grey calcareous siltstone.

**Mixed Oolitic and Bioclastic Grainstone** Dark gray mixed oolitic and bioclastic grainstone. Mollusks, crinoids, peloids and foraminfera are present. Overlies caliche crust.

**Mixed Oolitic and Bioclastic Grainstone** Dark gray to brown mottled oolitic and bioclastic grainstone with abundant peloids. Dark gray areas bioclastic grainstone, lt. brown areas oolitic with oomoldic porosity. Vuggy porosity poorly developed.

**Bioclastic Wackestone** Dark gray to light gray intensly mottled bioclastic wackestone. Pervasive (1-3mm) thick gray shale seams that grade into stylolites. Biota are small and disarticulated. Well burrowed.

**Bioclastic Wackestone** Lt. brown to gray mottled bioclastic grainstone. Large disarticulated brachiopods, brachiopod spines, crinoids, mollusks. Biota decreasing upward; brown color and mottling decreasing upward also. Few whispy shale seams.

**Bioclastic Wackestone** Lower portion dark gray and brown mottled wackestone. Large articulated brachiopods, crinoids, mollusks, brachiopod spines with phylloid algae at the base. (1-3mm) thick black whispy shale seams. Well burrowed.

Well Name: LEMON 7

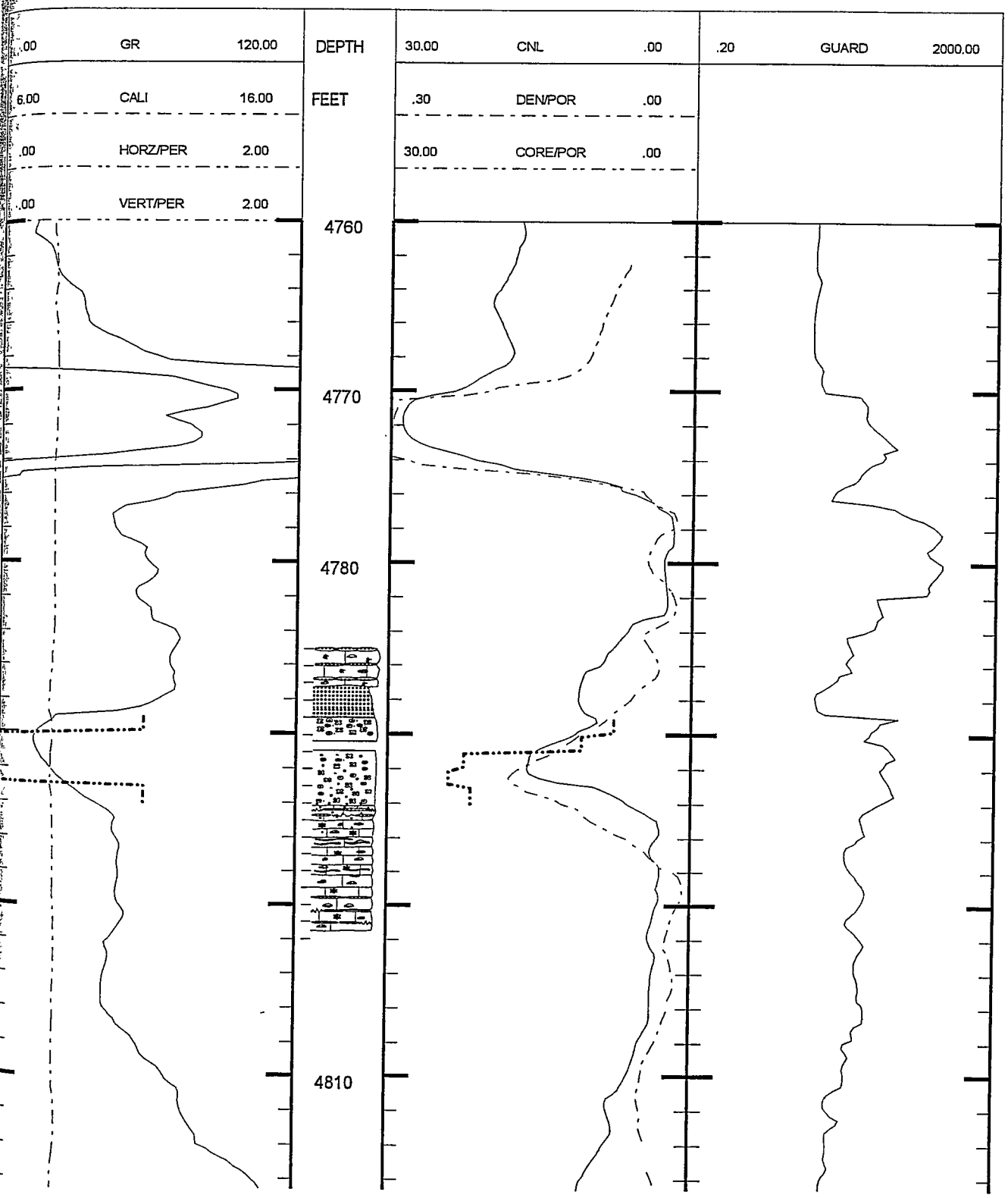


Lemon 7: Initial Production 84 BOPD (7/16/79) from Perfs: 4788-4794'

# LEMON 7

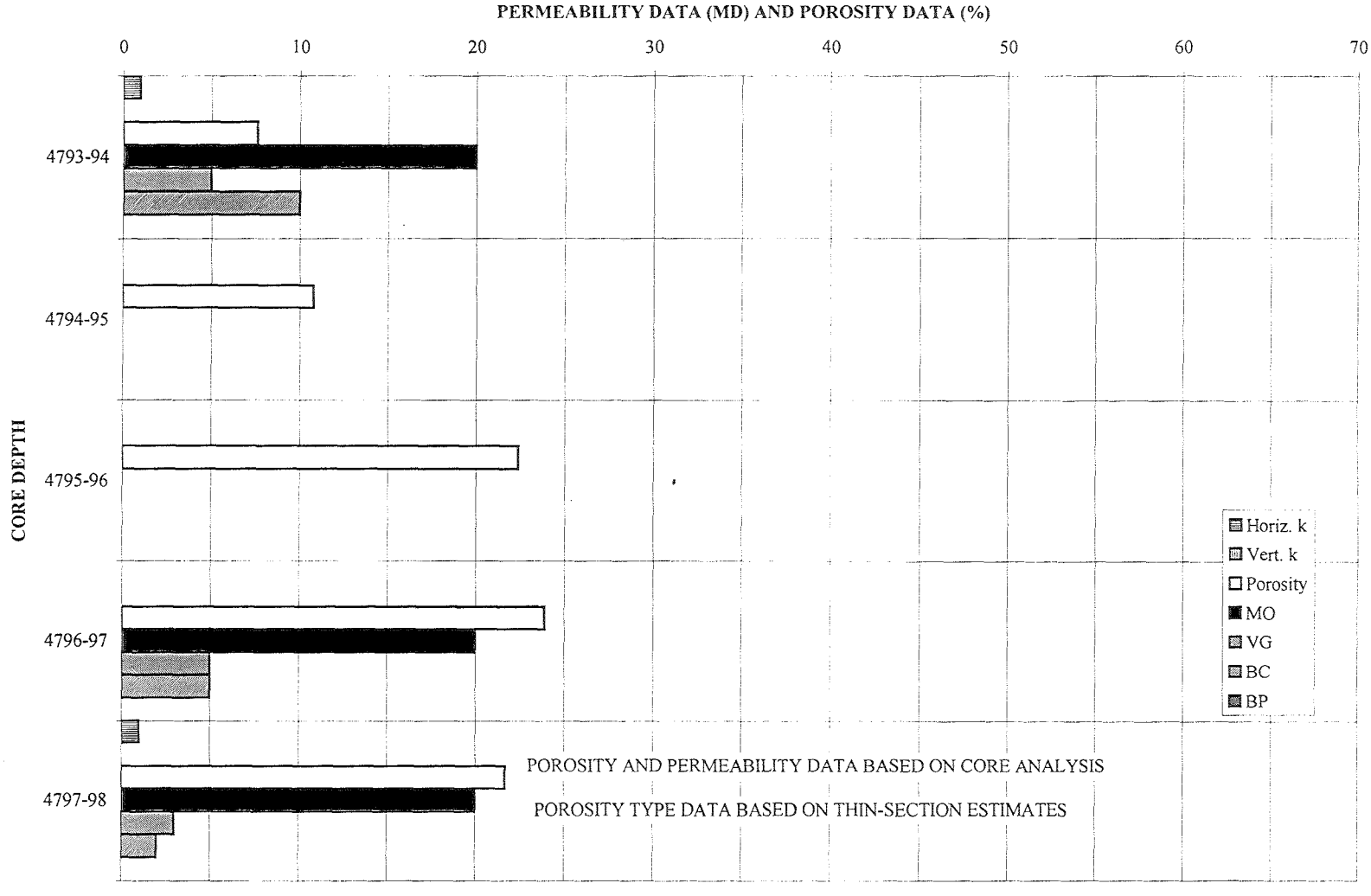
PERMEABILITY DATA (MD) AND POROSITY DATA (%)
0
10
20
30
40
50
60
70
CORE DEPTH
4793-94
4794-95
4795-96
4796-97
4797-98
Horiz. k
Vert. k
Porosity
MO
VG
BC
BP
POROSITY AND PERMEABILITY DATA BASED ON CORE ANALYSIS
POROSITY TYPE DATA BASED ON THIN-SECTION ESTIMATES

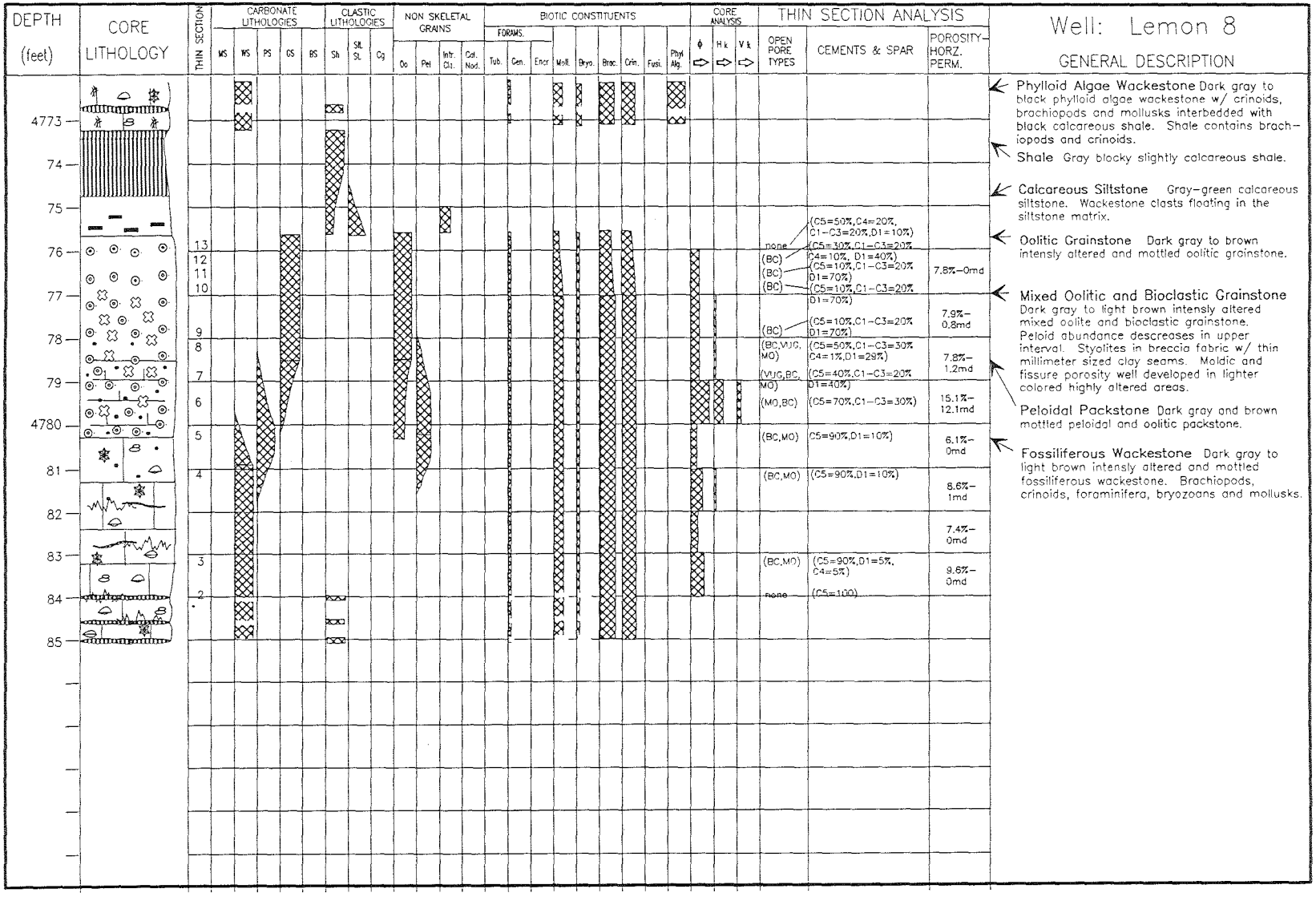
DEPTH (feet)
CORE LITHOLOGY
THIN SECTION
CARBONATE LITHOLOGIES
MS WS PS GS BS
CLASTIC LITHOLOGIES
Sh Slt Sl Cg
NON SKELETAL GRAINS
Oo Pel Intr. Clo. Cal. Nod.
BIOTIC CONSTITUENTS
FORAMS.
Tub. Cen. Encr Moll. Bryo. Brac. Crin. Fusi. Phyl Alg.
CORE ANALYSIS
ϕ H k V k
THIN SECTION ANALYSIS
OPEN PORE TYPES
CEMENTS & SPAR
POROSITY-HORZ. PERM.
4773
74
75
76
77
78
79
4780
81
82
83
84
85
13
12
11
10
9
8
7
6
5
4
3
2
none
(BC)
(BC)
(BC)
(BC)
(BC,MO)
(VUG,BC, MO)
(MO,BC)
(BC,MO)
(BC,MO)
none
(C5=50%,C4=20%, C1-C3=20%,D1=10%)
(C5=30%,C1-C3=20%
C4=10%, D1=40%)
(C5=10%,C1-C3=20% D1=70%)
(C5=10%,C1-C3=20% D1=70%)
(C5=10%,C1-C3=20% D1=70%)
(C5=50%,C1-C3=30% C4=1%,D1=29%)
(C5=40%,C1-C3=20% D1=40%)
(C5=70%,C1-C3=30%)
C5=90%,D1=10%)
(C5=90%,D1=10%)
(C5=90%,D1=5%, C4=5%)
(C5=100)
7.8%-0md
7.9%-0.8md
7.8%-1.2md
15.1%-12.1md
6.1%-0md
8.6%-1md
7.4%-0md
9.6%-0md
Well: Lemon 8
GENERAL DESCRIPTION
Phylloid Algae Wackestone Dark gray to black phylloid algae wackestone w/ crinoids, brachiopods and mollusks interbedded with black calcareous shale. Shale contains brachiopods and crinoids.
Shale Gray blocky slightly calcareous shale.
Calcareous Siltstone Gray-green calcareous siltstone. Wackestone clasts floating in the siltstone matrix.
Oolitic Grainstone Dark gray to brown intensly altered and mottled oolitic grainstone.
Mixed Oolitic and Bioclastic Grainstone Dark gray to light brown intensly altered mixed oolite and bioclastic grainstone. Peloid abundance descreases in upper interval. Styolites in breccia fabric w/ thin millimeter sized clay seams. Moldic and fissure porosity well developed in lighter colored highly altered areas.
Peloidal Packstone Dark gray and brown mottled peloidal and oolitic packstone.
Fossiliferous Wackestone Dark gray to light brown intensly altered and mottled fossiliferous wackestone. Brachiopods, crinoids, foraminifera, bryozoans and mollusks.

Well Name: LEMON 8

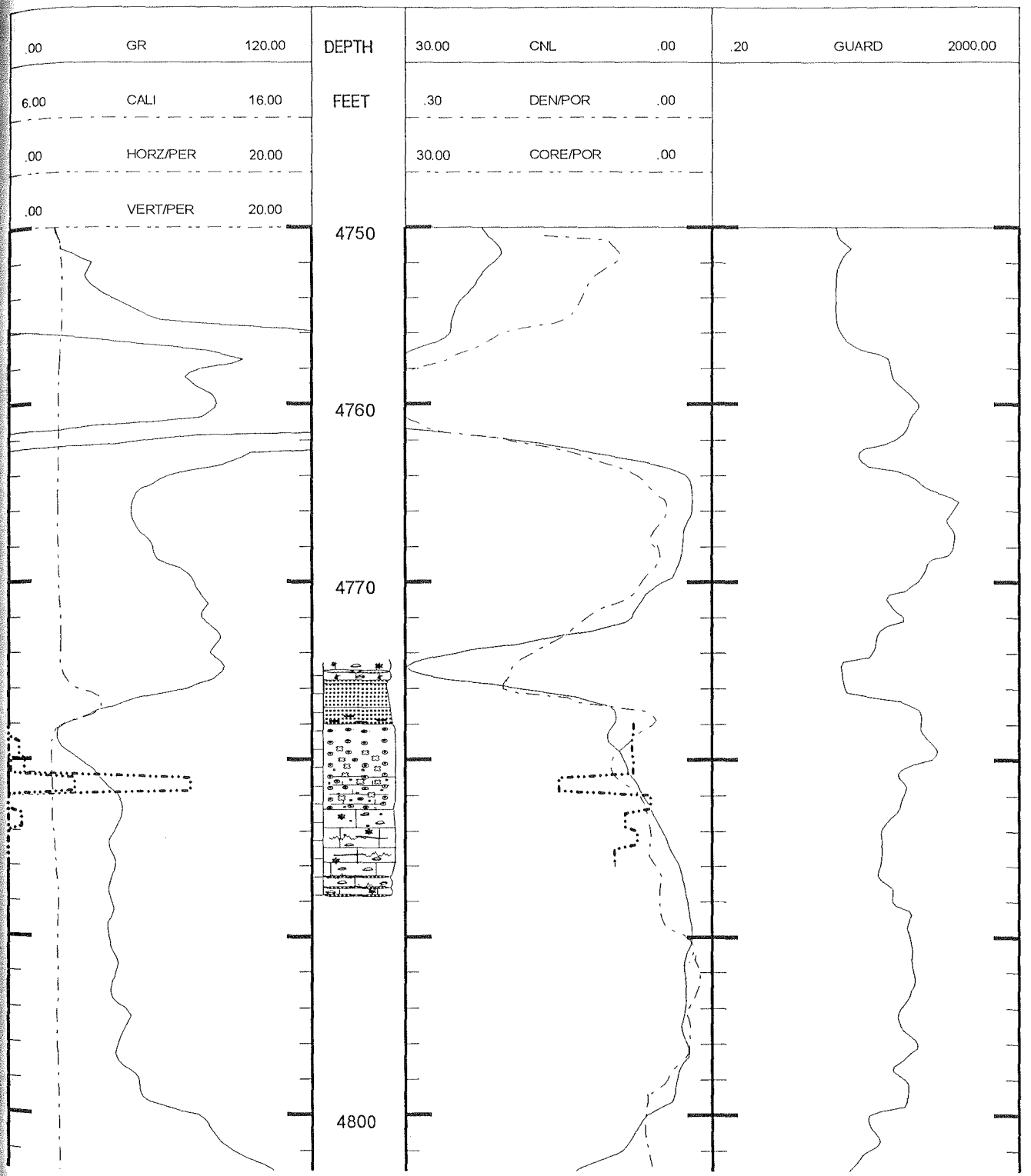


Lemon 8: Initial Production 115 BOPD (7/18/79) from Perfs: 4776-4782'

# LEMON 8

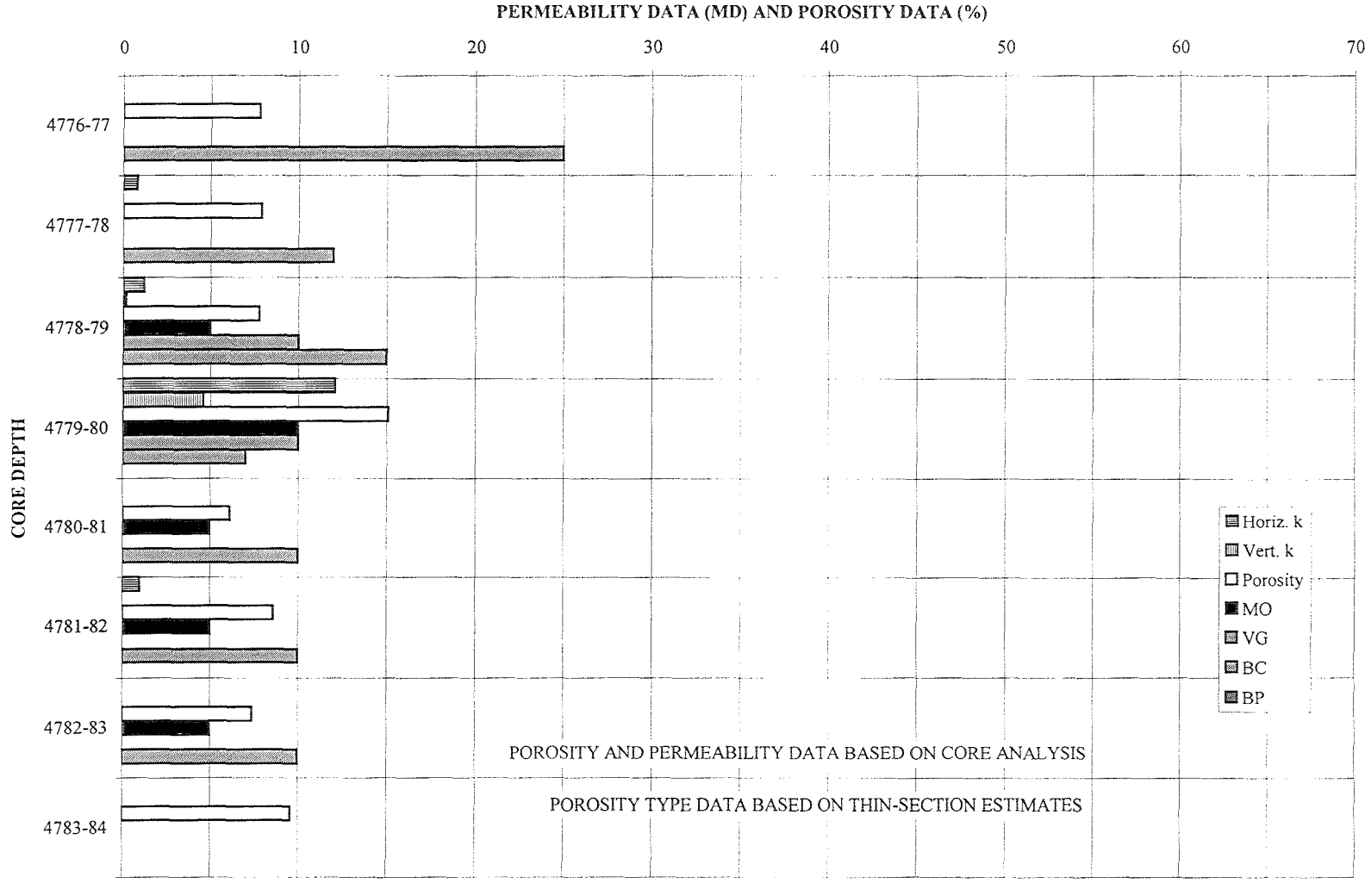
PERMEABILITY DATA (MD) AND POROSITY DATA (%)
0
10
20
30
40
50
60
70
CORE DEPTH
4776-77
4777-78
4778-79
4779-80
4780-81
4781-82
4782-83
4783-84
Horiz. k
Vert. k
Porosity
MO
VG
BC
BP
POROSITY AND PERMEABILITY DATA BASED ON CORE ANALYSIS
POROSITY TYPE DATA BASED ON THIN-SECTION ESTIMATES

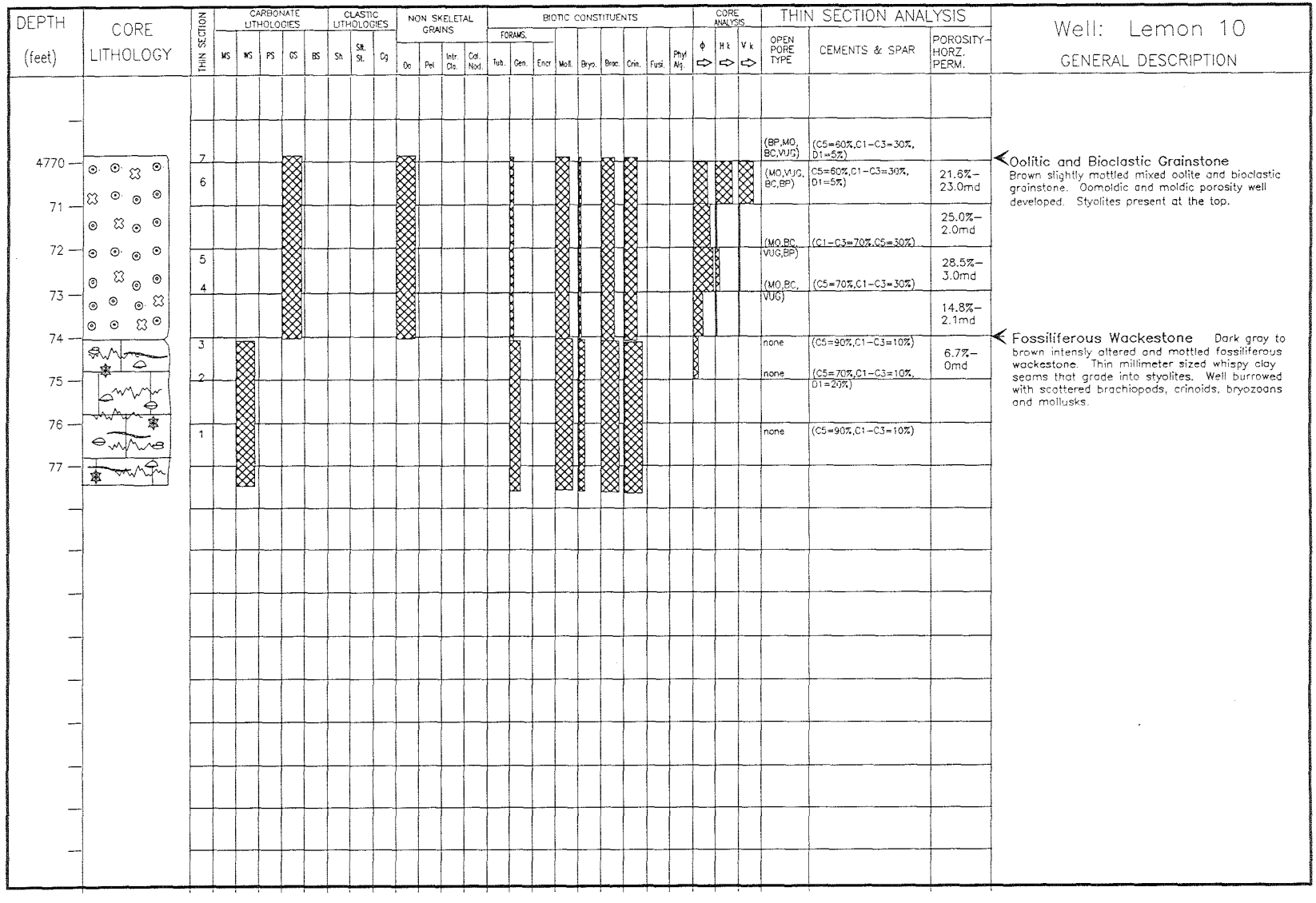
DEPTH (feet)
CORE LITHOLOGY
THIN SECTION
CARBONATE LITHOLOGIES
MS
WS
PS
GS
BS
CLASTIC LITHOLOGIES
Sh
Slt. St.
Cg
NON SKELETAL GRAINS
Oo
Pel
Intr. Clo.
Col. Nod.
BIOTIC CONSTITUENTS
FORAMS.
Tub.
Gen.
Encr
Moll.
Bryo.
Brac.
Crin.
Fusi.
Phyl Alg.
CORE ANALYSIS
φ
H k
V k
THIN SECTION ANALYSIS
OPEN PORE TYPE
CEMENTS & SPAR
POROSITY-HORZ. PERM.
Well: Lemon 10
GENERAL DESCRIPTION
4770
71
72
73
74
75
76
77
7
6
5
4
3
2
1
(BP,MO, BC,VUG)
(C5=60%,C1-C3=30%, D1=5%)
(MO,VUG, BC,BP)
C5=60%,C1-C3=30%, D1=5%)
21.6%-23.0md
(MO,BC, VUG,BP)
(C1-C3=70%,C5=30%)
25.0%-2.0md
28.5%-3.0md
(MO,BC, VUG)
(C5=70%,C1-C3=30%)
14.8%-2.1md
none
(C5=90%,C1-C3=10%)
6.7%-0md
none
(C5=70%,C1-C3=10%, D1=20%)
none
(C5=90%,C1-C3=10%)
Oolitic and Bioclastic Grainstone
Brown slightly mottled mixed oolite and bioclastic grainstone. Oomoldic and moldic porosity well developed. Stylolites present at the top.
Fossiliferous Wackestone
Dark gray to brown intensly altered and mottled fossiliferous wackestone. Thin millimeter sized whispy clay seams that grade into stylolites. Well burrowed with scattered brachiopods, crinoids, bryozoans and mollusks.

Well Name: LEMON 10

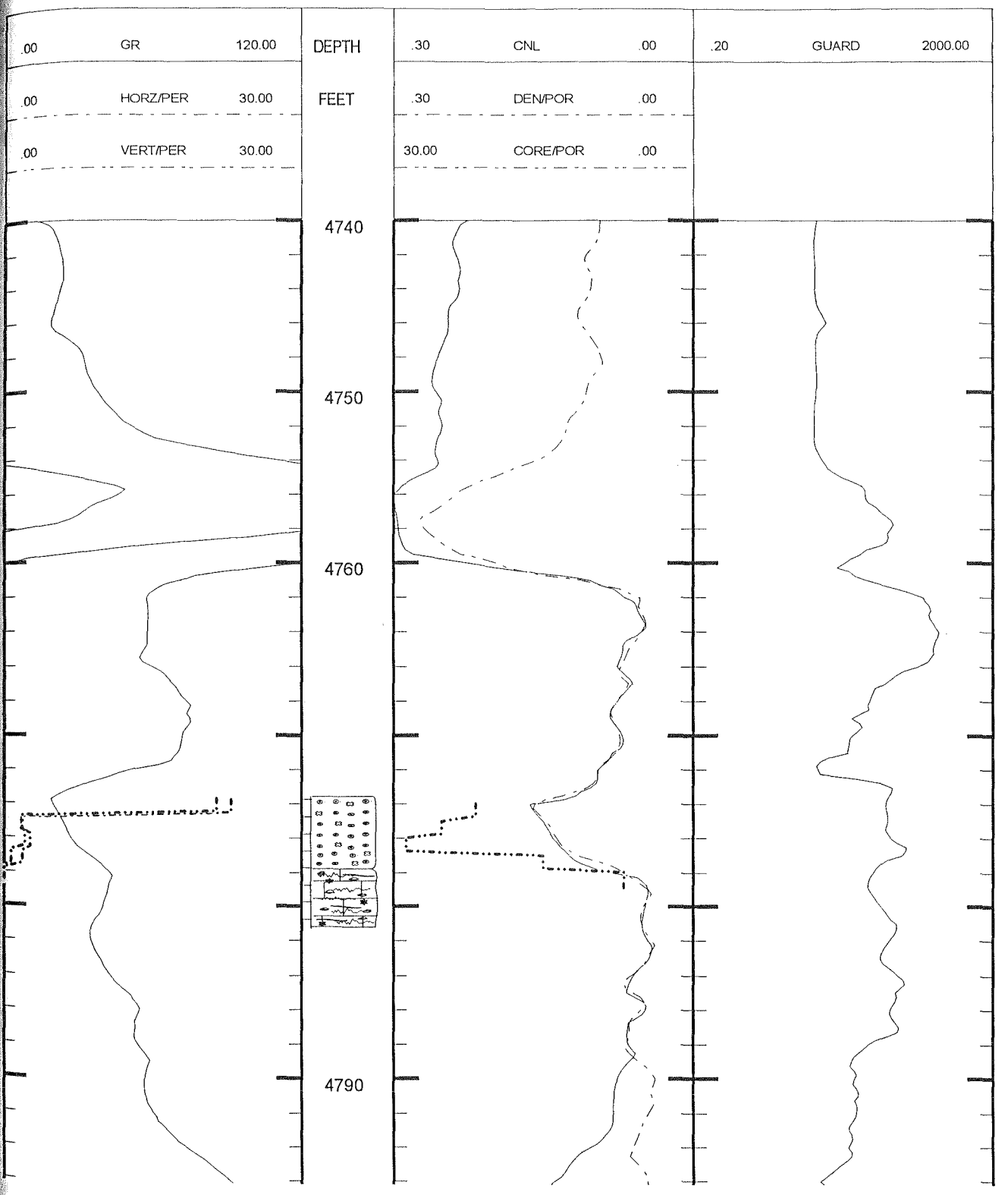


Lemon 10: Initial Production 40 BOPD, 35 MCFGPD (12/7/79) from Perfs: 4773-4778'

# LEMON 10

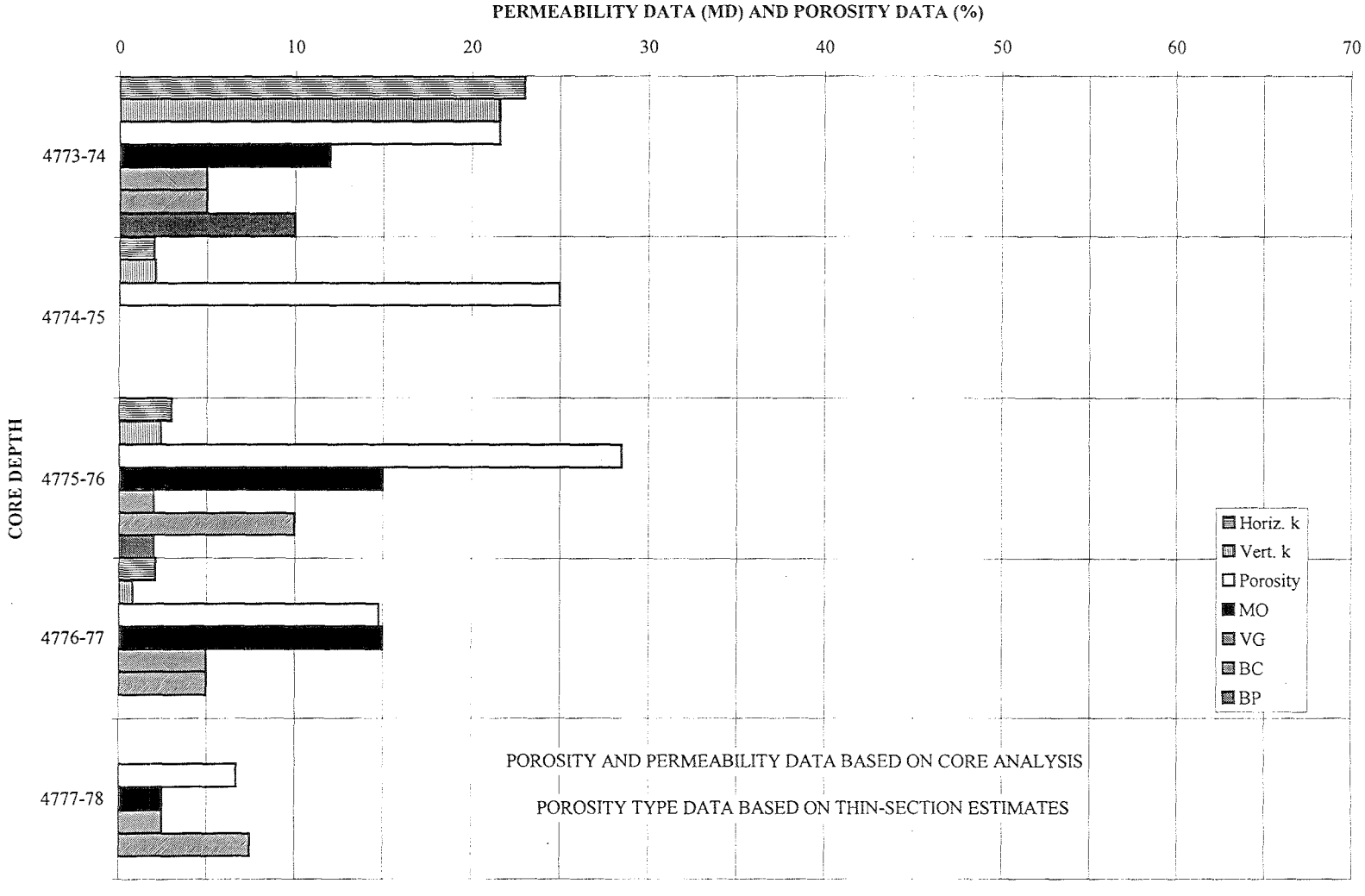
PERMEABILITY DATA (MD) AND POROSITY DATA (%)
0
10
20
30
40
50
60
70
CORE DEPTH
4773-74
4774-75
4775-76
4776-77
4777-78
Horiz. k
Vert. k
Porosity
MO
VG
BC
BP
POROSITY AND PERMEABILITY DATA BASED ON CORE ANALYSIS
POROSITY TYPE DATA BASED ON THIN-SECTION ESTIMATES

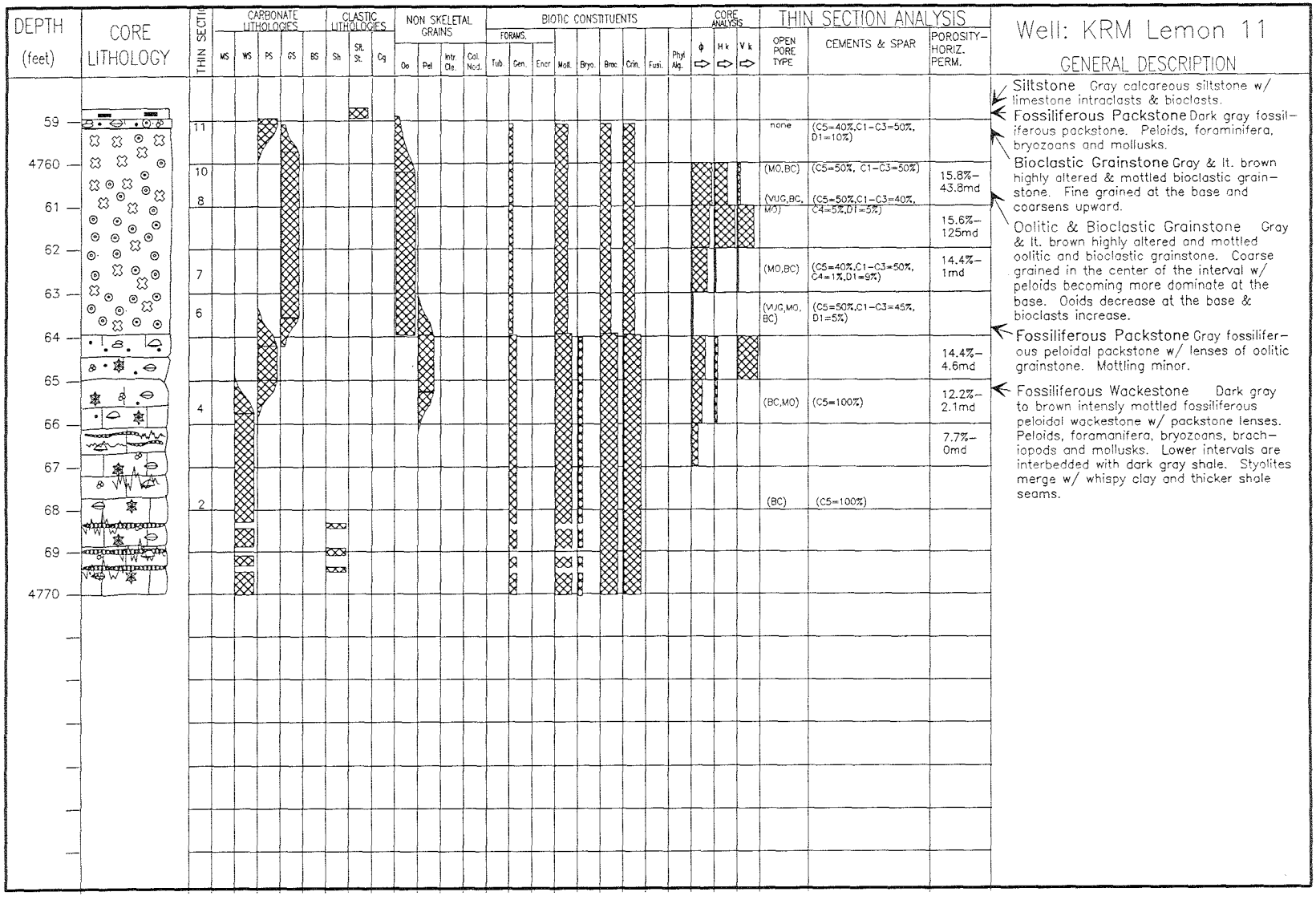


## Well: KRM Lemon 11

### GENERAL DESCRIPTION

**Siltstone** Gray calcareous siltstone w/ limestone intraclasts & bioclasts.

**Fossiliferous Packstone** Dark gray fossiliferous packstone. Peloids, foraminifera, bryozoans and mollusks.

**Bioclastic Grainstone** Gray & lt. brown highly altered & mottled bioclastic grainstone. Fine grained at the base and coarsens upward.

**Oolitic & Bioclastic Grainstone** Gray & lt. brown highly altered and mottled oolitic and bioclastic grainstone. Coarse grained in the center of the interval w/ peloids becoming more dominate at the base. Ooids decrease at the base & bioclasts increase.

**Fossiliferous Packstone** Gray fossiliferous peloidal packstone w/ lenses of oolitic grainstone. Mottling minor.

**Fossiliferous Wackestone** Dark gray to brown intensly mottled fossiliferous peloidal wackestone w/ packstone lenses. Peloids, foramanifera, bryozoans, brachiopods and mollusks. Lower intervals are interbedded with dark gray shale. Styolites merge w/ whispy clay and thicker shale seams.

Well Name: LEMON 11

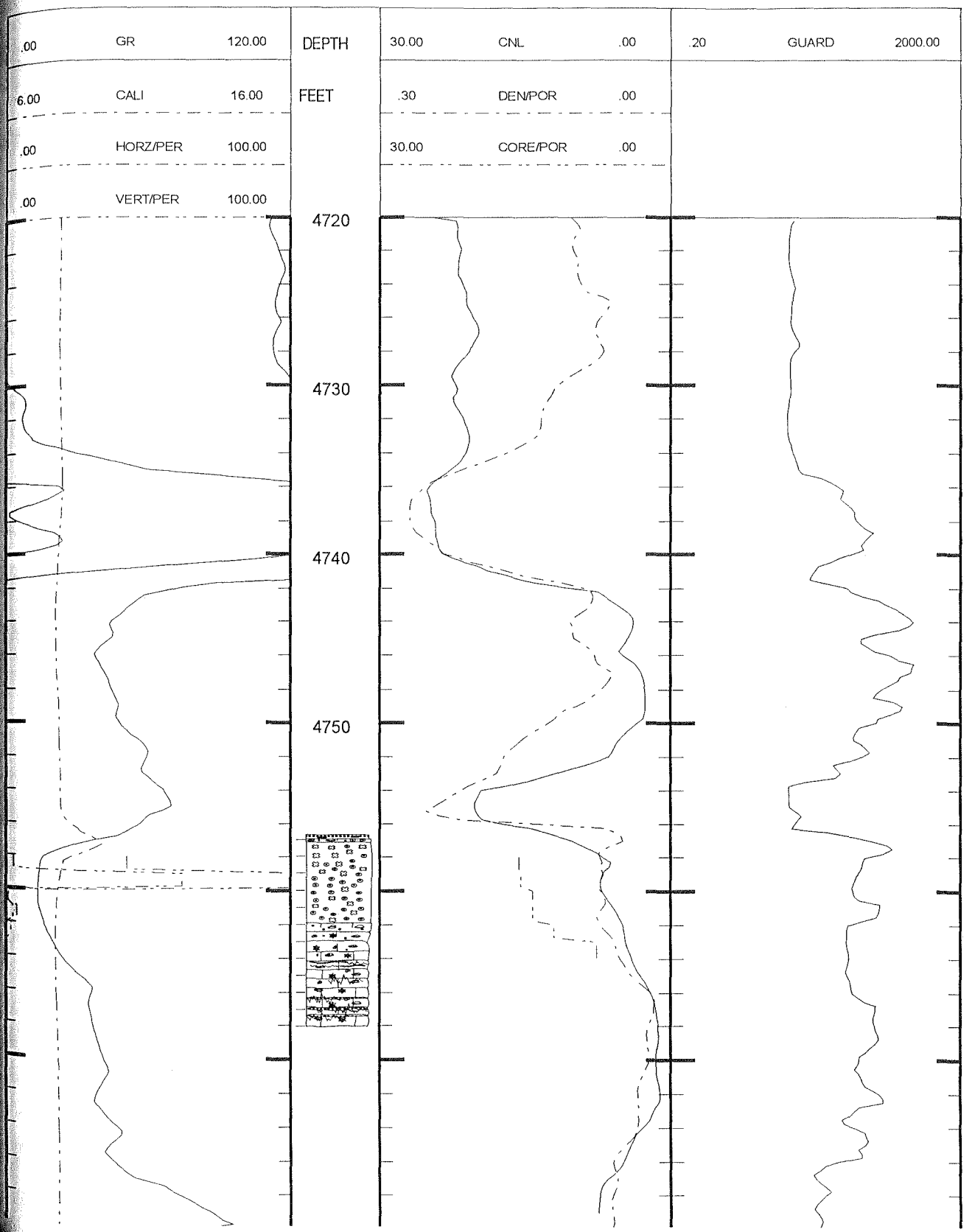


Lemon 11: Initial Production 2 BOPD, 920 MCFGPD (2/14/80) from Perfs: 4757-4764'

# LEMON 11

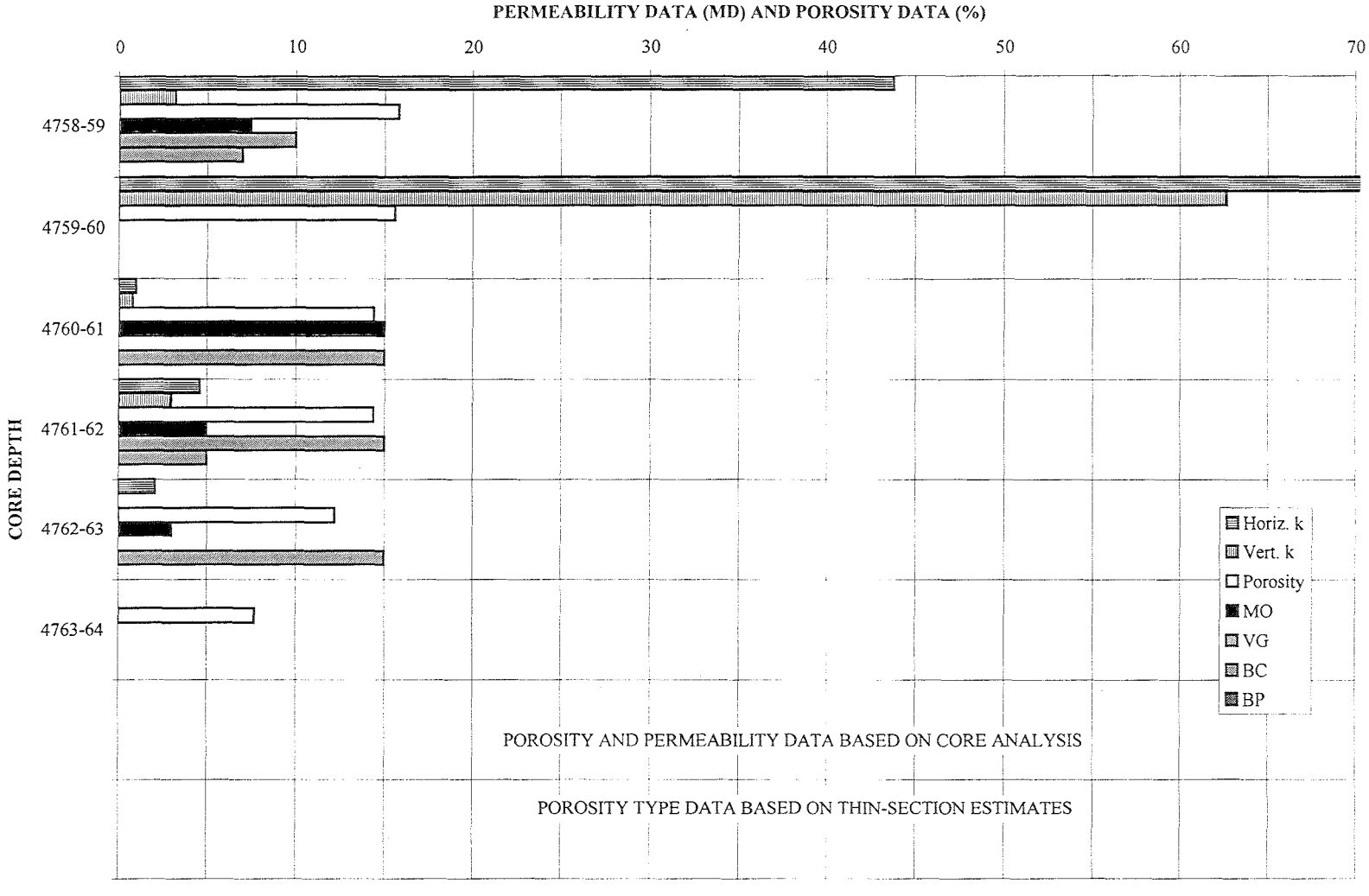
PERMEABILITY DATA (MD) AND POROSITY DATA (%)
0
10
20
30
40
50
60
70
CORE DEPTH
4758-59
4759-60
4760-61
4761-62
4762-63
4763-64
Horiz. k
Vert. k
Porosity
MO
VG
BC
BP
POROSITY AND PERMEABILITY DATA BASED ON CORE ANALYSIS
POROSITY TYPE DATA BASED ON THIN-SECTION ESTIMATES

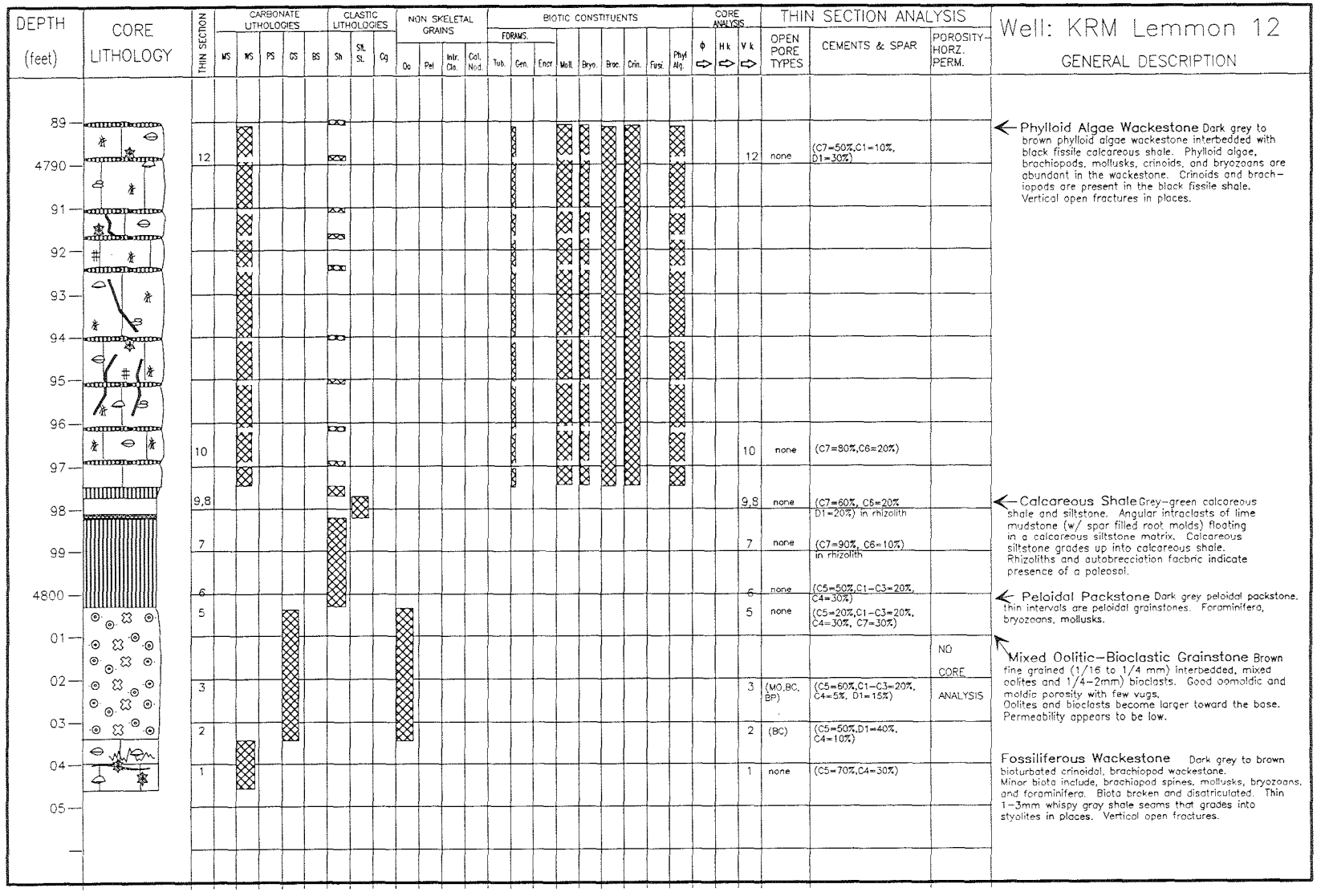


Well: KRM Lemmon 12

GENERAL DESCRIPTION

← **Phylloid Algae Wackestone** Dark grey to brown phylloid algae wackestone interbedded with black fissile calcareous shale. Phylloid algae, brachiopods, mollusks, crinoids, and bryozoans are abundant in the wackestone. Crinoids and brachiopods are present in the black fissile shale. Vertical open fractures in places.

← **Calcareous Shale** Grey-green calcareous shale and siltstone. Angular intraclasts of lime mudstone (w/ spar filled root molds) floating in a calcareous siltstone matrix. Calcareous siltstone grades up into calcareous shale. Rhizoliths and autobrecciation fabric indicate presence of a paleosol.

← **Peloidal Packstone** Dark grey peloidal packstone. thin intervals are peloidal grainstones. Foraminifera, bryozoans, mollusks.

↖ **Mixed Oolitic-Bioclastic Grainstone** Brown fine grained (1/16 to 1/4 mm) interbedded, mixed oolites and 1/4-2mm) bioclasts. Good oomoldic and moldic porosity with few vugs. Oolites and bioclasts become larger toward the base. Permeability appears to be low.

**Fossiliferous Wackestone** Dark grey to brown bioturbated crinoidal, brachiopod wackestone. Minor biota include, brachiopod spines, mollusks, bryozoans, and foraminifera. Biota broken and disatriculated. Thin 1-3mm whispy gray shale seams that grades into styolites in places. Vertical open fractures.

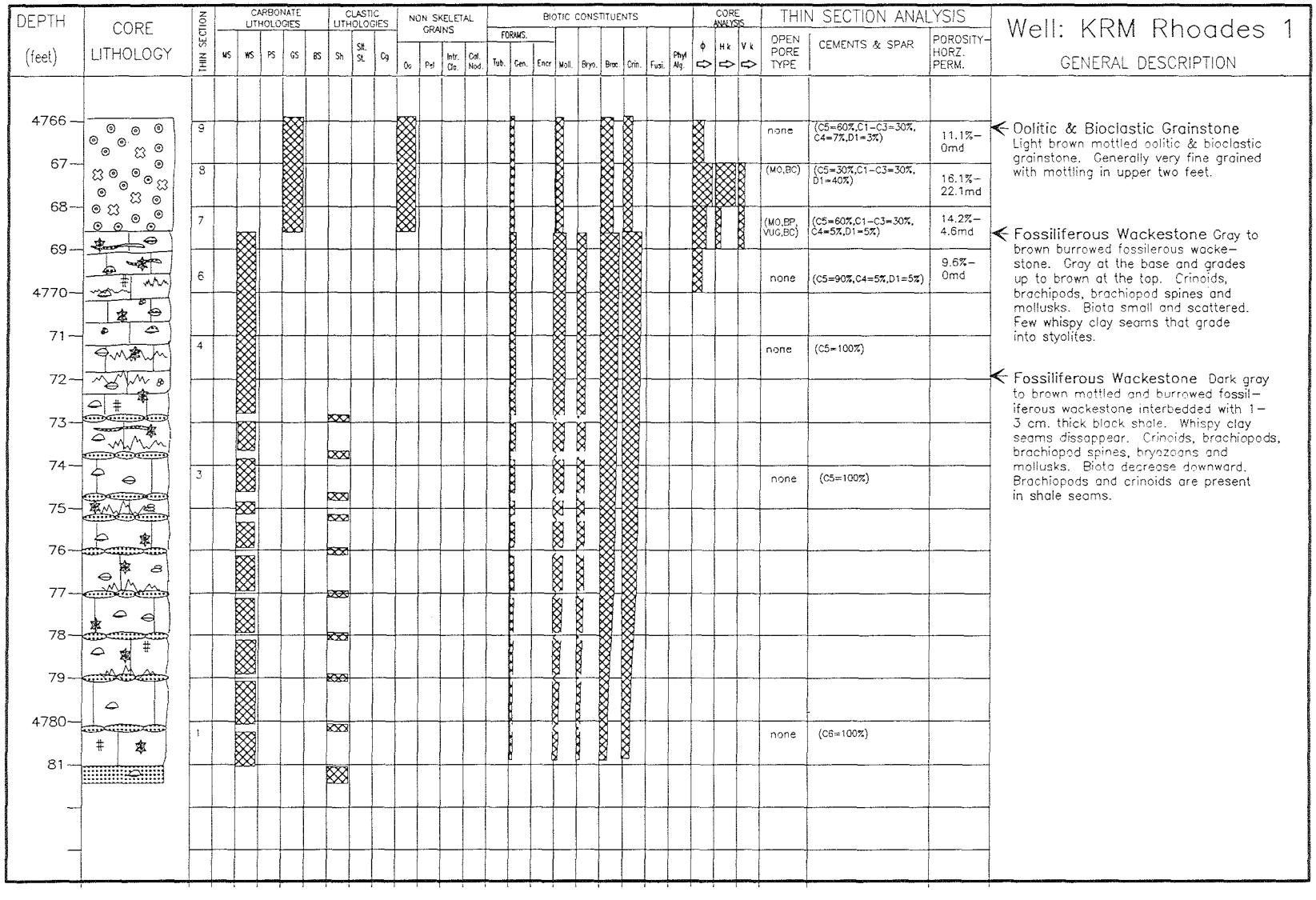
DEPTH (feet)
CORE LITHOLOGY
THIN SECTION
CARBONATE LITHOLOGIES
WS
WS
PS
GS
BS
CLASTIC LITHOLOGIES
Sh
Slt. St.
Cg
NON SKELETAL GRAINS
Oo
Pel
Intr. Clo.
Cal. Nod.
BIOTIC CONSTITUENTS
FORAMS.
Tub.
Gen.
Encr
Moll.
Bryo.
Brac.
Crin.
Fusi.
Phyl Alg.
CORE ANALYSIS
φ
H k
V k
THIN SECTION ANALYSIS
OPEN PORE TYPE
CEMENTS & SPAR
POROSITY-HORZ. PERM.
4766
67
68
69
4770
71
72
73
74
75
76
77
78
79
4780
81
9
8
7
6
4
3
1
none
(C5=60%,C1-C3=30%, C4=7%,D1=3%)
11.1%-0md
(MO,BC)
(C5=30%,C1-C3=30%, D1=40%)
16.1%-22.1md
(MO,BP, VUG,BC)
(C5=60%,C1-C3=30%, C4=5%,D1=5%)
14.2%-4.6md
(C5=90%,C4=5%,D1=5%)
9.6%-0md
(C5=100%)
(C6=100%)
Well: KRM Rhoades 1
GENERAL DESCRIPTION
Oolitic & Bioclastic Grainstone Light brown mottled oolitic & bioclastic grainstone. Generally very fine grained with mottling in upper two feet.
Fossiliferous Wackestone Gray to brown burrowed fossilerous wacke-stone. Gray at the base and grades up to brown at the top. Crinoids, brachipods, brachiopod spines and mollusks. Biota small and scattered. Few whispy clay seams that grade into styolites.
Fossiliferous Wackestone Dark gray to brown mottled and burrowed fossil-iferous wackestone interbedded with 1-3 cm. thick black shale. Whispy clay seams dissappear. Crinoids, brachiopods, brachiopod spines, bryozoans and mollusks. Biota decrease downward. Brachiopods and crinoids are present in shale seams.

Well Name: RHOADES 1

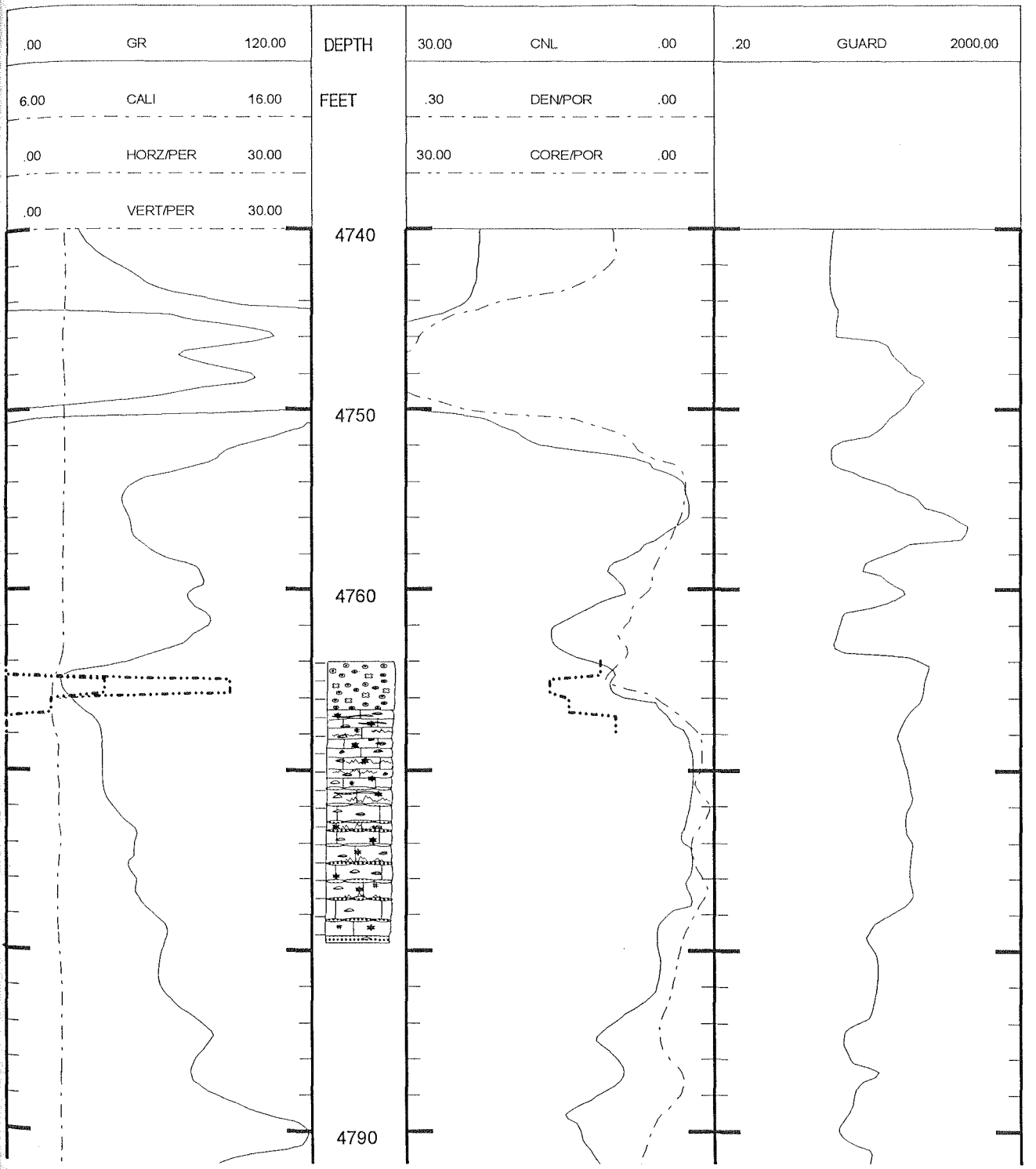


Rhoades 1: Initial Production 48 BOPD, 48 MCFGPD (7/19/79) from Perfs: 4763-4767'

# RHOADES 1

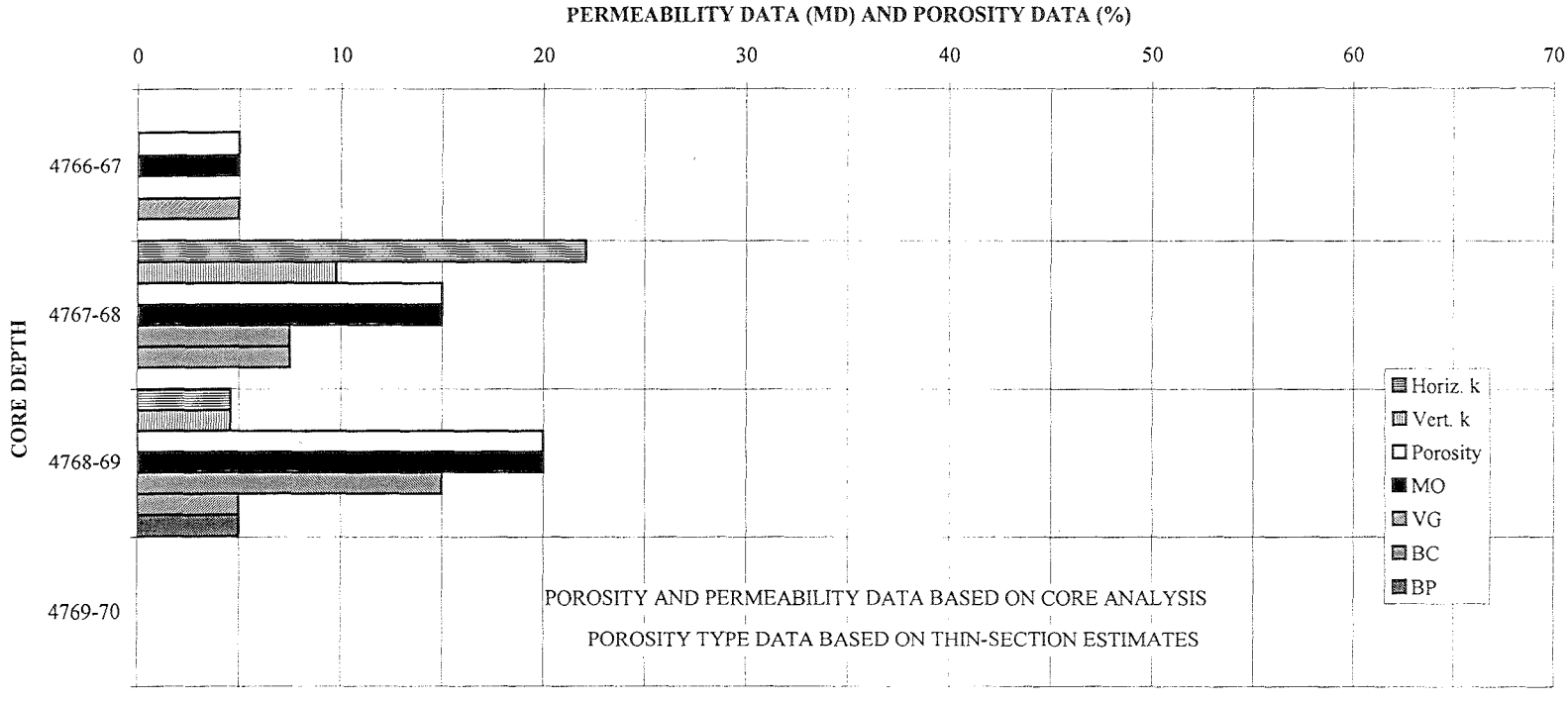
PERMEABILITY DATA (MD) AND POROSITY DATA (%)
0
10
20
30
40
50
60
70
CORE DEPTH
4766-67
4767-68
4768-69
4769-70
Horiz. k
Vert. k
Porosity
MO
VG
BC
BP
POROSITY AND PERMEABILITY DATA BASED ON CORE ANALYSIS
POROSITY TYPE DATA BASED ON THIN-SECTION ESTIMATES

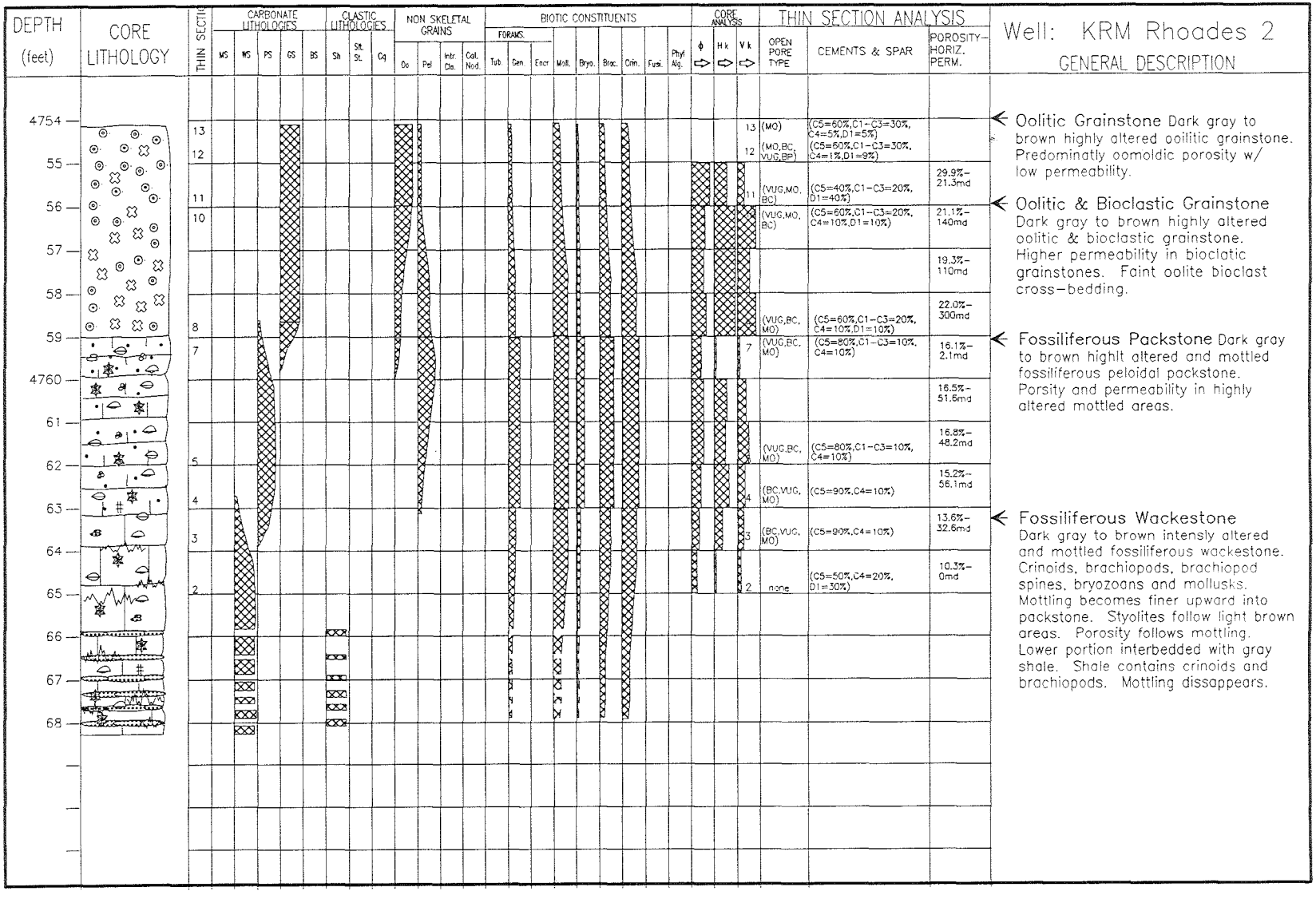


Well: KRM Rhoades 2

GENERAL DESCRIPTION

**Oolitic Grainstone** Dark gray to brown highly altered oolitic grainstone. Predominatly oomoldic porosity w/ low permeability.

**Oolitic & Bioclastic Grainstone** Dark gray to brown highly altered oolitic & bioclastic grainstone. Higher permeability in bioclatic grainstones. Faint oolite bioclast cross-bedding.

**Fossiliferous Packstone** Dark gray to brown highlt altered and mottled fossiliferous peloidal packstone. Porsity and permeability in highly altered mottled areas.

**Fossiliferous Wackestone** Dark gray to brown intensly altered and mottled fossiliferous wackestone. Crinoids, brachiopods, brachiopod spines, bryozoans and mollusks. Mottling becomes finer upward into packstone. Styolites follow light brown areas. Porosity follows mottling. Lower portion interbedded with gray shale. Shale contains crinoids and brachiopods. Mottling dissappears.

Well Name: RHOADES 2

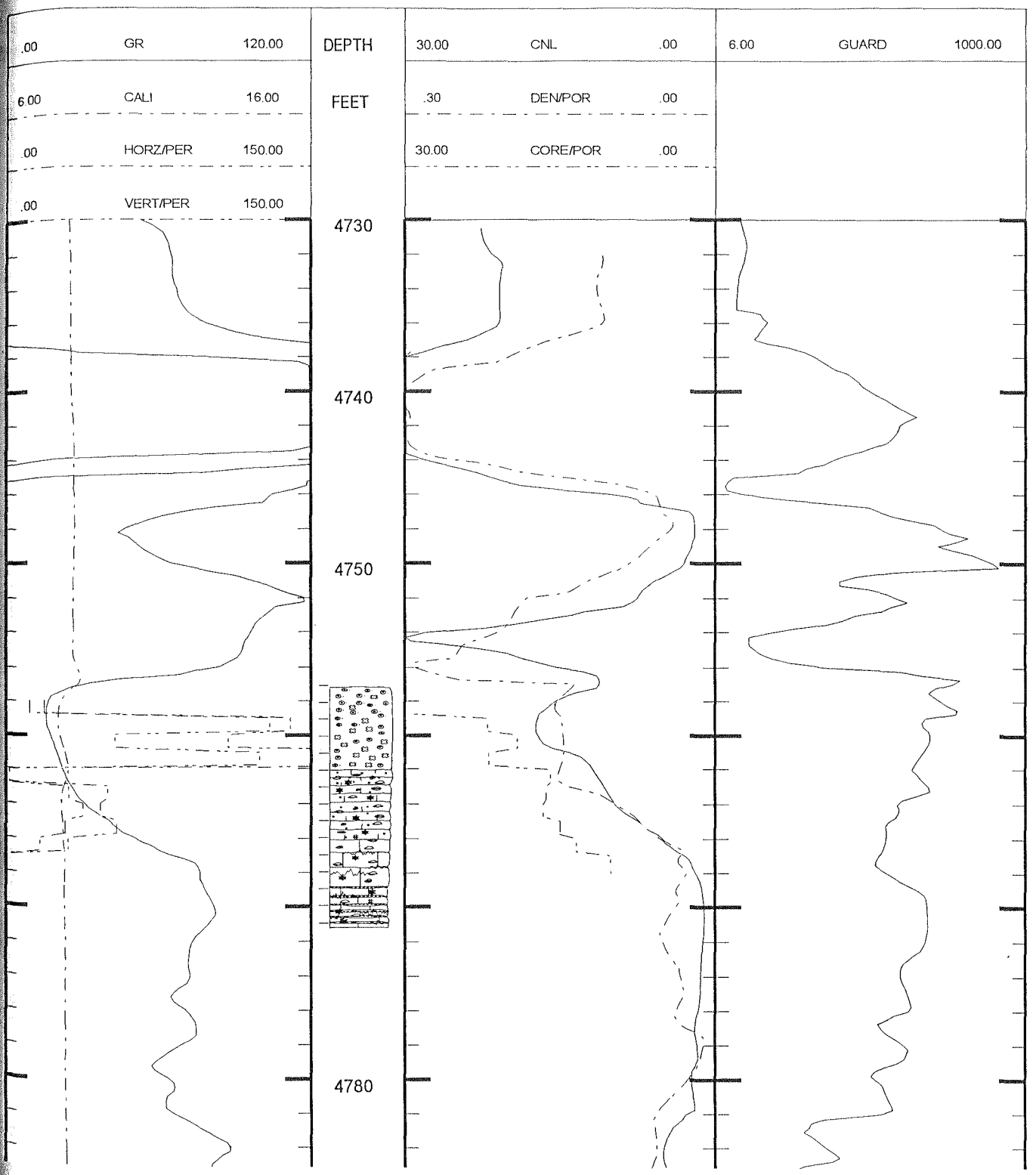


Rhoades 2: Initial Production 96 BOPD, 96 MCFGPD (7/19/79) from Perfs: 4754-4763'

# RHOADES 2

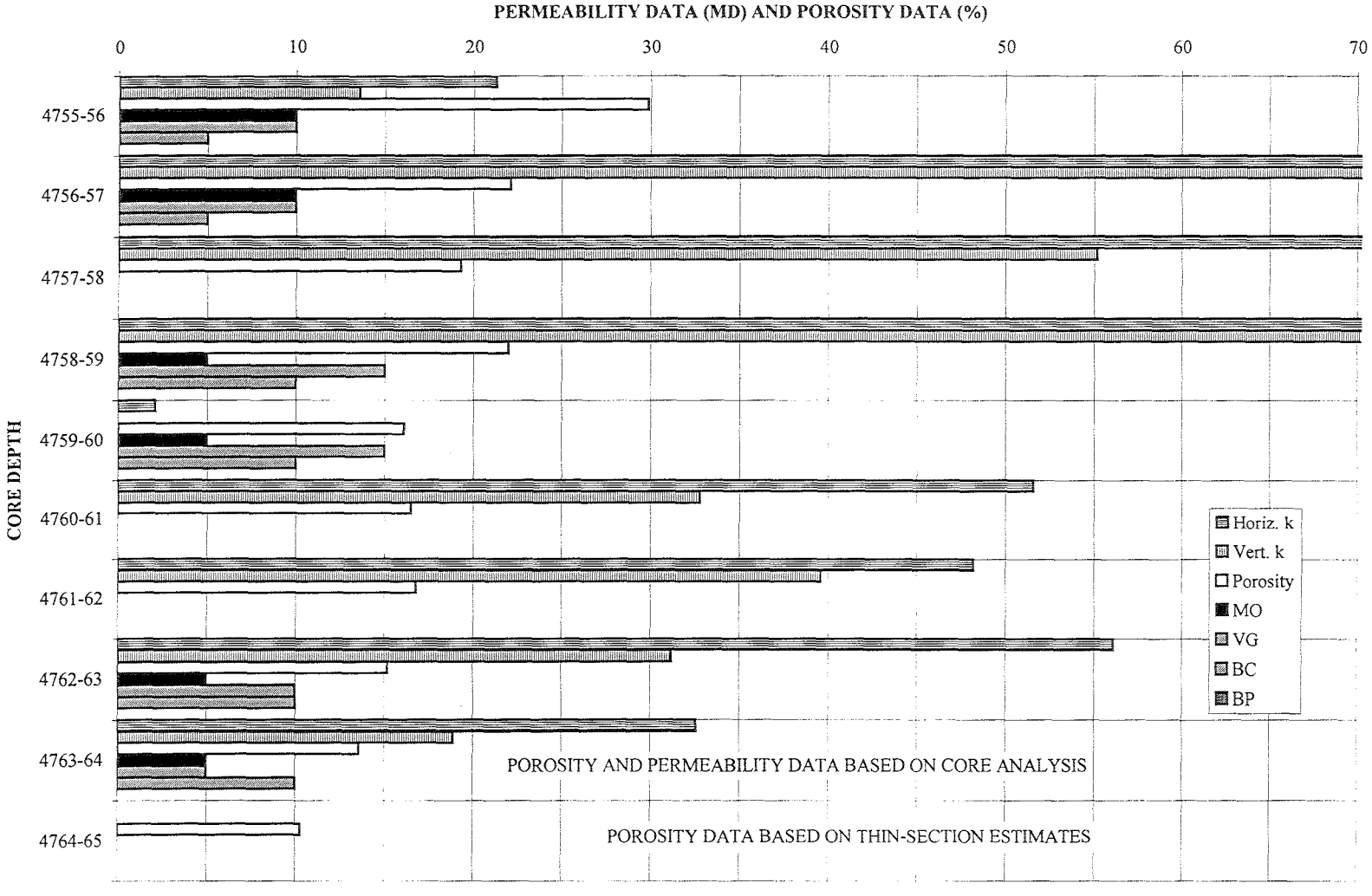
PERMEABILITY DATA (MD) AND POROSITY DATA (%)
0
10
20
30
40
50
60
70
CORE DEPTH
4755-56
4756-57
4757-58
4758-59
4759-60
4760-61
4761-62
4762-63
4763-64
4764-65
Horiz. k
Vert. k
Porosity
MO
VG
BC
BP
POROSITY AND PERMEABILITY DATA BASED ON CORE ANALYSIS
POROSITY DATA BASED ON THIN-SECTION ESTIMATES

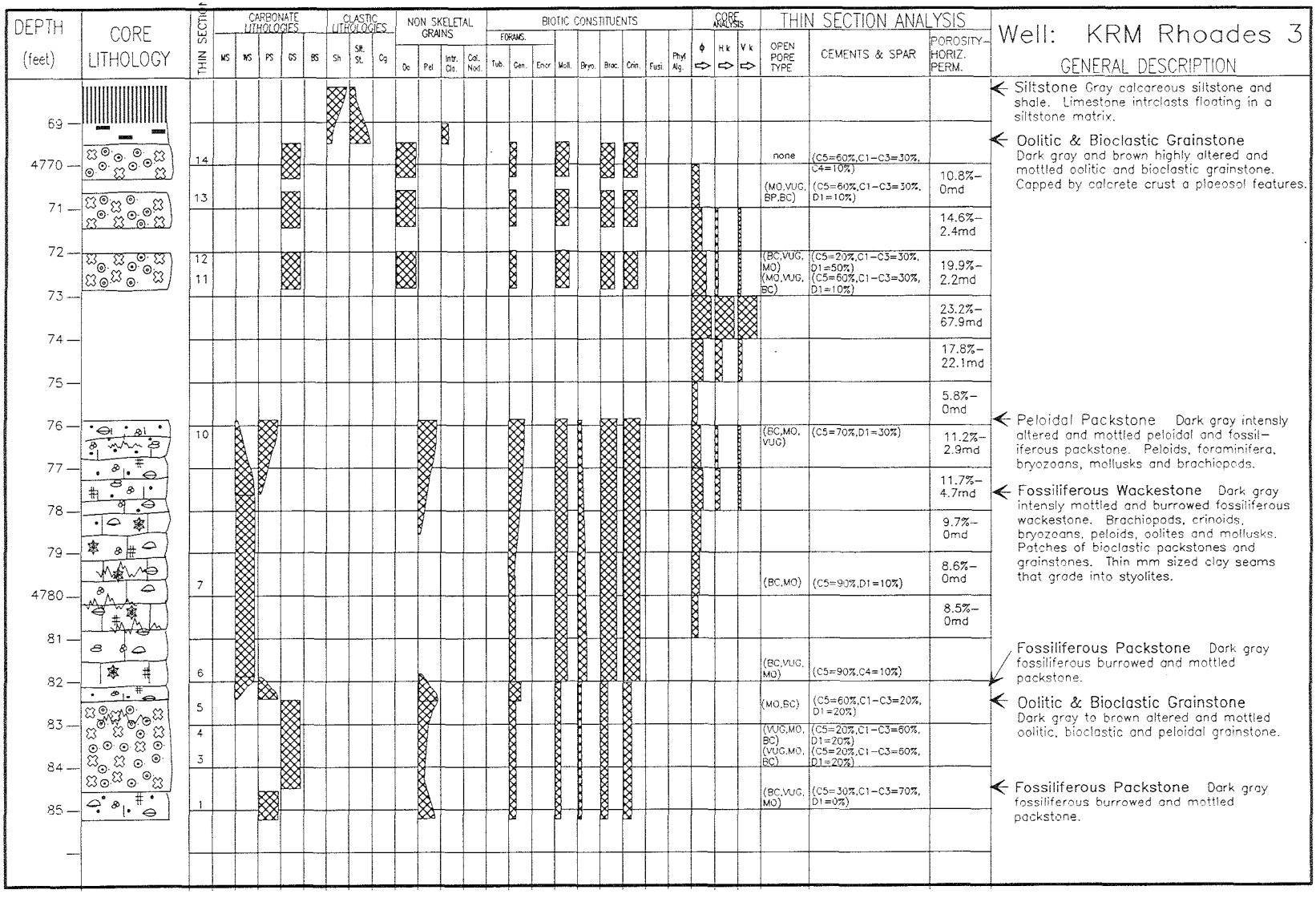
DEPTH (feet)
CORE LITHOLOGY
THIN SECTION
CARBONATE LITHOLOGIES
MS
WS
PS
GS
BS
CLASTIC LITHOLOGIES
Sh
Slt. St.
Cg
NON SKELETAL GRAINS
Oo
Pel
Intr. Clo.
Cal. Nod.
BIOTIC CONSTITUENTS
FORAMS.
Tub.
Gen.
Encr
Moll.
Bryo.
Broc.
Crin.
Fusi.
Phyl Alg.
CORE ANALYSIS
ϕ
H k
V k
THIN SECTION ANALYSIS
OPEN PORE TYPE
CEMENTS & SPAR
POROSITY–HORIZ. PERM.
Well: KRM Rhoades 3
GENERAL DESCRIPTION
69
4770
71
72
73
74
75
76
77
78
79
4780
81
82
83
84
85
14
13
12
11
10
7
6
5
4
3
1
none
(C5=60%,C1–C3=30%, C4=10%)
10.8%–0md
(MO,VUG, BP,BC)
(C5=60%,C1–C3=30%, D1=10%)
14.6%–2.4md
(BC,VUG, MO)
(C5=20%,C1–C3=30%, D1=50%)
19.9%–2.2md
(MO,VUG, BC)
(C5=60%,C1–C3=30%, D1=10%)
23.2%–67.9md
17.8%–22.1md
5.8%–0md
(BC,MO, VUG)
(C5=70%,D1=30%)
11.2%–2.9md
11.7%–4.7md
9.7%–0md
(BC,MO)
(C5=90%,D1=10%)
8.6%–0md
8.5%–0md
(BC,VUG, MO)
(C5=90%,C4=10%)
(MO,BC)
(C5=60%,C1–C3=20%, D1=20%)
(VUG,MO, BC)
(C5=20%,C1–C3=60%, D1=20%)
(VUG,MO, BC)
(C5=20%,C1–C3=60%, D1=20%)
(BC,VUG, MO)
(C5=30%,C1–C3=70%, D1=0%)
Siltstone Gray calcareous siltstone and shale. Limestone intrclasts floating in a siltstone matrix.
Oolitic & Bioclastic Grainstone
Dark gray and brown highly altered and mottled oolitic and bioclastic grainstone. Capped by calcrete crust a plaeosol features.
Peloidal Packstone Dark gray intensly altered and mottled peloidal and fossil–iferous packstone. Peloids, foraminifera, bryozoans, mollusks and brachiopods.
Fossiliferous Wackestone Dark gray intensly mottled and burrowed fossiliferous wackestone. Brachiopods, crinoids, bryozoans, peloids, oolites and mollusks. Patches of bioclastic packstones and grainstones. Thin mm sized clay seams that grade into styolites.
Fossiliferous Packstone Dark gray fossiliferous burrowed and mottled packstone.
Oolitic & Bioclastic Grainstone
Dark gray to brown altered and mottled oolitic, bioclastic and peloidal grainstone.
Fossiliferous Packstone Dark gray fossiliferous burrowed and mottled packstone.

Well Name: RHOADES 3

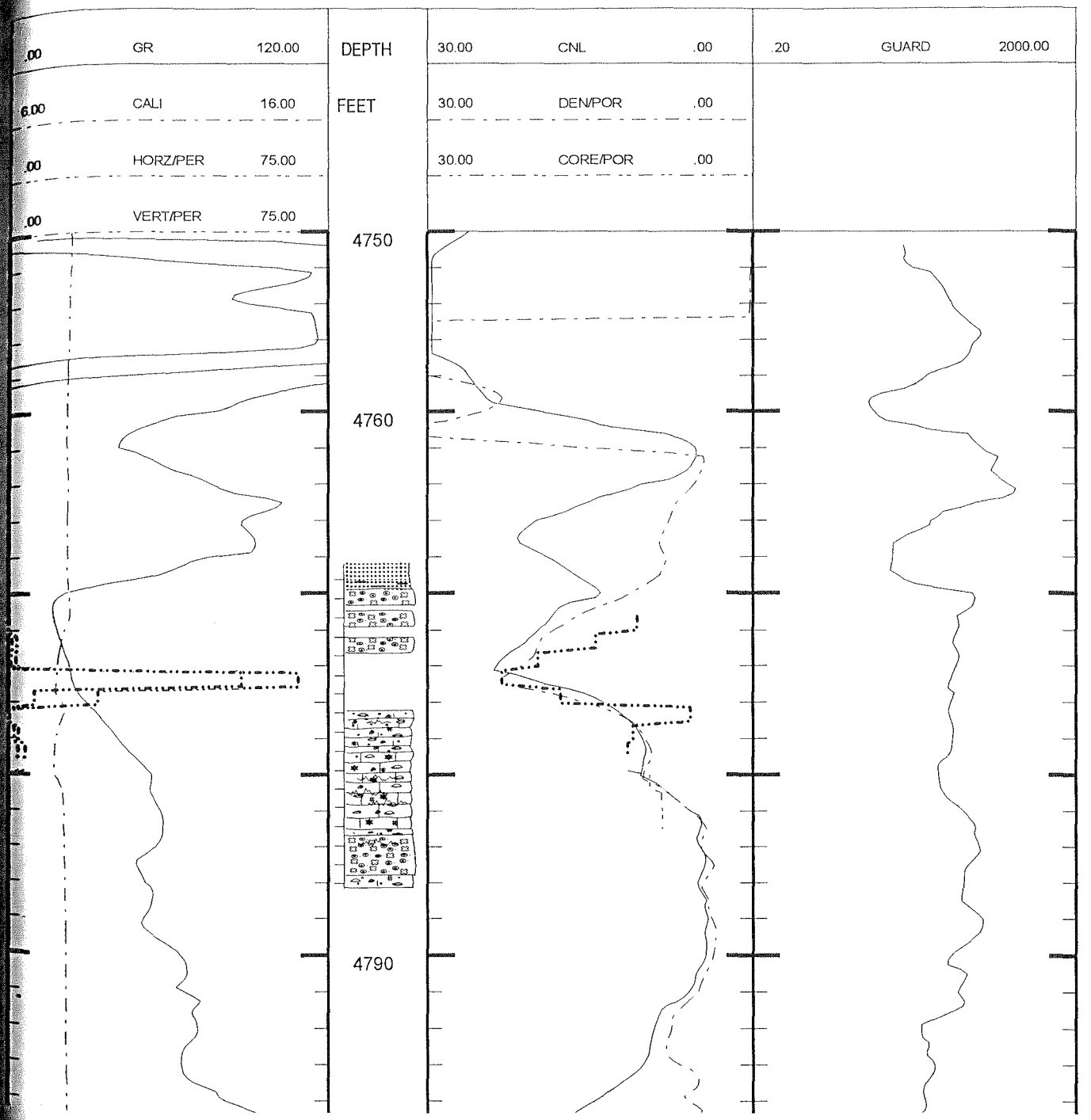


Rhoades 3: Initial Production 156 BOPD, 156 MCFPD (2/7/80) from Perfs: 4770-4780'

# RHOADES 3

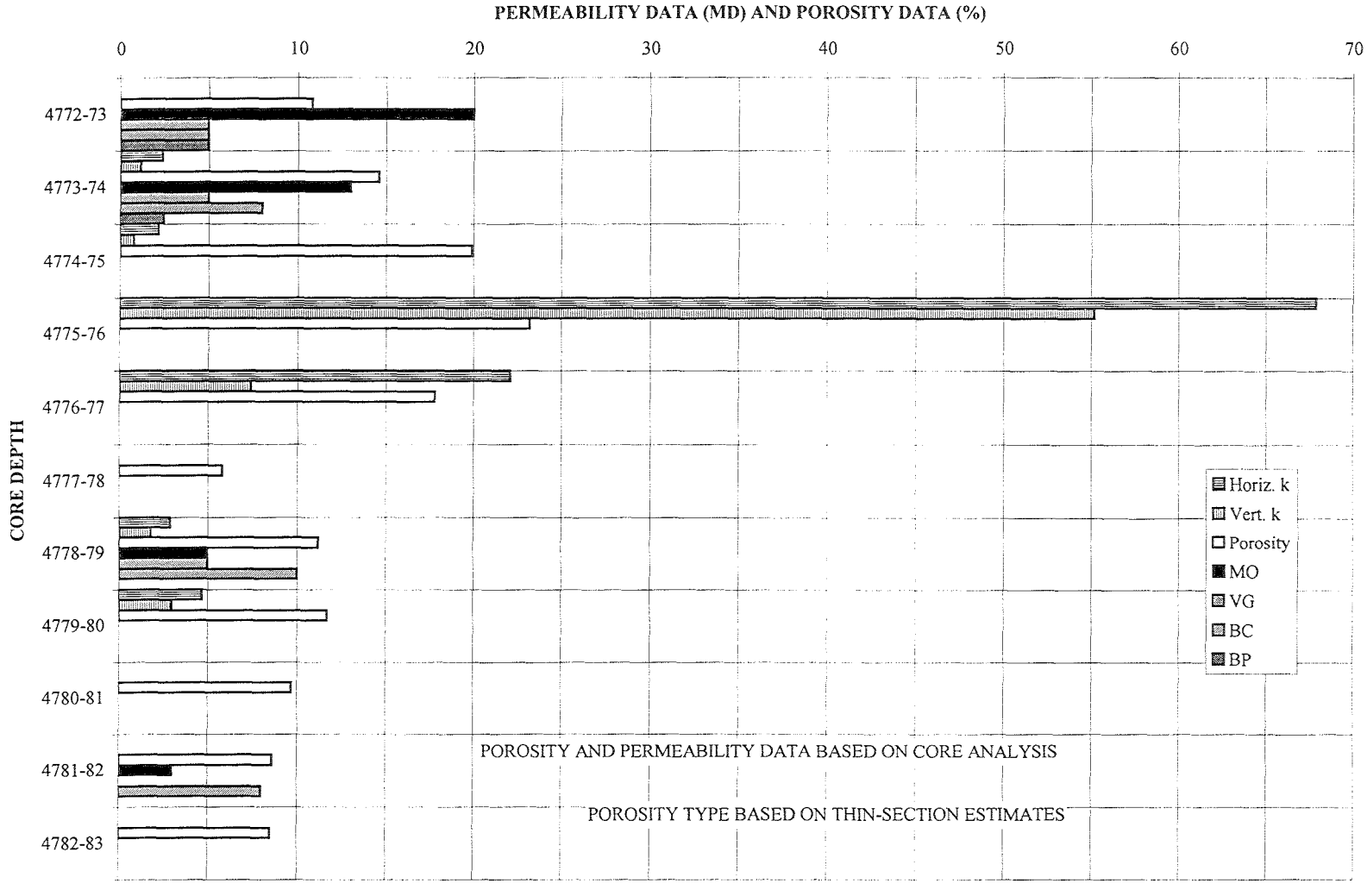
PERMEABILITY DATA (MD) AND POROSITY DATA (%)
0
10
20
30
40
50
60
70
CORE DEPTH
4772-73
4773-74
4774-75
4775-76
4776-77
4777-78
4778-79
4779-80
4780-81
4781-82
4782-83
Horiz. k
Vert. k
Porosity
MO
VG
BC
BP
POROSITY AND PERMEABILITY DATA BASED ON CORE ANALYSIS
POROSITY TYPE BASED ON THIN-SECTION ESTIMATES

# Appendix C

# Collier Flats Field
# Core Database

Whole Core Analysis Data

Lemon & Rhoades Leases
Sections 13,14, 23 & 24
T34S, R20W

Bethany Falls Limestone
Whole Core Analysis

| | A | B | C | D | E | F | G |
|---|---|---|---|---|---|---|---|
| 5 | Depth | Sample # | Horiz. Perm. | Vert. Perm. | Porosity | W. Sat | O. Sat |
| 49 | 4775-76 | L10-3 | 3 | 2.4 | 28.5 | 13.4 | 2.6 |
| 50 | 4776-77 | L10-4 | 2.1 | 0.8 | 14.8 | 34.1 | 17 |
| 51 | 4777-78 | L10-5 | 0 | 0 | 6.7 | 47.6 | 4.2 |
| 52 | Depth | Sample # | Horiz. Perm. | Vert. Perm. | Porosity | W. Sat | O. Sat |
| 53 | 4758-59 | L11-1 | 43.8 | 3.2 | 15.8 | 26.5 | 14 |
| 54 | 4759-60 | L11-2 | 125 | 62.7 | 15.6 | 32.6 | 13.6 |
| 55 | 4760-61 | L11-3 | 1 | 0.8 | 14.4 | 17.5 | 4.7 |
| 56 | 4761-62 | L11-4 | 4.6 | 3 | 14.4 | 30.3 | 11.7 |
| 57 | 4762-63 | L11-5 | 2.1 | 0 | 12.2 | 28 | 21.1 |
| 58 | 4763-64 | L11-6 | 0 | 0 | 7.7 | 31.8 | 17.5 |
| 59 | Depth | Sample # | Horiz. Perm. | Vert. Perm. | Porosity | W. Sat | O. Sat |
| 60 | 4766-67 | R1-1 | 0 | 0 | 11.1 | 31 | 9.1 |
| 61 | 4767-68 | R1-2 | 22.1 | 9.8 | 16.1 | 19.3 | 9 |
| 62 | 4768-69 | R1-3 | 4.6 | 4.6 | 14.2 | 18.2 | 13.7 |
| 63 | 4769-70 | R1-4 | 0 | 0 | 9.6 | 27.3 | 12.5 |
| 64 | Depth | Sample # | Horiz. Perm. | Vert. Perm. | Porosity | W. Sat | O. Sat |
| 65 | 4755-56 | R2-1 | 21.3 | 13.6 | 29.9 | 15 | 1.7 |
| 66 | 4756-57 | R2-2 | 140 | 130 | 22.1 | 21.6 | 10.1 |
| 67 | 4757-58 | R2-3 | 110 | 55.2 | 19.3 | 23.8 | 10.4 |
| 68 | 4758-59 | R2-4 | 300 | 125 | 22 | 19.3 | 13.2 |
| 69 | 4759-60 | R2-5 | 2.1 | 0 | 16.1 | 24.3 | 10.6 |
| 70 | 4760-61 | R2-6 | 51.6 | 32.8 | 16.5 | 28.2 | 9.8 |
| 71 | 4761-62 | R2-7 | 48.2 | 39.6 | 16.8 | 25.4 | 7.6 |
| 72 | 4762-63 | R2-8 | 56.1 | 31.2 | 15.2 | 24.9 | 6.3 |
| 73 | 4763-64 | R2-9 | 32.6 | 18.9 | 13.6 | 23.5 | 8.6 |
| 74 | 4764-65 | R2-10 | 0 | 0 | 10.3 | 36.2 | 5.1 |
| 75 | Depth | Sample # | Horiz. Perm. | Vert. Perm. | Porosity | W. Sat | O. Sat |
| 76 | 4772-73 | R3-1 | 0 | 0 | 10.8 | 33.6 | 7.8 |
| 77 | 4773-74 | R3-2 | 2.4 | 1.2 | 14.6 | 26.9 | 10 |
| 78 | 4774-75 | R3-3 | 2.2 | 0.8 | 19.9 | 32 | 12.9 |
| 79 | 4775-76 | R3-4 | 67.9 | 55.2 | 23.2 | 21.7 | 14.8 |
| 80 | 4776-77 | R3-5 | 22.1 | 7.4 | 17.8 | 19.3 | 16.9 |
| 81 | 4777-78 | R3-6 | 0 | 0 | 5.8 | 34.9 | 4.7 |
| 82 | 4778-79 | R3-7 | 2.9 | 1.8 | 11.2 | 26.6 | 9.2 |
| 83 | 4779-80 | R3-8 | 4.7 | 3 | 11.7 | 25.3 | 13.8 |
| 84 | 4780-81 | R3-9 | 0 | 0 | 9.7 | 27.2 | 12.4 |
| 85 | 4781-82 | R3-10 | 0 | 0 | 8.6 | 30.6 | 8.8 |
| 86 | 4782-83 | R3-11 | 0 | 0 | 8.5 | 47.1 | 2.9 |
| 87 | Depth | Sample # | Horiz. Perm. | Vert. Perm. | Porosity | W. Sat | O. Sat |
| 88 | '4780-81 | L3-1 | 78 | | 27 | | |
| 89 | '4782-83 | L3-2 | 63 | | 22 | | |
| 90 | '4783-84 | L3-3 | 8.7 | | 22.8 | | |
| 91 | | | | | | | |
| 92 | | | | | | | |

Bethany Falls Limestone
Whole Core Analysis

| | A | B | C | D | E | F | G |
|---|---|---|---|---|---|---|---|
| 5 | Depth | Sample # | Horiz. Perm. | Vert. Perm. | Porosity | W. Sat | O. Sat |
| 49 | 4775-76 | L10-3 | 3 | 2.4 | 28.5 | 13.4 | 2.6 |
| 50 | 4776-77 | L10-4 | 2.1 | 0.8 | 14.8 | 34.1 | 17 |
| 51 | 4777-78 | L10-5 | 0 | 0 | 6.7 | 47.6 | 4.2 |
| 52 | Depth | Sample # | Horiz. Perm. | Vert. Perm. | Porosity | W. Sat | O. Sat |
| 53 | 4758-59 | L11-1 | 43.8 | 3.2 | 15.8 | 26.5 | 14 |
| 54 | 4759-60 | L11-2 | 125 | 62.7 | 15.6 | 32.6 | 13.6 |
| 55 | 4760-61 | L11-3 | 1 | 0.8 | 14.4 | 17.5 | 4.7 |
| 56 | 4761-62 | L11-4 | 4.6 | 3 | 14.4 | 30.3 | 11.7 |
| 57 | 4762-63 | L11-5 | 2.1 | 0 | 12.2 | 28 | 21.1 |
| 58 | 4763-64 | L11-6 | 0 | 0 | 7.7 | 31.8 | 17.5 |
| 59 | Depth | Sample # | Horiz. Perm. | Vert. Perm. | Porosity | W. Sat | O. Sat |
| 60 | 4766-67 | R1-1 | 0 | 0 | 11.1 | 31 | 9.1 |
| 61 | 4767-68 | R1-2 | 22.1 | 9.8 | 16.1 | 19.3 | 9 |
| 62 | 4768-69 | R1-3 | 4.6 | 4.6 | 14.2 | 18.2 | 13.7 |
| 63 | 4769-70 | R1-4 | 0 | 0 | 9.6 | 27.3 | 12.5 |
| 64 | Depth | Sample # | Horiz. Perm. | Vert. Perm. | Porosity | W. Sat | O. Sat |
| 65 | 4755-56 | R2-1 | 21.3 | 13.6 | 29.9 | 15 | 1.7 |
| 66 | 4756-57 | R2-2 | 140 | 130 | 22.1 | 21.6 | 10.1 |
| 67 | 4757-58 | R2-3 | 110 | 55.2 | 19.3 | 23.8 | 10.4 |
| 68 | 4758-59 | R2-4 | 300 | 125 | 22 | 19.3 | 13.2 |
| 69 | 4759-60 | R2-5 | 2.1 | 0 | 16.1 | 24.3 | 10.6 |
| 70 | 4760-61 | R2-6 | 51.6 | 32.8 | 16.5 | 28.2 | 9.8 |
| 71 | 4761-62 | R2-7 | 48.2 | 39.6 | 16.8 | 25.4 | 7.6 |
| 72 | 4762-63 | R2-8 | 56.1 | 31.2 | 15.2 | 24.9 | 6.3 |
| 73 | 4763-64 | R2-9 | 32.6 | 18.9 | 13.6 | 23.5 | 8.6 |
| 74 | 4764-65 | R2-10 | 0 | 0 | 10.3 | 36.2 | 5.1 |
| 75 | Depth | Sample # | Horiz. Perm. | Vert. Perm. | Porosity | W. Sat | O. Sat |
| 76 | 4772-73 | R3-1 | 0 | 0 | 10.8 | 33.6 | 7.8 |
| 77 | 4773-74 | R3-2 | 2.4 | 1.2 | 14.6 | 26.9 | 10 |
| 78 | 4774-75 | R3-3 | 2.2 | 0.8 | 19.9 | 32 | 12.9 |
| 79 | 4775-76 | R3-4 | 67.9 | 55.2 | 23.2 | 21.7 | 14.8 |
| 80 | 4776-77 | R3-5 | 22.1 | 7.4 | 17.8 | 19.3 | 16.9 |
| 81 | 4777-78 | R3-6 | 0 | 0 | 5.8 | 34.9 | 4.7 |
| 82 | 4778-79 | R3-7 | 2.9 | 1.8 | 11.2 | 26.6 | 9.2 |
| 83 | 4779-80 | R3-8 | 4.7 | 3 | 11.7 | 25.3 | 13.8 |
| 84 | 4780-81 | R3-9 | 0 | 0 | 9.7 | 27.2 | 12.4 |
| 85 | 4781-82 | R3-10 | 0 | 0 | 8.6 | 30.6 | 8.8 |
| 86 | 4782-83 | R3-11 | 0 | 0 | 8.5 | 47.1 | 2.9 |
| 87 | Depth | Sample # | Horiz. Perm. | Vert. Perm. | Porosity | W. Sat | O. Sat |
| 88 | '4780-81 | L3-1 | 78 | | 27 | | |
| 89 | '4782-83 | L3-2 | 63 | | 22 | | |
| 90 | '4783-84 | L3-3 | 8.7 | | 22.8 | | |
| 91 | | | | | | | |
| 92 | | | | | | | |

# Appendix D

# Collier Flats Field
# Drill Stem Test Database

DST Analysis Worksheet

Wells Listed In Alphabetical Order

| | | | |
|---|---|---|---|
| DST Data | | | |
| GIRK 1 | | | |
| | | | |
| date | 9/24/80 | | |
| well bore diameter | 7.875 | inches | |
| drill-collar | 488.00 | feet | |
| drill-collar (ID) | 2.25 | inches | |
| drill-pipe | 4274.00 | feet | |
| drill-pipe (ID) | 3.80 | inches | |
| drill-collar-vol | 0.0049 | bbl/ft | |
| drill-pipe-vol | 0.0142 | bbl\ft | |
| initial flow time | 25.00 | min | |
| final flow time | 60.00 | min | |
| total flow time (T) | 85.00 | min | |
| 1st final flow pressure | 62.00 | psig | |
| 2nd final flow pressure | 66.00 | psig | |
| gauge depth | 4800.00 | psig | |
| mud wt. | 9.20 | lb/gal | |
| initial hydrostatic pressure | 2359.00 | psig | |
| final hydrostatic pressure | 2326.00 | psig | |
| bht | 124.00 | degrees f | |
| porous interval (h) | 6.00 | feet | |
| | | | |
| | | | |
| | | | |
| DST Quality Check | calculated hydrostatic pressure | 2294.02 | psig |
| | oil specfic gravity | 0.80 | g/cm^3 |
| | oil wt | 6.68 | lb/gal |
| | oil gradient | 0.35 | psi/ft |
| | theoretical 1st flow recovery | 129.73 | ft-mud |
| | theoretical 2nd flow recovery | 237.86 | ft-oil |
| | | | |
| Horner Plot Data | M | 45.00 | psi/cycle |
| | reservoir pressure (pi) | 790.00 | psig |
| | gas recovery (2nd flow) | 0.10 | mcfgpd |
| | fluid recovery (Ft.) | 150.00 | g&ocm,go |
| | production rate (Q) | 17.64 | STB/D |
| | ave porosity | 0.11 | |
| | production time (tp) | 1.42 | hours |
| | well bore radius | 0.33 | ft |
| | oil compressibility* | 1.39E-05 | |
| | viscosity* | 0.39 | cp |
| | formation factor (B)* | 1.49 | rb/stb |
| | oil gravity* | 46.00 | api |
| | perm (kh) | 37.04 | md-ft |
| | perm (k) | 6.17 | md |
| | | | |
| Skin Factor Data | pressure FSIP @ 1hr | 773.00 | psig |
| | skin factor | 12.88 | |
| | dP across skin | 503.34 | psig |
| | flow efficiency | 0.36 | |
| | | | |
| Initial Production | oil | 54.00 | bopd |
| on pump | gas | 160.00 | mcfpd |
| | water | 0.00 | bwpd |
| | perfs | 4795-4800 | ft |

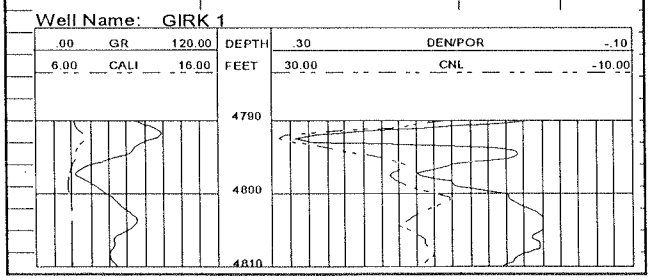

Hackney 2-13 DST Analysis

| | | | |
|---|---|---|---|
| DST Data | | | |
| HACKNEY 2-13 | | | |
| | | | |
| date | 10/26/81 | | |
| well bore diameter | 7.875 | inches | |
| drill-collar | 547.00 | feet | |
| drill-collar (ID) | 2.25 | inches | |
| drill-pipe | 4206.00 | feet | |
| drill-pipe (ID) | 3.80 | inches | |
| drill-collar-vol | 0.0049 | bbl/ft | |
| drill-pipe-vol | 0.0142 | bbl\ft | |
| initial flow time | 28.00 | min | |
| final flow time | 29.00 | min | |
| total flow time (T) | 57.00 | min | |
| 1st final flow pressure | 85.00 | psig | |
| 2nd final flow pressure | 88.00 | psig | |
| gauge depth | 4770.00 | psig | |
| mud wt. | 9.40 | lb/gal | |
| initial hydrostatic pressure | 2415.00 | psig | |
| final hydrostatic pressure | 2347.00 | psig | |
| bht | 110.00 | degrees f | |
| porous interval (h) | 4.00 | feet | |
| | | | |
| | | | |
| | | | |
| DST Quality Check | calculated hydrostatic pressure | 2329.24 | psig |
| | oil specfic gravity | 0.80 | g/cm^3 |
| | oil wt | 6.68 | lb/gal |
| | oil gradient | 0.35 | psi/ft |
| | theoretical 1st flow recovery | 174.07 | ft-mud |
| | theoretical 2nd flow recovery | 317.15 | ft-oil |
| | | | |
| Horner Plot Data | M | 215.00 | psi/cycle |
| | reservoir pressure (pi) | 1450.00 | psig |
| | gas recovery (2nd flow) | 156 | mcfgpd |
| | fluid recovery (Ft.) | 600.00 | mco |
| | production rate (Q) | 170.46 | STB/D |
| | ave porosity | 0.24 | |
| | production time (tp) | 0.95 | hours |
| | well bore radius | 0.33 | ft |
| | oil compressibility* | 1.39E-05 | |
| | viscosity* | 0.39 | cp |
| | formation factor (B)* | 1.49 | rb/stb |
| | oil gravity* | 46.00 | api |
| | perm (kh) | 74.91 | md-ft |
| | perm (k) | 18.73 | md |
| | | | |
| Skin Factor Data | pressure FSIP @ 1hr | 1415.00 | psig |
| | skin factor | 1.83 | |
| | dP across skin | 340.93 | psig |
| | flow efficiency | 0.76 | |
| | | | |
| Initial Production | oil | 76.00 | bopd |
| | gas | n/a | mcfpd |
| | water | 0.00 | bwpd |
| | perfs | 4770-76 | ft |

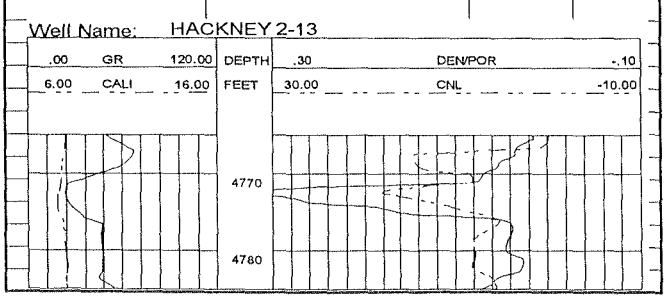

Selzer 1-35 DST Analysis

| | | | |
|---|---|---|---|
| DST Data | | | |
| SELZER 1-35 | | | |
| | | | |
| date | 2/22/81 | | |
| well bore diameter | 7.875 | inches | |
| drill-collar | 510.00 | feet | |
| drill-collar (ID) | 2.25 | inches | |
| drill-pipe | 4183.00 | feet | |
| drill-pipe (ID) | 3.80 | inches | |
| drill-collar-vol | 0.0049 | bbl/ft | |
| drill-pipe-vol | 0.0142 | bbl\ft | |
| initial flow time | 30.00 | min | |
| final flow time | 15.00 | min | |
| total flow time (T) | 45.00 | min | |
| 1st final flow pressure | 280.00 | psig | |
| 2nd final flow pressure | 344.30 | psig | |
| gauge depth | 4772.00 | psig | |
| mud wt. | 9.20 | lb/gal | |
| initial hydrostatic pressure | 2255.00 | psig | |
| final hydrostatic pressure | 2268.00 | psig | |
| bht | 117.00 | degrees f | |
| porosity thickness (h) | 12.00 | feet | |
| | | | |
| | | | |
| | | | |
| DST Quality Check | calculated hydrostatic pressure | 2280.64 | psig |
| | oil specfic gravity | 0.80 | g/cm^3 |
| | oil wt | 6.68 | lb/gal |
| | oil gradient | 0.35 | psi/ft |
| | theoretical 1st flow recovery | 585.87 | ft-mud |
| | theoretical 2nd flow recovery | 1240.85 | ft-oil |
| | | | |
| Horner Plot Data | M | 150.00 | psi/cycle |
| | reservoir pressure (pi) | 1800.00 | psig |
| | gas recovery (2nd flow) | 817 | mcfgpd |
| | fluid recovery (Ft.) | 1620.00 | ogcm,oil |
| | production rate (Q) | 584.35 | rbopd |
| | ave porosity | 0.25 | |
| | production time (tp) | 0.75 | hours |
| | well bore radius | 0.33 | ft |
| | oil compressibility* | 1.39E-05 | |
| | viscosity* | 0.39 | cp |
| | formation factor (B)* | 1.49 | rb/stb |
| | oil gravity* | 46.00 | api |
| | perm (kh) | 368.09 | md-ft |
| | perm (k) | 30.67 | md |
| | | | |
| Skin Factor Data | pressure FSIP @ 1hr | 1779.00 | psig |
| | skin factor | 5.57 | |
| | dP across skin | 725.50 | psig |
| | flow efficiency | 0.60 | |
| | | | |
| Initial Production | oil | 241.00 | bopd |
| | gas | 385.00 | mcfpd |
| | water | n/a | bwpd |
| | perfs | 4758-63 | ft |

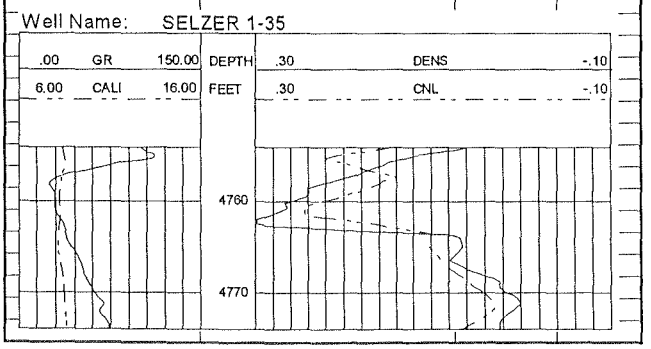

# Selzer 3-2 DST Analysis

| | | | |
|---|---|---|---|
| DST Data | | | |
| SELZER 3-2 | | | |
| | | | |
| date | 5/21/81 | | |
| well bore diameter | 7.875 | inches | |
| drill-collar | 557 | feet | |
| drill-collar (ID) | 2.25 | inches | |
| drill-pipe | 4161 | feet | |
| drill-pipe (ID) | 3.8 | inches | |
| drill-collar-vol | 0.0049 | bbl/ft | |
| drill-pipe-vol | 0.0142 | bbl\ft | |
| initial flow time | 30 | min | |
| final flow time | 30 | min | |
| total flow time (T) | 60 | min | |
| 1st final flow pressure | 123 | psig | |
| 2nd final flow pressure | 159 | psig | |
| gauge depth | 4752 | psig | |
| mud wt. | 8.9 | lb/gal | |
| initial hydrostatic pressure | 2278 | psig | |
| final hydrostatic pressure | 2246 | psig | |
| bht | 119 | degrees f | |
| porous interval (h) | 8 | feet | |
| | | | |
| | | | |
| | | | |
| DST Quality Check | calculated hydrostatic pressure | 2197.02 | psig |
| | oil specfic gravity | 0.80 | g/cm^3 |
| | oil wt | 6.68 | lb/gal |
| | oil gradient | 0.35 | psi/ft |
| | theoretical 1st flow recovery | 266.04 | ft-mud |
| | theoretical 2nd flow recovery | 573.03 | ft-oil |
| | | | |
| Horner Plot Data | M | 580 | psi/cycle |
| | reservoir pressure (pi) | 1815 | psig |
| | gas recovery (2nd flow) | 170 | mcfgpd |
| | fluid recovery (Ft.) | 600 | go |
| | production rate (Q) | 133.05 | STB/D |
| | ave porosity | 0.12 | |
| | production time (tp) | 1 | hours |
| | well bore radius | 0.33 | ft |
| | oil compressibility* | 1.39E-05 | |
| | viscosity* | 0.39 | cp |
| | formation factor (B)* | 1.49 | rb/stb |
| | oil gravity* | 46 | api |
| | perm (kh) | 21.68 | md-ft |
| | perm (k) | 2.71 | md |
| | | | |
| Skin Factor Data | pressure FSIP @ 1hr | 1712 | psig |
| | skin factor | -1.59 | |
| | dP across skin | -800.86 | psig |
| | flow efficiency | 1.44 | |
| | | | |
| Initial Production | oil | 123 | bopd |
| | gas | 192 | mcfpd |
| | water | 0 | bwpd |
| | perfs | 4748-54 | ft |

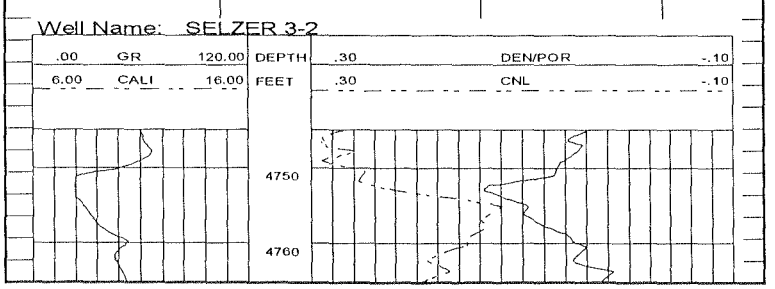

Selzer 3-34 DST Analysis

| | | | |
|---|---|---|---|
| DST Data | | | |
| SELZER 3-34 | | | |
| | | | |
| date | 2/16/82 | | |
| well bore diameter | 7.875 | inches | |
| drill-collar | 556.00 | feet | |
| drill-collar (ID) | 2.25 | inches | |
| drill-pipe | 4150.00 | feet | |
| drill-pipe (ID) | 3.80 | inches | |
| drill-collar-vol | 0.0049 | bbl/ft | |
| drill-pipe-vol | 0.0142 | bbl\ft | |
| initial flow time | 30.00 | min | |
| final flow time | 15.00 | min | |
| total flow time (T) | 45.00 | min | |
| 1st final flow pressure | 435.00 | psig | |
| 2nd final flow pressure | 440.00 | psig | |
| gauge depth | 4641.00 | psig | |
| mud wt. | 9.20 | lb/gal | |
| initial hydrostatic pressure | 2355.00 | psig | |
| final hydrostatic pressure | 2314.00 | psig | |
| bht | 120.00 | degrees f | |
| porous interval (h) | 5.00 | feet | |
| | | | |
| | | | |
| | | | |
| DST Quality Check | calculated hydrostatic pressure | 2218.03 | psig |
| | oil specfic gravity | 0.80 | g/cm^3 |
| | oil wt | 6.68 | lb/gal |
| | oil gradient | 0.35 | psi/ft |
| | theoretical 1st flow recovery | 910.19 | ft-mud |
| | theoretical 2nd flow recovery | 1585.76 | ft-oil |
| | | | |
| Horner Plot Data | M | 325.00 | psi/cycle |
| | reservoir pressure (pi) | 1610.00 | psig |
| | gas recovery (2nd flow) | 0.28 | mcfgpd |
| | fluid recovery (Ft.) | n/a | oil |
| | production rate (Q) | 50.00 | STB/D |
| | ave porosity | 0.17 | |
| | production time (tp) | 0.75 | hours |
| | well bore radius | 0.33 | ft |
| | oil compressibility* | 1.39E-05 | |
| | viscosity* | 0.39 | cp |
| | formation factor (B)* | 1.49 | rb/stb |
| | oil gravity* | 46.00 | api |
| | perm (kh) | 14.54 | md-ft |
| | perm (k) | 2.91 | md |
| | | | |
| Skin Factor Data | pressure FSIP @ 1hr | 1577.00 | psig |
| | skin factor | -0.43 | |
| | dP across skin | -121.08 | psig |
| | flow efficiency | 1.08 | |
| | | | |
| Initial Production | oil | 280.00 | bopd |
| | gas | 450.00 | mcfpd |
| | water | 0.00 | bwpd |
| | perfs | 4751-54 | ft |

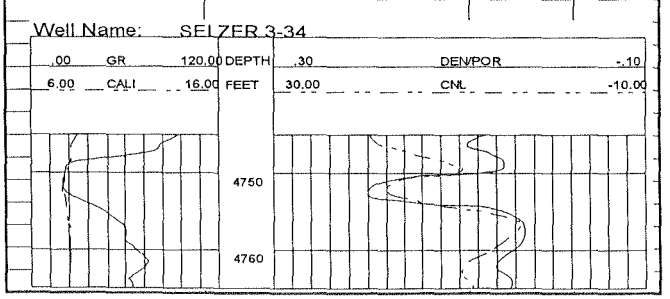

Selzer 3-34 DST Analysis

| | | | |
|---|---|---|---|
| DST Data | | | |
| SELZER 3-34 | | | |
| | | | |
| date | 2/16/82 | | |
| well bore diameter | 7.875 | inches | |
| drill-collar | 556.00 | feet | |
| drill-collar (ID) | 2.25 | inches | |
| drill-pipe | 4150.00 | feet | |
| drill-pipe (ID) | 3.80 | inches | |
| drill-collar-vol | 0.0049 | bbl/ft | |
| drill-pipe-vol | 0.0142 | bbl\ft | |
| initial flow time | 30.00 | min | |
| final flow time | 15.00 | min | |
| total flow time (T) | 45.00 | min | |
| 1st final flow pressure | 435.00 | psig | |
| 2nd final flow pressure | 440.00 | psig | |
| gauge depth | 4641.00 | psig | |
| mud wt. | 9.20 | lb/gal | |
| initial hydrostatic pressure | 2355.00 | psig | |
| final hydrostatic pressure | 2314.00 | psig | |
| bht | 120.00 | degrees f | |
| porous interval (h) | 5.00 | feet | |
| | | | |
| | | | |
| | | | |
| DST Quality Check | calculated hydrostatic pressure | 2218.03 | psig |
| | oil specfic gravity | 0.80 | g/cm^3 |
| | oil wt | 6.68 | lb/gal |
| | oil gradient | 0.35 | psi/ft |
| | theoretical 1st flow recovery | 910.19 | ft-mud |
| | theoretical 2nd flow recovery | 1585.76 | ft-oil |
| | | | |
| Horner Plot Data | M | 325.00 | psi/cycle |
| | reservoir pressure (pi) | 1610.00 | psig |
| | gas recovery (2nd flow) | 0.28 | mcfgpd |
| | fluid recovery (Ft.) | n/a | oil |
| | production rate (Q) | 50.00 | STB/D |
| | ave porosity | 0.17 | |
| | production time (tp) | 0.75 | hours |
| | well bore radius | 0.33 | ft |
| | oil compressibility* | 1.39E-05 | |
| | viscosity* | 0.39 | cp |
| | formation factor (B)* | 1.49 | rb/stb |
| | oil gravity* | 46.00 | api |
| | perm (kh) | 14.54 | md-ft |
| | perm (k) | 2.91 | md |
| | | | |
| Skin Factor Data | pressure FSIP @ 1hr | 1577.00 | psig |
| | skin factor | -0.43 | |
| | dP across skin | -121.08 | psig |
| | flow efficiency | 1.08 | |
| | | | |
| Initial Production | oil | 280.00 | bopd |
| | gas | 450.00 | mcfpd |
| | water | 0.00 | bwpd |
| | perfs | 4751-54 | ft |

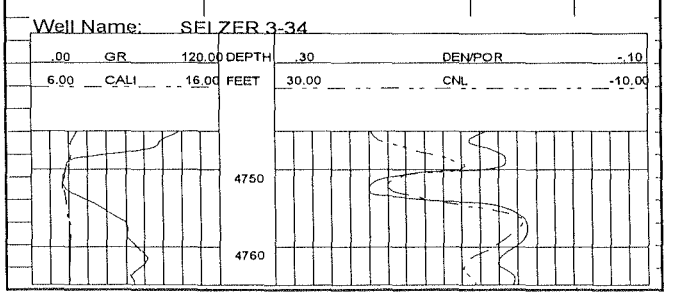

Selzer 4-2 DST Analysis

| | | | |
|---|---|---|---|
| DST Data | | | |
| SELZER 4-2 | | | |
| | | | |
| date | 6/11/81 | | |
| well bore diameter | 7.875 | inches | |
| drill-collar | 420.00 | feet | |
| drill-collar (ID) | 2.25 | inches | |
| drill-pipe | 4312.00 | feet | |
| drill-pipe (ID) | 3.80 | inches | |
| drill-collar-vol | 0.0049 | bbl/ft | |
| drill-pipe-vol | 0.0142 | bbl\ft | |
| initial flow time | 30.00 | min | |
| final flow time | 30.00 | min | |
| total flow time (T) | 60.00 | min | |
| 1st final flow pressure | 314.00 | psig | |
| 2nd final flow pressure | 233.00 | psig | |
| gauge depth | 4773.00 | psig | |
| mud wt. | 9.10 | lb/gal | |
| initial hydrostatic pressure | 2241.00 | psig | |
| final hydrostatic pressure | 2176.00 | psig | |
| bht | 124.00 | degrees f | |
| porous interval (h) | 10.00 | feet | |
| | | | |
| | | | |
| | | | |
| DST Quality Check | calculated hydrostatic pressure | 2256.32 | psig |
| | oil specfic gravity | 0.80 | g/cm^3 |
| | oil wt | 6.68 | lb/gal |
| | oil gradient | 0.35 | psi/ft |
| | theoretical 1st flow recovery | 664.23 | ft-mud |
| | theoretical 2nd flow recovery | 839.73 | ft-oil |
| | | | |
| Horner Plot Data | M | 45.00 | psi/cycle |
| | reservoir pressure (pi) | 1790.00 | psig |
| | gas recovery (2nd flow) | 0.48 | mcfgpd |
| | fluid recovery (Ft.) | 660.00 | gcm |
| | production rate (Q) | 262.37 | STB/D |
| | ave porosity | 0.17 | |
| | production time (tp) | 1.00 | hours |
| | well bore radius | 0.33 | ft |
| | oil compressibility* | 1.39E-05 | |
| | viscosity* | 0.39 | cp |
| | formation factor (B)* | 1.49 | rb/stb |
| | oil gravity* | 46.00 | api |
| | perm (kh) | 550.90 | md-ft |
| | perm (k) | 55.09 | md |
| | | | |
| Skin Factor Data | pressure FSIP @ 1hr | 1785.00 | psig |
| | skin factor | 33.70 | |
| | dP across skin | 1317.00 | psig |
| | flow efficiency | 0.26 | |
| | | | |
| Initial Production | oil | 113.00 | bopd |
| | gas | 195.00 | mcfpd |
| | water | 0.70 | bwpd |
| | perfs | 4762-69 | ft |

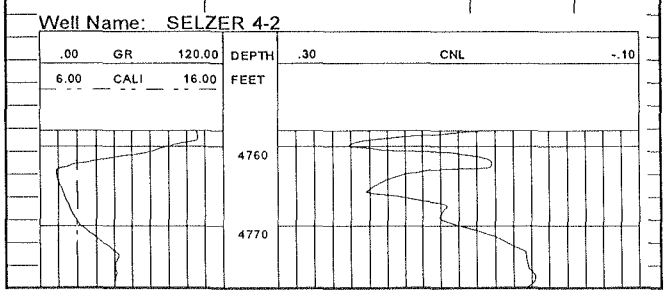

Selzer 4-35 DST Analysis

| DST Data | | | |
|---|---|---|---|
| SELZER 4-35 | | | |
| | | | |
| date | 12/2/81 | | |
| well bore diameter | 7.875 | inches | |
| drill-collar | 605.00 | feet | |
| drill-collar (ID) | 2.25 | inches | |
| drill-pipe | 4108.00 | feet | |
| drill-pipe (ID) | 3.80 | inches | |
| drill-collar-vol | 0.0049 | bbl/ft | |
| drill-pipe-vol | 0.0142 | bbl\ft | |
| initial flow time | 30.00 | min | |
| final flow time | 30.00 | min | |
| total flow time (T) | 60.00 | min | |
| 1st final flow pressure | 90.00 | psig | |
| 2nd final flow pressure | 60.00 | psig | |
| gauge depth | 4748.00 | psig | |
| mud wt. | 9.20 | lb/gal | |
| initial hydrostatic pressure | 2326.00 | psig | |
| final hydrostatic pressure | 2273.00 | psig | |
| bht | 118.00 | degrees f | |
| porous interval (h) | 5.00 | feet | |
| | | | |
| | | | |
| | | | |
| DST Quality Check | calculated hydrostatic pressure | 2269.17 | psig |
| | oil specfic gravity | 0.80 | g/cm^3 |
| | oil wt | 6.68 | lb/gal |
| | oil gradient | 0.35 | psi/ft |
| | theoretical 1st flow recovery | 188.32 | ft-mud |
| | theoretical 2nd flow recovery | 216.24 | ft-oil |
| | | | |
| Horner Plot Data | M | 73.00 | psi/cycle |
| | reservoir pressure (pi) | 1574.00 | psig |
| | gas recovery (2nd flow) | 0.15 | mcfgpd |
| | fluid recovery (Ft) | 65.00 | gcm |
| | production rate (Q) | 15.29 | STB/D |
| | ave porosity | 0.15 | |
| | production time (tp) | 1.00 | hours |
| | well bore radius | 0.33 | ft |
| | oil compressibility* | 1.39E-05 | |
| | viscosity* | 0.39 | cp |
| | formation factor (B)* | 1.49 | rb/stb |
| | oil gravity* | 46.00 | api |
| | perm (kh) | 19.79 | md-ft |
| | perm (k) | 3.96 | md |
| | | | |
| Skin Factor Data | pressure FSIP @ 1hr | 1557.00 | psig |
| | skin factor | 18.86 | |
| | dP across skin | 1195.51 | psig |
| | flow efficiency | 0.24 | |
| | | | |
| Initial Production | oil | 0.00 | bopd |
| | gas | 0.00 | mcfpd |
| | water | 0.00 | bwpd |
| | perfs | 4566-4569 | ft |

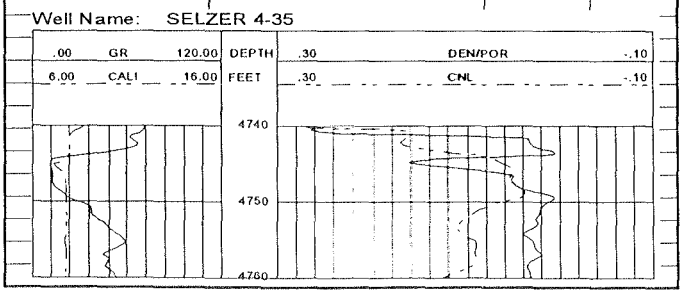

Selzer 6-2 DST Analysis

| DST Data | | | |
|---|---|---|---|
| SELZER 6-2 | | | |
| | | | |
| date | 9/21/81 | | |
| well bore diameter | 7.875 | inches | |
| drill-collar | 490.00 | feet | |
| drill-collar (ID) | 2.25 | inches | |
| drill-pipe | 4251.00 | feet | |
| drill-pipe (ID) | 3.80 | inches | |
| drill-collar-vol | 0.0049 | bbl/ft | |
| drill-pipe-vol | 0.0142 | bbl\ft | |
| initial flow time | 30.00 | min | |
| final flow time | 30.00 | min | |
| total flow time (T) | 60.00 | min | |
| 1st final flow pressure | 273.00 | psig | |
| 2nd final flow pressure | 498.00 | psig | |
| gauge depth | 4783.00 | psig | |
| mud wt. | 9.00 | lb/gal | |
| initial hydrostatic pressure | 2395.00 | psig | |
| final hydrostatic pressure | 2321.00 | psig | |
| bht | 129.00 | degrees f | |
| porous interval (h) | 12.00 | feet | |
| | | | |
| | | | |
| | | | |
| DST Quality Check | calculated hydrostatic pressure | 2236.20 | psig |
| | oil specfic gravity | 0.80 | g/cm^3 |
| | oil wt | 6.68 | lb/gal |
| | oil gradient | 0.35 | psi/ft |
| | theoretical 1st flow recovery | 583.92 | ft-mud |
| | theoretical 2nd flow recovery | 1794.79 | ft-oil |
| | | | |
| Horner Plot Data | M | 450.00 | psi/cycle |
| | reservoir pressure (pi) | 1780.00 | psig |
| | gas recovery (2nd flow) | 0.001 | mcfgpd |
| | fluid recovery (Ft.) | 1400.00 | go,w |
| | production rate (Q) | 735.50 | STB/D |
| | ave porosity | 0.20 | |
| | production time (tp) | 1.00 | hours |
| | well bore radius | 0.33 | ft |
| | oil compressibility* | 1.39E-05 | |
| | viscosity* | 0.39 | cp |
| | formation factor (B)* | 1.49 | rb/stb |
| | oil gravity* | 46.00 | api |
| | perm (kh) | 154.43 | md-ft |
| | perm (k) | 12.87 | md |
| | | | |
| Skin Factor Data | pressure FSIP @ 1hr | 1702.00 | psig |
| | skin factor | -2.12 | |
| | dP across skin | -826.90 | psig |
| | flow efficiency | 1.46 | |
| | | | |
| Initial Production | oil | 292.00 | bopd |
| | gas | 200.00 | mcfpd |
| | water | 0.00 | bwpd |
| | perfs | 4764-67 | ft |

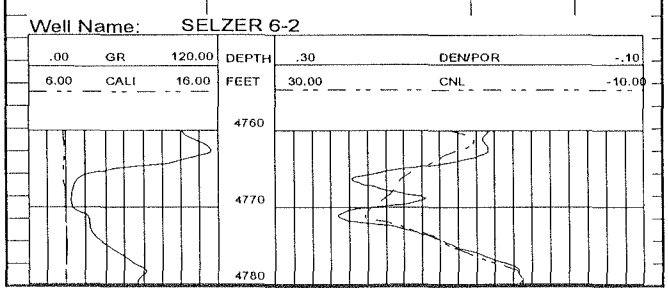

Selzer 9-2 DST Analysis

| | | | |
|---|---|---|---|
| DST Data | | | |
| SELZER 9-2 | | | |
| | | | |
| date | 12/15/82 | | |
| well bore diameter | 7.875 | inches | |
| drill-collar | 567.00 | feet | |
| drill-collar (ID) | 2.25 | inches | |
| drill-pipe | 4164.00 | feet | |
| drill-pipe (ID) | 3.80 | inches | |
| drill-collar-vol | 0.0049 | bbl/ft | |
| drill-pipe-vol | 0.0142 | bbl\ft | |
| initial flow time | 25.00 | min | |
| final flow time | 60.00 | min | |
| total flow time (T) | 85.00 | min | |
| 1st final flow pressure | 108.00 | psig | |
| 2nd final flow pressure | 139.00 | psig | |
| gauge depth | 4764.00 | psig | |
| mud wt. | 9.20 | lb/gal | |
| initial hydrostatic pressure | 2384.00 | psig | |
| final hydrostatic pressure | 2311.00 | psig | |
| bht | 117.00 | degrees f | |
| porous interval (h) | 6.00 | feet | |
| | | | |
| | | | |
| | | | |
| DST Quality Check | calculated hydrostatic pressure | 2276.81 | psig |
| | oil specfic gravity | 0.80 | g/cm^3 |
| | oil wt | 6.68 | lb/gal |
| | oil gradient | 0.35 | psi/ft |
| | theoretical 1st flow recovery | 225.98 | ft-mud |
| | theoretical 2nd flow recovery | 500.95 | ft-oil |
| | | | |
| Horner Plot Data | M | 3000.00 | psi/cycle |
| | reservoir pressure (pi) | 1250.00 | psig |
| | gas recovery (2nd flow) | 0.000 | mcfgpd |
| | fluid recovery (Ft.) | 185.00 | sogcm & m |
| | production rate (Q) | 21.76 | STB/D |
| | ave porosity | 0.15 | |
| | production time (tp) | 1.42 | hours |
| | well bore radius | 0.33 | ft |
| | oil compressibility* | 1.39E-05 | |
| | viscosity* | 0.39 | cp |
| | formation factor (B)* | 1.49 | rb/stb |
| | oil gravity* | 46.00 | api |
| | perm (kh) | 0.69 | md-ft |
| | perm (k) | 0.11 | md |
| | | | |
| Skin Factor Data | pressure FSIP @ 1hr | 395.00 | psig |
| | skin factor | -2.96 | |
| | dP across skin | -7709.27 | psig |
| | flow efficiency | 7.17 | |
| | | | |
| Initial Production | oil | 7.00 | bopd |
| | gas | n/a | mcfpd |
| | water | n/a | bwpd |
| | perfs | 4765-72 | ft |

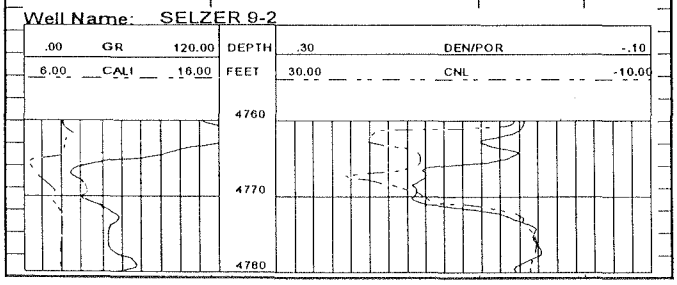

# Appendix E

# Collier Flats Field
# Reservoir Characterization Database

Individual Well Worksheet Summary

Wells Listed In Alphabetical Order

| WELL-NAME | ID | PCODE | TCODE | X | Y | LOW-GR | POR-FT | POR >10%-FT | AVE-GR | AVE-POR | POR*h | AVE-SW | AVE-PERM | PAY | NON-PAY | OOIP | EUR-23% | EUR-36% |
|---|---|---|---|---|---|---|---|---|---|---|---|---|---|---|---|---|---|---|
| Baker 1 | 132 | | 1 | 8.3602 | 12.5402 | 1.E+30 | 1.E+30 | 1.E+30 | 1.E+30 | 1.E+30 | 1.E+30 | 1.E+30 | 1.E+30 | 1.E+30 | 1.E+30 | 1.E+30 | 1.E+30 | 1.E+30 |
| Baker 1-34 | 129 | | 3 | 8.6838 | 17.5212 | 3 | 3 | 3 | 22 | 13 | 0.40 | 39 | 3 | 3 | 0 | 50,950 | 11,719 | 18,801 |
| Beyler 1 | 108 | | 3 | 10.6067 | 13.4645 | 1.E+30 | 1.E+30 | 1.E+30 | 1.E+30 | 1.E+30 | 1.E+30 | 1.E+30 | 1.E+30 | 1.E+30 | 1.E+30 | 1.E+30 | 1.E+30 | 1.E+30 |
| Beyler 2-11 | 107 | | 5 | 10.6076 | 14.1384 | 10 | 11 | 11 | 26 | 18 | 2.10 | 38 | 66 | 8 | 3 | 271,422 | 62,427 | 100,155 |
| Christian 1-11 | 87 | | 4 | 11.2956 | 14.1206 | 5 | 7 | 7 | 29 | 24 | 1.80 | 17 | 26 | 7 | 0 | 311,015 | 71,534 | 114,765 |
| Christian 2-11 | 86 | | 5 | 11.3040 | 13.4761 | 8 | 10 | 10 | 26 | 29 | 2.86 | 17 | 38 | 10 | 0 | 494,471 | 113,728 | 182,460 |
| Christian 3-11 | 64 | | 1 | 11.9507 | 13.4618 | 3 | 3 | 3 | 39 | 17 | 0.53 | 28 | 4 | 3 | 0 | 79,883 | 18,373 | 29,477 |
| Girk 1 | 40 | | 1 | 12.6712 | 19.4963 | 3 | 4 | 4 | 33 | 11 | 0.43 | 32 | 2 | 4 | 0 | 61,603 | 14,169 | 22,732 |
| Girk 11-1 | 122 | | 5 | 10.6339 | 12.2012 | 5 | 5 | 4 | 37 | 11 | 0.57 | 64 | 2 | 4 | 1 | 41,054 | 9,443 | 15,149 |
| Girk 11-2 | 101 | | 1 | 9.9304 | 12.1673 | 4 | 0 | 0 | 60 | 6 | 1.E+30 | 1.E+30 | 1.E+30 | 0 | 0 | 0 | 0 | 0 |
| Girk 2 | 43 | | 1 | 12.6649 | 18.8150 | 3 | 0 | 0 | 60 | 2 | 1.E+30 | 1.E+30 | 1.E+30 | 0 | 0 | 0 | 0 | 0 |
| Girk 3 | 29 | | 1 | 13.2573 | 19.4622 | 2 | 0 | 0 | 85 | 4 | 1.E+30 | 1.E+30 | 1.E+30 | 0 | 0 | 0 | 0 | 0 |
| Hackney 1 | 127 | | 1 | 12.6174 | 11.5539 | 2 | 1 | 0 | 20 | 8 | 0.08 | 47 | 1 | 1 | 0 | 9,008 | 2,072 | 3,324 |
| Hackney 2-13 | 50 | | 3 | 12.6169 | 10.8855 | 5 | 5 | 5 | 28 | 19 | 0.75 | 37 | 37 | 4 | 0 | 99,173 | 22,810 | 36,595 |
| Hallibur R. Baker 1 | 53 | | 1 | 12.4713 | 24.0010 | 2 | 0 | 0 | 30 | 4 | 1.E+30 | 1.E+30 | 1.E+30 | 0 | 0 | 0 | 0 | 0 |
| Halliburton Baker 3 | 48 | | 3 | 12.6300 | 22.1215 | 4 | 3 | 3 | 24 | 13 | 0.42 | 57 | 3 | 2 | 1 | 33,017 | 7,594 | 12,183 |
| Halliburton Norton 1 | 84 | | 1 | 11.3207 | 20.2003 | 1.E+30 | 1.E+30 | 1.E+30 | 1.E+30 | 1.E+30 | 1.E+30 | 1.E+30 | 1.E+30 | 1.E+30 | 1.E+30 | 1.E+30 | 1.E+30 | 1.E+30 |
| Holly Baker 1 | 103 | | 5 | 10.6264 | 16.8794 | 1.E+30 | 1.E+30 | 1.E+30 | 1.E+30 | 1.E+30 | 1.E+30 | 1.E+30 | 1.E+30 | 1.E+30 | 1.E+30 | 1.E+30 | 1.E+30 | 1.E+30 |
| Holly Baker 2 | 102 | | 5 | 10.6295 | 16.2207 | 1.E+30 | 1.E+30 | 1.E+30 | 1.E+30 | 1.E+30 | 1.E+30 | 1.E+30 | 1.E+30 | 1.E+30 | 1.E+30 | 1.E+30 | 1.E+30 | 1.E+30 |
| Holly Robert Wimmer 1 | 95 | | 1 | 11.2190 | 19.4900 | 4 | 0 | 0 | 30 | 3 | 1.E+30 | 1.E+30 | 1.E+30 | 0 | 0 | 0 | 0 | 0 |
| Lemon 1 | 80 | | 1 | 11.3368 | 10.1631 | 6 | 5 | 5 | 21 | 14 | 0.72 | 23 | 29 | 5 | 0 | 116,085 | 26,699 | 42,835 |
| Lemon 1-26 | 54 | | 3 | 12.1071 | 6.2732 | 3 | 7 | 6 | 41 | 11 | 0.77 | 87 | 2 | 0 | 7 | 0 | 0 | 0 |
| Lemon 10 | 39 | | 5 | 12.6950 | 8.9192 | 3 | 4 | 4 | 26 | 22 | 0.90 | 21 | 8 | 4 | 0 | 148,540 | 34,164 | 54,811 |
| Lemon 11 | 99 | | 3 | 10.6620 | 11.5521 | 6 | 5 | 5 | 17 | 14 | 0.72 | 26 | 30 | 5 | 0 | 111,282 | 25,595 | 41,063 |
| Lemon 12 | 27 | | 1 | 13.3539 | 8.2462 | 1.E+30 | 1.E+30 | 1.E+30 | 1.E+30 | 1.E+30 | 1.E+30 | 1.E+30 | 1.E+30 | 1.E+30 | 1.E+30 | 1.E+30 | 1.E+30 | 1.E+30 |
| Lemon 14 | 57 | | 1 | 12.026 | 8.2586 | 6 | 3 | 1 | 30 | 9 | 0.27 | 69 | 2 | 3 | 0 | 17,545 | 4,035 | 6,474 |
| Lemon 15 | 26 | | 1 | 13.3620 | 10.1845 | 4 | 0 | 0 | 50 | 4 | 1.E+30 | 1.E+30 | 1.E+30 | 0 | 0 | 0 | 0 | 0 |
| Lemon 2X | 98 | | 5 | 10.6742 | 10.1805 | 6 | 0 | 0 | 28 | 6 | 1.E+30 | 1.E+30 | 1.E+30 | 0 | 0 | 0 | 0 | 0 |
| Lemon 3 | 58 | | 5 | 12.0151 | 10.1682 | 6 | 6 | 6 | 22 | 15 | 0.93 | 20 | 43 | 6 | 0 | 154,881 | 35,623 | 57,151 |
| Lemon 4 | 82 | | 1 | 11.3295 | 9.5520 | 3 | 0 | 0 | 30 | 2 | 1.E+30 | 1.E+30 | 1.E+30 | 0 | 0 | 0 | 0 | 0 |
| Lemon 5 | 41 | | 5 | 12.6679 | 10.1762 | 3 | 5 | 5 | 33 | 23 | 1.12 | 16 | 35 | 5 | 0 | 196,783 | 45,260 | 72,613 |
| Lemon 6 | 55 | | 5 | 12.0431 | 9.5255 | 8 | 10 | 10 | 31 | 19 | 1.94 | 26 | 61 | 10 | 0 | 300,197 | 69,045 | 110,773 |
| Lemon 7 | 38 | | 3 | 12.7022 | 9.5399 | 4 | 6 | 4 | 27 | 18 | 1.08 | 33 | 1 | 4 | 2 | 83,062 | 19,104 | 30,650 |
| Lemon 8 | 56 | | 3 | 12.0328 | 8.8952 | 3 | 4 | 2 | 30 | 10 | 0.39 | 28 | 4 | 4 | 0 | 58,854 | 13,536 | 21,717 |
| Lemon 9 | 100 | | 5 | 10.6552 | 10.8805 | 3 | 3 | 3 | 32 | 14 | 0.43 | 37 | 3 | 3 | 0 | 56,338 | 12,958 | 20,789 |
| Lemon Bar 1 | 22 | | 1 | 14.8347 | 3.4699 | 3 | 0 | 0 | 1.E+30 | 1.E+30 | 1.E+30 | 1.E+30 | 1.E+30 | 0 | 0 | 0 | 0 | 0 |
| Luellia Mai 1 | 106 | | 1 | 10.6127 | 12.7866 | 6 | 5 | 4 | 17 | 11 | 0.59 | 44 | 2 | 5 | 0 | 68,743 | 15,811 | 25,366 |
| Marlene 1-23 | 96 | | 1 | 10.7258 | 6.8963 | 3 | 2 | 2 | 24 | 11 | 0.22 | 46 | 2 | 2 | 0 | 24,915 | 5,730 | 9,194 |
| Midwest Baker 1 | 51 | | 5 | 12.6168 | 21.5463 | 3 | 5 | 5 | 33 | 11 | 0.57 | 23 | 2 | 5 | 0 | 90,514 | 20,818 | 33,400 |
| Midwest Baker 2 | 30 | | 1 | 13.2447 | 22.1100 | 2 | 0 | 0 | 36 | 6 | 1.E+30 | 1.E+30 | 1.E+30 | 0 | 0 | 0 | 0 | 0 |
| Midwest Robert Wimmer | 74 | | 1 | 11.8846 | 19.4946 | 2 | 0 | 0 | 37 | 1.E+30 | 1.E+30 | 1.E+30 | 1.E+30 | 0 | 0 | 0 | 0 | 0 |
| Norton 1 | 69 | | 5 | 11.9066 | 20.8764 | 5 | 4 | 4 | 39 | 22 | 0.88 | 13 | 5 | 4 | 0 | 159,899 | 36,777 | 59,003 |
| Ora Baker 1 | 63 | | 1 | 11.9512 | 16.2203 | 1.E+30 | 1.E+30 | 1.E+30 | 1.E+30 | 1.E+30 | 1.E+30 | 1.E+30 | 1.E+30 | 1.E+30 | 1.E+30 | 1.E+30 | 1.E+30 | 1.E+30 |
| Ora Baker 4 | 66 | | 1 | 11.9353 | 16.8790 | 2 | 0 | 0 | 50 | 2 | 1.E+30 | 1.E+30 | 1.E+30 | 0 | 0 | 0 | 0 | 0 |
| Petro 11-1 | 78 | | 3 | 11.3634 | 12.1811 | 5 | 4 | 2 | 30 | 10 | 0.41 | 66 | 2 | 2 | 2 | 21,543 | 4,955 | 7,949 |
| Petro 11-2 | 59 | | 3 | 12.0065 | 12.1955 | 3 | 2 | 2 | 25 | 11 | 0.21 | 56 | 2 | 2 | 0 | 19,695 | 4,530 | 7,267 |
| Petro 11-3 | 83 | | 3 | 11.3258 | 12.8174 | 8 | 9 | 9 | 18 | 21 | 1.94 | 41 | 51 | 6 | 3 | 223,824 | 51,480 | 82,591 |
| Petro 11-4 | 61 | | 3 | 11.9882 | 12.8287 | 4 | 3 | 3 | 35 | 10 | 0.29 | 40 | 2 | 3 | 0 | 36,433 | 8,380 | 13,444 |
| Petro 12-1 | 23 | | 1 | 14.0621 | 13.4615 | 2 | 0 | 0 | 30 | 6 | 1.E+30 | 1.E+30 | 1.E+30 | 0 | 0 | 0 | 0 | 0 |
| Ralph Baker 5 | 42 | | 5 | 12.6678 | 17.5426 | 1.E+30 | 1.E+30 | 1.E+30 | 1.E+30 | 1.E+30 | 1.E+30 | 1.E+30 | 1.E+30 | 1.E+30 | 1.E+30 | 1.E+30 | 1.E+30 | 1.E+30 |
| Resource Baker 1 | 73 | | 3 | 11.8907 | 22.8719 | 4 | 4 | 4 | 19 | 14 | 0.55 | 43 | 3 | 4 | 0 | 64,630 | 14,865 | 23,848 |
| Rhoades 1 | 60 | | 5 | 11.9958 | 10.9032 | 3 | 2 | 2 | 25 | 15 | 0.30 | 19 | 13 | 2 | 0 | 51,273 | 11,793 | 18,920 |
| Rhoades 2 | 81 | | 5 | 11.3336 | 10.8792 | 6 | 9 | 9 | 30 | 19 | 1.72 | 22 | 79 | 9 | 0 | 277,585 | 63,845 | 102,429 |
| Rhoades 3 | 79 | | 5 | 11.3369 | 11.5762 | 6 | 6 | 6 | 30 | 16 | 0.98 | 25 | 17 | 6 | 0 | 153,894 | 35,396 | 56,787 |
| Rhoades 4 | 62 | | 5 | 11.9772 | 11.5555 | 5 | 6 | 6 | 34 | 16 | 0.99 | 30 | 48 | 6 | 0 | 144,472 | 33,229 | 53,310 |
| RJ Ora Baker 2 | 88 | | 5 | 11.2952 | 16.8712 | 3 | 3 | 2 | 26 | 11 | 0.35 | 53 | 2 | 3 | 0 | 34,898 | 8,026 | 12,877 |
| RJ Ora Baker 3 | 91 | | 5 | 11.2856 | 16.2189 | 3 | 5 | 4 | 28 | 14 | 0.74 | 44 | 34 | 5 | 0 | 86,163 | 19,817 | 31,794 |
| RJ Ralph Baker 1 | 35 | | 3 | 12.7538 | 16.2124 | 3 | 4 | 4 | 34 | 14 | 0.55 | 46 | 3 | 4 | 0 | 62,030 | 14,267 | 22,889 |

| | | | | | | | | | | | | | | | | | | |
|---|---|---|---|---|---|---|---|---|---|---|---|---|---|---|---|---|---|---|
| RJ Ralph Baker 2 | 44 | | 1 | 12.6550 | 18.2206 | 3 | 2 | 2 | 26 | 10 | 0.20 | 71 | 2 | 2 | 0 | 11,921 | 2,742 | 4,399 |
| RJ Ralph Baker 3 | 28 | | 1 | 13.3398 | 16.1976 | 2 | 0 | 0 | 28 | 6 | 1.E+30 | 1.E+30 | 1.E+30 | 0 | 0 | 0 | 0 | 0 |
| RJ Ralph Baker 4 | 37 | | 5 | 12.7248 | 16.9418 | 4 | 4 | 4 | 24 | 17 | 0.67 | 34 | 4 | 4 | 0 | 91,112 | 20,956 | 33,620 |
| RJ Robert Wimmer 1 | 92 | | 1 | 11.2506 | 17.5460 | 3 | 0 | 0 | 36 | 6 | 1.E+30 | 1.E+30 | 1.E+30 | 0 | 0 | 0 | 0 | 0 |
| RJ Robert Wimmer 2 | 67 | | 1 | 11.9321 | 17.5474 | 3 | 0 | 0 | 36 | 2 | 1.E+30 | 1.E+30 | 1.E+30 | 0 | 0 | 0 | 0 | 0 |
| RJ Robert Wimmer 3 | 70 | | 1 | 11.9065 | 18.2318 | 2 | 0 | 0 | 0 | 2 | 1.E+30 | 1.E+30 | 1.E+30 | 0 | 0 | 0 | 0 | 0 |
| RJ Robert Wimmer 4 | 94 | | 3 | 11.2441 | 18.2336 | 4 | 3 | 3 | 31 | 11 | 0.34 | 45 | 2 | 3 | 0 | 38,470 | 8,848 | 14,195 |
| Schweitzer 1 | 44 | | 3 | 11.8944 | 22.1071 | 6 | 2 | 2 | 21 | 16 | 0.32 | 31 | 3.6 | 2 | 0 | 46,102 | 10,604 | 17,012 |
| Schweitzer 2 | 85 | | 1 | 11.3175 | 21.5403 | 1.E+30 | 1.E+30 | 1.E+30 | 1.E+30 | 1.E+30 | 1.E+30 | 1.E+30 | 1.E+30 | 1.E+30 | 1.E+30 | 1.E+30 | 1.E+30 | 1.E+30 |
| Schweitzer 3 | 72 | | 3 | 11.8908 | 21.5287 | 4 | 6 | 4 | 43 | 14 | 0.86 | 36 | 3 | 6 | 0 | 115,357 | 26,532 | 42,567 |
| SELZER 1-2 | 65 | | 1 | 11.9484 | 15.4748 | 4 | 0 | 0 | 45 | 2 | 1.E+30 | 1.E+30 | 1.E+30 | 0 | 0 | 0 | 0 | 0 |
| SELZER 1-34 | 128 | | 1 | 9.2825 | 18.1940 | 3 | 0 | 0 | 36 | 6 | 1.E+30 | 1.E+30 | 1.E+30 | 0 | 0 | 0 | 0 | 0 |
| Selzer 1-35 | 109 | | 5 | 10.5977 | 17.5413 | 5 | 7 | 6 | 32 | 21 | 1.78 | 32 | 59 | 6 | 1 | 235,693 | 54,209 | 86,971 |
| SELZER 1-A | 125 | | 5 | 9.3208 | 16.8542 | 4 | 6 | 4 | 36 | 15 | 0.90 | 33 | 3 | 6 | 0 | 125,429 | 28,849 | 46,283 |
| Selzer 2-2 | 120 | | 3 | 9.9607 | 16.8877 | 4 | 5 | 4 | 34 | 12 | 0.62 | 34 | 2 | 5 | 0 | 85,208 | 19,598 | 31,442 |
| SELZER 2-34 | 135 | | 1 | 7.3717 | 19.5235 | 4 | 0 | 0 | 30 | 4 | 1.E+30 | 1.E+30 | 1.E+30 | 0 | 0 | 0 | 0 | 0 |
| Selzer 2-35 | 116 | | 5 | 9.9959 | 17.5176 | 5 | 5 | 4 | 27 | 14 | 0.75 | 23 | 3 | 5 | 0 | 120,830 | 27,791 | 44,586 |
| SELZER 2-A | 124 | | 5 | 9.3272 | 16.1826 | 5 | 7 | 7 | 35 | 14 | 1.06 | 54 | 3 | 6 | 1 | 100,015 | 23,003 | 36,906 |
| Selzer 3-2 | 117 | | 3 | 9.9831 | 16.2129 | 5 | 7 | 4 | 30 | 10 | 0.73 | 35 | 2 | 7 | 0 | 97,406 | 22,403 | 35,943 |
| Selzer 3-34 | 126 | | 5 | 9.2986 | 17.5032 | 6 | 4 | 4 | 25 | 18 | 0.72 | 29 | 4 | 4 | 0 | 106,035 | 24,388 | 39,127 |
| Selzer 3-35 | 110 | | 3 | 10.5849 | 18.2193 | 6 | 6 | 6 | 12 | 14 | 0.86 | 28 | 36 | 6 | 0 | 129,179 | 29,711 | 47,667 |
| SELZER 3-A | 123 | | 1 | 9.3369 | 15.4724 | 5 | 6 | 6 | 30 | 18 | 1.07 | 47 | 65 | 6 | 0 | 118,351 | 27,221 | 43,672 |
| Selzer 4-2 | 105 | | 5 | 10.6203 | 15.4880 | 6 | 7 | 8 | 18 | 14 | 1.15 | 40 | 35 | 6 | 2 | 131,813 | 30,317 | 48,639 |
| Selzer 4-34 | 133 | | 1 | 8.0054 | 18.1945 | 6 | 4 | 4 | 25 | 10 | 0.42 | 82 | 2 | 2 | 2 | 11,966 | 2,752 | 4,416 |
| Selzer 4-35 | 114 | | 1 | 10.0181 | 18.2149 | 5 | 2 | 2 | 12 | 12 | 0.24 | 57 | 2 | 2 | 0 | 21,525 | 4,951 | 7,943 |
| Selzer 5-2 | 121 | | 5 | 9.9579 | 15.4834 | 8 | 10 | 10 | 38 | 19 | 1.92 | 43 | 61 | 8 | 2 | 215,586 | 49,585 | 79,551 |
| Selzer 6-2 | 104 | | 5 | 10.6235 | 14.8197 | 8 | 11 | 11 | 37 | 17 | 1.89 | 50 | 53 | 8 | 3 | 181,682 | 41,787 | 67,041 |
| Selzer 7-2 | 89 | | 5 | 11.2891 | 14.8243 | 5 | 5 | 5 | 31 | 16 | 0.88 | 48 | 51 | 4 | 1 | 92,146 | 21,194 | 34,002 |
| Selzer 8-2 | 90 | | 4 | 11.2860 | 15.4670 | 6 | 9 | 9 | 20 | 20 | 1.92 | 35 | 59 | 8 | 1 | 255,362 | 58,733 | 94,229 |
| Selzer 9-2 | 119 | | 3 | 9.9642 | 14.8183 | 5 | 6 | 5 | 38 | 14 | 0.85 | 61 | 3 | 6 | 0 | 69,711 | 16,034 | 25,723 |
| Selzer B-1 | 130 | | 5 | 8.6554 | 15.4678 | 4 | 4 | 2 | 20 | 9 | 0.38 | 84 | 2 | 0 | 0 | 0 | 0 | 0 |
| Smith Weede 1 | 19 | | 1 | 15.4916 | 16.0091 | 3 | 0 | 0 | 30 | 2 | 1.E+30 | 1.E+30 | 1.E+30 | 0 | 0 | 0 | 0 | 0 |
| Thornhill 1 | 52 | | 3 | 12.5661 | 22.8380 | 4 | 5 | 4 | 31 | 10 | 0.53 | 25 | 2 | 5 | 0 | 83,151 | 19,125 | 30,683 |
| Thornhill 2 | 31 | | 1 | 13.2348 | 23.5239 | 3 | 0 | 0 | 35 | 6 | 1.E+30 | 1.E+30 | 1.E+30 | 0 | 0 | 0 | 0 | 0 |
| Waters 1-25 | 25 | | 3 | 13.4286 | 5.5765 | 3 | 4 | 4 | 36 | 13 | 0.52 | 89 | 3 | 0 | 0 | 0 | 0 | 0 |
| Waters 2-25 | 34 | | 1 | 12.7633 | 6.2558 | 2 | 0 | 0 | 45 | 2 | 1.E+30 | 1.E+30 | 1.E+30 | 0 | 0 | 0 | 0 | 0 |
| Wesley Girk 1 | 36 | | 1 | 12.7317 | 15.4894 | 2 | 0 | 0 | 45 | 2 | 1.E+30 | 1.E+30 | 1.E+30 | 0 | 0 | 0 | 0 | 0 |
| Wesley Girk 2 | 24 | | 1 | 13.9866 | 15.4631 | 5 | 4 | 4 | 28 | 14 | 0.56 | 62 | 3 | 4 | 0 | 44,033 | 10,128 | 16,248 |
| Willems A-1 | 112 | | 3 | 10.5725 | 18.8266 | 5 | 5 | 5 | 28 | 19 | 1.01 | 27 | 65 | 5 | 0 | 152,792 | 35,142 | 56,380 |
| Willems 2-A | 115 | | 1 | 9.9959 | 18.8640 | 2 | 0 | 0 | 30 | 5 | 1.E+30 | 1.E+30 | 1.E+30 | 0 | 0 | 0 | 0 | 0 |
| Willems A-3 | 111 | | 3 | 10.5725 | 19.4822 | 5 | 6 | 6 | 43 | 20 | 1.17 | 41 | 53 | 6 | 0 | 144,341 | 33,198 | 53,262 |
| Willems A-4 | 118 | | 3 | 9.9738 | 19.4873 | 4 | 2 | 1 | 32 | 9 | 0.17 | 52 | 1 | 2 | 0 | 17,337 | 3,987 | 6,397 |
| Willems A-5 | 97 | | 3 | 10.6996 | 20.2087 | 5 | 5 | 4 | 38 | 11 | 0.60 | 62 | 2 | 5 | 0 | 47,730 | 10,978 | 17,612 |
| Willems 6-A | 113 | | 5 | 10.0373 | 20.1976 | 3 | 0 | 0 | 40 | 6 | 1.E+30 | 1.E+30 | 1.E+30 | 0 | 0 | 0 | 0 | 0 |
| Winn Baker 1 | 45 | | 1 | 12.6529 | 19.9847 | 1.E+30 | 1.E+30 | 1.E+30 | 1.E+30 | 1.E+30 | 1.E+30 | 1.E+30 | 1.E+30 | 1.E+30 | 1.E+30 | 1.E+30 | 1.E+30 | 1.E+30 |
| Woolfolk 1 | 32 | | 1 | 13.0822 | 4.6281 | 1.E+30 | 1.E+30 | 1.E+30 | 1.E+30 | 1.E+30 | 1.E+30 | 1.E+30 | 1.E+30 | 1.E+30 | 1.E+30 | 1.E+30 | 1.E+30 | 1.E+30 |
| Woolfolk 1-34 | 76 | | 1 | 11.4107 | 7.5825 | 5 | 5 | 4 | 22 | 10 | 0.49 | 95 | 2 | 0 | 0 | 0 | 0 | 0 |
| YUCCA ORA BAKER 1 | 93 | | 1 | 11.2442 | 22.8737 | 3 | 0 | 0 | 25 | 6 | 1.E+30 | 1.E+30 | 1.E+30 | 0 | 0 | 0 | 0 | 0 |
| YUCCA ORA BAKER 2 | 68 | | 1 | 11.9160 | 23.5853 | 3 | 0 | 0 | 35 | 6 | 1.E+30 | 1.E+30 | 1.E+30 | 0 | 0 | 0 | 0 | 0 |
| Yucca Ralph Baker 1 | 47 | | 3 | 12.6426 | 20.1518 | 4 | 4 | 4 | 50 | 16 | 0.64 | 24 | 4 | 4 | 0 | 101,480 | 23,340 | 37,446 |
| Yucca Ralph Baker 2 | 46 | | 3 | 12.6507 | 20.4538 | 3 | 2 | 1 | 23 | 10 | 0.21 | 38 | 2 | 2 | 0 | 27,090 | 6,231 | 9,996 |
| | | | | | | | | | | | | | | | | | | |